

Towards improving cell culture processes for biotherapeutic production: novel tools and strategies

by

Jyoti Rawat

10BB17J26054

A thesis Submitted to the
Academy of Scientific & Innovative Research
for the award of the degree of
DOCTOR OF PHILOSOPHY

in
SCIENCE

Under the Supervision of
Dr Mugdha Gadgil



CSIR-National Chemical Laboratory, Pune

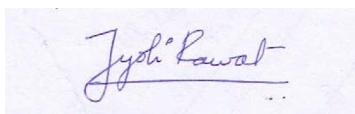


Academy of Scientific and Innovative Research
AcSIR Headquarters, CSIR-HRDC campus
Sector 19, Kamla Nehru Nagar,
Ghaziabad, U.P. – 201 002, India

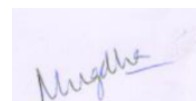
December 2021

CERTIFICATE

This is to certify that the work incorporated in this Ph.D. thesis entitled, “*Towards improving cell culture processes for biotherapeutic production: novel tools and strategies*”, submitted by *Ms. Jyoti Rawat* to Academy of Scientific and Innovative Research (AcSIR) in partial fulfilment of the requirements for the award of the Degree of *Doctor of Philosophy in Science*, embodies original research work carried-out by the student. We, further certify that this work has not been submitted to any other University or Institution in part or full for the award of any degree or diploma. Research material(s) obtained from other source(s) and used in this research work has/have been duly acknowledged in the thesis. Image(s), illustration(s), figures(s), table(s) etc., used in the thesis from other source(s), have been duly cited and acknowledged.



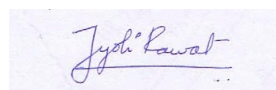
Jyoti Rawat
16/12/21
(Student)



Dr Mugdha Gadgil
17/12/21
(Research advisor)

STATEMENTS OF ACADEMIC INTEGRITY

I Jyoti Rawat, a Ph.D. student of the Academy of Scientific and Innovative Research (AcSIR) with Registration No.10BB17J26054 hereby undertake that, the thesis entitled “Towards improving cell culture processes for biotherapeutic production: novel tools and strategies” has been prepared by me and that the document reports original work carried out by me and is free of any plagiarism in compliance with the UGC Regulations on “*Promotion of Academic Integrity and Prevention of Plagiarism in Higher Educational Institutions (2018)*” and the CSIR Guidelines for “*Ethics in Research and in Governance (2020)*”.

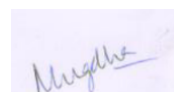


Signature of the Student

Date : 16/12/21

Place : Pune

It is hereby certified that the work done by the student, under my/our supervision, is plagiarism free in accordance with the UGC Regulations on “*Promotion of Academic Integrity and Prevention of Plagiarism in Higher Educational Institutions (2018)*” and the CSIR Guidelines for “*Ethics in Research and in Governance (2020)*”.



Signature of the Supervisor

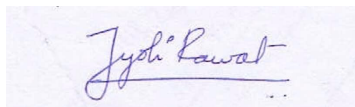
Name : Mugdha Gadgil

Date :17/12/21

Place : Pune

DECLARATION BY RESEARCH SCHOLAR

I, Jyoti Rawat hereby declare that the work incorporated in the thesis entitled 'Towards improving cell culture processes for biotherapeutic production: novel tools and strategies' submitted by me to the Academy of Scientific and Innovative Research (AcSIR), for the degree of Doctor of Philosophy in Biological Sciences has been carried out by myself. All the work has been carried out at CSIR-National Chemical Laboratory, Pune under the guidance of Dr. Mugdha Gadgil. The reported work is original and has not been submitted to any other university or institution for the award of any degree or diploma. Such material, as has been obtained from other sources, has been duly acknowledged.

A rectangular box containing a handwritten signature in blue ink that reads "Jyoti Rawat". The signature is written in a cursive style and is underlined.

Jyoti Rawat
Date: 15/12/21
Place: Pune

Acknowledgements

I would like to thank my advisor Dr Mugdha Gadgil for accepting to be a supervisor to a naïve masters intern and with that introducing me to the world of research. I cannot thank her enough for the numerous woman hours she spent making me not only a good researcher but a better human being.

I thank by my doctoral advisory committee consisting of Dr Anu Raghunathan, Dr Rahul Bhambure and Dr Paresh Dhepe for their valuable scientific inputs and support. I thank Dr Ramchandra Gadre for generously helping us establish the HPLC protocols. I would also like to thank my collaborators Dr Beena Pillai and Dr Aksheev Bhambri from CSIR-IGIB for the RNA-Seq analysis.

I thank all my lab mates, particularly, Vishwanath, Anuja, Tanaya, Tejal, Rupali, Kathik, Samay and Santosh for their help and support during my time at the cell culture engineering lab. I also thank my colleagues at MBL and NCL for their support, guidance and some very creative out of the box troubleshooting techniques. I would also like to thank Vishwanath for being a supportive spouse.

I thank CSIR for the research fellowship and CSIR-NCL for hosting me. I cannot thank my parents, friends and family enough for their love and support.

Table of Contents

CERTIFICATE	iii
STATEMENTS OF ACADEMIC INTEGRITY	v
DECLARATION BY RESEARCH SCHOLAR	vi
Acknowledgements	vii
List of Figures	xiii
List of Tables	xv
Abbreviations	xvii
Abstract	xxi
Chapter I. Introduction	1
1.1 Thesis organization	7
Chapter II. Background	9
2.1 Replacement of serum	10
2.2 Components of serum-free media	11
2.2.1 Carbohydrate source	12
2.2.2 Amino acids	14
2.2.3 Glutamine	16
2.2.4 Protein Hydrolysates	17
2.2.5 Vitamins	18
2.2.5.1 Vitamin C	20
2.2.6 Lipoic acid	20
2.2.7 Hormones	21
2.2.8 Lipids	21
2.2.9 Ions	22
2.2.10 Trace metals	22
2.2.11 Miscellaneous	23
2.3 Designing serum-free medium for biotherapeutic production	24
2.4 Effective feeding strategy for the production of biotherapeutics	25
2.5 Conclusion	27
Chapter III. Methods	31
3.1 Materials	31
3.2 Cell culture	31
3.2.1 CHO-S cells	32
3.2.2 K562	32
3.2.3 CHO cells expressing IgG	32
3.3 Adaptation to HDFE 3 without hydrolysate	33
3.4 Adaptation to low amino acid media	34
3.5 Single amino acid supplementation	34
3.6 Bioreactor experiment	34
3.7 RNA seq library preparation	35
3.8 Specific metabolite consumption	36
3.9 Hydrogel synthesis	36
3.9.1 Release kinetics for amino acids	37

3.10 Volumetric IgG Quantification	38
3.11 Flow apparatus	38
3.12 Transfection	39
3.13 Calculation of transfection efficiency	39
3.14 Statistical analysis	40
Chapter IV. Shear stress and its implication on large-scale transient transfection for biopharmaceutical production.....	41
4.1 Summary	41
4.2 Introduction.....	42
4.3 Results.....	47
4.3.1 Developing a scale-down device to investigate a wide range of shear stress on mammalian cells.....	47
4.3.2 Exposure to shear stress in the presence of lipoplex reduces transfection efficiency and increases cell death.....	49
4.3.3 Shear stress does not affect the transfectability of the lipoplex complex.....	51
4.3.4 Shear stress affects the transfectability of CHO-S cells	52
4.3.5 Toxicity of lipoplex is not solely attributable to liposome	53
4.3.6 Shear stress does not affect the toxicity of lipoplex in inefficiently transfected K562 cell line.....	54
4.4 Discussion	56
4.5 Conclusion	58
Chapter V. Towards establishing continuous nutrient release using hydrogels:	
Hydrogel development and characterization	59
5.1 Summary	59
5.2 Introduction.....	60
5.3 Methods.....	64
5.3.1 Synthesis of hydrogels	64
5.3.2 Release kinetics for amino acids.....	65
5.4 Results.....	66
5.4.1 Standardizing the hydrogel geometry for sustained release in mammalian cell culture: Effect of crosslinking, nutrient payload and hydrogel geometry	66
5.4.2 Toxicity profile for NutriGel in CHO cell culture	68
5.4.3 Standardizing the amount of nutrient payload suitable for supporting animal cell culture.....	69
5.4.4 Hydrogels can maintain a continuous supply of amino acids for an extended duration suitable for supporting animal cell culture	70
5.4.5 Effect of abundance and solubility	75
5.5 Conclusion	77
Chapter VI. Towards in situ continuous feeding via controlled release of complete nutrients for the fed-batch culture of animal cells	79
6.1 Summary	79
6.2 Introduction.....	80
6.3 Methods.....	82
6.3.1 Hydrogel synthesis.....	82
6.3.2 Cell culture.....	83
6.3.3 Statistical analysis	84
6.4 Results and discussion	84

6.4.1 Continuous feeding of complex nutrient feed using NutriGel ₁ improves culture longevity and volumetric productivity of recombinant CHO cell culture	85
6.4.2 NutriGel ₁ hydrogels also supply other classes of nutrients that help in improving culture longevity.....	86
6.4.3 Vitamins and trace elements are released from the NutriGels and contribute to improving culture longevity	87
6.4.4 Use of NutriGel ₂ ^{HVT,T} to reduce the differences in release rates of all amino acids in fed-batch cultures	89
6.4.5 A completely closed continuous in situ feeding via hydrogels for animal cell culture requiring no operator handling.....	91
6.4.6 Utilizing NutriGel ₁ ^T for a nutrient-rich media and other suspension cell lines.....	94
6.5 Conclusion	95
Chapter VII.	97
Lean amino acid medium formulation and its implication on culture performance....	97
7.1 Summary	97
7.2 Introduction.....	97
7.3 Methods.....	99
7.3.1 Cell culture.....	99
7.3.2 RNA isolation and library preparation.....	100
7.3.3 Transcriptome analysis	100
7.3.4 Bioreactor culture.....	101
7.4 Results.....	101
7.4.1 Growth response of CHO cells under diverse amino acid conditions	101
7.4.2 GCNP transcriptional activation as a response to nutrient limitation	105
7.4.3 Differential expression of amino acid sensors	108
7.4.3.1 Amino acid transporters.....	108
7.3.4 Cell cycle arrest observed when cells are cultured in LAA.....	116
7.4.5 Autophagy.....	118
7.4.6 Other differentially expressed genes.....	120
Mafk.....	120
RNF182.....	120
KLHL24.....	120
KLF5	121
TNFAIP3	122
Trp53inp1.....	122
CHAC1	122
TRIB	122
SGK	123
Elov16.....	123
CHD5	124
EGR1.....	124
Pim 3	125
GPER1	125
NNMT.....	125
MED12.....	126
GFOD1.....	127

INSIG1	127
IRS1	127
ALDOA.....	127
DNA2	127
DUSP14 and DUSP7	128
CREBRF	128
7.4.7 Supplementation of single amino acid in a lean amino acid background does not improve growth or productivity in CHO cell culture	132
7.4.8 Developing a feeding strategy to complement LAA condition while maintaining low amino acid concentrations.....	135
7.5 Conclusions.....	144
Chapter VIII. Conclusions	147
8.1 Future directions	149
Appendix.....	151
Custom medium formulation	151
References.....	161
ABSTRACT.....	193
List of publications and patent.....	194
(1) List of publications and patent	194
(2) Poster presentation	195
(3) Copy of all SCI publication(s)	197

List of Figures

Figure 1.1: Typical route for the production of any recombinant biotherapeutic.....	2
Figure 1.2: Clonal selection and scale-up for recombinant biotherapeutic production ..	5
Figure 2.1: Overview of transport mechanisms for various media components	12
Figure 2.2: Representation depicting the mechanism of system ASC for amino acid transport	15
Figure 2.3: Representation depicting the mechanism of systems A and L for amino acid transport.....	15
Figure 2.4: Modes of cell culture routinely used for the production of biotherapeutics	27
Figure 4.1: Summary of the energy dissipation rate in the literature.....	43
Figure 4.2: A simple scale-down flow device to subject CHO cells to a shear stress.	47
Figure 4.3 The effect of shear stress on cell density and viability of CHO-S cells. ...	49
Figure 4.4 Cell density, viability, and transfection efficiency of CHO-S cells when exposed to shear stress in the presence of lipoplex.....	50
Figure 4.5 Shear stress does not affect the transfectability of the lipoplex.	51
Figure 4.6 Shear stress reduces the transfectability of CHO-S cells.	53
Figure 4.7 Exposure of CHO-S cells to shear stress in the presence or absence of liposome causes a reduction in cell growth.	54
Figure 4.8 Effect of shear stress on cell density and transfection efficiency of K562 cells in the presence or absence of the lipoplex.....	55
Figure 5.1: Comparative influence of crosslinking, loading and geometry on glutamine release	67
Figure 5.2: CHO cell culture supplemented with hydrogels do not show enhanced toxicity	68
Figure 5.3 Standardization of nutrient payload for assisting feeding in mammalian cell culture	70
Figure 5.4: Amino acid composition for the two nutrient mixture payloads to create NutriGels.....	73
Figure 5.5: Cumulative amino acid release profile from two different compositions of amino acid in the NutriGel payload viz NutriGel ₁ and NutriGel ₂ ^H	74
Figure 5.6: Effect of inclusion of HEPES in the payload on the release rate constant	75
Figure 6.1: In situ delivery of nutrients through NutriGel ₁ ^T leads to improved culture performance	86
Figure 6.2: In situ release of only amino acids does not improve cell growth.	87
Figure 6.3: Effect of different classes of nutrients from the payload of the NutriGel on culture longevity	88
Figure 6.4: Overcoming low amino acid concentration through NutriGel ₂ ^{HVT,T}	91
Figure 6.5: Complete in situ release of nutrients for CHO IgG culture.....	93
Figure 6.6: Utilizing NutriGel ₁ ^T for alternative nutrient-rich media and other suspension cell lines.....	95
Figure 7.1: Effects of amino acid starvation in mammalian cells.....	99
Figure 7.2: Evaluating the effects of diverse media formulation on CHO cell culture performance	103
Figure 7.3: Major biological processes enriched during growth in LAA	105

Figure 7.4: GCNP transcriptional activation in mammalian cells	106
Figure 7.5: Alterations in SLC transporter gene expression following growth in LAA condition	112
Figure 7.6: The amino acid transporters in cancer cells.	113
Figure 7.7 Disruption in cell cycle regulation following growth in LAA condition ..	118
Figure 7.8: Disruption in cell cycle regulation following growth in LAA condition	119
Figure 7.9: No significant difference in cell culture performance with single amino acid supplementation under LAA background	134
Figure 7.10: In situ, continuous feeding of amino acids through NutriGel in low amino acid (LAA) conditions can sustain CHO cell culture	135
Figure 7.11: Feeding strategy designed on release rates from NutriGel led to culture performance on a bench scale comparable bioreactor system.....	136
Figure 7.12: Representation of the defined continuous feeding approach developed in this study	137
Figure 7.13: Optimizing cell culture performance in low amino acid media by utilizing specific amino acid consumption rates.....	139
Figure 7.14: Improved specific productivity is observed as amino acid concentration is maintained above 0.1 mM with an improved feeding strategy	140
Figure 7.15: Optimizing cell culture performance in low amino acid media by utilizing specific amino acid consumption rates.....	142
Figure 7.16: Controlling glucose while maintaining low amino acid concentration contributes to higher cell densities.....	144

List of Tables

Table 1. Plasma membrane transporters for glutamine.	17
Table 3: Summary of commercial cultivation systems.....	63
Table 4: Compositions of payloads used in this study.....	76
Table 5: Differentially expressed SLC genes	114
Table 6: List of differential expressed genes in CHO cells cultured in LAA.....	129
Table 7: Feed composition for the various reactor runs	138

Abbreviations

Acronym	Expansion
CHO	Chinese hamster ovary
CAGR	Compound annual growth rate
DHFR	dihydrofolate reductase
GS	Glutamine synthetase
FACS	Fluorescence-activated cell sorting
PTM	Post translational modification
SGE	Stable cell line generation
TGE	Transient gene expression
VCD	Viable cell density
IVCD	Integral viable cell density
AA	Amino acid
LAA	Low amino acid
DE	Differentially expressed
OFAT	One factor at a time approach
DoE	Design of expedient
QbD	Quality by Design
RSM	Response surface methodology
ROS	reactive oxygen species
rAlb	recombinant human albumin
SLC	Solute carrier
Cbl	Cobalamin
POT	Proton-coupled Oligopeptide Transporter
PTR/ PEPT	Peptide Transporter
PHT	Peptide/Histidine Transporter 1
THTR	Thiamin transporter
SMVT	Sodium-dependent multivitamin transporter
RFT1	Riboflavin transporters-1
DHLA	dihydrolipoic acid

LA	Lipoic acid
DMEM	Dulbecco's Modified Eagle's Medium
SFM	Serum-free media
SCP2	Non-specific lipid-transfer protein
CNT	Concentrative nucleoside transporters
ENT	Equilibrative nucleoside transporters
HEMA	2-hydroxyethyl methacrylate
EGDMA	Ethylene glycol dimethacrylate
PITC	Phenylisothiocyanate
ELISA	Enzyme-linked immunoassay
EDR	Energy dissipation rate
EC	Endothelial cells
HUVECs	Human umbilical vein endothelial cells
FDA	Food and Drug administration
mTOR	Mammalian target of rapamycin
BSA	Bovine serum albumin
PBS	Phosphate-buffered saline
AAR	Amino acid response
ISR	Integrated stress response
ATG13	Autophagy 13
HAA	High amino acid
ATF4	Activating transcription factor 4
PP1	protein phosphatase 1
4E-BP	4E-binding protein 1
Rheb	Ras homologue enriched in brain
TSC2	Tuberous sclerosis complex 2
LARS	Leucyl-tRNA synthetase
TOP	5' terminal oligopyrimidine
LAMTOR	Late endosomal/lysosomal adaptor
ULK1	UNC51-like kinase 1
CDK	Cyclin dependent kinase
CDKI	Cyclin dependent kinase inhibitors
CHD5	Chromodomain helicase DNA binding protein 5
VPS34	Vacuolar protein sorting 34

PPP	Pentose phosphate pathway
SAM	S-adenosylmethionine
TCA	Tricarboxylic cycle

Abstract

Mammalian cell culture-based processes are essential for producing effective recombinant therapeutics such as monoclonal antibodies. A typical production process involves the introduction of the gene of interest in the host cell, selecting a clone with desired productivity characteristics, process and medium development for the selected clone, followed by production runs in larger scale bioreactors, which are currently predominantly fed-batch mode. For preclinical analysis, the material can be produced by transient expression of the protein without selecting a clone. Each of these steps has scope for improvement. In this thesis, I have explored three problems associated with these steps (1) Understanding whether shear stress affects the productivity of transient protein expression, which is of importance when scaling up such processes (2) Developing a hydrogel-based tool for simultaneous in situ delivery of >20 nutrients in small scale culture which can enable fed-batch culture at small scale without any additional infrastructure, and help in better identification of high productivity clones at the screening stage (3) Evaluated whether a medium formulation strategy of maintaining amino acids at low concentrations via continuous feeding may be beneficial for increasing culture longevity and productivity.

Large scale TGE is a crucial method for rapidly producing a large amount of recombinant protein for initial characterizations. Mammalian cells are subjected to varying degrees of shear during various stages of bioprocessing. The effect of shear has been mainly studied in adherent cells but has been studied to a lower degree in suspension cells, especially in the bioprocessing context. Shear stress affects transfection efficiency and increases liposomal toxicity. And this effect increases as the magnitude of shear stress increases because of the synergistic effect of shear on liposomal toxicity and the cells.

During cell line development, selecting a robust high producer is the primary requirement for any successful cell line development program. Screening clones under conditions similar to the final production process reduces the chances of sub-

par clone performance at a higher scale. I have investigated whether it is possible to culture fed-batch mode in small scale platforms without requiring any additional infrastructure. I have developed a nutrient delivery system for in situ feeding of CHO cells in small scale culture platforms, capable of delivering a large number of nutrients such as amino acids, vitamins and trace elements. I have shown that it is possible to modulate the delivery of 18 amino acids, improving cell culture performance. Such a system will also aid in creating a completely closed system for small scale platforms for cultivating CHO cells.

Medium development is another critical parameter that can affect the process. Recent reports caution against the use of a nutritionally rich medium as a result of the catabolic by-products of amino acids. I have investigated whether maintaining amino acids at low concentrations through continuous feeding can improve culture performance. Results from these experiments do not suggest an improvement in culture performance. However, with developments in online metabolite measurements, precise at-line control of amino acids may enable further refined experimentation.

Chapter I.

Introduction

Biotherapeutics refers to therapeutic materials produced using a suitable biological host, including recombinant DNA technology. They are the fastest-growing class of therapeutics, with 53 approved drugs in 2020 [1]. In 2020, biotherapeutics had a global market of over US\$ 325 billion, and it is expected to increase to US\$ 496.71 billion in 2026, with a compound annual growth rate of 7.32% over the period 2021-2026[2]. Monoclonal antibodies (mAbs) account for a dominating fraction of these biopharmaceutical approvals and comprise about 65% of the total sales[3]. Current top-selling therapeutics on the market produced from CHO cells include Humira (adalimumab; anti-TNF, Sandoz), Enbrel (Etanercept, Sandoz, Pfizer), Rituxan (Rituximab, Sandoz, Celltrion, Genentech), Herceptin (Trastuzumab, Merck, Celltrion, Genentech), Benefix (recombinant Coagulation factor IX, Genetics Institute), Avone (Interferon β -1a, Biogen), and TNKase (Tenecteplase, Genentech), ReFacto (recombinant Antihemophilic factor, Genetics Institute) [3].

Unlike the simpler chemically synthesized molecules, biopharmaceuticals are complex molecules requiring complex modifications like protein folding and post translations to be functional and efficient. Chinese hamster ovary (CHO) cell-based system remains the most preferred mammalian cell line in use for the production of mAbs. In 2017, 84% (57 of the 68 mAbs) were produced in CHO, with the remaining mAbs being produced in either NS0 or Sp2/0 cells (murine myeloma-based cell line) [3]. There are multiple advantages to choosing CHO cells over the other available expression systems. CHO cells can appropriately process the correct post-translational modification. They can also be adapted to grow in suspension and make large-scale production possible, increasing production capacity. CHO cells cannot host human viral pathogens and hence offer a lower chance of transmittances and are therefore considered safer for the production of biopharmaceuticals. CHO cells are also preferred because of the accepted safety guidelines and the long history of being used

as the host for the production of recombinant proteins. Because of the long history of the production of biomolecules, it can prove easier to get regulatory approvals.

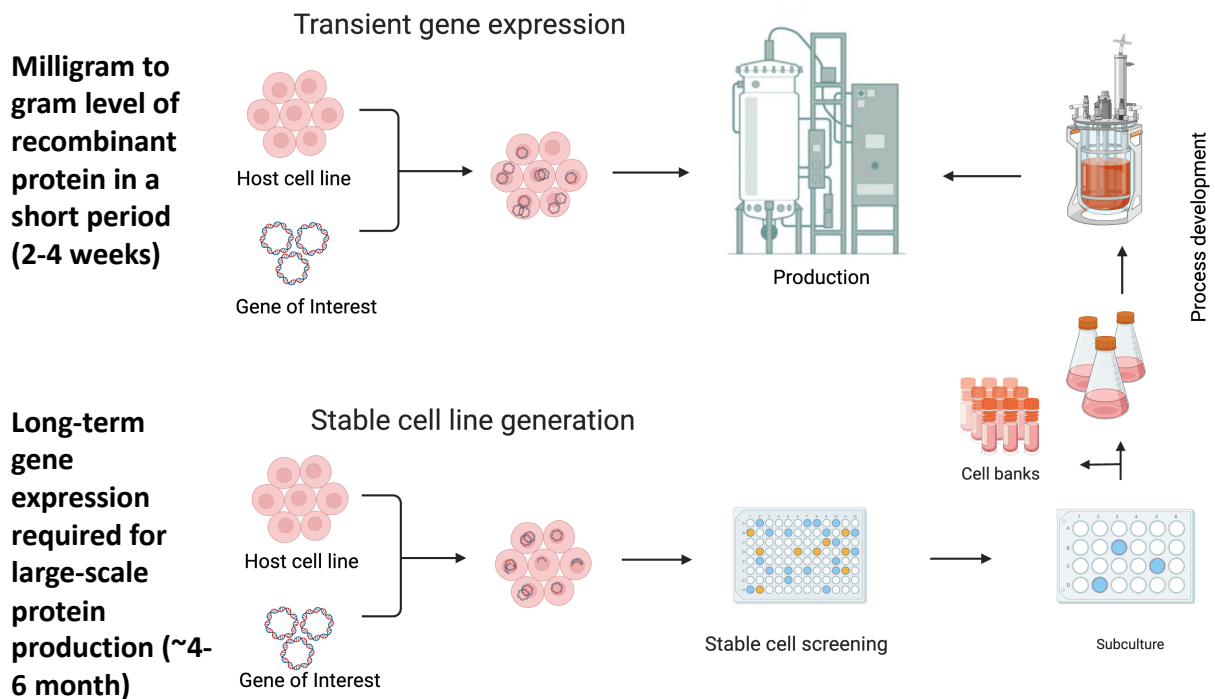


Figure1.1: Typical route for the production of any recombinant biotherapeutic

Created with BioRender.com

The typical production of a recombinant biotherapeutic begins by generating a stable, robust production cell line (Figure1.1). The first step to obtaining a robust production cell line is the insertion of the gene of interest in the appropriate host cell line with a suitable selection and amplification system. Robust selection systems help select clones with the maximum number of copies of the gene of interest integrated into the host genome. Because the high producers are crowded among low producers, extensive screening steps involving multiple evaluation stages ensure the highest, most robust producer cell strain selection. After insertion of the gene of interest, selection of clones with the integrated gene of interest and amplification of the gene of interest using various selection and amplification systems like DHFR and GS system is performed (Figure1.2). Screening is usually performed in small-scale culture platforms like shake flasks and spin tubes. High-throughput devices such as CClonePix and FACS are also increasingly being utilized for screening. At this stage,

the primary criteria for clone selection include high protein expression levels with the desired PTM and genetic stability. This makes screening one of the most resource and labour-intensive steps in cell line development. Depending on the timelines and the stage of drug development and the amount of recombinant biotherapeutic required, either stable cell line generation (SGE) or transient gene expression (TGE) can be chosen. A transient gene expression route can also be taken to produce milligram to gram quantities of the product of interest in preclinical trials and product characterization. TGE differs from SGE by not involving the permanent integration of the gene of interest in the genome. Hence, large-scale TGE is utilized to produce the recombinant product of interest rapidly.

Further development strategies for enhancing cell performance, productivity, and product quality, are based on the medium, feed composition optimization, and process parameters, such as pH, aeration, agitation, and temperature. Various parameters like viable cell density, cell viability, metabolism, titre, and product quality, are used as indicators for process development. Different medium designs, feed, and feeding strategies are also tested to improve productivity and product quality while limiting waste metabolite production during process development. The best cell clone with good productivity, product quality, growth, and metabolic characteristics are stored in a master cell bank and further in working cell banks to be used for production.

Irrefutably, the medium formulation and feeding strategy used for culturing these cells to produce recombinant biotherapeutic products is vital because environmental changes and nutrient availability affect cell culture characteristics. The cell culture medium acts as a source of nutrients for cell proliferation and protein production. A cell culture medium is an osmotically balanced mixture of a carbon source, amino acids, vitamins, trace elements, antioxidants, and other vital nutrients. It plays an essential role in process development as it directly affects product titre and quality. The growth of cells can be divided into three phases. Initially, growth occurs exponentially where a growth rate is accompanied by nutrient (high glucose and amino acid (AA)) consumption. Higher nutrient consumption results in escalated waste metabolite generation. After reaching a peak VCD (viable cell density), cell growth stagnates while mAb production increases. In that phase, glucose and amino

acid consumption are reduced, lactate starts getting consumed, and ammonia accumulation slows down. During the cell death phase, cell viability starts to drop.

The batch, fed-batch, and continuous or perfusion modes of cultivation can be used to produce recombinant protein-based biotherapeutics. Culturing cells in batch mode can lead to nutrient limitation, negatively affecting productivity. To overcome the nutrient limitation, currently, production is preferentially carried out in fed-batch mode, which utilizes concentrated bolus feeds to replenish the exhausted nutrients in the basal medium. Bolus feeding during process development may also lock in production processes to have intermittent feeding strategies. The value of such feeding strategies is to achieve a multifold increase in cell growth and culture longevity [2,5,7,8]. Various traditional approaches, one factor at a time approach (OFAT), medium blending along with statistical techniques like Design of experiment (DoE), Quality by Design (QbD), full factorial design, response surface methodology (RSM) are also being used to optimize media and feed formulations [4,5]. Some feeding strategies are based on nutrient consumption and by-product accumulation. While the most conventional approach to developing a feed is to concentrate the basal medium, sophisticated medium optimization strategies must balance promoting growth and improving volumetric productivity. It has been shown that high-producing clones selected at small-scale culture may not necessarily be high producers at the production scale. Such differences can be attributed to differences in medium and feeding profiles during the screening and the production stage [6,7].

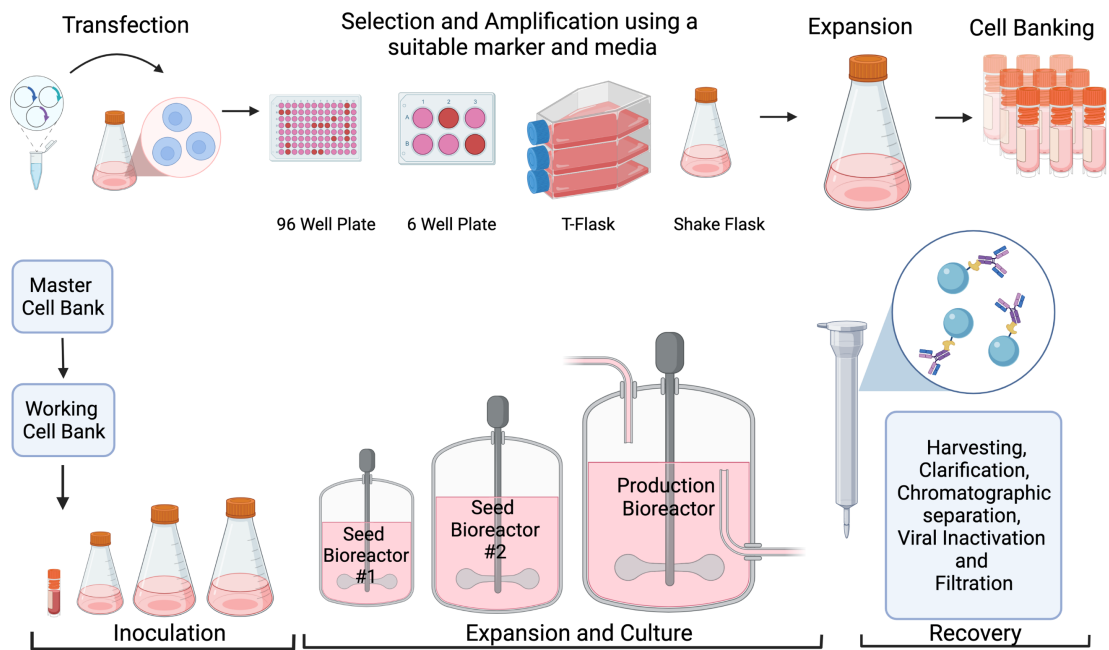


Figure1.2: Clonal selection and scale-up for recombinant biotherapeutic production

Created with BioRender.com

The use of powerful -omics approaches like proteomics, lipidomics, transcriptomics and metabolomics has helped fabricate specialized media designs. This has recently led to identifying certain amino acids such as phenylalanine, tyrosine, tryptophan, methionine, leucine, serine, threonine, and glycine, that produce novel toxic by-products; therefore, they should be added at lower non-limiting concentrations [8]. In rCHO cells, transcriptome analysis using RNA-seq has been used to compare mRNA profiles between high producers and low producers to decipher suitable target genes that may contribute to higher q_p [9,10]. It has been shown that nutritionally rich cell culture medium formulations in routine use can lead to metabolic artefacts. The in vivo metabolic environment may be better reproduced by a nutritionally leaner medium mimicking human plasma [11,12]. Toxic metabolite accumulation and nutrient depletion activate autophagy or apoptosis. Hence, adding autophagy inhibitors [7,8] or apoptosis inhibitors [15–17] can improve cell longevity. However, these inhibitors are unfavourable from a cost and regulatory standpoint. Thus, maintaining amino acids at low concentrations presents unexplored opportunities to devise strategies for controlling waste metabolite generations for robust manufacturing of biotherapeutics.

The mode in which CHO cells are grown significantly impacts their growth and productivity. Fed-batch culture is labour-intensive and, if performed manually, makes the culture more error and contamination prone. Automation in the form of robotic liquid handling systems is a considerable capital investment. Concentrated bolus feeding may also lead to underfeeding or overfeeding nutrients depending on the medium design. Fed-batch cultures also have complications related to the preparation of concentrated feed and pH adjustment, which lead to a significant step-change in pH and nutrient levels when added to the culture [18,19]. Such substantial step changes can interfere with the internal metabolic homeostasis. Cell metabolism can critically affect productivity and product quality. In perfusion culture, the medium is continuously circulated through culture while retaining the cells to maintain higher cell densities, allowing simultaneous waste removal and nutrient replenishment [18,19]. Owing to operational complexity, perfusion culture is still being developed for recombinant protein manufacturing [20]. Continuous bioprocessing is also evolving as a novel strategy for recombinant protein production with the aim to facilitate production and process development while limiting resource footprint. Process development also includes scale-up to ensure attaining robust process performance at a large scale. Various high throughput devices have also been developed for rapid process development; these include microtiter plates and micro bioreactors [23] Microbioreactors like Ambr, which is a 10-15 mL bioreactor with automated feeding and sampling, and BioLector, which is a 0.8 to 2.4 mL well plate with pH and oxygen sensors are popular high throughput system used in cell line and bioprocess development. But such robotic systems are capital and operationally intensive, rendering them unsuitable in many academic and industrial settings.

Bioreactor type and process control are other factors to consider that can impact successful process optimization and process development. The bioreactors used for biotherapeutic production include stirred tank bioreactors and airlift reactors. Process parameters like aeration and shear stress have also been critical process parameters, for example, as demonstrated in the large scale production of oncolytic measles virus using Vero cells [24]. Mammalian cells, when cultured in a large-scale reactor or under various stages of bioprocessing, are subjected to diverse ranges of shear, from agitation due to the impellers to the bursting of bubbles. Such diverse shear stress can impact bioprocessing, as seen by its effect on culture viability, metabolism, and

recombinant protein production. More importantly, as shown by various reports on endothelial cells, shear can impact membrane properties which can have an impact on processes like TGE.

For a complete understanding of recombinant protein production, it is also important to recognize the downstream process. The downstream manufacturing process usually includes the following steps. The typical steps include cell harvesting (using centrifugation and depth filtration), and proteins are further purified using microfiltration and Protein A chromatography. If the protein is expressed as an inclusion body, cell disruption methods are employed along with solubilization and refolding. Viral inactivation is also employed. This is followed by chromatographic purifications like affinity and ion-exchange chromatography and diafiltration and formulation to give an active recombinant protein.

1.1 Thesis organization

In chapter 2, literature on serum-free medium, its components, and their metabolic functions, along with a review of literature related to their transport and regulation. In chapter 3, common methods used across chapters 4, 5, 6, 7, and 8 are described. Any other method specific to a chapter is described in the respective chapter. Shear stress routinely observed due to various hydrodynamic forces that can impact processes like TGE; in chapter 2, we understand the implications of shear for large-scale TGE and gene therapies. A novel hydrogel-based method nutrient delivery system, NutriGel, is described in chapter 4, the kinetics of simultaneous release of 18 amino acids through various NutriGel formulations is described in chapter 4, and the effect of supplementation of various NutriGels to CHO cell culture is described in chapter 5. We demonstrate the application of this hydrogel for complete in situ feeding to a suspension-adapted CHO cell line expressing IgG. In situ supply of a feed mixture with a composition identical to the culture medium with the exception of glucose and bulk salts (with bolus feeding of glucose as required) led to a significant improvement in integral viable cell density and volumetric productivity while creating a completely closed system for shake flasks. In chapter 6, results from the RNA-Seq study to characterize transcriptomics changes when cells are cultured in a lean amino acid-based environment are described. In chapter 7, using the transcriptomics dynamic, we

explore the utility of low amino acid-based condition and feeding strategy and evaluate its effect on culture performance. In chapter 8, conclusions and future outlook are presented.

Chapter II.

Background

Effective growth and productivity are affected by the mode of cultivation and require media that can support growth and sustain productivity. Medium composition, its design, and choice of feeding strategy are critical factors in the biotherapeutic space. The understanding and evaluation of which culture medium and components define its possible usefulness in process development, although this evaluation is still an empirical search. This current understanding of medium composition, its evolution and how cells utilize nutrients, along with the responses of mammalian cells to nutrient limitation, is briefly introduced in this chapter.

Cell culture medium selected to culture cells *in vitro* has undeniably a critical impact on the cells either used for the production of biotherapeutics or physiological studies. Different types of cell culture media have evolved with diverse purposes, like keeping cells and tissue alive for a short period for transporting clinical samples, studying the physiology of tissues and organs *ex vivo*, for large-scale production of viral vaccines, therapeutics, and recently cultivating embryos *in vitro* for assisted reproductive technology.

Ringer first realized the milestone work of keeping cells alive outside the body in 1882. Ringer developed bicarbonate based buffered saline to successfully keep a frog's heart beating post dissection for a relatively extended period, variants of which are still in use [25,26]. This basal salt solution was the ancestor of modern cell culture media. In order to mimic the *in vivo* conditions and keep cells alive for a longer period, medium development began with the addition of tissue components like blood clots, plasma, embryo extracts etc. [27,28]. This led to the foundational studies by Harrison, where he successfully grew frog nerve fibre tissue alive for weeks outside the body by supplementing it with frog lymph [29].

Various attempts to make synthetic media succeeded only with adding an undefined component like serum or plasma from various sources. With the addition

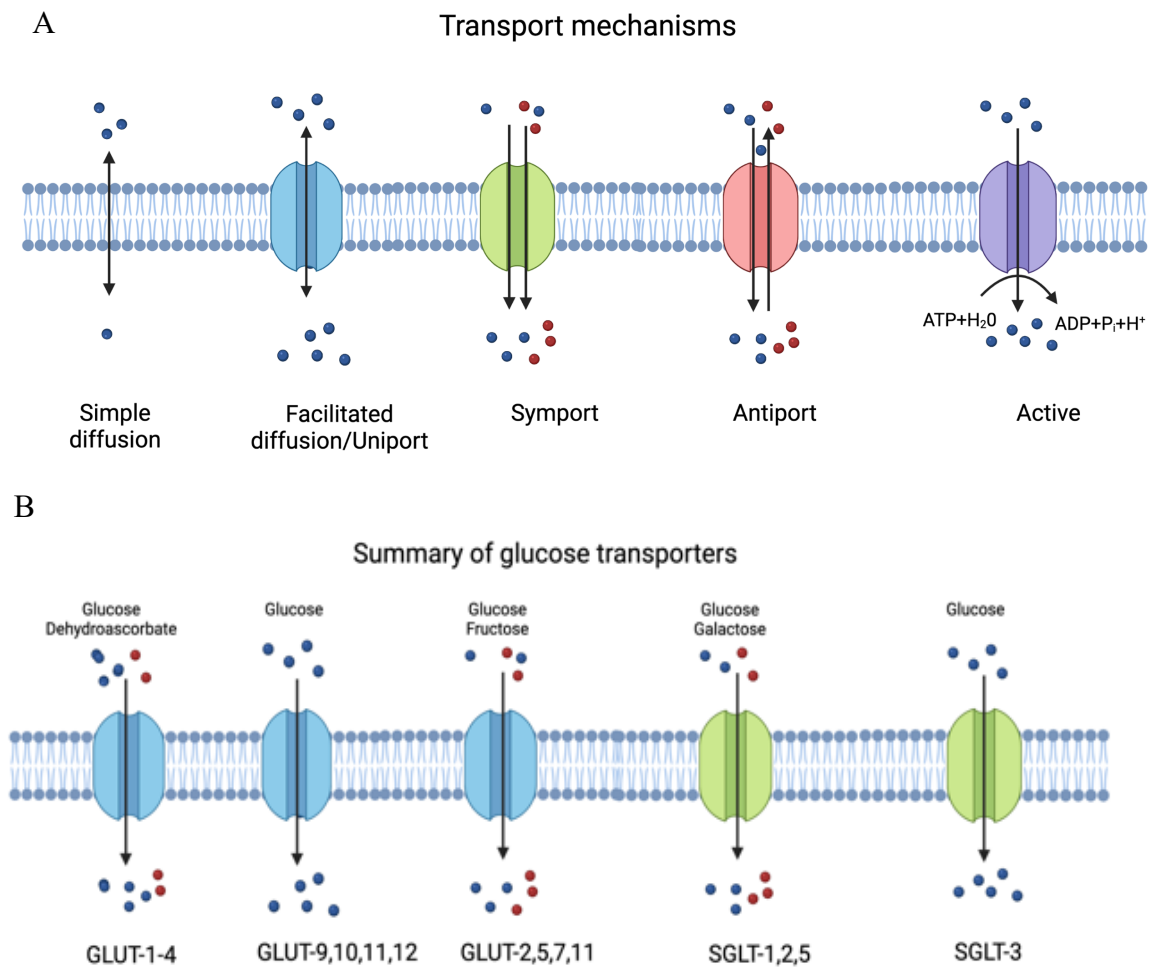
of serum in media, a lot of cells could be cultured and expanded. Different methods of purifying and fractioning serum were developed for use in cell culture[30]. With the development of continuous cell lines like HeLa and the advent of hybridoma technology, a necessity arose to industrially produce biotherapeutics where serum had to be removed, reduced or replaced.

2.1 Replacement of serum

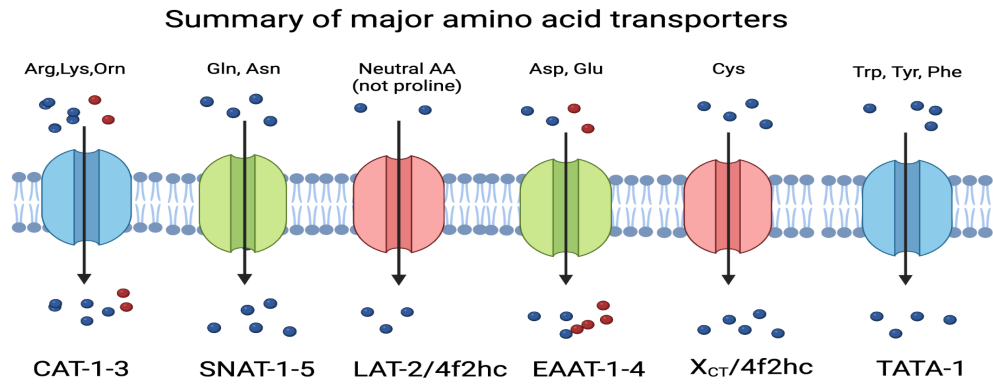
The serum is an excellent nutritional supplement containing vitamins, amino acids, hormones, trace elements, and antioxidants having diverse functions. The addition of serum in cell culture media has many advantages. It is a paradox that though some cells cannot proliferate without serum supplementation, cells can also not grow in 100% serum [31]. Various studies conducted to scrutinize the quality of commercially available serum revealed a lot of batch to batch variation [32,33]. The main complication of using serum has been its ambiguous composition and difficulty in downstream purification due to its high protein load [34]. Societal and ethical concerns regarding the killing of fetuses and safety concerns relating to the transmission of contaminants like mycoplasma and bovine viruses have also discouraged the use of serum or any animal-based component [35]. Finally, economic concerns due to the high cost of serum have paved the way for replacing serum in cell culture medium [36]. Extensive work was done with the foresight of replacing serum completely, either for studying the functions of various biomolecules or cells or for large scale production of biotherapeutics. The albumin is a 69 kDa acidic water-soluble protein found in animal sera. Albumin is the major component of serum present at around 50 mg/mL, where it makes up about 60% of the total serum protein [37,38]. The primary function of albumin in vivo and in vitro is being a sacrificial antioxidant and transporter of many molecules like fatty acids, trace elements, vitamins, and hormones. The trace metals like Cu^+ and Fe^+ routinely present in cell culture media can react with other media components like ascorbic acid can cause reactive oxygen species (ROS) generation in cell culture media. Albumin has a dedicated high-affinity binding site for Cu^+ and Ni^+ that prevents their participation in ROS production. There are 35 cysteine residues in albumin that form

disulfide bridges, leaving, Cys-34 as a free reduced thiol that helps albumin exert its antioxidant function. Albumin is also widely recognized for preventing lipid peroxidation [37]. Albumin supplementation is serum sparing and effective in enhancing cell growth. Supplementation with recombinant albumins has been successfully employed to eliminate an animal-derived component like albumin in cell culture media^{18,19}. Further albumins derived from animals are also being replaced by recombinant human albumin (rAlb) produce using yeasts to further improve safety issues, especially with cell therapies and stem cell applications [38,41].

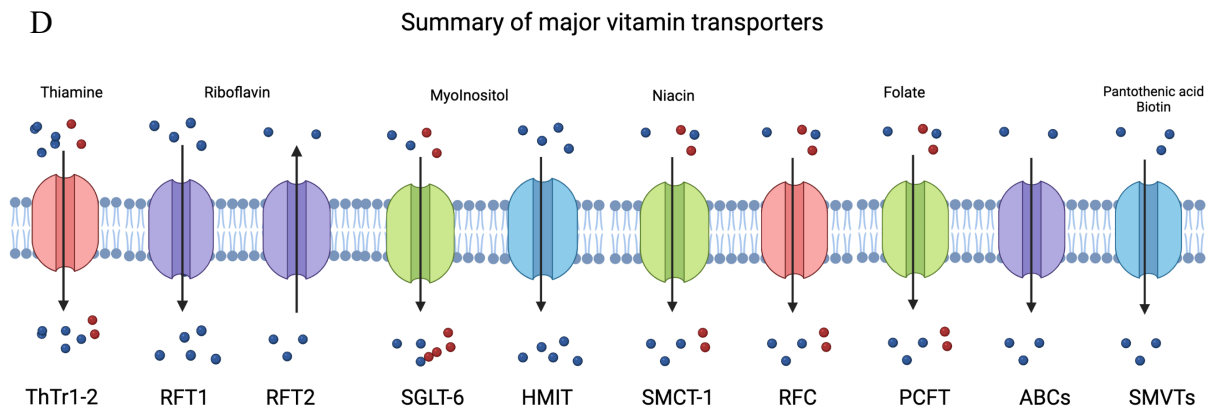
2.2 Components of serum-free media



C

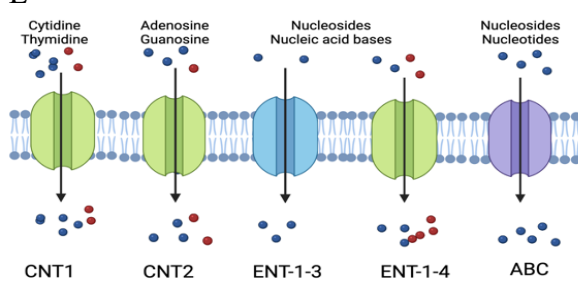


D



E

Summary of major nucleotide transporters



F

Summary of major fatty acid transporters

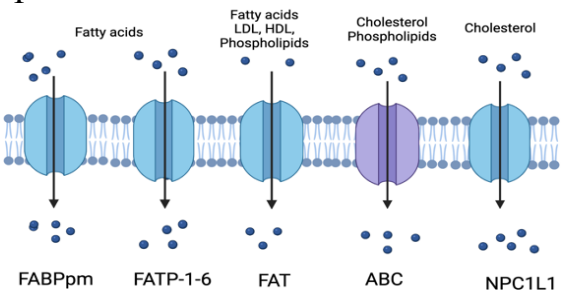


Figure 2.1: Overview of transport mechanisms for various media components

(A) The basic modes for metabolite transport based on the energy association (categorized into active and passive modes) are shown (B–F) Major transport proteins involved in the transport of various substrates belonging to the major nutrient classes in the media like carbohydrate, amino acid, lipid, nucleoside, vitamins. Created with BioRender.com

2.2.1 Carbohydrate source

Glucose is the most frequently used carbohydrate source in cell culture media. It is generally present at high concentrations (5 to 55 mM) in cell culture media. But CHO cells can maintain viability at low glucose concentration (3 mM) [42]. In many

traditional media[43], the concentration is similar to blood plasma concentrations (5.5 mM), whereas proprietary media have higher glucose concentrations to sustain higher cell densities²¹. Other alternate sugar sources that have been used to substitute glucose with varying degrees of success are D-galactose, D-mannose, D-ribose, trehalose, turanose, D-maltose, D-fructose, including glucose-6-phosphate and glucose-1-phosphate [45]. The in vivo functions of glucose are the generation of energy in the form of ATP, NADH, NADPH, synthesis of nucleotides, fatty acids and amino acids. It is metabolized principally by glycolysis to form pyruvate, which may be converted to lactate or is oxidized to form CO₂ via the tricarboxylic acid cycle (TCA). However, glucose can also be converted to lactate without entering the TCA cycle. This leads to the accumulation of lactic acid in the medium, which has harmful effects on cell growth and productivity [46]. In mammalian cell lines, only a fraction of glucose is completely oxidized (less than 5%), about 8% of utilized glucose is metabolized via the pentose phosphate pathway (PPP), and almost 90% is converted to lactate. 20-30% of the utilized glucose is utilized for cellular pathways other than glycolysis, the TCA cycle, or the PPP. An important aspect to note is that glucose and glutamine metabolisms are interlinked and interactive with the availability of each other [47]. At low glucose concentration, the primary function of glucose is to provide ribosyl units for nucleotide synthesis [47]. Galactose is an important alternative carbohydrate source that, like glucose, is also converted to pyruvate via glycolysis. In media containing both glucose and galactose, CHO cells prefer to use glucose first, followed by galactose consumption. This metabolic shift leads to lower lactate production and higher lactate consumption [48]. However, a complete replacement of glucose with galactose is not ideal as it leads to reduced growth and viability [49]. Glucose is transported into the cells by facilitative diffusion by two families of transporters- the GLUT and SGLT(1-6). SGLT-2 from the SGLT family has a low affinity but high capacity for glucose and galactose transport (Figure 2.1) [50]. Substituting the carbon source has had many advantages, mainly lowering lactate accumulation in the medium [49,51]. Glutamine is also a major energy source in CHO cell culture and is metabolized via glutaminolysis entering the TCA cycle via α -ketoglutarate, and is discussed in detail in the next section.

2.2.2 Amino acids

Amino acids essential for cells in vitro were first identified based on the systematic study by Eagle [52–54]. He established all 13 essential amino acids are necessary for culturing mammalian cells in-vitro (Arginine, Cysteine, Glutamine, Histidine, Isoleucine, Leucine, Lysine, Methionine, Phenylalanine, Threonine, Tryptophan, Tyrosine, and Valine) and are present in high concentrations (0.5–4 mM). However, later the seven non-essential amino acids were also supplemented to lower the metabolic burden [55]. Non-essential amino acids, particularly serine, have been used to demonstrate enhanced cloning efficiency for some primary and continuous cell lines [56]. As amino acids are the building blocks of recombinant proteins, they have been identified as nutritional supplements for increasing productivity [57,58]. Duval et al. showed that supplementing hybridoma cell lines with four rapidly consumed amino acids led to an increase in productivity by increasing the VCD and culture longevity [58]. Altamirano et al. have shown that systematic medium supplementation with proline, serine, and asparagine, along with lipid and vitamins, led to an 80% higher t-PA production in CHO TF70R cells [49]. Sophisticated studies designed to understand the specific amino acid requirement for increasing productivity have used statistical tools like Plackett-Burman (PB) multifactorial design [4]. Amino acids cannot simply diffuse into the cells are transported inside the cell with the assistance of 10 SLC families and 17 distinct transport systems, classically classified into transport systems ASC (neutral amino acid transporters from the SLC1 family, Figure1) and systems A and L (SLC38 members, Figure 2.1-2.3) based on substrate specificities [59]. Some of these transport systems are ubiquitous (e.g., systems A, ASC, L, y^+ and X^-_{AG}), and some have tissue-specific transport systems (e.g., systems $B^{o,+}$, N^m , and $b^{o,+}$)[60]. With the advent of "omics technology", these systems were refined and renamed based on their SLC gene, and further intricate regulation mechanisms were confirmed.

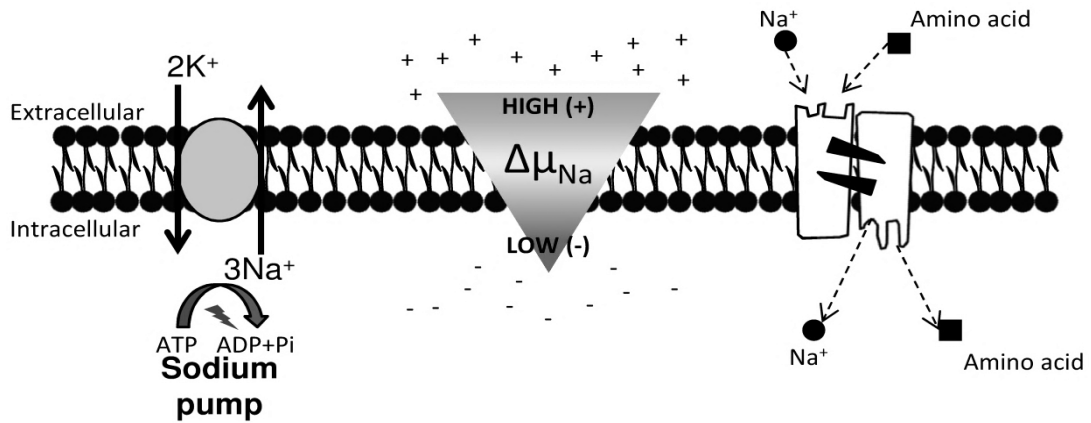


Figure 2.2: Representation depicting the mechanism of system ASC for amino acid transport

System ASC is a stereoselective, sodium-dependent antiporter that is powered by a sodium gradient and is involved in the uptake of amino acids with linear side chains like alanine and glutamine but also has a preference for some polar amino acids, such as cysteine, serine and threonine. Reproduced from [61]. System ASC is the SLC1A4/5 family of the transporter.

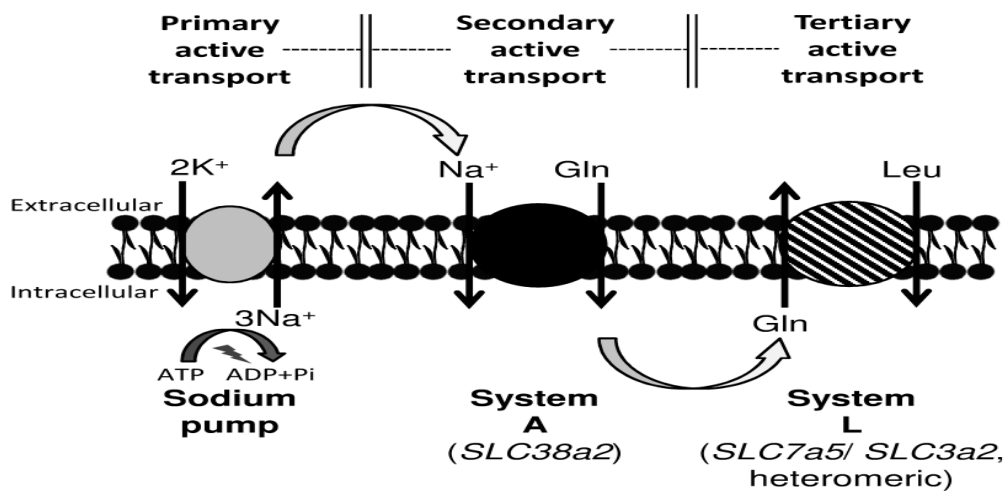


Figure 2.3: Representation depicting the mechanism of systems A and L for amino acid transport

System A is a sodium-ion dependent secondary active transport system responsible for importing unbranched amino acids and imino acids (proline). System L is a tertiary active transport system that imports amino acids against their concentration gradient (e.g. leucine) by expelling amino acids accumulated by other systems (e.g. glutamine). Reproduced from [61]

2.2.3 Glutamine

Eagle identified the 10-100-fold higher glutamine requirement by cells in vitro. He further investigated how nutrients could reduce this higher demand for glutamine. Arginine, ornithine, α -ketoglutaric acid, and proline could not substitute for glutamine [62]. Glutamate only at a higher concentration of 20 mM in the presence of ATP and NH_4 could substitute for glutamine in HeLa cells. With radiolabelling experiments, the carbon chain of glutamine was confirmed to give rise to aspartic acid and proline, probably via glutamic acid [63]. Glutamine is the main respiratory fuel and can be catabolized using the following three pathways. The first one is by the complete oxidation to CO_2 through the TCA cycle. The second and the third are the partial oxidation to lactate or aspartate by aspartate or alanine (via aminotransferases). In HeLa cells, 70% of ATP is produced from glutamine metabolism, even in the presence of glucose. HeLa cells, when grown in the absence of glucose and the presence of alternate carbon sources like fructose, obtain 98% of their energy requirement from glutamine metabolism. The carbon from fructose is exclusively directed to the pentose-phosphate pathway for nucleotide synthesis [47,64]. On the other hand, glutamine supplies only up to 40% of the energy requirements of fibroblast cells [65] and of CHO cells [66]. Glutamine is an essential nutrient in CHO cell culture, and its absence delays the start of the exponential growth phase [67]. Glutamine supplementation has been previously reported to improve cell viability, reduce lactate accumulation and increase productivity, even in the case of CHO-GS cells which produces glutamine via transfected glutamine synthetase [68,69]. During glutaminolysis, however, glutamine is converted to glutamate, leading to ammonium accumulation in the medium [70]. High ammonium concentration are known to have a detrimental effect on the cell culture by reducing cell growth rate, increasing the glycoform heterogeneity, and affecting the consumption rate of other amino acids [71,72]. Glutamine is hydrophilic and water-soluble, and hence the import of glutamine into cells is mediated by specific SLC families of transporters. There are fourteen transporters that accept glutamine as a substrate. Transporters are not specific for a particular amino acid, and multiple transporter families are involved in the uptake of particular amino acid. These transporters are not specific for glutamine, and not all of these transporters function in the influx of glutamine under normal physiologic conditions. These fourteen transporters belong to four SLC families: SLC1, SLC6, SLC7, and SLC38 (one

transporter in SLC1, two transporters in SLC6, five transporters in SLC7, and six transporters in SLC38) (Figure 2.1) [73,74]. The members of the SLC38 gene family are generally regarded as the major glutamine transporters in mammalian cells.

Table 1. Plasma membrane transporters for glutamine.

Gene name	Protein name	Amino acid substrates	The direction of glutamine flux
SLC1A5	ASCT2	Neutral	Influx/Efflux
SLC6A14	ATB ^{0,+}	Neutral & Cationic	Influx
SLC6A19	B ⁰ AT1	Neutral	Influx
SLC7A5	LAT1	Neutral	Influx/Efflux
SLC7A6	y ⁺ LAT2	Neutral & Cationic	Influx
SLC7A7	y ⁺ LAT1	Neutral & Cationic	Influx
SLC7A8	LAT2	Neutral	Efflux
SLC7A9	b ^{0,+} AT	Neutral & Cationic	Efflux
SLC38A1	SNAT1	Neutral	Influx
SLC38A2	SNAT2	Neutral	Influx
SLC38A3	SNAT3	Neutral	Influx/Efflux
SLC38A5	SNAT5	Neutral	Influx/Efflux
SLC38A7	SNAT7	Neutral, Cationic & Anionic	Influx
SLC38A8	SNAT8	Neutral, Cationic & Anionic	Influx

2.2.4 Protein Hydrolysates

Hydrolysates are protein digests constituting amino acids, peptides, carbohydrates, vitamins, growth factors and minerals obtained by hydrolysis of proteins by various enzymes, acids, and alkali that provide nutrient supplements to the media [75]. They are sourced from animal tissues (Primatone RL, tryptose broth, etc.), plants (soy, wheat etc.), milk (lactalbumin, casein, etc.) or yeasts. Plant-based hydrolysates from soy, wheat and yeast are also commonly used to support cell growth in serum-free cell culture media. Protein hydrolysates are used to deliver amino acids and small peptides. There are contradictory reports on the effect of a protein hydrolysate; some studies report a beneficial effect [76–79], while other studies demonstrated no effect or detrimental effect on cell density and product quality at higher concentrations [80]. Protein hydrolysates are chemically not defined and may cause problems in reproducibility because of their compositional complexity and lot-to-lot variations. A few possible explanations for the beneficial effect of protein hydrolysates are that

they provide free amino acids and low molecular weight nutrients. Large oligopeptides can also be growth factors for cells or mimic in part sequences of growth-promoting factors [76,81]. These speculations have led to the development of synthetic peptides that show a positive effect on cell density and productivity [82,83]. Hydrolysates provide a large number of oligopeptides as a source of amino acids for CHO cells. However, proteins and long peptides have to be digested into shorter di- or tripeptides before being available for CHO cells to be utilized. Such peptides are transported by peptide transporters that have been grouped in the Proton-coupled Oligopeptide Transporter (POT) superfamily, also known as the Peptide Transporter family. Two peptide transporters, designated peptide transporter 1 (PEPT1, SLC15A1) and peptide transporter 2 (PEPT2, SLC15A2), several new POT members, including Peptide/Histidine Transporter 1 (PHT1) and Peptide/Histidine Transporter 2 (PHT2) and their splice variants have also been identified that are involved in peptide transport (Figure 2.1) [84,85].

2.2.5 Vitamins

Vitamins functions as enzyme co-factors in a wide variety of metabolic reactions; for example, Riboflavin, niacin, and vitamin C are essential in maintaining the redox balance; thiamine and biotin are involved in macronutrient metabolism; and folate, vitamin B12 or cobalamin (Cbl), pyridoxine, and riboflavin play important roles in nucleotide synthesis. Initially, 7 vitamins were established as essential by Eagle for cell growth and proliferation: choline, folic acid, nicotinamide, pantothenate, pyridoxal, riboflavin, and thiamine and cytopathic effects of vitamin deficiency were reversible[86]. As Eagle used dialyzed serum-supplemented basal media, it was later realized that many vitamins could be supplied by serum. Biotin and Inositol were found to be essential under specific conditions. Hence all B-vitamins are necessary for cell culture in-vitro and are included in DMEM as well as in Ham-F-12 [55]. However, the vitamin requirement has been found to be strain-specific and dependent on the complex interactions with other nutrients in the medium. For example, biotin routinely present in serum-free media NCTC 109 was found essential only when the number of other vitamins is reduced to 7 instead of 18, and nucleic acid derivatives from 5 to 2 along with the absence of sodium glucuronate. When cells were cultured in a medium devoid of all nucleic acid derivatives except

deoxycytidine, an essential requirement for folic acid was demonstrated [87,88]. Myo-Inositol was an essential growth factor for the survival and multiplication of a wide variety of normal and malignant human cells [89]. The folic acid requirement of cells is also found to be dependent on the origin of cells, with primary cell lines showing a higher requirement [90]. Vitamins are susceptible to heat, strong light, and long-term air exposure. Among the vitamins present in CHO cell culture media, ascorbic acid and tocopherols are vulnerable to oxidation; thiamine, riboflavin, cobalamin, and ascorbic acid are sensitive to light; and thiamine and pantothenic acid are thermolabile [91]. As a result, protection from light and heat is important during the storage of culture media affecting the shelf life and reproducibility.

With the exception of folinic acid, coenzymes are generally able to replace their constituent vitamins [92]. The water-soluble vitamins also have specific membrane transporter families responsible for their transport across the plasma membrane. The absorption of Cbl is complex, requiring multiple processes involving four different binding proteins. Interestingly, vitamins like folate, biotin, and riboflavin can be transported across colonic epithelial cells in the human body. Four SLC families are involved in vitamin or co-factor transport. SLC19 participates in folate and thiamine transport, whereas SLC46 is responsible for folic acid transport (Figure 2.1) [93]. The molecular identity of thiamin uptake systems thiamine transporter (THTR)-1 (SLC19A2) and THTR-2 (SLC19A3) has been recently elucidated [2]. Thiamin-mono- and di-phosphates, Monoglutamyl folates, including folic acid, are transported by Riboflavin transporters-1, -2 and/or -3 (RFT-1, -2, SLC19A1 SLC52A1/3 respectively), whereas 5 Methyltetrahydrofolate is transported by folate receptors FOLR1,2,3 and PCFT. Sodium-dependent multivitamin transporter (SMVT) transports the vitamins pantothenic acid, biotin and lipoate. SVCT family of transporters (SLC23A1 and 2) is responsible for ascorbic acid transport, whereas dehydroascorbic acid transport is facilitated by GLUT1 and GLUT3 (Figure 2.1). Cobalmine is also transported by GIF, CUBN, and AMA. Riboflavin is transported by RFT3 (SLC52A2). SGLT-6 (SLC5A11) and SMIT (SLC5A3) are myo-inositol transporters (Figure 2.1) [86].

2.2.5.1 Vitamin C

Ascorbic acid is a routinely used water-soluble vitamin in a cell culture medium. It is highly unstable. It acts as an antioxidant that protects unsaturated fatty acids from peroxidation by converting lipid peroxy and alkoxy radicals to stable lipid hydroperoxides and hydroxides, respectively. Alpha-tocopherol donates hydrogen to lipid peroxy radicals and gets reduced. Ascorbic acid also regenerates the oxidized lipid peroxy radicals and indirectly limits lipid peroxidation in cell membranes [94][95]. Ascorbic acid facilitates the import of copper from ceruloplasmin in the serum into cells. It is involved in the catabolism of amino acids (phenylalanine and tyrosine) to acetyl-CoA and the synthesis of collagen. It was found to be a potent antioxidant in L929 fibroblast that could mitigate glutathione toxicity. However, these cells were also shown to grow in the absence of any reducing agent, including vitamin C [87]. SLC23 is involved in ascorbic acid transport (Figure 2.1) [93].

2.2.6 Lipoic acid

Lipoic acid (LA) is a media component that functions primarily as an antioxidant [96,97]. LA was first introduced into the cell culture medium by Ham in Ham's Nutrient Mixtures for the clonal growth of CHO cells, where its utility is uncertain. Lipoic acid can be synthesized by eukaryotic cells [98]. As lipoamide, it functions as a co-factor in the pyruvate decarboxylase multienzyme complex [96]. As LA and its reduced form, dihydrolipoic acid (DHLA) is closely involved in amino acid metabolism (glycine, leucine, isoleucine and valine), as well as in defence against oxidative stress and apoptosis. LA and DHLA regenerate endogenous antioxidants, remove transition metals from redox reactions by chelation and scavenge reactive oxygen species [98]. The availability of cysteine is a rate-limiting step in the synthesis of glutathione which is an important intracellular antioxidant. LA stimulates glutathione synthesis by improving cystine utilization by reducing cystine to cysteine, which can be taken up by cells [99]. Lipoic acid has been established to be transported by SMVT and also by MCT (Figure 2.1) [100,101].

2.2.7 Hormones

Supplementation of hormones began with the hypothesis that the primary function of serum is delivering hormones to cells. Hormone supplemented serum-free cultures could be used to grow a variety of cell lines, both primary cell lines and continuous cell lines like HeLa-S. Hormone supplemented media could be used to select specific cell types from primary cultures or help cells express cell-specific functions [102]. The hormone requirement of cells is different for various types of cells; for example, five components- Epidermal growth factor (EGF), Fibroblast growth factor (FGF), transferrin, insulin, hydrocortisone (aldosterone)-can replace the serum requirement for HeLa cells [103]. While transferrin, Insulin, EGF and Thrombin are required for serum-free propagation of cell line Chinese hamster lung fibroblast [104].

2.2.8 Lipids

Lipids can be classified into triacylglycerol, phospholipids, and sterols. These lipids are broken down into free fatty acids, monoacylglycerols, and cholesterol, which are subsequently absorbed in vivo. The principal function of lipids is to provide structural units for the permeability barrier of membranes (The main forms of lipids present in cell membranes are phospholipids and cholesterol). It is also used as a stored metabolic fuel (triglyceride) for the synthesis of hormones (Cholesterol acts as a precursor for steroid hormones and bile acids) and, to a lesser extent, as signalling molecules (Lipids also act as precursors for second messengers).

Most cells in vitro are known to employ fatty acids in the medium. Human skin fibroblasts (GM-10 cells) proved that cells could use fatty acids to synthesize triacylglycerol when fatty acids were included in a lipid-free medium [105]. Cells have also been shown to grow in serum-free media (SFM) lacking any lipid supplementation and yet have been found to sustain indefinite cell growth and complete function. It appears that fatty acids essential in vivo are not critical for cell proliferation in vitro [106,107]. Some cultured cells can be auxotrophs for particular lipids, the most famous being NS0, a myeloma cell line that requires supplementation with cholesterol [108]. Supplementing lipid has been a long-standing problem due to its low solubility and instability in the cell culture medium. This issue has been resolved with limited success with the help of carrier molecules

like albumin and cyclodextrin [108]. Supplementation of the medium with unsaturated fatty acids can improve cell yield and volumetric monoclonal antibody titre (58%), as illustrated in the case of B-lymphocyte hybridoma [109]. Lipids can diffuse across the plasma membrane due to their hydrophobic nature. But specific transporters also exist (1) fatty acid transport proteins, including FATP1-6 (SLC27A1-6), (2) the membrane-associated fatty acid transporters FABPpm (GOT2) and fatty acid translocase FAT (CD36) (3) ATP binding cassette transporters (ABC) (4) various lipoproteins (i.e., chylomicrons, low-density lipoprotein, and high-density lipoprotein) and (5) lipid transporters, such as non-specific lipid-transfer protein (SCP2), acyl CoA binding protein (DBI), fatty acid-binding proteins/ cytoplasmic fatty acid-binding proteins [i.e., FABPc (FABP1-9)] (Figure 2.1).

2.2.9 Ions

The ions demonstrably essential for survival and growth *in vitro* are Na^+ , K^+ , Ca^{2+} , Mg^{2+} , Cl^- , and H_2PO_4^- [92]. The bulk ions are primarily required for homeostasis and physiological roles, such as maintenance of membrane potentials and osmotic balance, rather than any nutritive requirement. However, some ions can act as co-factors for various enzymatic reactions [92]. The bicarbonate ion is also required for a number of biosynthetic reactions such as urea synthesis [110] and helps to buffer the medium pH, and must be supplied exogenously when the cellular population is sparse [111].

2.2.10 Trace metals

Initially, trace elements were supplied to the cells through serum and as contaminants from water used for preparing media. Selenium was the first trace element demonstrated to be essential in human fibroblast in 1976 [112]. Selenium acts as an antioxidant as part of the enzymes like glutathione and thioredoxin reductases, glutathione peroxidases, and selenoprotein P as the amino acid selenocysteine [113–115]. Trace elements like copper and iron are essential for the growth and survival of cells *in-vitro*. But trace element management in serum-free media is a double-edged sword owing to trace metal toxicity. Some trace elements can be toxic to certain cell lines; for example, manganese is toxic to GH₃ cells [116].

Iron is required by cells as heme or a non-heme component of various enzymes. As a heme component of enzymes like catalase and peroxidase, it prevents oxidative damage. It participates in cellular respiration by forming the heme-containing part of cytochrome located in the mitochondria [117]. The transfer of electrons by cytochromes for the generation of ATP involves oxidation and reduction cycling of iron. As the non-heme form, it is a part of succinate dehydrogenase. As an enzyme co-factor, iron prevents cellular oxidative damage. It is frequently added to cell culture media as a nitrate or sulfate salt to replace transferrin [104]. Copper in serum is delivered by albumin and ceruloplasmin. Copper is a part of various copper oxidases like cytochrome c oxidase, superoxide dismutase, and tyrosinase [118]. The copper oxidases; ceruloplasmin, ascorbate oxidase, and lactase are the only known oxidases capable of reducing molecular oxygen to water along with the transfer of four electrons. Zinc is found in Zn and Cu superoxide dismutase and helps protect cells from superoxide radical damage. Zinc is a part of several enzymes like alcohol dehydrogenase, glutamic acid dehydrogenase, carbonic anhydrase as a coordinating cation and several NAD-dependent dehydrogenases as zinc proteins [118];[119]. Other trace elements Cr, I, Co, Mn, and Mo, are also added to various proprietary formulations. Trace metals are transported into the cells by 6 SLC families, with SLC 31 involved in copper influx SLC31, SLC39 involved in Zn^{2+} , Fe^{2+} , Cu^{2+} and Mn^{2+} , SLC40 and 41 involved in iron and magnesium transport, respectively (Figure 2.1) [93].

2.2.11 Miscellaneous

Serum-free medium are often supplemented with Insulin, transferrin, ethanolamine and selenium (ITES), combined with mercaptoethanol (BITES) or hydrocortisone (HITES) for the cultivation of a wide range of cells. Ethanolamine was reported to be an essential growth factor for hybridomas in serum-free culture [120]. Glutathione is a water-soluble tripeptide antioxidant that can be synthesized by cells. Glutathione is the preferred substrate of a number of selenoproteins to cope with the intra- and extra-cellular oxidative stress [37]. Glutathione can regenerate ascorbate and inhibits the copper-mediated autoxidation of ascorbate. Glutathione may serve as a reservoir of cysteine for protein synthesis [121]. Nucleosides and nucleic acid bases are transported across membranes by concentrative nucleoside transporters (CNT) [122],

equilibrative nucleoside transporters (ENT) [122], and members of the ABC transporter family

Table 2: Basic functions of components in serum-free medium

Components	Functions
Carbohydrate source	Generation of energy in the form of ATP, NADH, NADPH, synthesis of nucleotides, fatty acids and amino acids
Amino acids	Protein synthesis, cell signalling, oxidative stress management, nucleotide synthesis
Glutamine	Generation of TCA metabolites, nucleotide synthesis, amino acid and vitamin synthesis
Vitamins	Required as co-factors/ precursor of co-factors. Vitamin C is required as an antioxidant
Hormones	Required for cell proliferation of a variety of cells
Protein Hydrolysates	Supply vitamins, amino acids, peptides, growth factors
Ions	Maintaining osmotic balance and membrane potential
Lipids	structural units for membranes, stored metabolic fuel, synthesis of hormones, and signalling molecules
Trace elements	Required as co-factors for enzymes. Se is required for the management of oxygen toxicity
Miscellaneous	Reductants are added to maintain the intracellular redox balance

2.3 Designing serum-free medium for biotherapeutic production

All cell lines do not have identical nutritional needs, and an important step in the optimization of mAb production is the optimization of media formulation that is tailored to meet the specific growth and productivity requirements of any given industrially production cell line. Medium development is a complex process aimed at achieving maximum cell growth and or productivity. It involves optimization of numerous interacting components to their final concentrations with the aim of achieving robust cell growth and productivity. The traditional approach to medium development described in the previous chapter was pioneered by Ham and co-workers'. It is an iterative approach, also known as one factor at a time (OFAT) strategy, where a series of titrations of individual medium component while keeping all other components at a constant concentration is performed. At the end of the first round of titrations, a working optimum is set for the selected component. Then the next round of titrations is performed for each component while keeping the first component at optimum. It is the simplest systematic approach with drawbacks like

being low throughput, time and labour intensive, and lack of an ability to optimize interacting components [123]. With factorial designs, concentrations of several components can be varied simultaneously, and thus one can identify interacting components and find the optimal combinations of components. Factorial designs have been used as medium development tools for bacterial and mammalian systems [124–126] and for mammalian cells such as CHO cells [127–131]. Petiot et al. [132], by using fractional factorial design to rapidly screen serum-free medium components for Vero cells, Deshpande et al. [133] used central composite design to optimize the concentrations of media components like glucose, glutamine, and inorganic salts for the cultivation of CHO cells. Plackett-Burman statistical design, which is used for screening a large number of medium supplements combination, has also been demonstrated to develop serum-free medium [4,134]. An innate drawback of factorial designs is the large number of experiments required to be performed, which can make the process potentially time-consuming and error-prone. Alternative approaches for medium optimization, such as metabolic flux analysis, consumption profile study [135–138], medium blending [139] and DOE, have also been demonstrated [131,140]. Medium blending is a strategy to quickly generate newer formulations as it relies on mixing existing formulations, but technically the components having beneficial or adverse impacts are not identifiable. Spent medium analysis allows rational medium development by understanding the nutrient consumption profiles along with metabolites that are accumulating.

Since the number of components is large, an automated high throughput system is preferable. For example, systems like bioLector, Ambr or micro bioreactors are becoming increasingly useful in accurately representing the production process. It is also to understand other factors to be considered during media development, like regulatory requirements and choosing appropriate models for the media development experiments (scaled-down cell culture methods and using appropriate end-points).

2.4 Effective feeding strategy for the production of biotherapeutics

During the batch mode of cultivation, generally, a nutrient-rich medium is chosen to culture cells. The cells consume nutrients from the medium that leads to growth and protein production, but this also results in nutrient depletion and accumulation of

inhibitory metabolites. The fed-batch mode is currently the most frequently used mode for operation for the production of biotherapeutics. The fed-batch mode relies on optimizing a feed and a feeding regimen in order to maximize both cell culture performance and productivity. The type of mode and the timing of feeding, and the methodology employed to deliver the feeds is an important consideration in producing the desired therapeutic product. It is well established that under-feeding a culture has a negative impact on its performance; likewise, a process that over-feeds can also have deleterious effects on the culture. The amount of feed, as well as the frequency of feeding, are important factors to be considered when devising a robust fed-batch process. Optimal feed concentrations and feeding regimes should be determined experimentally. Though this evaluation method is the most effective and gives detailed results, it is resource-intensive and may be limited by the number of individual parameters that can be evaluated simultaneously. Again, because individual parameters are evaluated independently from others, the potential interaction of one experimental variable on another may not be detectable using this evaluation method. Experimentation by a statistical DOE approach is another screening method utilized in process development to optimize feeding regimens. The advantage of this screening method over an iterative approach is that it results in comprehensive results (including potential interactions between experimental conditions)—however, this knowledge of advanced statistical methods and computational and technical expertise. However, fed-batch cultures improve on them in principle by supplying key nutrients to prevent depletion, but this increases the culture volume. Continuous cultures employ a similar feeding strategy, but an equal volume is removed beforehand to avoid increasing the working volume and diluting the culture; however, this results in a decrease in total viable cell number at the time of feeding. Perfusion culture techniques improve upon this by filtering out spent media and cell debris while retaining whole cells. A comparison of these culturing methodologies is shown in Figure 2.4.

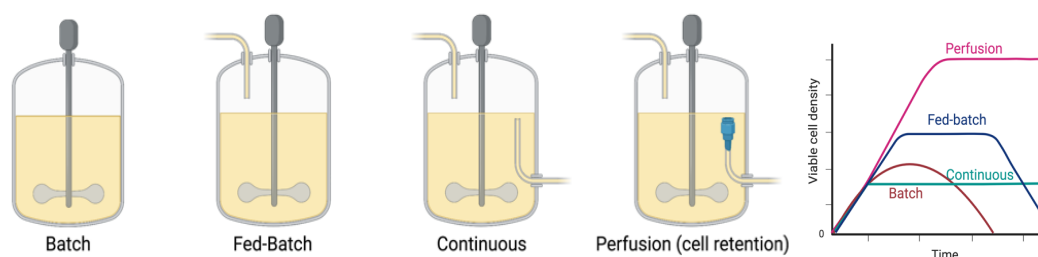


Figure 2.4: Modes of cell culture routinely used for the production of biotherapeutics

Various modes of operation are used to produce biotherapeutics- batch, fed-batch, continuous, and perfusion cultures. Created with BioRender.com

2.5 Conclusion

The development of serum-free cell culture media has encouraged the understanding of nutritional requirements, physiology, and functions of various types of cells.

Removing an incredibly complex component like serum requires an extensive understanding of the diverse array of functions it performs and the imperfections it conceals in the basal medium. But the advantages of serum-free media come with a cautionary note of an in-depth understanding of the nature of the components, their functions and interactions in the medium. Various components like cysteine, vitamin C, iron and copper are involved in complex redox reactions and can have a pro-oxidant or antioxidant role depending on given redox conditions. Rational media design and feeding strategy require an understanding of the specific cell line and finding a middle ground between toxicity and nutrient insufficiency. Omics approaches can help provide better insights and develop and optimize media enabling efficient and consistent cell culture process development for biotherapeutics.

Chapter III.

Methods

This chapter describes common methods used across multiple approaching chapters. Any other methods specific to a particular chapter are described in the methods section of its chapter.

3.1 Materials

Suspension CHO-DG44 based cells producing recombinant IgG were provided by Inbiopro Solutions (Bengaluru, India). They were regularly passaged custom-made DMEM:F12 based HDFE medium (composition in Appendix 1). Unless otherwise mentioned, all chemicals were purchased from Merck (Kenilworth, NJ, USA). Lipofectamine 2000 (11668027) was purchased from Invitrogen Corporation (Carlsbad, CA, USA). CHO-S- SFM II and DMEM were purchased from Invitrogen Corporation (12052-114 and 12320-032, respectively).

Fetal Bovine Serum (RM1112, FBS) was purchased from Hi Media Laboratories (Mumbai, India). Cell culture compatible silicone tubing ID 2 mm 9 OD 4 mm was purchased from Ami Polymers (Mumbai, India). 24 well plates were purchased from Nest Scientific USA (Rahway, NJ, USA) and used for seeding K562 cells. Ultra-low binding 24 well plates were purchased from Sigma-Aldrich (St. Louis, MO, USA) and used for CHO-S cells.

3.2 Cell culture

All cultures were incubated in a humidified incubator set at 37 °C and 10% CO₂ and shaken at 110 rpm or 130 rpm for high density cultures. No antibiotics or serum was used in any of the CHO cultures. Culture volume of 20 mL, in a 100 mL glass conical

flask with a screw cap, was used for all cultures. Cultures were sampled regularly for cell density and extracellular metabolite measurements.

3.2.1 CHO-S cells

CHO-S cell line was purchased from Invitrogen Corporation (Invitrogen, CA, USA). Cells were seeded at a density of 0.2×10^6 cells/mL in CHO-SFM II and passaged every second day. Cells were maintained at 37 °C, 10 % CO₂ and 110 rpm, and used from passage 9–40.

3.2.2 K562

K562, human chronic myelogenous leukemic cell line was obtained from National Centre for Cell Sciences (NCCS, Pune, India). K562 cells were maintained in DMEM (Invitrogen, CA, USA) supplemented with 10 % FBS and cultured at 37°C, 10 % CO₂ and 110 rpm. K562 cells were used from passage 39–50. Plasmid containing mCherry gene was used for transfection with fluorescent mCherry protein used as a reporter.

3.2.3 CHO cells expressing IgG

A suspension CHO cell line expressing IgG, provided by Inbiopro Solutions (Bangalore, India), was used to evaluate the effect of the addition of the hydrogels to increase culture longevity and productivity. Cells were inoculated at a density of 0.3×10^6 cells/mL in 25 mL culture volume in 100 mL Erlenmeyer flasks (Borosil). Cells were regularly passaged in our in-house medium formulation based on DMEM:F12 containing 3 g/L glucose and 5 mM glutamine. The complete medium formulation is provided in Supplementary Table 1. For fed batch experiments, shake flasks cultures were incubated at 37°C, 10% CO₂, 110 rpm. Glucose was fed to bring its concentration back to 2 g/L: at viability above 85%, glucose was fed when its concentration decreased below 2 g/L, while at viability below 85%, glucose was fed when the concentration decreased below 1.5 g/L. For cultures supplemented with NutriGel₂^{HVT,T}, cells were inoculated at 5×10^6 cells/mL in 50 mL culture volume. These cultures were incubated at 37°C, 10% CO₂, 130 rpm. Glucose was fed to bring its concentration back to 4 g/L: at viability above 85%, glucose was fed when its

concentration decreased below 4 g/L, while at viability below 85% glucose was fed when the concentration decreased below 2.5 g/L. The hydrogel was added on day 3 for all the cultures and at day 0 for the NutriGel₂^{HVT,T} cultures. For bolus fed cultures the composition of the bolus liquid feed was the same as NutriGel_T. While standardizing the payload, cultures were fed with 50 mg of the corresponding feed on day 3 and 6 and a total of a total of 2.5 mL liquid feed was added to 25 mL culture volume of the bolus fed cultures. This resulted in the addition of 100 mg of the feed. For other bolus fed culture 0.5X of the corresponding feed (20X) was fed on day 3,6,8,10 or day 3,4,6,8. A total of 2X of the feed was added, where 1X corresponds to medium concentration without the bulk salts. A total of 2.5 mL liquid feed was added to 25 mL culture volume of the bolus fed cultures. The hydrogel is added as a pre-swollen solid, so there is no volume change due to hydrogel addition. The composition of the bolus liquid feed was the same as NutriGel_T. The amount of payload in NutriGel_T was 250 mg, while the liquid bolus feed addition resulted in the addition of 125 mg of the feed, both to the same initial culture volume. The hydrogel payload was kept higher due to loss of payload during the initial washing and pre-incubation of the hydrogel for at least 2.5 days to remove unpolymerized monomers. The loss of payload was variable for the different components. Glucose was fed to maintain glucose concentration between 2–2.5 g/L, and a total of 7 mM of glutamine was also fed to the cultures. Samples were taken on alternate days for measuring cell density, viability, glucose concentration. Cell density was quantified by manual counting using a hemocytometer. Viability was assessed using the trypan blue dye exclusion assay. Glucose concentration was measured using a YSI Biochemistry Analyzer.

3.3 Adaptation to HDFE 3 without hydrolysate

CHO-IgG GC cells were adapted to DMEM/F12 based formulation without vegetable-based protein hydrolysate present in the original medium formulation. Adaptation was carried out by passaging the cells on every 3rd day and seeding at a density of 0.5×10^6 cells/ mL by resuspending in fresh medium. At every passage the percentage of hydrolysate in the media (gradual decrease in hydrolysate was from 75,50,25,25 and 0 percent) was reduced.

3.4 Adaptation to low amino acid media

To adapt suspension adapted CHO cell line expressing IgG, provided by Inbiopro Solutions (Bangalore, India), grown in DMEM/F12 media without hydrolysate, to an inhouse low amino acid media (0.1 mM amino acid concentration and 0.5 mM glutamine, this media will be henceforth referred to as LAA: Low amino acid medium) cells were passaged every 3 days and seeded at 0.3×10^6 cells/ mL. Cells being adapted to low amino acid media showed no significant growth for 30 days with eventually the cells death.

3.5 Single amino acid supplementation

A suspension adapted CHO cell line expressing IgG, provided by Inbiopro Solutions (Bangalore, India), was used to evaluate the effect of individual amino acid supplementation, on cell growth and productivity. Cells were inoculated at a density of 1×10^6 cells/mL in 20 mL culture volume in 100 mL Erlenmeyer flasks (Borosil). Cells were allowed to acclimatize to nutritionally limited medium by culturing them in a custom made low amino acid (LAA) medium containing all amino acids at 0.1 mM, glutamine at 0.5 mM, glucose at 2 g/L for 24 hours. Post 24 hours cells were resuspended in fresh LAA medium, along with 2mM of individual amino acids and an supplemented control culture. To minimize carryover from the previous medium, at each resuspension an additional wash with LAA medium was included. Cells were sampled at alternate days for 6 days and viable cell density and viability was measured using trypan blue dye exclusion assay on a hemocytometer. The supernatant was used to perform glucose assay using GOD/POD based kit according to the manufacturers instruction (Beacon diagnostics).

3.6 Bioreactor experiment

In order to test if feeding continuously at a constant lower rate can maintain amino acids at a low concentration while improving culture longevity (unlike the hydrogels where the release rates of amino acid reduces over time) we utilized a bioreactor. To feed amino acids to try to maintain low amino acid concentration to restrict amino acid overflow metabolism, we created a feed comprising of amino acids, vitamins and

trace elements based on NutriGel experiment. The culture was seeded at 1×10^6 cells/mL and fed the same amount of amino acids as supplemented through the NutriGel, through a pump throughout the entire culture duration in a controlled environment using the bioreactor.

A benchtop bioreactor with a working volume of one-litre (Celligen 115, New Brunswick Scientific, Edison, NJ, USA) was used for bioreactor cultures. An initial culture volume of 500 mL was used. Identical basal medium, seeding density, inoculum, feed and feeding strategy was developed from E85 shake flask cultures. Culture temperature was maintained at 37 °C. Dissolved oxygen was maintained above 30% (of saturation) using cascaded control of agitation and gas flow. The culture was agitated using a marine blade impeller between 100 and 130 rpm. Culture pH was maintained at 7 ± 0.02 for cultures. CO₂ gas and 0.1 mM sodium bicarbonate were used as acid and base, respectively, for pH management. Increase in culture volume and increase in cell density was accounted while feeding the bioreactor. Simethicone was added to control foaming whenever necessary. Clustered heatmaps were plotted using Datawrapper.

Amino acid quantification was carried out using HPLC. Briefly the samples were subjected to precolumn derivatization with phenylisothiocyanate (PITC) and the derivatized amino acids were quantified on HPLC (Agilent 1200 infinity series) with reverse phase C18 column (Purosphere star RP18 (5 µm) end-capped, Merck, Darmstadt, Germany).

3.7 RNA seq library preparation

For creation of RNA seq library, suspension adapted CHO cells producing IgG regularly passaged in a custom DMEM: F12 based medium without hydrolysate were resuspended in LAA. The different conditions tested were a low amino acid background containing amino acids at 0.1 mM, a high amino acid background containing most amino acids at 1 mM and the passage medium. After 24 hours of adjustment period, the cells were again resuspended in the respective low or high amino acid media along with the routinely used passaging medium. The cells were seeded at 1×10^6 cells/mL in a 20 mL culture volume. To minimize carryover from the

previous media, additional washing step was included with the respective media. Post 24 hours of growth the cells were counted and 1×10^6 cells were pelleted by centrifugation at 1000 rpm for 5 mins. The pellet was then washed with PBS once. About 100 μL of fresh PBS was added to loosen up the pellet and resuspend the cells followed by addition of 500 μL of RNA later. The cell pellet was then stored at -80°C till RNA extraction.

3.8 Specific metabolite consumption

Specific glucose consumption rates were calculated as the slope of the plot of cumulative glucose consumption versus integrated viable cell density (IVCD) in the indicated period.

3.9 Hydrogel synthesis

Hydrogels are polymers with insoluble polymeric backbone with hydrophilic functional groups attached to it, that are insoluble in water. Poly-HEMA hydrogels were synthesized using 2-hydroxyethyl methacrylate (HEMA, 97% pure, Sigma-Aldrich Corp, USA) monomer and ethylene glycol dimethacrylate (EGDMA, Sigma-Aldrich Corp, USA) crosslinker at 86:14 mol/mol HEMA:EGDMA in the presence of an initiator Azobisisobutyronitrile (0.5%, Sigma Aldrich Corp, USA). A bottom layer of the hydrogel was created by polymerizing 200 μL of the HEMA:EGDMA mixture in a 1.3 cm diameter glass disc at 75°C for 1.5 h. A cavity was then formed over the bottom layer using an appropriate mould and 400 μL of the HEMA:EGDMA mixture by incubation at 75°C for 1.25 h. The diameter of the cavity was 9 mm. Subsequently, the solid powder of the payload was added into this cavity. The exact composition of the payload varies in different experiments and is described in Table 1. Four hundred and fifty microliters of the HEMA:EGDMA mixture was used to create the monolithic central reservoir and final layer of the hydrogel, sealing the cavity. The hydrogels were then washed in sterile ultrapure water for two days. After washing, the hydrogels were sterilized using UV for 25 min on each side of the hydrogel. Hydrogels were incubated overnight in culture medium before addition to

the cultures. The HEMA:EGDMA hydrogel was previously assessed for cytotoxicity and demonstrated to be non-toxic [21].

3.9.1 Release kinetics for amino acids

The release kinetics of amino acids were analysed at 37 °C. The hydrogel was added into phosphate-buffered saline (PBS) with 0.05% sodium azide under shaking conditions to simulate conditions during release in shake flasks. Samples were taken on alternate days for amino acid concentration measurement for 16 days. Amino acid quantification was carried out using HPLC. The samples were subjected to precolumn derivatization with phenylisothiocyanate (PITC) and the phenylthiocarbamyl derivatised (PTC-amino acids) amino acids were quantified on HPLC (Agilent 1200 infinity series) with reversed phase C18 column (Purosphere star RP18 (5µm) end-capped, Merck, Darmstadt, Germany). Briefly, 100 µL of the sample was spiked with 15 µg of norleucine as internal standard and lyophilized. Subsequently, 20 µL of methanol:water:trimethylamine 2:1:1 (v/v) was added, vortexed and lyophilized. Further, 20 µL of methanol:water:trimethylamine:PITC 7:1:1:1 (v/v) was added, vortexed, incubated for 20min at room temperature and lyophilized. Derivatized samples were resuspended in 1 mL of eluent A (85 mM sodium acetate and 0.3 mM sodium azide in 98% water and 2% acetonitrile, pH 5.2, (w/v)). Chromatography was carried out after injecting 5 µL of derivatized sample using elution gradient of $T_{0 \text{ min}} = 3\%$ eluent B (100% acetonitrile), $T_{25 \text{ min}} = 13\%$ eluent B, $T_{45 \text{ min}} = 50\%$ eluent B, $T_{46 \text{ min}} = 3\%$ eluent B. Flow rate was maintained at 0.8 mL min⁻¹. Eluted derivatives were detected with a diode array detector at 254 nm with a bandwidth of 4 nm. The peak area for each amino acid was normalized to the internal standard. Amino acid concentration was calculated using response factor calculated from the peak area of the respective amino acid (normalized to norleucine) in a standard containing 15 µg/mL of aspartate, glutamate, glutamine, glycine, asparagine, serine, histidine, threonine, arginine, alanine, proline, tyrosine, valine, methionine, cystine, isoleucine, leucine, phenylalanine, tryptophan and lysine. It is important to note that in this method for amino acid measurement, cysteine and cystine were not resolved as separate peaks but coeluted as a single peak and hence could not be accurately quantified.

3.10 Volumetric IgG Quantification

Volumetric IgG titer was determined by a sandwich ELISA. Briefly, ELISA plates were coated with capture antibody-rabbit anti-human IgG and subsequently blocked with 1% bovine serum albumin (BSA) in phosphate-buffered saline (PBS). 0.01% Tween 20 in PBS was used to wash plates. Human IgG was used to generate a standard curve for quantitation. HRP conjugated rabbit anti-human IgG (GeNei Laboratories Pvt Ltd, India) was used to detect IgG in culture followed by the addition of substrate TMB/H₂O₂ (GeNei Laboratories Pvt Ltd, India). The reaction was stopped using 1M H₂SO₄. Absorbance was measured at 450 nM on Bio-Rad iMark microplate reader (Bio-Rad Laboratories, Mumbai, India). Samples selected for ELISA had a viability of 60% or more.

3.11 Flow apparatus

A flow apparatus with a reservoir for cell suspension and a peristaltic pump (Longer pumps BT100-2J Low Flow Rate Peristaltic Pump with the 6-roller pump head DG-2) was used to flow cells at a flow rate of 19 mL/min through a cell culture compatible silicone tubing (ID 2 mm 9 OD 4 mm, Ami polymers). For low shear stress, cells were flowed only through the silicone tube of 2 mm inner diameter. A glass capillary of 0.5 mm diameter and length of 8 cm was attached to generate moderate shear stress and a silicone tube of 0.25 mm diameter of length 1.2 cm was inserted to generate high shear stress. Under an assumption of incompressible walls and no slip at the wall, these correspond to a wall shear stress of ~2, 220 and 2000 dynes/cm² under the three conditions respectively. The experiment was repeated at least three times, and cells were seeded into two wells for each repetition. To control for any effect of shear stress due the squeezing action of the peristaltic pump head, the flow rate was kept constant under all three conditions. The pump head design allowed varying occlusion using a ratchet wheel. The extent of cell death observed when cells alone were flowed through the pump head varied for different values of this parameter with cell death increasing at higher levels of occlusion. The highest occlusion was identified for each cell type such that there was minimal cell death immediately subsequent to exposure to low shear stress, and was then kept constant for all experiments with that cell type. The selected level of this parameter was higher for CHO-S compared to K562.

3.12 Transfection

Transfection for CHO-S was performed using Lipofectamine 2000 (Invitrogen Corporation) as per the manufacturer's instructions. Transfections were carried out using cells on the second day of passage. 1 μg DNA and 5 μl Lipofectamine 2000 was used per milliliter of the cell suspension. Depending on the experiment, the lipoplex complex or lipid alone were added to 4 ml of the cell suspension and flowed through the flow apparatus for 2 h. After 2 h, 500 μl of the culture was incubated in 24 well plate at 37 °C, 10 % CO₂ and 110 rpm. Samples were taken for measuring cell density immediately before and after flowing the cells, and after allowing cells to recover for one day after exposure to shear stress. Cell density was measured using a hemocytometer after appropriate dilution and viability was measured using trypan blue dye exclusion method. After 24 h of incubation, some clumping was observed for all transfected CHO-S cultures with clumps of approximately 5–20 cells. Clumps were counted as a single cell for calculation of cell density. Each experiment was repeated at least 3 times.

Transfection for K562 was performed using Lipofectamine 2000 as per a modified protocol suggested by the manufacturer. 2.4 μg DNA and 5 μL Lipofectamine 2000 was used per milliliter of the cell suspension for transfection. The complex was mixed in serum free DMEM medium and incubated for 20 min at room temperature before addition to the culture.

3.13 Calculation of transfection efficiency

Twenty-four hours post transfection, cells were harvested from the 24 well plate. After washing with PBS, the CHO-S cells were then imaged on EVOS Fluid Cell Imaging Station (Life Technologies, Carlsbad, CA, USA). Transfection efficiency for CHO-S cells was calculated by counting the percentage of cells that showed red fluorescence due to expression of fluorescent mCherry protein. A minimum of fifteen fields per well were recorded with the Fluid Cell Imaging Station and the number of fluorescent cells and total cells was counted.

Due to the very low transfection efficiencies for K562 cells, transfection efficiency was measured using flow cytometry (BD Accuri C6 Flow Cytometer, BD Bio-

sciences) and data were analyzed using the BD Accuricflow software (BD Biosciences, San Jose, CA, USA).

3.14 Statistical analysis

Two-tailed Student's t-test was used to determine the significance of the difference between each pair of data. All p values lower than the significance level of 0.05 are denoted by asterisks in figures. A p value < 0.05 is denoted by *, < 0.005 by **, and < 0.0005 by ***.

Chapter IV.

Shear stress and its implication on large-scale transient transfection for biopharmaceutical production

4.1 Summary

A typical manufacturing process for biotherapeutics begins with pre-clinical trials on the protein of interest produced by large-scale transient gene expression of the protein of interest. Suspension-adapted CHO cells are the workhorse for biopharmaceutical production. About 70% of the top 10 recombinant proteins are produced in CHO cells. Animal cells in suspension experience a wide range of shear stress in different situations, such as in vivo due to hemodynamics or in vitro due to agitation in large-scale bioreactors. Shear stress affects cell physiology, including binding and uptake of extracellular cargo, and is studied comprehensively in adherent cells. There are, however, no reports on the effect of shear stress on extracellular cargo delivery to suspension cells. This chapter describes the impact of shear stress on the transfection of CHO-S cells using Lipofectamine 2000 using a simple flow apparatus. Our results show decreased cell growth and transfection efficiency upon lipoplex-assisted transfection of CHO-S while being subjected to shear stress. This effect is not seen to the same extent when cells are exposed to shear stress in the absence of the lipoplex complex and subsequently transfected, or if the lipoplex is subjected to shear stress and subsequently used to transfect the cells. It is also not seen to the same extent when cells are exposed to shear stress in the presence of liposome alone, suggesting that the observed effect is dependent on the interaction of the lipoplex with cells in the presence of shear stress. These results indicate that studies involving liposomal DNA delivery should account for the effect of shear during lipoplex-assisted DNA delivery, especially for large-scale transient production of biotherapeutics.

4.2 Introduction

Liposome, polymer, and viral transfection are well-known methods of introducing a transgene into a host cell. Compared to non-viral methods, viral transfection can have potential mutations, immune responses, and genetic alterations due to integration [141]. Liposomal formulations are a popular vehicle for delivering the transgene to cells in culture and are also being evaluated for gene and drug delivery in human clinical trials. Large scale transient transfection is an important approach for producing biotherapeutics needed to produce substantial amounts of recombinant protein for pre-clinical trials. CHO cells are the preferred host for biotherapeutics production and are subject to agitation during transient transfection at large-scale culture in bioreactors.

Large-scale cell cultures require an efficient mass transfer system determined by the bioreactors' agitation and aeration configuration. Impeller speed and aeration strategy are critical parameters for bioreactor scale-up but also result in generating shear stress which has been well reported. For example, impeller tip speed above 1.5 m/s can induce cellular damage [24,142]. In a reactor, these hydrodynamic stresses vary with time, adding to the complexity and resulting in cells being subjected to a range of hydrodynamic stresses. Hence different parameters are used by the fluid dynamics community to understand, estimate and characterize these forces. One parameter that is preferred is the energy dissipation rate, EDR. EDR is a scalar value used to represent the rate of dissipation of kinetic energy per unit of mass or volume. It has been also demonstrated that the EDR in the impeller region varies and has been reported to be over 103 times higher than the EDR away from the impeller region [143–146]. The average range of EDR levels caused by impeller agitation are in the range of 0.01–1 w/kg, while the threshold at which mammalian cells are subjected to damage is approximately 2–4 orders of magnitude higher [147,148]. Typically mammalian cells in a reactor are subjected to shear stress well within these ranges of EDRs. A summary of critical process parameters reported in the literature to correlate the effect of hydrodynamic forces on cells in vitro is presented in Godoy-Silva et al. [149] (Figure 4.1). Compared to lethal cell damage, sub-lethal effects encountered by cells due to hydrodynamic stresses in suspended culture are more difficult to recognize and demonstrate, especially because of the complex fluid dynamics in the

bioprocessing context.

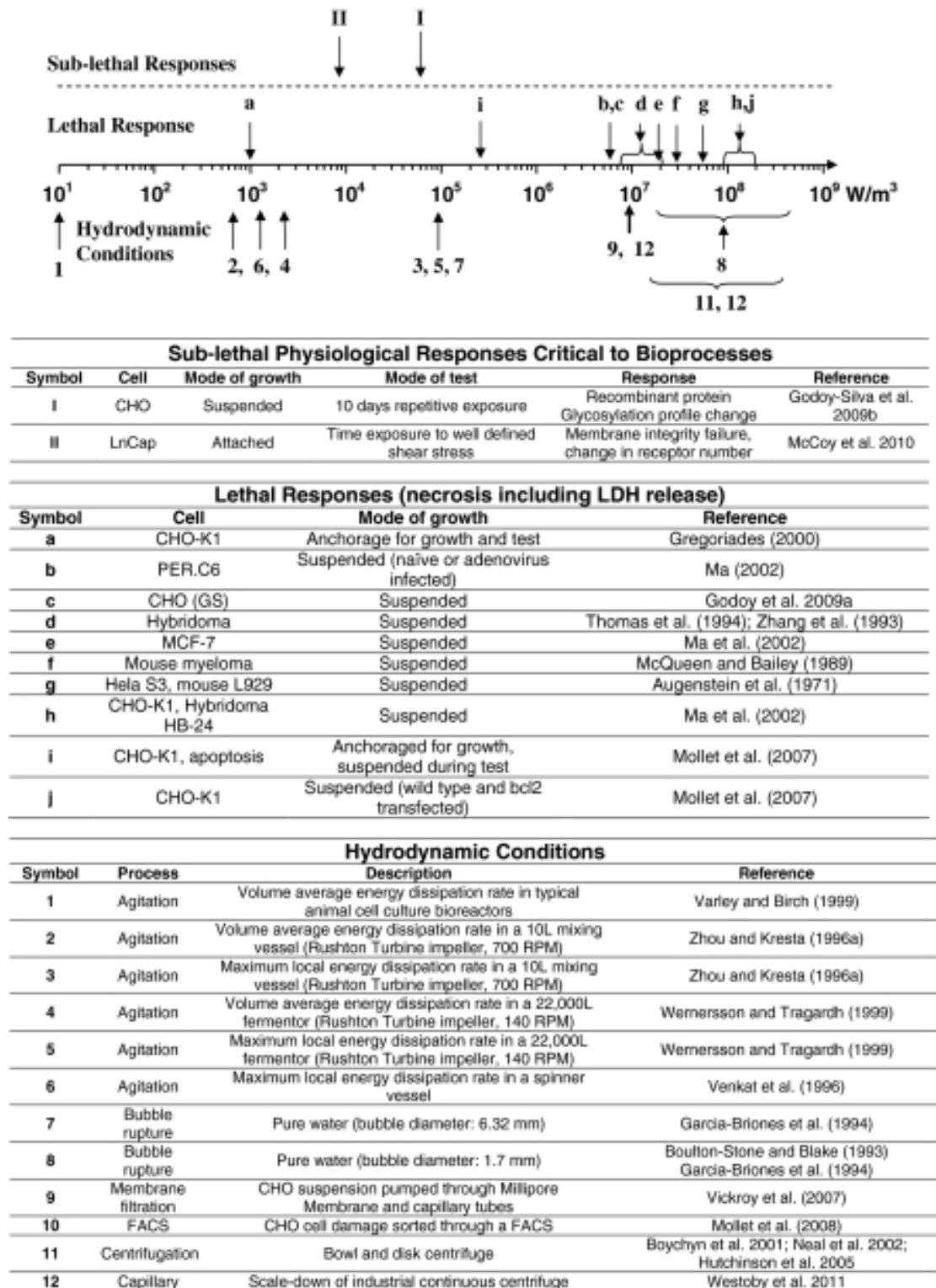


Figure 4.1: Summary of the energy dissipation rate in the literature

Summary of the reported EDRs in literature, at which cells are damaged as well as the reported levels of EDR in various bioprocess environments. Adapted from Godoy-Silva et al. [149]

In contrast, endothelial cells (EC), which line the walls of arteries and veins, are subjected to a wider range of shear stress and have been extensively studied. For example, they are subjected to a wide range of shear stress of about 15 dynes/cm² for arterial circulation and 1–6 dynes/cm² for venous circulation to 3000 dynes/cm² at certain places in the body like the vessel bifurcations, in the heart, and near the walls of large blood vessels [150,151]. Hence, the effect of shear stress has been primarily studied in adherent cells mostly due to interest in the impact of shear stress on various aspects of endothelial cell biology and is known to affect multiple aspects of other cell lineages like cell physiology, including cell morphology, size, and metabolism [152–155]. A large body of work is reported on various hybridomas subjected to diverse levels of shear by different techniques that show the shear sensitivity of cells is cell line-specific. Shear sensitivity of hybridoma cells is described to be attributed to the culture conditions like the presence of low shear or no shear in slowly agitated spinner flasks or T flask versus rapidly agitated flasks, stage of the cell cycle, time of exposure, and the health of the population. From a bioprocessing perspective, shear stress also affects quality attributes like glycosylation, as shown in a study, producing Type II glycoform of Recombinant tissue-type Plasminogen Activator Protein in CHO cells [152].

Shear stress has been reported to affect particle adhesion in ECs, which can potentially affect uptake. Exposure to shear stress has been reported to transiently increase fluid-phase endocytosis and caveolae density [156–158]. Endocytosis of extracellular cargo requires the association of the cargo with the cell membrane as the first step in transfection [159]. These effects can vary depending on the particle size and the level of shear stress. There are contradicting reports on the impact of shear and size. Patil et al. have reported that at a higher shear rate, adhesion depends on the size of the particle, i.e., the rate of attachment of 5-20 μm diameter microspheres decreased with increasing size at shear rates of 400 s⁻¹ to 600 s⁻¹ [160]. Charoenphol et al. showed that binding efficiency for spherical particles increased with increasing particle size at a shear rate of 200 s⁻¹, and for a given size, the binding efficiency increased when the wall shear rate was increased from 200 to 1500 s⁻¹ [161]. Such contrariety may be attributed to the different ligands used, the different modes of

adhesion of the carrier particle, and the different shear stress at which the experiments were performed. For the nanoscale particles, there exists an inverse relationship between shear and particle uptake [162]. In addition to size, particle shape also affects the binding of particles under shear stress. For example, the adhesion of elongated and flattened particles was found to be significantly higher than that of spheres [163]. For spherical particles, the binding efficiency increased with an increasing size [20]. This may be of relevance to the effectiveness in the presence of shear stress of carriers such as liposomes, which can deform in the presence of shear.

The duration and magnitude of cellular exposure to shear stress are important parameters that can also affect the uptake of particles. Chronic exposure to shear affects the uptake of nanoparticles differently versus acute exposure. Chronic shear is known to reduce the internalization of spherical particles; for example, constant exposure to Human umbilical vein endothelial cells (HUVECs) cells leads to reduced internalization of FITC-labelled polystyrene spheres coated with anti-PECAM ~180 nm in diameter and 80 nm spherical gold nanoparticles (AuNPs). In contrast, acute exposure leads to increased internalization [164,165]. The magnitude of the shear stress also matters for binding/uptake: for example, nanoscale particles showed an inverse relationship between shear stress and particle uptake [162]. Cell membrane properties can also be affected by shear stress, with membrane fluidity reported to increase with shear stress in endothelial cells. Mardikar and Niranjana subjected various animal cells in suspension to shear in a concentric viscometer which led to the observation such as the formation of pores and papillation shrinkage. They theorized that damage to the cells might begin with the formation of pores followed by the oozing out of the cytoplasm from the cells. Depending on the shear forces, this extruded cytoplasm gets cleaved from cell leading to cell shrinkage, which can be a possible explanation for the various reports on the effect of shear on cell size and formation of pores for delivery of macromolecules. It is conceivable that such formation of pores could affect the uptake of extracellular cargo [166,167]. Shear stress can also affect cell membrane by inducing membrane fusion, suggesting that under some conditions, the interaction of liposomal carriers with cells, and hence their ability to deliver cargo, is also affected by shear stress [168].

All reported effects of shear on intracellular delivery of cargo have been evaluated on adherent cells where the flow has an additional effect of improving access of the liposome: DNA complex to the cell [169]. Flow can have a positive effect of improving access of the lipoplex to the adhered cell, which can increase its uptake, but at the same time, can reduce the binding affinity of the lipoplex to the cells [170]. Nonetheless, above a threshold shear, the hemodynamic forces lead to a decrease in the uptake of the cargo [171,172]. In a bioreactor, the range of the hydrodynamic stress encountered by the suspended cells covers several orders of magnitudes, and the development of a downscale device that can subject cells to wide ranges of shear stress is unreported. A small-scale set-up is developed here, being capable of simulating the high and low-stress regions while giving the possibility to determine a cell-specific threshold. To our knowledge, there are no reports on the effect of shear stress on carrier-assisted delivery of cargo to suspension cells. Such scenarios are relevant to large-scale transfections carried out in bioreactors for transient expression of recombinant protein and to liposomal gene and drug delivery to blood cells where the liposomal complex is injected into blood vessels.

Since shear stress is known to affect cellular uptake of extracellular cargo, exposure to shear stress is being evaluated as a strategy for delivering macromolecules into cells. It is possible that shear stress experienced by CHO cells during routine bioprocessing processes can affect transient transfection. Different methods of employing shear stress have led to devices such as those made by Hallow et al. and Sharei et al. that use shear stress as the fundamental principle for intracellular delivery [173,174]. However, the exact mechanism is yet unclear.

In this study, we employ uncomplicated flow apparatus to investigate the ability of liposomal carriers to deliver DNA to suspension cells for transgene expression in the presence or absence of shear stress. We find that exposure to shear stress during transfection with lipoplex results in a decrease in transfection efficiency and reduced cell density compared to transfection carried out in the absence of shear stress in well-plates in CHO-S cells, which are efficiently transfected by Lipofectamine 2000. This effect is not seen to the same extent when cells are exposed to shear stress in the absence of the lipoplex and subsequently transfected, or if the lipoplex is exposed to shear stress and subsequently used to transfect cells not exposed to shear.

4.3 Results

4.3.1 Developing a scale-down device to investigate a wide range of shear stress on mammalian cells

Cells were subjected to shear stress by pumping them in a closed-loop at a constant flow rate using a peristaltic pump (Figure 4.2). The use of a peristaltic pump allowed continuous unidirectional flow allowing cells to be precisely verified exposed to shear stress for extended periods of time. The use of such a set-up enabled maintaining sterility and flexibility in terms of the range of shear stress that the cells could be subjected to using this simple flow set-up. Cells were subjected to shear stress by pumping them for 2 h either through a silicone tube of 2 mm inner diameter, henceforth referred to as 'low shear,' which corresponds to about ~ 2 dynes/cm². Or a silicone tube of 2 mm diameter with an attached glass capillary of 0.5 mm inner diameter and length of 8 cm referred to as 'moderate shear,' which corresponds to about ~ 200 dynes/cm² or a silicone tube of 2 mm diameter with a silicone tube of 0.25 mm diameter and length 1.2 cm referred to as 'high shear' which corresponds to about ~ 2000 dynes/cm².

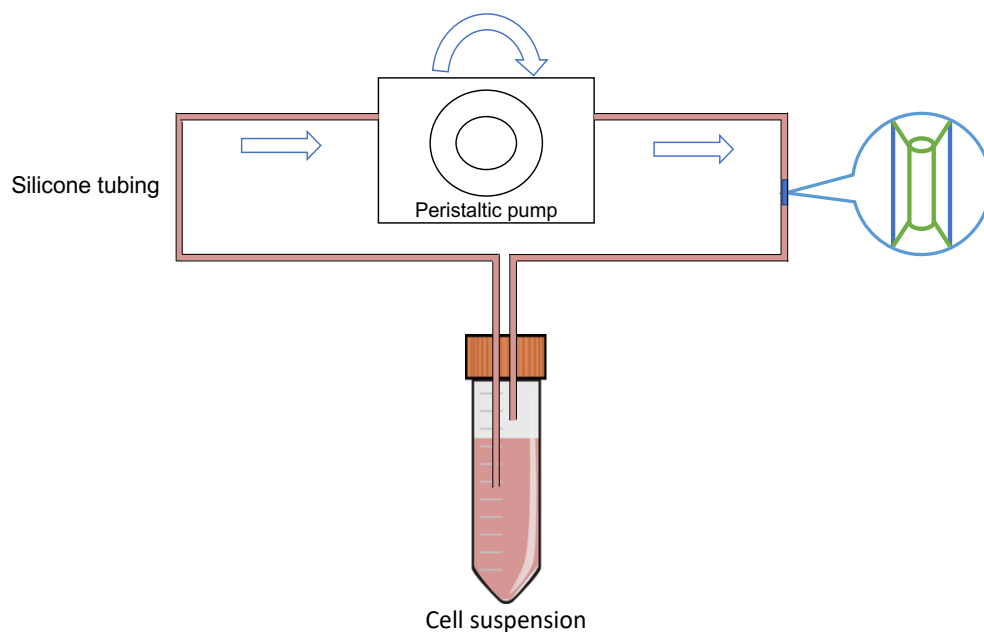


Figure 4.2: A simple scale-down flow device to subject CHO cells to a shear stress

We first evaluated the effect of shear stress on CHO-S cells to validate the use of the flow apparatus. This was done by evaluating the immediate effect of shear stress on cell death by measuring any decrease in VCD immediately after exposure to shear stress. The biochemical changes induced by shear may not immediately be obvious, and it is possible that it takes a time scale of the order of a cell-generation time before changes can be detected. And any longer-term effect on cell growth was measured at the end of 24 h after exposure to shear stress. Mechanical damage, on the other hand, is immediately detectable. The immediate decrease in VCD due to shear stress is small at low shear stress (8% decrease) but significantly increases at high shear stress (50% decrease, Figure 4.3). This is not surprising as cells are being subjected to a high shear stress of ~ 2000 dyne/cm². Exposure to shear stress also leads to liposomal toxicity and affects subsequent cell growth. Cells exposed to low shear stress showed an average of 0.9 population doublings over 24 h, compared to the growth of cells maintained throughout in a 24 well plate showing an average of 1.2 population doublings. However, cells exposed to high shear stress show a considerable decrease in VCD (average 73% decrease in 24 h). This is similar to lysis caused at a shear stress of 1800 dyne/cm² reported by McQueen et al. and Vickroy et al., validating the use of our flow apparatus [175,176]. Cell viability is, however, not substantially reduced after exposure to shear at all levels of shear stress (Figure 4.3b), indicating the decrease in viable cell density at high shear stress is likely due to cell lysis. Due to high cell death at high shear stress, the effect of shear stress on the transfection of CHO-S cells using lipoplex was further evaluated only at low and moderate shear stress.

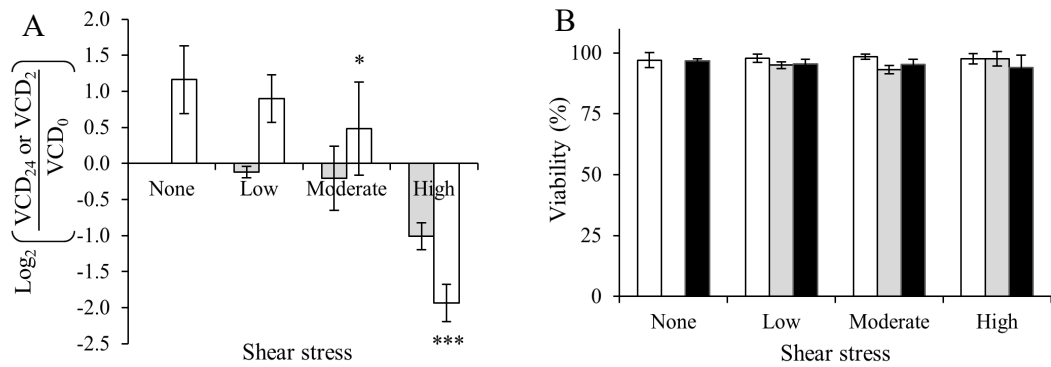


Figure. 4.3 The effect of shear stress on cell density and viability of CHO-S cells.

CHO-S cells were subjected to shear stress (low, moderate, and high, see Methods chapter for details on shear stress levels) for 120 min and monitored for changes in viable cell density and viability immediately after flow and after 24 h of incubation. CHO-S cells not subjected to shear stress were used as control. a Viable cell density (VCD) normalized to initial viable cell density. Immediately after subjecting cells to shear stress (filled bars), after 24 h (open bars). Initial viable cell density (VCD₀), viable cell density immediately after flow (VCD₂), and 24 h after flow (VCD₂₄). Log₂ transformation is used to represent cell growth in terms of population doublings and make the data symmetric for changes in both directions (growth and death). b Viability. Initial (white bars), immediately after subjecting the cells to shear stress (grey bars) and after 24 h (black bars). n ≥ 3, error bars indicate a 95 % confidence interval. ***p < 0.0005; **p < 0.005; *p < 0.05 for comparison to no shear condition

4.3.2 Exposure to shear stress in the presence of lipoplex reduces transfection efficiency and increases cell death

We further evaluated the effect of exposure of cells to shear stress in the presence of lipoplex (lipofectamine 2000: DNA complex). The immediate effect of shear stress on cell death was similar to the case when cells were exposed to shear stress without the lipoplex. However, surprisingly, the adverse effects with the presence of lipoplex were more pronounced. VCD at 24 h after exposure to shear stress was substantially reduced even at low shear stress (Figure. 4.4a). An average 25% decrease in VCD was observed at low shear and a 40 % decrease at moderate shear, compared to cell growth at an average 0.4 population doublings observed in cells transfected in the well plate. This decrease in VCD is partly caused due to greater clumping of cells in the presence of shear stress during transfection, though that alone is not sufficient to

explain the difference, as verified by including the cells in clumps during cell counting. Viability was again, however, not substantially affected, suggesting the decrease in VCD is due to increased cell lysis in the presence of lipoplex during exposure to shear stress (Figure 4.4b). Transfection efficiency decreased significantly when cells were subjected to shear stress in the presence of lipoplex (Figure 4.4c).

Higher cell death and lower transfection efficiency of the lipoplex in the presence of shear stress could possibly be due to the effect of shear on cells: for example, reduced cell growth upon exposure to shear stress could lead to reduced transfection efficiency. On the other hand, shear stress could have an effect on the lipoplex characteristics, which in turn affect their ability to cause DNA uptake. Both these mechanisms could, by themselves or in a concerted fashion, produce the effect of increased toxicity and reduced transfection efficiency in the presence of shear stress.

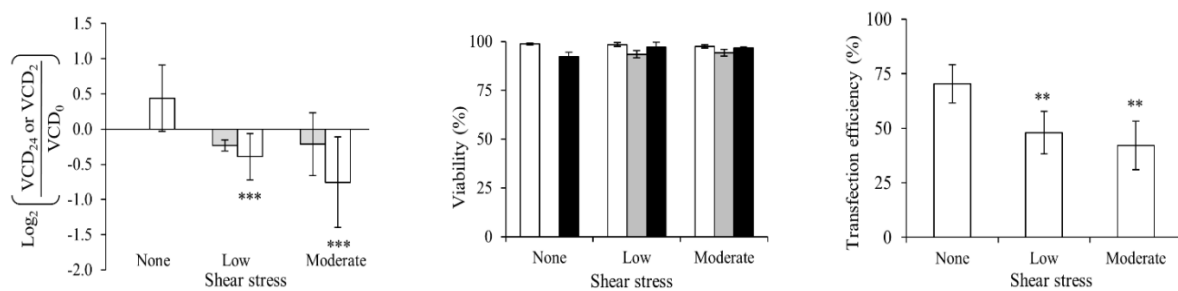


Figure 4.4 Cell density, viability, and transfection efficiency of CHO-S cells when exposed to shear stress in the presence of lipoplex.

CHO-S cells were subjected to shear stress (low and moderate shear stress levels) for 120 min in the presence of lipoplex and monitored for changes in cell density and viability immediately after flow and after 24 h of incubation. The control culture was not subjected to shear stress. a Viable cell density (VCD) normalized to initial viable cell density. Immediately after subjecting cells to shear stress (filled bars), after 24 h (open bars). Initial viable cell density (VCD₀), viable cell density immediately after flow (VCD₂), 24 h after flow (VCD₂₄). b Viability. Initial (white bars), immediately after subjecting the cells to shear stress (grey bars) and after 24 h (black bars). c Transfection efficiency. n ≥ 3, error bars indicate a 95 % confidence interval. ***p < 0.0005; **p < 0.005; *p < 0.05 for comparison to no shear condition

4.3.3 Shear stress does not affect the transfectability of the lipoplex complex

To test whether the observed effect on cell toxicity could be explained solely by the effect of shear stress on cells or on the lipoplex in any way, we subjected either only the lipoplex or the cells to shear stress prior to transfection. Further experiments were only carried out at low shear stress. The lipoplex was exposed to low shear stress for 2 h and subsequently used to transfect CHO-S cells. A control culture was also transfected with lipoplex incubated for the same period of time in the absence of shear stress to control for the effect of increased incubation time on the efficacy of the complex. There is no remarkable difference in the transfection efficiency of lipoplexes sheared for 15 min (Figure 4.5a). The slight decrease in transfection efficiency of lipoplex sheared for 2 h may be attributed to the higher incubation time compared to the manufacturer's suggested optimal duration, as it is also seen in the case of the lipoplex incubated for 2 h in the absence of any shear stress. Surprisingly, there is higher cell growth when cells are transfected with lipoplex sheared for 2 h, seen from the 1.2 population doublings for cells transfected with sheared lipoplex compared to the 0.6 population doublings for cells transfected with lipoplex incubated for 2 h without shear (Fig. 4.5b). Our data does not suggest any explanation for this observation of comparable transfectability and reduced growth inhibition by lipoplex subjected to shear stress.

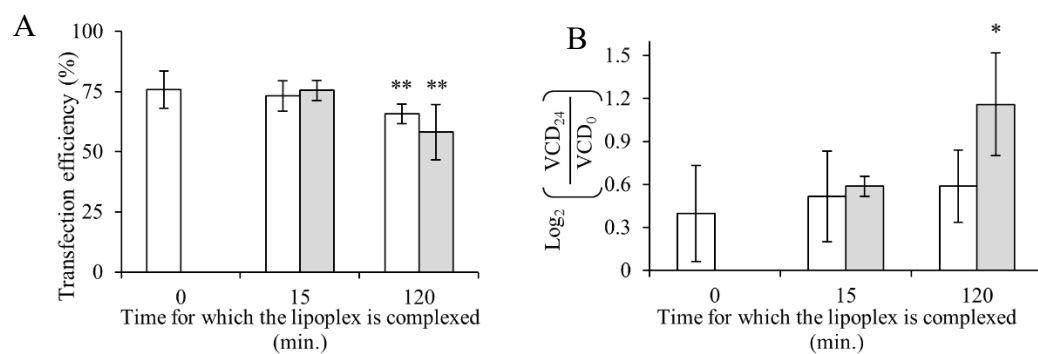


Figure 4.5 Shear stress does not affect the transfectability of the lipoplex.

Lipoplex was subjected to low shear stress for 120 min, and its unsheared control was used for transfecting CHO-S cells at different time points. a Transfection efficiency. Lipoplex not subjected to shear stress (white bars) and sheared lipoplex (grey bar). b Viable cell density (VCD) normalized to initial viable cell density. Cells transfected with unsheared lipoplex at indicated time points after complexation (white bars), cells transfected with sheared lipoplex at indicated time points (sheared for

15 and 120 min) (grey bars). Initial viable cell density (VCD_0), 24 h after flow (VCD_{24}). The error bars indicate 95 % confidence interval, $n = 3$. ** $p < 0.005$; * $p < 0.05$

4.3.4 Shear stress affects the transfectability of CHO-S cells

To test whether the observed effect on cell toxicity could be explained solely by the effect of shear stress on cells or on the lipoplex in any way (lipoplex size, density, etc.), we subjected CHO-S to low shear stress for varying durations of time and subsequently immediately transfected them. Figure 4a shows the transfection efficiency of cells transfected without exposure to shear stress or transfected after 15 and 120 min of exposure to shear stress. A short duration of 15 min exposure of cells to shear stress did not decrease their transfectability significantly. The transfection efficiency, however, decreased significantly when the cells were subjected to shear stress for 2 h prior to transfection. As expected from the previous results, VCD did not change significantly immediately after exposure of cells to shear stress (see grey bars in Fig. 4.6b). The average number of 0.9 population doublings in 24 h after exposure to shear stress was significantly higher for cells exposed to shear stress for a short duration prior to transfection compared to the cells transfected without exposure to shear (average 0.5 population doublings, see white bars in Fig. 4b).

For both cases where either the lipoplex or cells are subjected to shear stress followed by transfection, VCD increases in the 24 h post-transfection. This is unlike the case when cells are exposed to shear stress in the presence of lipoplex, where the VCD decreases in the 24 h period after exposure to shear. A comparison of figures 4.3a, 4.4b, and 4.6b thus suggests that cell growth is adversely affected by the presence of lipoplex during exposure of cells to shear stress.

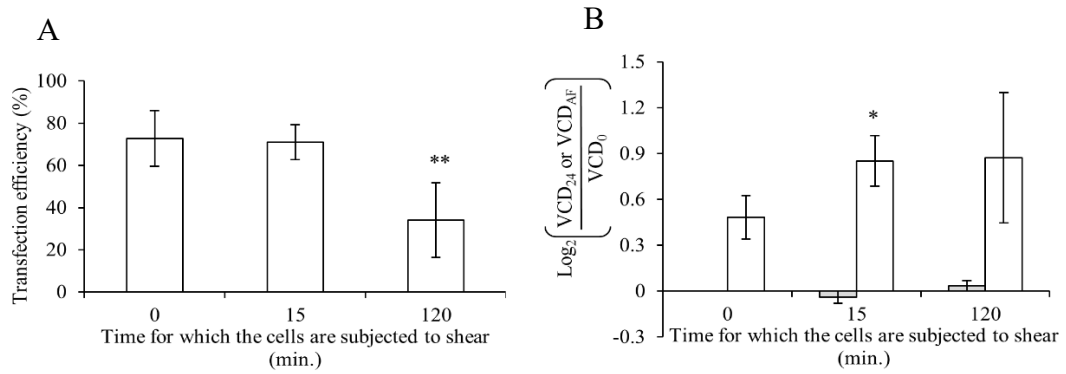


Figure 4.6 Shear stress reduces the transfectability of CHO-S cells.

CHO-S cells were subjected to low shear stress for 120 min and subsequently transfected at different time points. a Transfection efficiency. b Viable cell density (VCD) normalized to initial viable cell density. Immediately after subjecting cells to shear stress (grey bars), 24 h after subjecting cells to shear stress for the indicated time (white bars). Initial viable cell density (VCD₀), viable cell density immediately after flow for the indicated time (VCD_{AF}). 24 h after flow (VCD₂₄). The error bars indicate 95 % confidence interval, n = 3. **p < 0.005; *p < 0.05

4.3.5 Toxicity of lipoplex is not solely attributable to liposome

To understand whether the effect of shear stress during lipofection is exclusively due to the liposome, we subjected CHO-S cells to shear stress in the presence of liposome at a concentration equivalent to its concentration in the lipoplex. In the absence of shear stress, an average of 1.9 and 1.2 population doublings were observed in 24 h in the absence and presence of liposomes, respectively (Figure 4.7). Thus the presence of liposomes by itself adversely affects cell growth. When cells are exposed to shear stress in the absence and presence of liposomes, cells show growth at a lower average of 1.6 and 0.6 population doublings. Thus the adverse effect of liposomes on cell growth is substantially enhanced in the presence of shear. This is, however, in contrast to the case when cells are subjected to shear stress, the presence of the lipoplex, where a 25 % decrease in VCD was observed (Figure 4.4a). This suggests that the adverse effect on cell growth seen when cells are exposed to shear in the presence of the lipoplex is not attributable solely to the liposome.

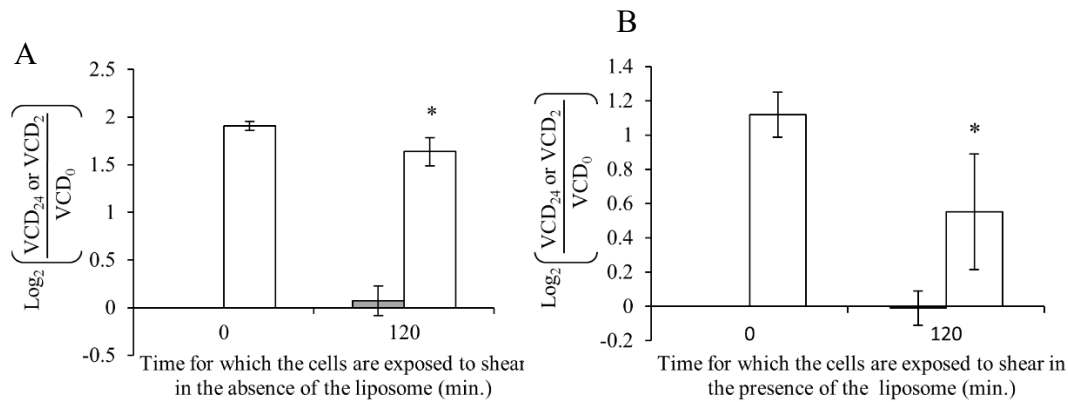


Figure 4.7 Exposure of CHO-S cells to shear stress in the presence or absence of liposome causes a reduction in cell growth.

CHO-S cells were subjected to shear stress in the presence or absence of lipofectamine 2000 for 120 min and monitored for changes in cell density immediately after 120 min of flow and after 24 h of incubation. a Viable cell density (VCD) normalized to initial viable cell density for CHO-S cells subjected to low shear stress without the liposome. b Viable cell density normalized to initial viable cell density for CHO-S cells subjected to low shear stress with the liposome. Viable cell density immediately after subjecting cells to shear stress for 120 min (grey bars), after 24 h of incubation (white bars). Initial viable cell density (VCD₀), viable cell density immediately after flow (VCD₂), and 24 h after flow (VCD₂₄). The error bars indicate 95 % confidence interval, n = 3. *p < 0.05

4.3.6 Shear stress does not affect the toxicity of lipoplex in inefficiently transfected K562 cell line

Liposomes used for gene delivery are initially evaluated in vitro in cultured cells under static conditions for their ability to deliver cargo inside the cell. The initial evaluations are thus carried out in the absence of shear, which the liposomal formulations get subjected to upon injection into blood vessels in animals. Liposomes with low toxicity, when evaluated in cell cultures, have resulted in significant toxicity to blood cells in the form of transient leukopenia and neutropenia, both in animal models and human clinical trials.

The results in CHO-S cells above indicate that toxicity of lipoplex is increased in the presence of shear stress. A study done by Mardikar and Niranjana evaluated the robustness of various cell lines and found shear sensitivity in the following order HL60 > U937 > SF9 > PUTKO > DA6.21 > K562, with HL60 being the most shear-

sensitive cell line and K562 the most robust. Hence we next evaluated whether the same effects of liposomal toxicity are seen in K562 cells, a naturally suspended cell line. K562 cells are not as efficiently transfected by Lipofectamine 2000 as CHO-S cells. There was no substantial cell death immediately after exposure of cells to shear stress, both in the absence or presence of lipoplex (grey bars in Figure 4.8a,b). The cell density of K562 cells doubled 24 h post-transfection irrespective of whether cells were incubated with lipoplex in the absence or presence of shear stress (white bars Figure 4.8a, b). The transfection efficiency of K562 cells is low and is slightly, but not significantly, increased in the presence of shear (Figure 4.8c). Thus the adverse effect of lipoplex on cell growth in the presence of shear is not seen in the inefficiently transfected K562 cell line.

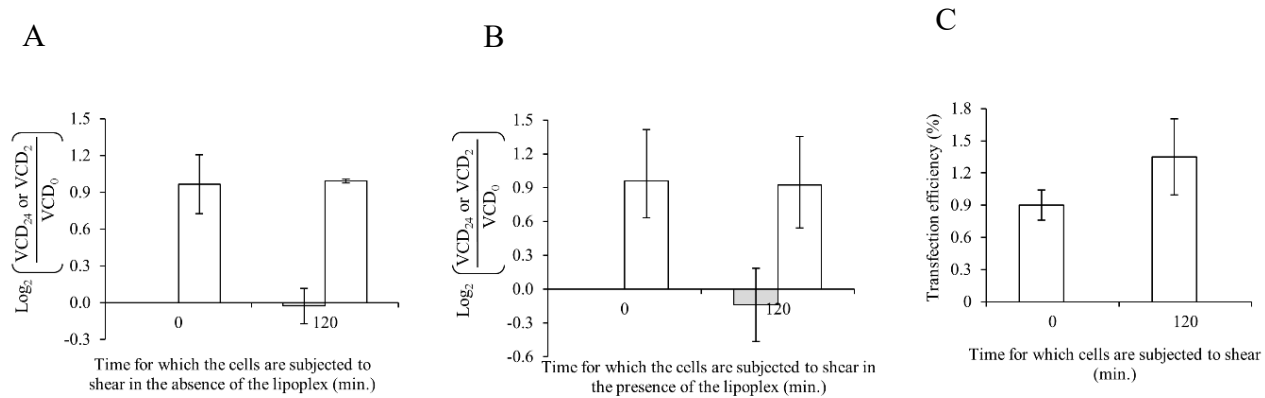


Figure 4.8 Effect of shear stress on cell density and transfection efficiency of K562 cells in the presence or absence of the lipoplex

K562 cells were subjected to low shear stress for 120 min in the presence or absence of the lipoplex and monitored for changes in cell density and viability immediately after flow and after 24 h of incubation. a Viable cell density (VCD) normalized to initial viable cell density for K562 cells subjected to low shear stress for 120 min. b Viable cell density normalized to initial viable cell density for K562 cells subjected to low shear stress in the presence of lipoplex for 120 min. Immediately after subjecting cells to shear stress (grey bars), after 24 h (white bars). Initial viable cell density (VCD₀), viable cell density immediately after flow (VCD₂), 24 h after flow (VCD₂₄). c Transfection efficiency. The error bars indicate 95 % confidence interval, n = 2

4.4 Discussion

Shear stress is a meaningful parameter known to affect various aspects of cell physiology like endocytosis and pinocytosis [156,157,177], membrane fluidity [166,167], inducing membrane fusion [168], and more recently, it was shown to facilitate uptake of extracellular macromolecules [173,174], possibly through formation of transient pores in the cell membrane [178]. Hence shear stress can also potentially modulate transgene delivery, and, given the number of liposomal formulations in human clinical trials, it is a significant parameter that warrants careful consideration. It is already established that high levels of shear stress are deleterious to suspension cells [175]. Our simple flow apparatus comprising of pumping suspension cells using a peristaltic pump also showed similar results for CHO-S cells with high levels of cell death at high wall shear stress but not at the low and moderate shear stress levels. Though shear stress has been known to affect cell survival and, for reasons described above, can be expected to affect liposomal delivery of cargo to suspension cells, to our knowledge, there have been no studies explicitly analysing the effect of shear stress on liposomal DNA delivery to suspension cells. Harris and Giorgio demonstrated that convective flow enhances lipoplex delivery to cellular monolayers in vitro. They discussed that convective flow increases the collision rate of lipoplex onto cell surfaces. This is why the hydrodynamic environment must be considered when executing vector design for transfection and gene delivery experiments [169].

We report that exposure of CHO-S cells to shear stress in the presence of lipoplex reduced transfection efficiency and cell growth in the subsequent 24 h period while causing greater cell clumping. We further evaluated whether this effect could be attributed simply to the interaction of the cells with lipid in the presence of shear. The size and zeta potential of lipofectamine 2000 has been reported to change upon complexation with DNA [179]. In an uncomplexed state, the reported zeta potential was -4 mV, and upon complexation with plasmid DNA, it was -24 mV. The hydrodynamic diameter in a complexed state was reported to increase to 488 nm from 319 nm in an uncomplexed state [179]. Shearing of cells in the presence of liposome alone also reduces cell growth in the subsequent 24-h period, though not to an extent similar to that due to the lipoplex. This suggests that the increased toxicity is not

entirely explained by the interaction of the liposome alone with the cell in the presence of shear stress. This could be due to the differences in zeta potential and/or size of the liposome and lipoplex reported in the literature. To further check if the increased toxicity due to lipoplex in the presence of shear stress might be due to long-lasting modification of the lipoplex with shear, we subjected the lipoplex to shear, subsequently using the sheared lipoplex for transfection. It was observed that there is only a slight reduction in efficiency following the 2 h incubation of lipoplex both in the presence and absence of shear stress. Such slight loss of transfection efficiency was previously reported where the DNA–Lipofectamine 2000 complexes were relatively stable and continued to provide high transfection efficiency even up to 2 h after complexation [180]. This, however, does not preclude a change in shape and therefore increased toxicity when lipoplex is sheared along with cells. Interestingly, there is a slight increase in cell growth when cells are transfected with sheared lipoplex compared to the cell growth upon transfection with lipoplex incubated under static conditions.

The reduced transfection efficiency and increased lipoplex toxicity observed at low shear stress could also possibly be due to the effect of shear stress on cells, making the cells more susceptible to lipoplex toxicity. In that case, these effects should be seen when transfection is carried out immediately after subjecting cells to shear stress. Indeed, subjecting CHO cells to sustained low shear stress prior to transfection (for 2 h, resulted in reducing the transfectability of CHO cells but did not increase cell death. This indicates that the observed effect of reduced transfection efficiency could be due to shear stress affecting the ability of cells to uptake and/or deliver the foreign DNA to the nucleus. This also suggests that the increased toxicity of lipoplex in the presence of shear stress results from cellular interaction with lipoplex in the presence of shear stress and likely not due to other long-term cellular changes upon exposure to shear stress. Lipoplexes with low toxicity *in vitro*, when injected into the bloodstream where they are subjected to shear stress, have resulted in significant toxicity to blood cells in the form of transient leukopenia and neutropenia both in animal models and human clinical trials [181–183], though the cause of this is not clear. We did not observe a similar effect of higher toxicity in the presence of shear stress in K562 cells. K562 cells were not efficiently transfected by the lipoplex used in this study, whereas

CHO-S are efficiently transfected. It remains to be seen whether transfectability has any role in the relationship between shear stress and toxicity of the lipoplex.

Such large modulation of lipoplex delivery by shear stress raises a potentially significant issue in traditional routinely performed static *in vitro* transfections. Shear stress can have a large impact on results, especially in the field of transient transfection in bioprocessing. We find that exposure to shear after mixing cells with liposome: DNA complex, i.e., during transfection, results in a decrease in transfection efficiency and cell growth compared to transfection carried out under static conditions. This effect is not seen to the same extent when cells are exposed to shear in the absence of the liposome: DNA complex, or if the liposome: DNA complex exposed to shear is subsequently used to deliver DNA into cells not exposed to shear. Thus, evaluating the performance of liposomal delivery agents in the presence of shear could prove useful as an *in vitro* intermediate testing step before animal studies.

4.5 Conclusion

In conclusion, enhanced toxicity and reduced transfection efficiency of lipoplex are observed in CHO-S cells exposed to shear stress. Further studies will be necessary to fully understand the mode of toxicity. We propose that this factor should be taken into account in the design and careful curation for large-scale transfections in bioreactors for transient protein expression. Our results may also be relevant to gene therapy where shear stress may contribute to the performance of *in vitro* static cell cultures not being predictive of performance in animal models where the lipoplex is intravenously injected, and evaluation of liposomal delivery agents in the presence of shear stress could be considered as an intermediate testing step before animal studies for gene therapy.

Chapter V.

Towards establishing continuous nutrient release using hydrogels: Hydrogel development and characterization

5.1 Summary

The upstream development of bioprocesses for the production of recombinant biotherapeutics consists of the four stages initiating with clone selection, clone stability testing, process development and scale-up experiments. During clone selection, hundreds of clones with the gene of interest are grown under the stationary condition in 96 well format to find the fastest growers and highest producer clones based on productivity. The selected clones are then advanced to the next stage of selection, where they are grown in small scale culture formats like tube spin and shake flasks, which resembles the agitated environment similar to production bioreactors but without any pH temperature, dissolved oxygen (DO) or feed rate control. Identifying desirable high producers with the highest productivity and product quality traits in a transfected pool of cells requires screening of a large number of clones. Clone screening is a time consuming, resource-intensive step and poses a bottleneck in cell-line development. Growth and productivity vary enormously among clones [6,7]. Feeding can be a key difference affecting traditional clonal selection. This selection process is error-prone because there is evidence that clone selection from measuring growth and productivity is not a predictor for selecting a stable cell line [184]. From the shake flask experiments, only a few clones are selected and transferred to bench-scale reactor experiments before scaling up to large scale industrial bioreactors because of the expensive and resource-intensive nature of this stage of process development. Moreover, shake flasks are deficient in controlling pH, DO or feeding; hence may not be able to select the highest producer with the desired glycosylation profile since the product titre and quality can be affected by the actual process conditions [185]. Therefore, an inexpensive, effective solution is desired in the conventional upstream development space that can have continuous feeding making the scale down model comparable to an industrial bioreactor

with sufficient volume for the multiplicity of offline characterization of product titre, quality and other important process conditions and parameters.

5.2 Introduction

Shake flasks, predominantly used for batch and fed-batch modes of operation, are widely used in an academic and industrial setting. As explained while introducing the thesis, in batch culture, an excess of nutrients is supplied to the culture at the beginning without replenishing any nutrients that get exhausted during the production. However, this mode leads to exhaustion of nutrients and hence results in lower titres. Exhaustion of key nutrients like amino acids may lead to a change in the amino acid sequence of antibodies [186]. A compromise between regular feeding and optimum cell densities is achieved by using a nutrient-enriched medium. This can lead to the following drawbacks: Higher waste metabolites and/or formation of inhibitors. An excess of nutrients also leads to sub-optimal performances of cells. One of the ways to solve this problem is by feeding at regular intervals to maintain a constant supply of nutrients without the complications of overfeeding and nutrient limitation. The universal small-scale cultivation platforms like shake flasks, which allow a fed-batch mode of operation, are critical for fast and reliable early process development. The use of the fed-batch mode of operation in early process development stages leads to scalable and accurate results from small-scale to larger process development stages [187–190].

Typically, cells are grown in a chemically defined medium containing an osmotically balanced and buffered cocktail of carbon source, amino acids, vitamins, trace elements, antioxidants and other vital nutrients. Amino acids are the building blocks required for protein synthesis and are hence supplemented in excess for recombinant protein production. The cells cultured *in vitro* have different requirements than cells growing *in vivo*. An excess of these nutrients leads to by-product accumulation, like lactate and ammonia, which are known to be growth inhibitory and also affect the product quality.

Continuous feeding, which requires automation, is not feasible for small-scale culture platforms due to its expensive nature. The use of nutrient delivery systems that can achieve a fed-batch mode without all the automation is highly desirable. In this study, we propose using hydrogel to deliver various nutrient feeds that allow higher

productivity and maintain higher peak cell densities for longer. Since their synthesis in 1954 by Wichterle and Lim in 1954, hydrogels have been a subject of a growing multidisciplinary field of research [191]. Hydrogel technologies have been successfully used for an array of applications, from tissue engineering, regenerative medicines, and biomedical applications to pharmaceuticals [192,193]. Hydrogels are three-dimensional polymer networks that can be swollen by water and loaded with the desired feed for the controlled slow release of nutrients. Such slow release of nutrients can be customized using a different proportion of the polymer and the crosslinking agent used. Different variants of diffusion-based delivery systems have been previously reported for microbial systems for the maintenance of pH and glucose from our group [194–196].

In terms of bacterial bioprocess development, various systems have enabled shake flask ranging from simple silicone discs to sophisticated equipment for applications like screening. Among the ever-growing spectrum of polymer-based devices for release in small scale cultivation devices, an early example would be silicone elastomer discs for shake flasks and deep well plates [195,197]. These discs embedded with sodium carbonate help control the pH [198]. The EnBase system developed by Panula-Perälä et al. [194] is a gel layer comprising of starch which is covered with a medium containing the enzyme glucoamylase. The EnBase system is based on the enzymatic degradation of the starch molecules by glucoamylase, and once starch diffuses into the liquid, consequently, glucose is released. The EnBase system has been commercialized into the EnBase Flo cultivation system. In all these increasing applications of various polymeric systems, the payload (compound of interest, substrate for an enzyme, carbon source or the pH-regulating agent) is embedded in the polymer matrix. Once the controlled-release system comes into contact with liquid, water diffuses into the matrix dissolving the embedded payload, which diffuses out of the matrix into the medium. The release rate depends on material characteristics (e.g., hydrophobicity, degree of crosslinking, particle size, and other material properties) and the concentration gradient. Using this approach, a scale-up to 100 L was demonstrated for a bacterial process.

One challenge with these systems is the restriction to the substrate, glucose in the case of the EnBase system and lack of control over the feeding rates and active process control. Advanced systems like the fed-batch microtiter plate (FB-MTP BioLector) have been developed to solve this by having active process control along with online

monitoring with the flexibility of adding any desired compound to the culture. BioLector has been proven to enable multiple parallel fed-batch experiments at a small scale. A channel connects a reservoir well with a culture well, and the desired compound diffuses from the reservoir into the culture well. Hence, the feed rate can be adjusted to the experiment's needs by changing the geometry of the channel and the concentration gradient [199]. The bioLector system could also be coupled with robotic liquid handling systems. Hence preliminary system has also been replaced by micropumps making feeding automated and more robust along with pH and DO control [200,201]. However, these systems require significant investment and operational costs. A summary of various commercial sophisticated high throughput systems has been listed in table 3.

In the case of mammalian cultures, glucose loaded hydrogels have been previously shown to significantly reduce lactate accumulation in mammalian cells. Hydrogels have also been demonstrated as in situ pH management system for mammalian cells [202]. Many systems like Ambr have been developed to aid the earlier stages of process development. Hydrogels have been extensively used for biomedical applications like the slow release of drugs, hormones, growth factors etc. [192]. They have not yet been attempted to emulate the fed-batch mode to cultivate mammalian cells. The application of these hydrogels in primary screening would most likely enable rapid screening and identification of the optimal cell clones for the expression of the desired product. This slow-release system is easy to manage with the possibility of running parallel cultures in a confined space, leading to screening a large number of clones without additional infrastructure.

Table 3: Summary of commercial cultivation systems

Micro Flask by Duetz	24- and 6-well sensor dishes	BioLector	Micro-24	Micro-matrix	Ambr
<p>Miniature shaken vessel Combination of a microtiter plate, sandwich cover, and clamp units No process control</p>	<p>Miniature shaken vessel (well): Oxygen and pH sensors integrated with 6/24-well microtiter plate with the florescent reader Only one parameter, either pH or DO, can be monitored but not controlled</p>	<p>Miniature shaken well (flower shape): Microtiter plate formats and operates with non-invasive, optical sensors. Real-time culture monitoring With liquid handling system option to upgrade it to a fully automatic unit</p>	<p>24 bubble column microbioreactor: 24 simultaneous cultures independent control of each reactor's gas supply, temperature and pH Single-use 24 column cassette with pH and DO sensors Independent control of each column Continuous real-time monitoring logging and controlling each column bioreactor's DO, temperature and pH</p>	<p>24 bioreactors in microtiter format: 24 bioreactors on a plate offer independent controls pH, temperature, and DO can be measured and controlled Individual liquid additions, including feeding profiles Up to four separate gas additions under individual control</p>	<p>Micro-stirred tank bioreactor: Single-use individual micro-bioreactor Closed-loop control of pH and DO with independent control of O₂ and CO₂ for each vessel Automated liquid handling for reactor set-up, feeds, base addition and sampling Integrated Vi-CELL[®] cell viability analysis optional</p>
<p>24 square deep-well plate: 2.5–4 mL/well</p>	<p>6- or 24-microtiter</p>	<p>Flower-plate: 0.8–1.5 mL/well</p>	<p>Working volume: 3–7 mL/column</p>	<p>Working volume: 1–7 mL/well</p>	<p>10–15 mL/vessel</p>

96 square deep-well: 0.3–0.75 mL/well 24 round low-well plate: 0.75–1.5 mL/well 96 round low-well plate: 0.1–0.2 mL/well	plate, and 24 deep-plate Culture volume 0.1–6 mL				
Feeding not possible	Feeding not possible	Needs a liquid handling station for feeding	Integrated liquid feed individually per well	Integrated liquid feed individually per well	Automated liquid handling for reactor set-up, feeds, base addition and sampling
[203–205]	[197,206,207]	[201,208]	[209,210]	applikon-bio.com	[211,212]

5.3 Methods

5.3.1 Synthesis of hydrogels

Synthesis of a single layer or two-layer gels: For single layer gel, 4 mg tyrosine and either 14.6 or 30 mg glutamine was added as the payload. A glass vessel of diameter 1.3 cm was used for creating these hydrogels using 150 μ L of the HEMA: EGDMA polymer mixture. There was no washing prior to measuring the release. For 2 layer gel, 100 μ l of the polymer was again used to synthesize a bottom layer with 150 mg of AT8801A feed with 2 mg tyrosine and 14.6 mg of glutamine as the payload. Over this, a 2nd layer was synthesized using 300 μ l of the polymer. The 3 layer gel was

synthesized as mentioned in the methods section, loaded with 150 mg of AT8801A feed with 2 mg tyrosine and 14.6 mg of glutamine as the payload.

5.3.2 Release kinetics for amino acids

The release kinetics of amino acids were analysed at 37 °C. The hydrogel was added into phosphate-buffered saline (PBS) with 0.05% sodium azide under shaking conditions to simulate conditions during the release in shake flasks. Samples were taken on alternate days for amino acid concentration measurement for 16 days. Amino acid quantification was carried out using HPLC. The samples were subjected to pre-column derivatization with phenylisothiocyanate (PITC), and the derivatized amino acids were quantified on HPLC (Agilent 1200 infinity series) with reverse phase C18 column (Purosphere star RP18 (5 µm) end-capped, Merck, Darmstadt, Germany). Briefly, 100 µL of the sample was spiked with 15 µg of norleucine as internal standard and lyophilized. Subsequently, 20 µL of methanol:water: trimethylamine 2:1:1 (v/v) was added, vortexed and lyophilized. Further, 20 µL of methanol:water:trimethylamine: PITC 7:1:1:1 (v/v) was added, vortexed, incubated for 20 minutes at room temperature and lyophilized. Derivatized samples were resuspended in 1 mL of eluent A (85 mM sodium acetate and 0.3 mM sodium azide in 98% water and 2% acetonitrile, pH 5.2, (w/v)). Chromatography was carried out after injecting 5 µL of the derivatized sample using an elution gradient of $T_{0 \text{ min}} = 3\%$ eluent B (100% acetonitrile), $T_{25 \text{ min}} = 13\%$ eluent B, $T_{45 \text{ min}} = 50\%$ eluent B, $T_{46 \text{ min}} = 3\%$ eluent B. Flow rate was maintained at 0.8 mL min⁻¹. Eluted derivatives were detected with a diode array detector at 254 nm with a bandwidth of 4 nm. The peak area for each amino acid was normalized to the internal standard. The amino acid concentration was calculated using a response factor calculated from the peak area of the respective amino acid (normalized to norleucine) in a standard containing 15 µg/mL of aspartate, glutamate, glutamine, glycine, asparagine, serine, histidine, threonine, arginine, alanine, proline, tyrosine, valine, methionine, cystine, isoleucine, leucine, phenylalanine, tryptophan and lysine. It is important to note that in this method for amino acid measurement, cysteine and cystine were not resolved as separate peaks but coeluted as a single peak and could not be accurately quantified.

5.4 Results

It has already been established that hydrogels can deliver glucose and protein hydrolysates to CHO cells and have shown to be an effective pH management system in mammalian cells. Here we have attempted to standardize the hydrogel for delivering an optimal feed to improve peak cell densities, maintain the peak density for longer, and increase productivity without the need for continuous monitoring and complicated feeding regimes.

We standardized different gel formulations intending to identify acceptable release rates that can sustain a nutrient release for longer and are suitable for sustaining mammalian cultures. The three fundamental components of preparing a hydrogel are monomer, initiator, and crosslinker. A crosslinker in the hydrogel is added to introduce the right degree of cross-linking in this polymeric network. After formation, the hydrogel needs to be washed to remove impurities, and these include a non-reacted monomer, initiators, crosslinkers, and unwanted by-products of side reactions left from the polymer preparation process. Hydrogels are synthesized by reacting hydrophilic monomers with multifunctional crosslinkers. Various polymerization techniques can be used to form gels, including bulk, solution, and suspension polymerization. The bulk polymerization of monomers results in a homogeneous hydrogel producing a glassy, hard and transparent polymer. When submerged in water, the glassy matrix swells to become soft and flexible. The polymerization can be initiated thermally, via UV-irradiation, by redox initiator or by introducing small molecules.

5.4.1 Standardizing the hydrogel geometry for sustained release in mammalian cell culture: Effect of crosslinking, nutrient payload and hydrogel geometry

Hydrogels can be prepared via various methods like free radical polymerization. The free radical initial may be excited thermally or via UV irradiation exposure. The percentage of crosslinking agent can be varied to adjust the crosslinking density that controls the swelling and hence the release rate of the nutrient payload according to the requirement. Glutamine is used as a representative amino acid to measure the release of amino acids and Ethylene glycol dimethacrylate (EGDMA) as a crosslinking agent with Azobisisobutyronitrile (AIBN) as a free radical initiator. Crosslinking at a higher

percentage led to sustained release over a longer period of time. 20% concentration was found to work better than 5% and 10% (Figure 5.1). Higher the cross-linking, lower is the release rate, as seen in Figure 5.1. The release was in 25 mL PBS with 0.05 % azide at 37° C under shaking conditions with 250 mg AT8801A feed and 25 mg glutamine. There was no washing involved for any release measurement. An even higher crosslinking would make the release even slower but would make the hydrogels brittle. Henceforth, all gels have been synthesized using the 20% Ethylene glycol dimethacrylate as a crosslinker.

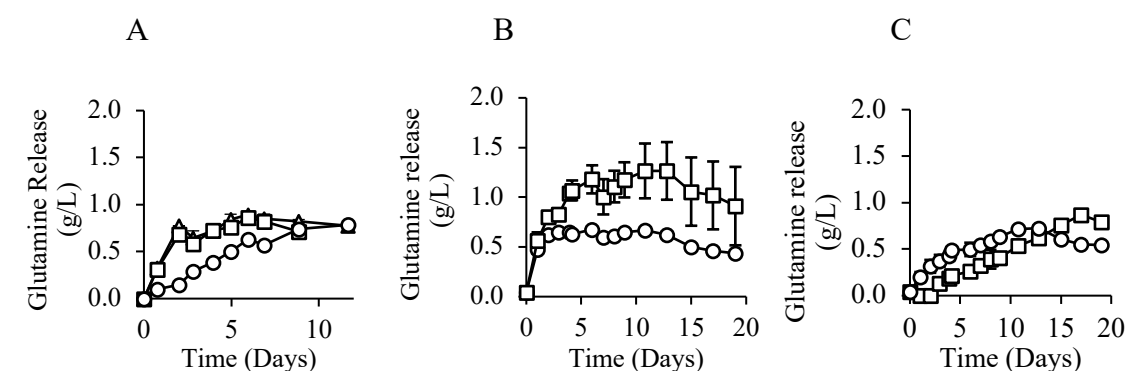


Figure 5.1: Comparative influence of crosslinking, loading and geometry on glutamine release

(A) Release kinetics of glutamine loaded hydrogel with different percentages of crosslinking monitored in sterile PBS; Δ - Hydrogel with 5% crosslinking, \circ - Hydrogel with 20% crosslinking, \square - Hydrogel with 10% crosslinking (B) \circ - Single-layer hydrogel with 15 mg glutamine, \square - Single layer hydrogel with 30 mg glutamine (C) \circ -Three-layer hydrogel with 45 mg glutamine, \square - Two-layer hydrogel with 45 mg glutamine

After establishing the percentage of crosslinking, the geometry and the types of gels were established. Previously simple disc-shaped gels have been used in a growing number of studies. We synthesized simple single layer gel, two-layer gel and a cylindrical 3-layer gel to compare release suitable for mammalian cell culture. Again glutamine was used as an indicator to measure the approximate release rate for amino acids that have similar abundance or solubility or both. For single layer and two-layer gel, tyrosine and glutamine were added as a payload on a disc, whereas for three-layer gel, a cavity was formed where the nutrient payload was placed. Measuring glutamine release with two different payloads demonstrates increasing the payload also led to an

increase in the release rate for glutamine. This indicates loading is among the important factor regulating release. Measurement of glutamine release only through single layer gel indicates a very high release rate in the 1st three days, which indicates additional loss of the amino acid payload compared to two layer and three layer gels. Such a release profile won't be able to efficiently supply amino acids to animal cell cultures as they last for several days as compared to bacterial cultures. With the two or three-layer gel, we could also observe sustained release for at least 6-7 days, which is suitable for mammalian cell culture application.

5.4.2 Toxicity profile for NutriGel in CHO cell culture

We further tested if this basic formulation does not have any toxicity effects in CHO cells. A suspension adapted CHO cell culture was supplemented with either a single or two-layer gel. As seen in Figure 5.2, supplementation of single or two-layer hydrogel does not lead to any toxicity in CHO cells. Since the gels have to be washed before being used in cultures, the majority of the payload is released during the washing step in single and two-layered gels, making them equivalent to empty gels without any payload. The cultures supplemented with the hydrogel grow to similar density and have similar longevity as the control cultures without hydrogels. Also, it is important to note that there is no improvement in culture properties because, as expected, there is a significant loss of the nutrient payload during the washing.

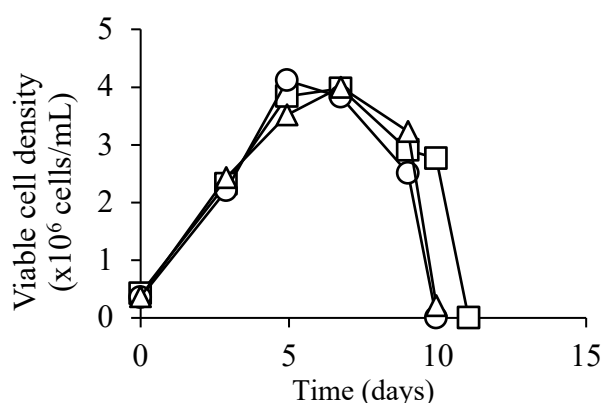


Figure 5.2: CHO cell culture supplemented with hydrogels do not show enhanced toxicity

Viable cell densities of CHO cells being supplemented with ○- single layer hydrogel, △- two-layer hydrogel, □- Unsupplemented control culture.

5.4.3 Standardizing the amount of nutrient payload suitable for supporting animal cell culture

The actual performance of varying amounts of feed was tested on IgG producing CHO cells (Figure 5.3), and the 3 layer gels were synthesized as described in the methods sections. The cavity was again adjusted according to the payload, and the top layer was filled using the following volume of the monomer, 100 μ l for 50 mg and 100 mg, 200 μ l for 150 mg feed and 370 μ L of 250 mg feed to fabricate the hydrogel. CHO cell cultures were supplemented with these hydrogels along with an unsupplemented control culture. As a positive control culture, we also supplemented CHO cell culture with the traditional bolus feeding equivalent to the nutrient payload in the hydrogel. For bolus fed cultures, cultures were fed with 1X of the corresponding feed (20X) on days 3, and 6. A total of 2X of the feed was added, where 1X corresponds to medium concentration without the bulk salts. A total of 2.5 mL liquid feed was added to the 25 mL culture volume of the bolus fed cultures. The amount of payload in NutriGel_T was 250 mg, while the liquid bolus feed addition resulted in the addition of 100 mg of the feed, both to the same initial culture volume. The hydrogel payload was kept higher due to loss of payload during the initial washing and pre-incubation of the hydrogel for at least 2.5 days to remove unpolymerized monomers. The loss of payload was variable for the different components. Supplementing hydrogels with an increasing amount of feed aided in improving culture performance. Supplementing cultures with 250 mg feed improved culture performance comparable to the traditional bolus fed cultures. Hence we continued our further experiments with 250 mg of feed.

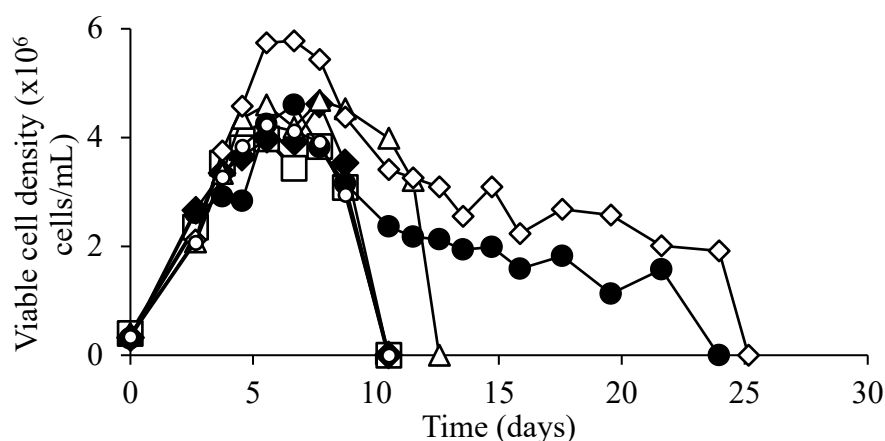


Figure 5.3 Standardization of nutrient payload for assisting feeding in mammalian cell culture

Viable cell densities of CHO cells being supplemented with three-layer hydrogel with different payloads, □-a hydrogel with 50 mg nutrient feed, ○-Control culture without any hydrogel supplementation, ●-Control culture with traditional bolus feeding, ◆-hydrogel with 100 mg nutrient feed, △- hydrogel with 150 mg nutrient feed, ◇- hydrogel with 250 mg nutrient feed.

5.4.4 Hydrogels can maintain a continuous supply of amino acids for an extended duration suitable for supporting animal cell culture

A hydrogel formed by the bulk polymerization of HEMA with EGDMA as a crosslinker was evaluated for in situ release of a nutrient mixture including 18 amino acids. Since alanine and glycine are typically excreted by cells in culture, they were not included in the feed. Briefly, this hydrogel comprises a central monolithic reservoir system surrounded by a hydrogel layer. The nutrient payload is dispersed as a solid powder within the hydrogel matrix in the central reservoir. We first formulated a simple feed mixture having the same composition as the culture medium but without bulk salts. These hydrogels will be subsequently called NutriGel₁ (composition in Table 4, Figure 5.4). The release of amino acids from washed and pre-swollen NutriGel₁ was monitored in PBS buffer over a duration of 2 weeks. Cysteine/cystine could not be accurately quantified. Figure 5.6 a, b shows the cumulative release of 17 amino acids in the feed mixture. All amino acids continue to be released from the hydrogel for a period of at least seven days.

Release rate constants were further calculated for all amino acids. Assuming a 0.75 void fraction in the central reservoir and after accounting for the amino acid content lost during the wash, we calculate that at the initial amino acid loadings used, the concentrations of all amino acids in the reservoir except cysteine/cystine and tyrosine will be less than their solubility at 37°C. Hence, the release rate is assumed to follow first-order release kinetics as described by the equation [213]

$$\frac{dm_i}{dt} = k_i (m_{0i} - m_i), \text{ resulting in } m_i = m_{0i} \left(1 - \frac{1}{e^{k_i t}}\right) \dots (1)$$

for $i=1$ to 17, where m_i is the amount of i^{th} amino acid released at time t , m_{0i} is the initial loading of the i^{th} amino acid in the reservoir, and k_i is the rate constant for release for the i^{th} amino acid. The amino acid release data for the first seven days was fit to the above equation (1) for all amino acids except tyrosine to obtain the release rate constants. The r^2 values for all fits were above 0.95 except for proline, phenylalanine ($r^2 > 0.92$) and aspartate ($r^2 > 0.68$). For amino acids with very low solubility, i.e., cystine and tyrosine, a zero-order release is expected, as described by [213]:

$$\frac{dm_i}{dt} = k_i, \text{ resulting in } m_i = k_i t \dots (2)$$

For tyrosine, the amino acid release data was fit to the above equation (2) to obtain the release rate constants ($r^2 > 0.84$). It should be noted that consistent with its low solubility, the release rate for tyrosine is very low, and the release rate of cysteine/cystine is also expected to be very low. Figure 1e, f shows the release rate constants for all amino acids. As per equation (1), the amino acid release rates are proportional to the initial loading of the amino acid within the central reservoir. Thus, this provides a simple tool to vary individual amino acid release rates for all amino acids (except cysteine/cystine and tyrosine) by varying their initial loading.

To independently confirm the effect of initial loading in the central reservoir on the release rate, we next evaluated a feed mixture comprising 8 mg each of all 18 amino acids along with 100 mg HEPES (composition in Table 4). These hydrogels will be referred to as NutriGel₂^H. Figures 5.5 c, d, and e, f shows the cumulative release profile and release rate constants for the release of all amino acids from NutriGel₂^H. The release rate constants are similar to those calculated for NutriGel₁, indicating that the release rate is indeed proportional to the initial loading of the amino acid in the reservoir except

for tyrosine and is not substantially affected by changes in the composition of the other amino acids in the reservoir.

A plot of release rate constant in NutriGel₂^H vs solubility at 37° C shows a weak positive correlation (Figure 5.5g) (amino acid solubility at 37° C was calculated using the Sober equation, δ and θ for the equation were obtained from Bowden, 2018 [214]). There is no correlation between the release rate constants of the amino acids and their molecular weight (data not shown). This is not surprising since the molecular weights of all amino acids lie within a narrow range. The local pH in the reservoir, which is not known, could affect the charge on the amino acids and hence their release. Due to the buffering action of HEPES and the effect of pH on the solubility of amino acids, we next assessed whether the presence of HEPES in the payload had any effect on release rates. The release rates for the amino acid formulations in NutriGel₂ were then analysed in the presence of an equal amount of glucose instead of HEPES (NutriGel₂^G). With the exception of lysine, there was no substantial difference between the release rate constants in the presence or absence of HEPES (Figure 5.6).

To increase the release rates of tyrosine, the amino acid with the lowest release rate constant, we dispersed 4 mg of tyrosine directly in the bottom layer of the hydrogel. Release kinetics of tyrosine from such a matrix was separately measured and found to be 0.09 mg/day. All hydrogels containing tyrosine thus dispersed are indicated by including ^T in the superscript in the name of the hydrogel. Since an oversupply of cysteine can cause toxicity [215], no further loading of cysteine/cystine was evaluated. However, a similar strategy can increase the supply of cysteine/cystine if desired.

With the demonstrated ability of NutriGels to release amino acids over at least a week, we next explored whether such hydrogels could be used to achieve a closed in situ feeding system for animal cell culture. Though the release rate of only amino acids has been measured here, other low abundance components of cell culture medium like vitamins, trace elements, and antioxidants also play an essential role [216,217] and have been included in the feed mixture payload of the hydrogels used for cell culture. We have used a recombinant CHO cell line expressing IgG as a model culture system to assess whether in situ feeding of amino acids and other micronutrients can enable an increase in longevity of the culture in order to increase productivity. We first use a

hydrogel with a nutrient feed payload having the same composition as the culture medium but without the bulk salts (NutriGel₁).

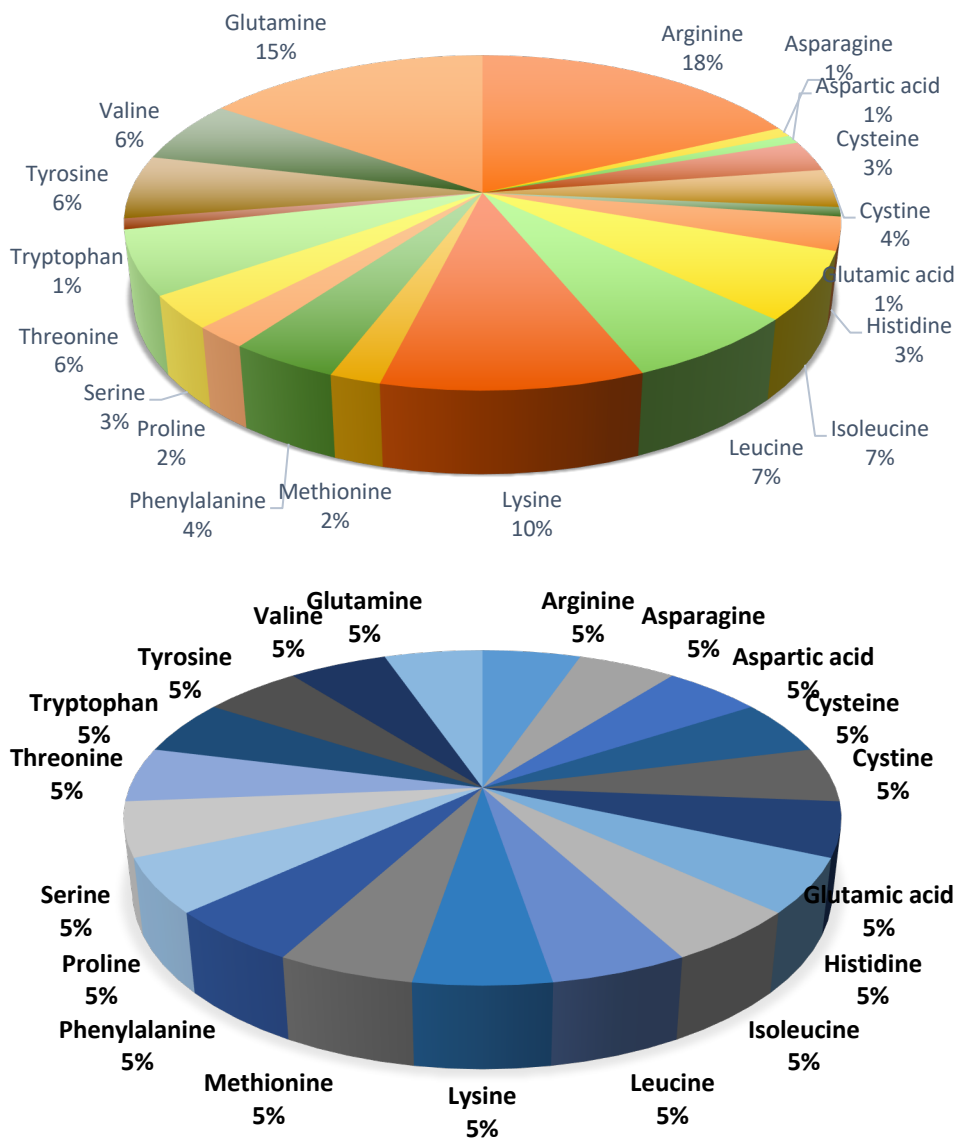


Figure 5.4: Amino acid composition for the two nutrient mixture payloads to create NutriGels

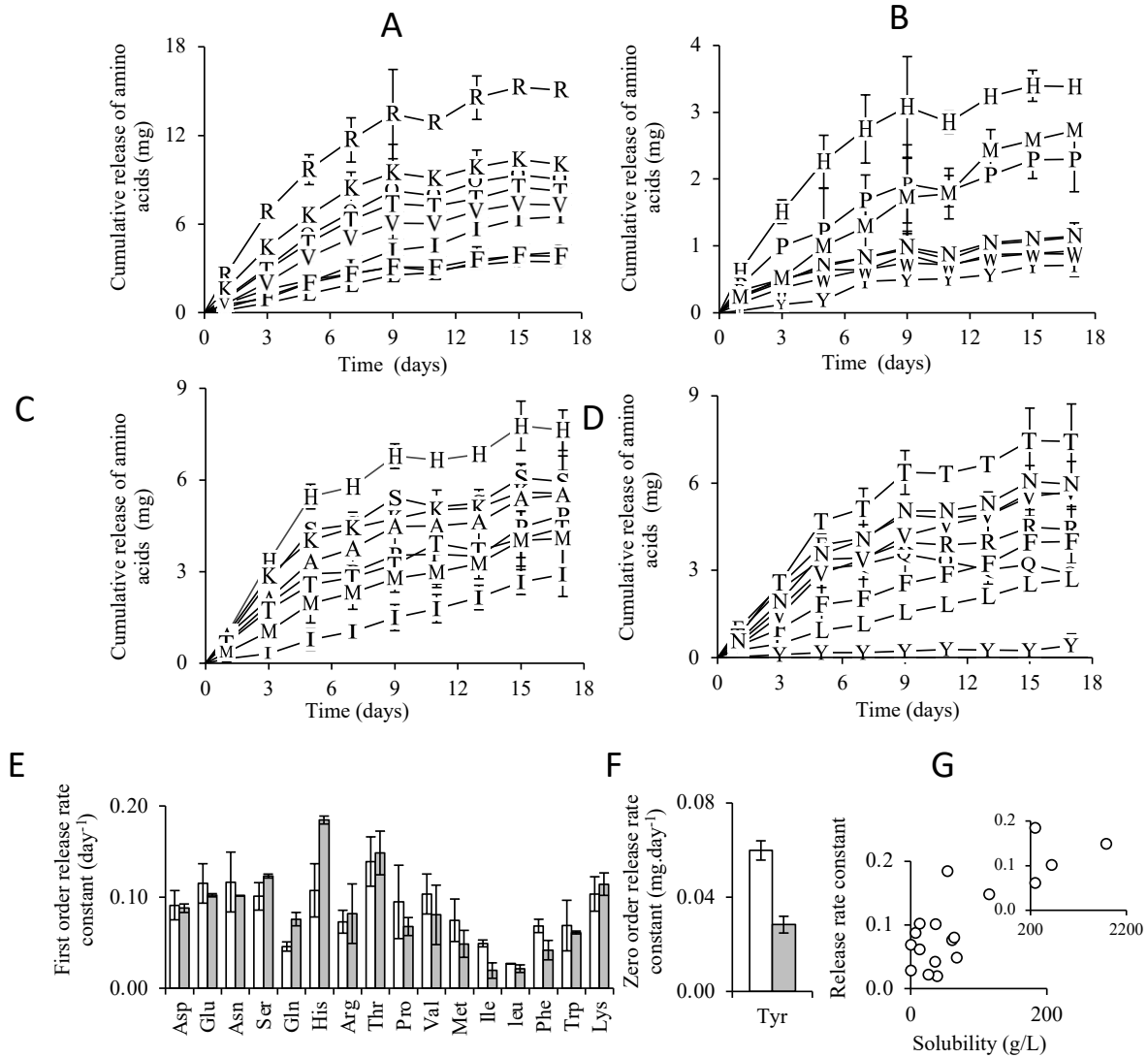


Figure 5.5: Cumulative amino acid release profile from two different compositions of amino acid in the NutriGel payload viz NutriGel₁ and NutriGel₂^H

Release kinetics of amino acids for prewashed NutriGel₁ or NutriGel₂^H were characterized in 25 mL PBS with 0.05% sodium azide incubated at 37°C under shaking conditions. Amino acid concentrations were quantified by reversed-phase HPLC. (A, B) Cumulative amino acid release profile from NutriGel₁. Markers depict single amino acid abbreviations. (C,D) Cumulative amino acid release profile from NutriGel₂^H. Markers depict single amino acid abbreviations. (E, F) Release rate constants for NutriGel₁ gel (white bar) and NutriGel₂^H (grey bar). (G) Relationship between release rate constant and solubility. Error bars indicate 95% confidence interval, n=2.

5.4.5 Effect of abundance and solubility

In Figure 5.5, we observe how release rates depend on the abundance in the feed and the solubility of individual amino acids. The highest release rates were observed for arginine and lysine, amino acids with the highest abundance in the formulation and high solubility (Figure 5.6). The lowest release rates were observed for amino acids cysteine/cysteine, tyrosine, aspartate and glutamate. These amino acids either have very low solubility or have low abundance in the feed mixture. A plot of release rates vs abundance in the feed mixture of AT880A indicates that the release rates are correlated to the loading of the amino acid ($R^2 = 0.90$, $p < 0.00001$) Figure 5.6).

The abundance of the amino acid in the feed mixture inside the hydrogel and their solubility are thus the two parameters which have the most effect on the release rates of the amino acids. The dependence on solubility is expected since it affects the concentration gradient for diffusion. The dependence on abundance may stem from its effect on the concentration of the amino acid that can be maintained at the edge of the inner core, which influences the concentration gradient for diffusion and hence the release rate through the hydrogel.

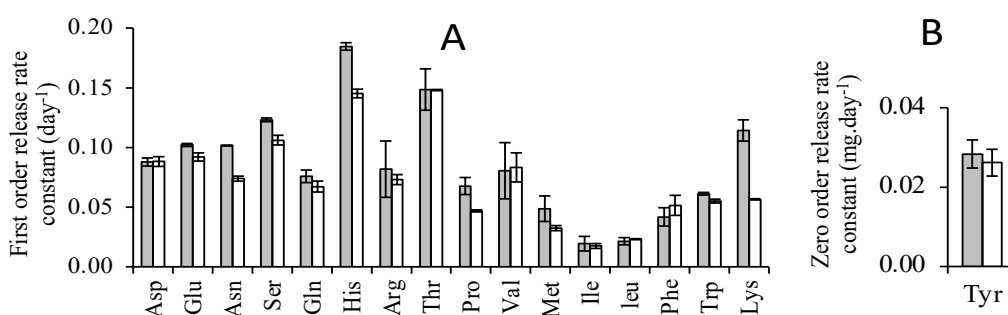


Figure 5.6: Effect of inclusion of HEPES in the payload on the release rate constant

Release kinetics of amino acids for prewashed NutriGel^{2H} or NutriGel^{2G} were characterized in 25 mL PBS with 0.05% sodium azide at 37 °C under shaking conditions. Amino acid concentrations were quantified by reversed-phase HPLC. Release rate constants for NutriGel^{2H} (grey bars) and NutriGel^{2G} (white bars). Release rate constants for NutriGel^{2H} are taken from Figure 5.5 e,f. Error bars indicate 95% confidence interval, n=2

Table 4: Compositions of payloads used in this study

	Amino acids ^{a,b}	HEPES	Glucose	Vitamins	Trace elements	Thioctic acid	Antioxidant	Nucleoside precursors	Linoleic acid
NutriGel ₁	+ ^a	+		+	+	+	+	+	+
NutriGel ₂ ^H	+ ^b	+							
NutriGel ₂ ^G	+ ^b		+						
NutriGel ₁ ^T	+ ^a	+		+	+	+	+	+	+
NutriGel ₁ ^{AA,T,G}	+ ^a		++						
NutriGel ₁ ^{T-V}	+ ^a	+	+		+	+	+	+	
NutriGel ₁ ^{T-TE}	+ ^a	+	+	+		+	+	+	
NutriGel ₁ ^{T-AO}	+ ^a	+	+	+	+	+		+	
NutriGel ₁ ^{T-N}	+ ^a	+	+	+	+	+	+		
NutriGel ₁ ^{T-TA}	+ ^a	+	+	+	+		+	+	
NutriGel ₂ ^{HVT,T}	+ ^b	+		++++	++++	+	+	+	
NutriGel ₁ ^{T,G}	+ ^a	+	++	+	+	+	+	+	+

(x-number of + indicates x-times of concentration indicated below, ^{a,b} indicate the amino acid composition type, ^T Indicates the presence of 4 mg tyrosine in the bottom layer of the hydrogel

L-Amino acids ^a (mg)	Arginine hydrochloride 29, Asparagine monohydrate 2, Aspartic acid 1, Cysteine dihydrochloride 5, Cystine hydrochloride monohydrate 6, Glutamic acid 1.5, Histidine hydrochloride monohydrate 5, Isoleucine 11, Leucine 11, Lysine hydrochloride 16, Methionine 3, Phenylalanine 7, Proline 4, L-Serine 5, Threonine 10, Tryptophan 1.7, Tyrosine 10, Valine 10, Glutamine 25
L-Amino acids ^b (mg)	Arginine hydrochloride 8, Asparagine monohydrate 8, Aspartic acid 8, Cysteine dihydrochloride 8, Cystine hydrochloride monohydrate 8, Glutamic acid 8, Histidine hydrochloride monohydrate 8, Isoleucine 8, Leucine 8, Lysine hydrochloride 8, Methionine 8, Phenylalanine 8, Proline 8, Serine 8, Threonine 8, Tryptophan 8, Tyrosine 8, Valine 8, Glutamine 8
Trace elements (mg)	Ammonium metavanadate 0.00006, Ammonium molybdate tetrahydrate 0.0006, Copper sulphate pentahydrate 0.0001, Ferric nitrate nonahydrate 0.005, Ferrous sulphate heptahydrate 0.04, Nickel chloride 0.00001, Sodium metasilicate nonahydrate 0.001, Sodium selenite 0.001, Stannous chloride dehydrate 0.00001, Zinc sulphate heptahydrate 0.04
Vitamins (mg)	Ca-D-Pantothenic acid 0.2, Choline chloride 0.9, D-Biotin 0.0004, Folic acid 0.3, Niacinamide 0.2, Pyridoxal hydrochloride 0.2, Pyridoxine hydrochloride 0.003, Riboflavin 0.02, Thiamine hydrochloride 0.2, Vitamin B12 0.07, Myo-Inositol 1.3

Antioxidants (mg)	L-Ascorbic acid 2, Ethanolamine hydrochloride 1.4, Glutathione reduced 0.2, Putrescine dihydrochloride 0.01
Nucleoside precursors (mg)	Hypoxanthine 0.2, Thymidine 0.04
Miscellaneous (mg)	Linoleic acid 0.004
Glucose (mg)	Glucose 100
Thioctic acid (mg)	Thioctic acid 0.011
HEPES (mg)	HEPES 100

5.5 Conclusion

We tried to establish an alternate application for hydrogels as a nutrient delivery system. Release studies using glutamine as a marker led us to understand the correct percentage of the cross-linking agent. It also highlighted that the mode of release is diffusion and is correlated to the surface area size of the cavity. The hydrogel includes the complex nutrient feed dispersed in the form of a solid in a central reservoir.

We demonstrate that it is possible to modulate the release rates of individual amino acids through this hydrogel by changing their initial loading in the central reservoir, with the exception of low solubility amino acids tyrosine and possibly cystine/cysteine. This provides the ability to tailor release rates for individual amino acids as required for the specific application. The release rates of these low solubility amino acids can be increased if required by loading them outside the hydrogel reservoir. The use of modified amino acids, such as phosphotyrosine disodium salt, (with higher solubility/stability) can also allow control over the release rate of the low solubility amino acids through the reservoir if desired [218,219].

Chapter VI.

Towards in situ continuous feeding via controlled release of complete nutrients for the fed-batch culture of animal cells

6.1 Summary

The small-scale culture of animal cells in suspension is important for many applications. At a small-scale, fed-batch is achieved either by manual bolus feeding or the use of liquid handling robots. In this study, we report an alternate application of a hydrogel for in situ continuous delivery of a nutrient feed comprising 18 amino acids, vitamins, antioxidants, and trace elements. We show that amino acid release is sustained for at least seven days. Importantly, the release rates of individual amino acids can be independently modulated by changing their loading. We demonstrate the application of this hydrogel for complete in situ feeding of nutrients to a suspension adapted CHO cell line expressing IgG leading to a 2.7-fold and a 4-fold improvement in integral viable cell density (IVCD) and volumetric productivity, respectively. This is similar to improvements obtained by bolus liquid feeding. Further, supplying glucose from the same hydrogel to eliminate manual feeding led to a 1.8-fold increase in IVCD accompanied by a 3-fold increase in volumetric productivity as compared to batch culture. In summary, this study provides a proof of concept that hydrogels can enable completely closed in situ feeding for mammalian cell culture, requiring no external intervention. Such continuous in situ delivery can potentially enable closed culture systems while maintaining nutrients at low levels mimicking physiological concentrations.

6.2 Introduction

Small-scale culture of animal cells in suspension is of importance for many applications such as process development for the production of recombinant proteins and viral vaccines, stem cell culture, and cell therapy applications such as the recently FDA approved CAR-T therapy [3]. Increasing culture longevity and/or cell growth is of importance for such applications. In vitro culture of animal cells requires a large number of nutrients, including sugars such as glucose, most amino acids, vitamins, antioxidants, bulk ions, and trace elements. Some of these nutrients, such as glucose and amino acids, are substantially consumed during culture, while others, such as bulk salt, may not show an appreciable change in concentration [220]. Recent reports indicate that high initial nutrient concentrations above physiological levels may result in metabolic differences in cells in culture, which can result in reduced biological relevance of in vitro cell culture models [12]. Feeding nutrients during the course of the culture enables replenishment of the exhausted nutrients to prevent their limitation while at the same time avoiding initial oversupply and associated waste metabolite production, which could be inhibitory to cell growth [42,221,222]. The value of such feeding strategies to achieve higher cell growth and culture longevity has been amply demonstrated in the development of fed-batch processes for recombinant protein production [220,221,223,224]. In small-scale cultures, nutrient feeding is predominantly made possible by the bolus addition of highly concentrated feed solutions. This is usually carried out using liquid handling robots in the case of micro bioreactors or manually for the ubiquitous shake flasks or spinner flasks.

Bolus feed addition has several limitations. The solubility of some components, such as tyrosine, is low at neutral pH, and pH adjustments are necessary to achieve the desired solubility [218,225]. These can contribute to increasing the osmolarity of the culture. Feeding such concentrated solutions can also lead to large step increases in concentration and pH at the time of feeding, which may be undesirable [18,19]. Bolus feeding during process development may lock in production processes to have intermittent feeding strategies. Manual feeding also requires frequent handling of the cultures, which increases the chances of operator-induced errors. Lesser manual intervention and fewer steps with limited exposure to the environment reduce the probability of contamination. This is especially important for the imminent cell-based

therapies where a limited quantity of patient-derived cells are available, and cells are the final product of interest that cannot be subjected to sterilization [226].

The disadvantages of manual bolus feeding can be overcome through the use of a continuous feeding process, not requiring manual intervention. Automated closed systems have been demonstrated for ex vivo production of cells such as human placental, human CD4, and CD8 T lymphocytes [227], and stem cell [228] for cell-derived therapies. Automated continuous feeding for small-scale platforms cannot, however, be achieved without upgrading to additional infrastructure and robotic platforms [210,229,230]. These systems require appreciable capital investment. An alternative approach for continuous feeding is the continuous in situ delivery of nutrients via diffusion through hydrogels. Hydrogels are three-dimensional polymer networks that swell in water [191]. Hydrogels have been extensively used for biomedical applications like the slow release of drugs, hormones, and growth factors [192]. Our group has previously described the use of hydrogels for continuous in situ feeding of individual nutrients such as glucose in shake flasks [231]. However, mammalian cells in culture require feeding a complex mixture comprising multiple nutrients. This study aimed to investigate the feasibility of developing hydrogels for simultaneous in situ release of all nutrients provided in feed formulations for a fed-batch culture of mammalian cells, such as glucose, amino acids, and vitamins. Such in situ diffusion-based continuous delivery of nutrients can enable a fed-batch culture in a completely closed system requiring only gas exchange.

In this study, we have used suspension adapted CHO cells expressing recombinant IgG as a model system to establish the proof of concept for using hydrogels for in situ feeding of all nutrients required for the culture of animal cells. We characterize the individual rate constants for a simultaneous release of amino acids through the hydrogel. Alanine and glycine are formed as waste metabolites during culture and are not included in the feed. In the range of loading evaluated, we show that the amino acid release rates are proportional to the initial loading of the amino acid. This feature enables independent control of the release rates for all amino acids as per the requirement of the particular cell line. Tyrosine and cystine are expected to be an exception due to their poor solubility, and indeed tyrosine, whose release rate is measured, shows a constant zero-order release. We show that in situ delivery of all

nutrients led to a 1.8-fold (*p-value* 0.004) increase in IVCD accompanied by a 3-fold (*p-value* 0.011) increase in volumetric productivity compared to batch culture. To our knowledge, this study demonstrates, for the first time, the feasibility of achieving a completely closed in situ feeding platform for continuous feeding of complex nutrient feeds to animal cells, which does not require manual intervention or liquid handling technology.

6.3 Methods

6.3.1 Hydrogel synthesis

Poly-HEMA hydrogels were synthesized using 2-hydroxyethyl methacrylate (HEMA, 97% pure, Sigma-Aldrich Corp, USA) monomer and ethylene glycol dimethacrylate (EGDMA, Sigma-Aldrich Corp, USA) crosslinker at 86:14 mol/mol HEMA: EGDMA in the presence of an initiator Azobisisobutyronitrile (0.5%, Sigma Aldrich Corp, USA). A bottom layer of the hydrogel was created by polymerizing 200 μL of the HEMA: EGDMA mixture in a 1.3 cm diameter glass disc at 75 °C for 1.5 hours. A cavity was then formed over the bottom layer using an appropriate mould and 400 μL of the HEMA: EGDMA mixture by incubation at 75 °C for 1.25 hours. The diameter of the cavity was 9 mm. Subsequently, the solid powder of the payload was added to this cavity. The exact composition of the payload varies in different experiments and is described in Table 1. Four hundred and fifty microliters of the HEMA: EGDMA mixture were used to create the monolithic central reservoir and final layer of the hydrogel, sealing the cavity. The hydrogels were then washed in sterile ultrapure water for two days. After washing, the hydrogels were sterilized using UV for 25 minutes on each side of the hydrogel. Hydrogels were incubated overnight in a culture medium before addition to the cultures. The HEMA: EGDMA hydrogel was previously assessed for cytotoxicity to CHO cells and found to be non-toxic as processed [231].

6.3.2 Cell culture

A suspension CHO cell line expressing IgG, provided by Inbiopro Solutions (Bangalore, India), was used to evaluate the effect of the addition of the hydrogels to increase culture longevity and productivity. Cells were inoculated at a density of 0.3×10^6 cells/mL in 25 mL culture volume in 100 mL Erlenmeyer flasks (Borosil). Cells were regularly passaged in our in-house medium formulation based on DMEM: F12 containing 3 g/L glucose and 5 mM glutamine. For fed-batch experiments, shake flasks cultures were incubated at 37 °C, 10% CO₂, and 110 rpm. Glucose was fed to bring its concentration back to 2 g/L: at viability above 85%, glucose was fed when its concentration decreased below 2 g/L, while at viability below 85%, glucose was fed when the concentration decreased below 1.5 g/L. For cultures supplemented with NutriGel₂^{HVT,T}, cells were inoculated at 5×10^6 cells/mL in 50 mL culture volume. These cultures were incubated at 37 °C, 10% CO₂, and 130 rpm. Glucose was fed to bring its concentration back to 4 g/L: at viability above 85%, glucose was fed when its concentration decreased below 4 g/L, while at viability below 85%, glucose was fed when the concentration decreased below 2.5 g/L. The hydrogel was added on day 3 for all the cultures and day 0 for the NutriGel₂^{HVT,T} cultures. For bolus fed cultures, cultures were fed with 0.5X of the corresponding feed (20X) on days 3,6,8,10 or days 3,4,6,8. A total of 2X of the feed was added, where 1X corresponds to medium concentration without the bulk salts. A total of 2.5 mL liquid feed was added to the 25 mL culture volume of the bolus fed cultures. The hydrogel is added as a pre-swollen solid, so there is no volume change due to hydrogel addition. The composition of the bolus liquid feed was the same as NutriGel^T. The amount of payload in NutriGel^T was 250 mg, while the liquid bolus feed addition resulted in the addition of 125 mg of the feed, both to the same initial culture volume. The hydrogel payload was kept higher due to loss of payload during the initial washing and pre-incubation of the hydrogel for at least 2.5 days to remove unpolymerized monomers. The loss of payload was variable for the different components. Glucose was fed to maintain glucose concentration between 2 to 2.5 g/L, and a total of 7 mM of glutamine was also fed to the cultures. Samples were taken every alternate day to measure cell density, viability, and glucose concentration. Cell density was quantified by manual counting using a hemocytometer. Viability was assessed using the trypan blue dye exclusion assay. Glucose concentration was measured using a YSI Biochemistry Analyzer. Volumetric

IgG titer was determined by a sandwich ELISA. Briefly, ELISA plates were coated with capture antibody-rabbit anti-human IgG and subsequently blocked with 1% bovine serum albumin (BSA) in phosphate-buffered saline (PBS). 0.01% Tween 20 in PBS was used to wash plates. Human IgG was used to generate a standard curve for quantitation. HRP conjugated rabbit anti-human IgG (Merck Millipore, Mumbai, India) was used to detect IgG in culture, followed by the addition of substrate TMB/H₂O₂ (GeNei Laboratories Pvt Ltd, India). The reaction was stopped using 1 M H₂SO₄. Absorbance was measured at 450 nm on Bio-Rad iMark microplate reader (Bio-Rad Laboratories, Mumbai, India). Samples selected for ELISA had a viability of 60% or more.

6.3.3 Statistical analysis

Two-tailed Student's *t*-test was used to determine the significance of the difference between each pair of data. All *p* values lower than the significance level of 0.05 are denoted by asterisks in the figures. A *p*-value <0.05 is denoted by *, <0.005 by **, and <0.0005 by ***.

6.4 Results and discussion

Glucose and glutamine are the vital nutrients significantly consumed in vitro by mammalian cells. Amino acids other than glutamine have been shown to account for the majority of the cell mass in proliferating mammalian cell lines, also indicating their importance to cell growth [232]. Various cell lines producing recombinant proteins have been shown to improve their productivity and product quality and delay apoptosis upon supplementation of customized amino acid feed [4,216,217,233–235]. Depletion of even non-essential amino acids, such as asparagine, has been reported to result in the misincorporation of other amino acids during translation. This indicates the importance of maintaining an adequate amino acid supply [236–238]. At the same time, recent reports have also shown that high concentrations of amino acids in the culture lead to the accumulation of inhibitory metabolites [8]. Thus, feeding amino acids is essential to maintain an adequate supply of nutrients while avoiding a large initial excess. We have previously reported an alternate approach for the use of hydrogels for the in situ delivery of glucose to animal cell cultures. We now explore

whether similar hydrogels can enable simultaneous in situ delivery of a mixture including 18 amino acids.

6.4.1 Continuous feeding of complex nutrient feed using NutriGel₁^T improves culture longevity and volumetric productivity of recombinant CHO cell culture

NutriGel₁^T was evaluated with a suspension CHO cell culture producing IgG to assess whether the in situ supply of nutrients through the hydrogel has a beneficial effect on productivity and/or culture longevity. A culture without NutriGel₁^T served as control. Glucose was bolus fed to all the cultures, as described in the methods section. The NutriGel₁^T hydrogel was added on the 3rd day of the culture inoculated at a density of 0.3×10^6 cells/mL. Figure 6.1 shows the effect of the addition of NutriGel₁^T on culture performance for a representative culture. The biological replicate cultures had differences in cell density in the later stages of the culture beyond day 13 and are hence not averaged. We also compared NutriGel₁^T to the traditional bolus fed cultures, where the bolus feed had the same composition as the payload of NutriGel₁^T and was supplemented as a liquid feed at fixed intervals. Figure 6.1 also provides a comparison between the continuous mode of feeding through a hydrogel and the manual bolus mode of feeding. The viability of the cultures without the hydrogel decreased below 60% beyond day 8, while the addition of NutriGel₁^T or bolus feed resulted in maintenance of viability above 60% for at least 13 days among all replicates, thus substantially increasing the culture longevity. This is reflected in an average 2.7-fold (*p-value* 0.002) increase in IVCD and an average 4 fold and 4-fold (*p-value* 0.001) increase in volumetric productivity of IgG (Figure 6.1d) with NutriGel₁^T. Bolus feeding led to an average 2-fold (*p-value* 0.003) increase in IVCD and an average 3.8 (*p-value* 0.0001) fold increase in volumetric productivity of IgG compared to the control. The differences between the bolus and NutriGel fed cultures are not statistically different. Thus, supplying the feed nutrient mixture through the hydrogel led to significantly increased culture longevity and volumetric productivity compared to the control demonstrating the proof-of-concept that a large number of nutrients can be simultaneously supplied in situ to support cell culture. It should be noted that the composition of the nutrient feed mixture loaded into the hydrogel is identical to the medium formulation, with the exception of the omission of bulk salts and glucose, and has not been optimized for improved culture performance.

Nutrients in cell culture medium other than amino acids, such as vitamins, trace elements, and antioxidants, also have a significant impact on cells in culture and have been shown to improve growth and productivity [217]. The NutriGel₁^T hydrogels have a payload of vitamins, antioxidants, trace elements, and other micronutrients, as listed in Table 4, in addition to amino acids. Though the release rates of these other nutrients included in small quantities in the payload have not been quantified, we questioned whether the release of any of these other nutrients contributed to the increased culture longevity. We investigated this by making hydrogels identical to NutriGel₁^T, but without particular classes of nutrients such as vitamins, trace elements and antioxidants and analysing their effect on culture longevity.

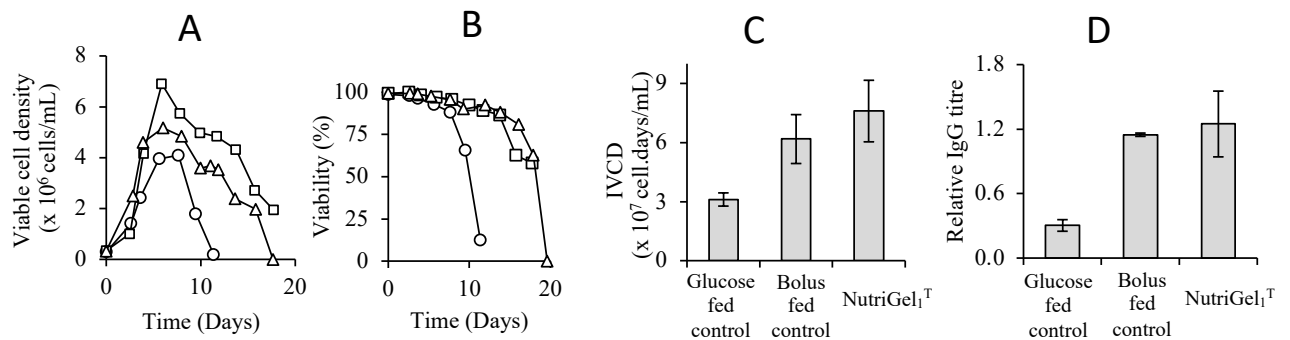


Figure 6.1: In situ delivery of nutrients through NutriGel₁^T leads to improved culture performance

Suspension adapted CHO cells expressing IgG were inoculated at 0.3×10^6 cells/mL. Cultures were either bolus fed only glucose (control), bolus-fed complete nutrient feed (bolus fed control) or NutriGel₁^T was added to the culture on the 3rd day and cultures were bolus fed glucose as required (NutriGel₁^T). (A) Viable cell density. A representative growth curve is shown. (B) Viability (C) IVCD (D) Relative IgG titer. ○ – control, △ -bolus fed control, □ – NutriGel₁^T. Error bars indicate 95% confidence interval, n=5 for cultures supplemented with NutriGel₁^T, n=4 for control cultures, n=2 for bolus-fed control cultures

6.4.2 NutriGel₁ hydrogels also supply other classes of nutrients that help in improving culture longevity

We first formulated NutriGel₁^{AA,T,G} with a payload of only amino acids in a composition identical to that in NutriGel₁ along with glucose. The NutriGel₁^{AA,T,G} were similarly added to the culture on day 3, and the culture was fed with glucose as a

bolus when the glucose concentration decreased below 2 g/L. The culture data shown in Figure 6.2 indicates that in situ supply of only amino acids through NutriGel₁^{AA,T,G} does not result in a culture performance similar to NutriGel₁^T (Figure 6.2). Viable cell densities of cultures supplemented with NutriGel₁^{AA,T,G} are similar to control cultures without the hydrogel and show no increase in IVCD. This supports the conclusion that at least some of the other micro-nutrients are being delivered to the culture through the NutriGel₁^T and their release contributes to the improved culture longevity.

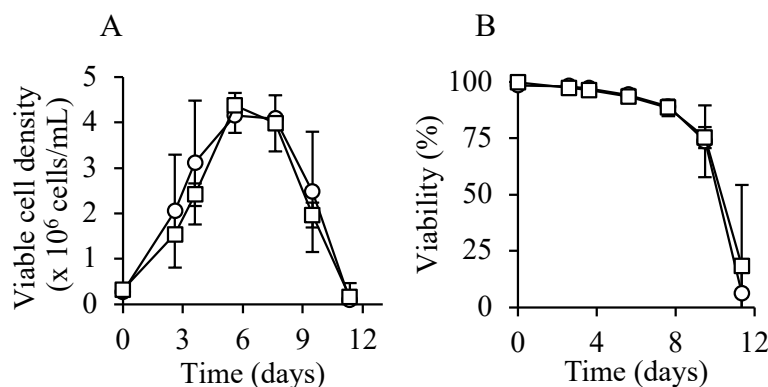


Figure 6.2: In situ release of only amino acids does not improve cell growth.

Suspension adapted CHO cells expressing IgG were inoculated at 0.3×10^6 cells/mL. NutriGel₁^{AA,T,G} was added on the 3rd day. Cultures were bolus-fed with glucose as required. (A) Viable cell density. (B) Viability. ○ – control, □ – NutriGel₁^{AA,T,G}. Error bars indicate 95% confidence interval, n=2 for control cultures and n=3 for cultures supplemented with NutriGel₁^{AA,T,G}.

6.4.3 Vitamins and trace elements are released from the NutriGels and contribute to improving culture longevity

In order to perform an individual elimination of individual components, we had to first establish the commercial purchased feed can be mimicked by its individual constituents. Amino acid release profiles have previously indicated this. Hence we synthesized NutriGel₁^{mimic} by making the nutrient feed from its individual nutrient classes and supplementing NutriGel₁^{mimic}, leading to a similar cell density and growth. With the possibility of making the complete feed, we could remove each component and test the actual essentiality of each component (Figure 6.3). Vitamins led to the lowest peak density, followed by trace elements, and also had lower longevity.

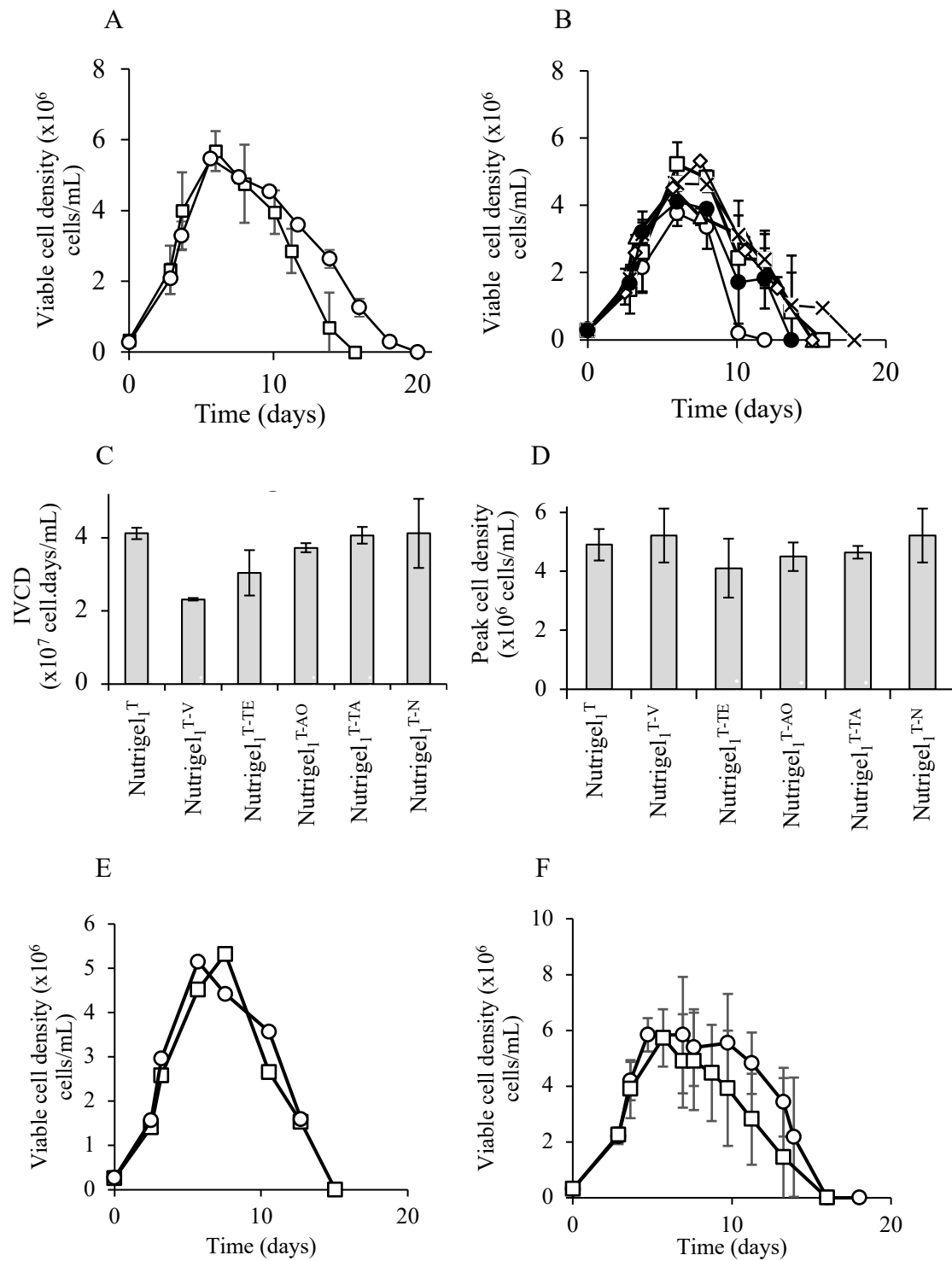


Figure 6.3: Effect of different classes of nutrients from the payload of the NutriGel on culture longevity

Suspension adapted CHO cells expressing IgG were inoculated at 0.3×10^6 cells/mL. Cultures were either supplemented with ○- NutriGel^T (control), □ – NutriGel^{Tmimic} or NutriGel^T was added to the culture on the 3rd day and cultures were bolus fed glucose as required (NutriGel^T). (A) Viable cell density (B) NutriGels deficient in a single class of nutrients were added on the 3rd day, and cultures were bolus fed glucose as required. ◇ – NutriGel^T, ○ – NutriGel^{T-V} (without vitamins), ● – NutriGel^{T-TE} (without trace elements), □ – NutriGel^{T-N} (without nucleoside precursor), △ –

Nutrigel₁^{T-AO} (without antioxidants), -**×**-Nutrigel₁^{T-TA} (without thioctic acid). Error bars indicate 95% confidence interval, n=2. (C) IVCD and (D) Peak viable cell density. Error bars indicate 95% confidence interval, n=2. See table 1 for the detailed formulation of the NutriGels. Error bars indicate 95% confidence interval, n=2 for cultures supplemented with Nutrigel₁^{Tmimic}, n=1 for control cultures. (E) Viable cell density ○- Nutrigel₁^{T4XV}, □- Nutrigel₁^{Tmimic} (control), (F) Viable cell density, ○- bolus fed cultures with 2x Vitamins and Trace elements, □- bolus fed cultures (control)

To identify the nutrients essential for enhanced culture longevity in NutriGel₁^T as compared to NutriGel₁^{AA,T,G}, we supplemented CHO cultures with hydrogels identical to NutriGel₁^T, but with one category of micro-nutrients absent. The payload in these experiments was assembled by mixing all individual components in solid form for the macronutrients, while the micronutrients were added as a stock solution followed by drying due to their low levels. These hydrogels were NutriGel₁^{T-V}, NutriGel₁^{T-TE}, NutriGel₁^{T-AO}, NutriGel₁^{T-TA}, and NutriGel₁^{T-N} lacking vitamins, trace elements, antioxidants (ethanolamine, putrescine, glutathione, and vitamin C), thioctic acid and nucleoside precursors respectively. Figure 6.3 shows the IVCD, and peak viable cell density for NutriGel₁^T, NutriGel₁^{T-V}, NutriGel₁^{T-TE}, NutriGel₁^{T-AO}, NutriGel₁^{T-TA}, and NutriGel₁^{T-N}. The absence of vitamins in the hydrogel led to the lowest IVCD, followed by the absence of trace elements, indicating their importance in maintaining culture longevity. When NutriGel₁^{AA,T} was supplemented with vitamins and trace elements in the payload, the IVCD was restored to levels similar to NutriGel₁^T (Figure 6.3). On the other hand, when 4x vitamins were added to the mimic, they reached a higher density similar to the control cultures. Bolus feeding of nutrient feed and with additional vitamins and trace elements lead to high densities proving that trace elements and vitamins indirectly help in improving culture longevity.

6.4.4 Use of NutriGel₂^{HVT,T} to reduce the differences in release rates of all amino acids in fed-batch cultures

The amino acid composition in the payload for NutriGel₁ is similar to the culture medium. As shown above, the release rates of amino acids are proportional to the initial loading in the reservoir. Thus, amino acids, such as arginine, which are already in high abundance in the medium, have a high release rate. It is increasingly becoming

evident that excessive supplementation of amino acids can lead to the production of inhibitory metabolites [8]. Amino acids like arginine have also been shown to have a negative impact on protein production [134]. At the same time, amino acids like aspartate, which are present at low concentrations in the medium, have low release rates, which could limit their availability [239]. Consequently, in order to support cultures at higher viable cell density, we next examined the effect of using NutriGel₂^H hydrogels containing 8 mg each of all amino acids instead of NutriGel₁^T. Additional vitamin and trace element loading was included in the NutriGel₂^H hydrogels since the release of these two groups of micro-nutrients was seen to be essential for the increased culture longevity. This hydrogel is referred to henceforth as NutriGel₂^{HVT,T}.

We evaluated the effect of in situ feeding cultures seeded at a higher cell density of 5×10^6 cells/mL. NutriGel₂^{HVT,T} was added to the culture at the time of inoculation, while no hydrogel was added to the control culture. Both cultures were bolus fed glucose as described in the methods section. There is no difference in peak viable cell density with the addition of NutriGel₂^{HVT,T} indicating the per cell supply of nutrients achieved in this condition does not support higher cell growth. In the absence of NutriGel₂^{HVT,T}, cell viability was maintained above 80% till day 6. The addition of NutriGel₂^{HVT,T} led to viability above 80% till day 10, with an average 1.2-fold higher IVCD (*p-value* 0.24) and a 1.9-fold (*p-value* 0.014) increase in volumetric productivity of IgG compared to the control. Volumetric productivity of 1.5 g/L was achieved with NutriGel₂^{HVT,T} (Figure 6.4). This again demonstrates the ability to improve culture performance by in situ release of nutrients. Though this particular hydrogel loading formulation did not support higher growth, culture volume and/or amino acid loading can be trivially changed to adjust the per cell release rates to further optimize the release rates per unit volume for increased growth if desired.

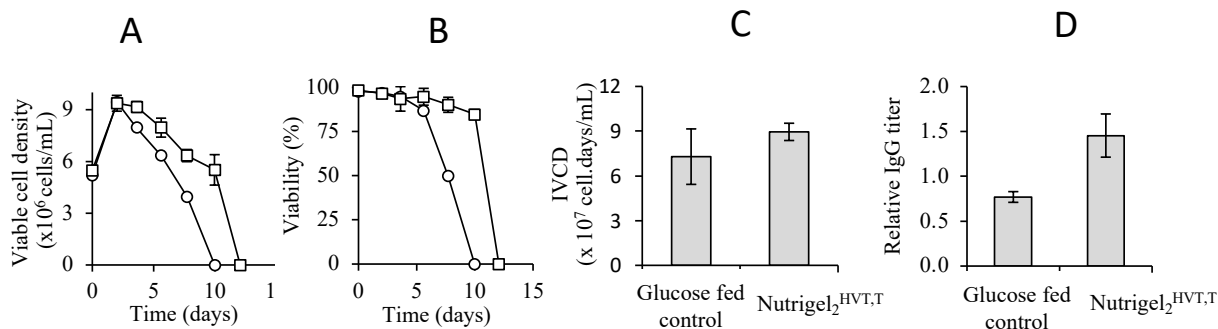


Figure 6.4: Overcoming low amino acid concentration through NutriGel₂^{HVT,T}

CHO-IgG cells were seeded at 5×10^6 cells/mL, and NutriGel₂^{HVT,T} was added on day zero. Cells were counted on a hemocytometer every other day. Cell density and viability were monitored using trypan blue dye exclusion assay. (A) Cell density (B) Viability (C) IVCD, (D) Relative IgG titre, O – control, □ – NutriGel₂^{HVT,T}. Representative growth curve. Error bars indicate ±95% confidence interval n=2

6.4.5 A completely closed continuous in situ feeding via hydrogels for animal cell culture requiring no operator handling

With NutriGel₁^T, we successfully demonstrated the utility of a hydrogel to feed amino acids and other nutrients to improve culture performance in terms of growth and productivity, but glucose was supplied via bolus additions. To make a complete in situ feeding system, glucose was also delivered through the same hydrogel to avoid bolus feeding. NutriGel₁^{T,G} has an identical payload as NutriGel₁^T with the addition of 200 mg glucose. Release kinetics for hydrogels loaded with 200 mg of glucose is shown in Figure 6.5a. Cultures supplemented with NutriGel₁^{T,G} hydrogel on day 3 led to improved culture longevity with an average 1.8-fold (*p-value* 0.004) higher IVCD along with a 3-fold (*p-value* 0.01) higher volumetric productivity of IgG compared to the control cultures in batch mode (Figure 6.5 e, f). Importantly, with the addition of NutriGel₁^{T,G}, there is no requirement for operator handling to feed cultures (Figure 6.5). The statistical significance of the differences between this completely closed culture and the NutriGel added cultures which were bolus fed glucose as described above, is *p-value* 0.03 and *p-value* 0.21 for IVCD and titer, respectively. This indicates no significant difference in titer when glucose is either fed as a bolus or through the NutriGel. The difference in IVCD may be due to the nature of the glucose release kinetics through the hydrogel. A separate hydrogel could be used for glucose

delivery to provide independent control on the rate and duration of glucose release. The use of other slowly metabolizing sugars in addition to glucose may result in further improvements to the culture performance. A separate glucose loaded hydrogel can also be used to obtain independent control over the glucose release rate. Galactose solely or with glucose was also tested as an alternative to bolus feeding of glucose (Figure 6.5 g,h). Though galactose cultures had a lower peak density of 30%, they had a 2 fold increase in productivity (Figure 6.5 g,h). The cultures with glucose and galactose had a similar peak density and productivity to those with glucose through the gel.

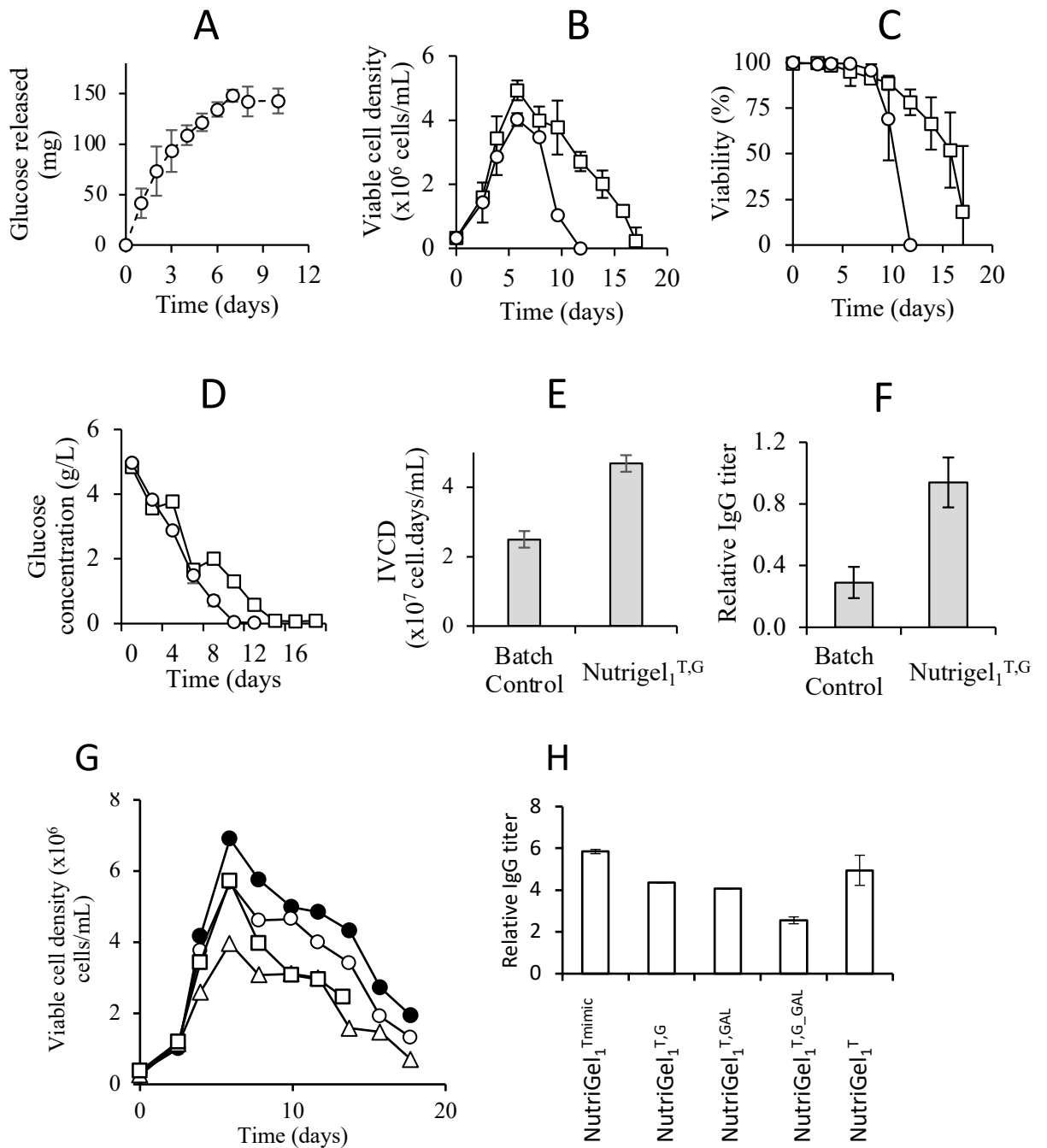


Figure 6.5: Complete in situ release of nutrients for CHO IgG culture

CHO-IgG cells were inoculated at 0.3×10^6 cells/mL, and NutriGel₁ with or without a carbohydrate source was added on the 3rd day. Cells were counted on a hemocytometer every other day. Cell density and viability were monitored using trypan blue dye exclusion assay. (A) Release kinetics of glucose through glucose-loaded hydrogel (B) Viable cell density (C) Viability (D) Glucose concentration (E) IVCD (F) Relative IgG titer. ○– batch control, □– NutriGel₁^{T,G}. (G) Viable cell density, ○– NutriGel₁^{T,G}, ●–NutriGel₁^{Tmimic}, △- NutriGel₁^{T,GAL}, ◻– NutriGel₁^{T,G,GAL}. (H) Relative IgG titer. Error

bars indicate $\pm 95\%$ confidence interval, n=2 for control, n=1 for NutriGel₁^{T,G}, NutriGel₁^{Tmimic}, NutriGel₁^{T,GAL}, NutriGel₁^{T,G_GAL} and n=3 for cultures supplemented with NutriGel₁^{T,G} and glucose release kinetics.

6.4.6 Utilizing NutriGel₁^T for a nutrient-rich media and other suspension cell lines

CD-CHO is a chemically defined commercial media that allows the growth of cells to a high density. We wanted to test if using the NutriGel₁^T with the same nutrient feed that enhances culture performance in a custom made media based on DMEM/F12 can also lead to a further increase in cell density in CD CHO media. This custom DMEM/F12 media formulation is also utilized to routinely culture CHO cells, and compared to CD, CHO is a nutritionally lean formulation. As seen in Figure 6.6, CD-CHO media supplemented with NutriGel₁^T and with CD-CHO media powder through the gel does not perform better than the control cultures (Figure 6.6). The CD-CHO media powder supplemented through the NutriGel in CD-CHO media possibly did not work because of higher contents of salt in the media that might lead to the high osmolarity of cultures or due to washing away of the nutrients.

K562, myelogenous leukaemia suspension cell line was also supplemented with NutriGel₁^T. However, they do not perform better than the control (Figure 6.6). This highlights the differences which may be due to metabolic changes and cell origin changes.

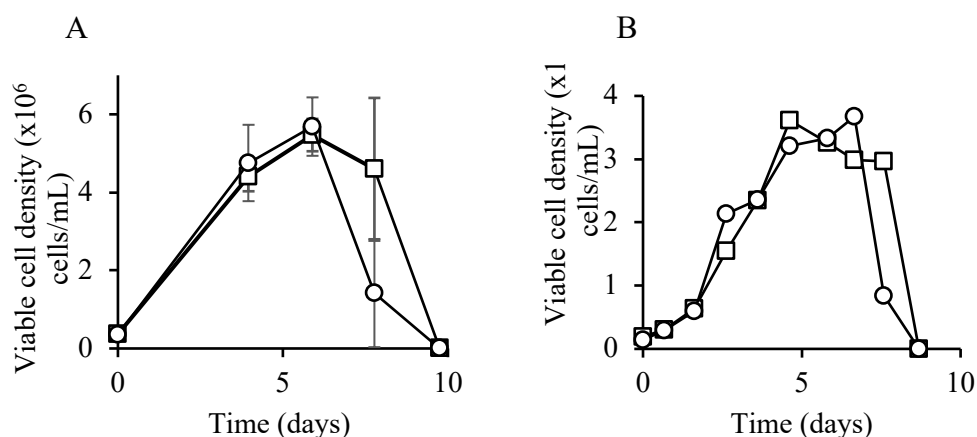


Figure 6.6: Utilizing NutriGel^T for alternative nutrient-rich media and other suspension cell lines

CHO-IgG cells or K562 cells were inoculated at 0.3×10^6 cells/mL, NutriGel^T with glucose was fed as a bolus, and NutriGel was added on the 3rd day. Cells were counted on a hemocytometer every other day. Cell density and viability were monitored using trypan blue dye exclusion assay. (A) Viable cell density for CHO cells ○– NutriGel^{T,G}, □– control culture. (B) Viable cell density for K562 cells ○– NutriGel^{T,G}, □–control Error bars indicate $\pm 95\%$ confidence interval, $n=2$ for control and NutriGel^{T,G} supplemented in CHO cell cultures $n=1$ for control and NutriGel^{T,G} for K562 cell cultures

6.5 Conclusion

In this study, we report for the first time the development and application of a diffusion-based inexpensive hydrogel system for continuous in situ feeding of a complex mixture of all nutrients required for mammalian cell cultures, including amino acids, vitamins, and trace elements. The hydrogel includes the complex nutrient feed dispersed in the form of a solid in a central reservoir. This prevents dilution of the culture seen in traditional fed-batch cultures where the feed is added as a concentrated solution whose strength is limited by the solubility of the nutrients included. At the end of the culture, the culture can be pipetted/pumped out from the culture vessel, leaving the hydrogel behind. No additional separation step is required. Though the release rates of the other micronutrients like vitamins and trace elements were not measured, we show that their incorporation was essential for the improved culture performance. This indirectly confirms that at least some of the other nutrients are indeed delivered through the hydrogel. Further characterization of release rates of micronutrients will help optimise the feed loaded in the reservoir.

The effect of NutriGel₁^T on CHO cells is not simply because of the higher glutamine that is being supplied through the gel. It is evident that amino acids are not limiting for cells to achieve peak density. Trace elements and vitamins are essential to reach higher densities. But beyond a threshold, increasing them does not affect cell density and productivity, indicating a secondary problem that arises due to cell metabolism within the initial growth phase. pH can be that issue as HEPES affects only when the cell is devoid of other nutrients.

Cells grown in CD-CHO media and supplemented with NutriGel₁^T or gels with NutriGel^T with CD-CHO media powder as the payload do not perform as well as the cells grown in DMEM and F12 based medium (Media based on supplemented with a feed based on the same media). This justifies cell line-specific optimization and feeding to be developed complementary to the basal medium design. This mode of feeding could not be successfully applied to another cell line, K562, which is a leukaemia cell line dependent on serum for its growth and more sensitive than CHO cell lines. Hence the difference in robustness and metabolism may have led to the ineffectiveness of the NutriGels.

Such systems can help small-scale animal cell culture platforms to achieve continuous nutrient feeding in a completely closed use-and-throw format without any additional infrastructure. We have not evaluated the shear sensitivity of the NutriGel, but such studies can guide exploration of application in small scale single-use bioreactors like the WAVE bioreactor. In situ continuous feeding at small-scales can also allow the development and use of a leaner culture medium, which is more representative of conditions encountered by cells in vivo [240] since cell growth will no longer be limited by the initial nutrient concentrations in the medium. In situ nutrient feeding reported in this study, in addition to in situ pH management described previously [196], can enable completely closed systems in single-use platforms requiring no operator intervention, which may be of use in bioprocessing as a screening tool for animal cell-based bioprocesses and in production of patient-specific cell-based therapies.

Chapter VII.

Lean amino acid medium formulation and its implication on culture performance

7.1 Summary

Cell culture medium has non-physiological amino acid concentrations, which can potentially alter metabolism, leading to inhibitory metabolite production. Detailed reports have described that the composition of basal media has a consequential influence on the outcome. Effects of lean culture media and supplementation remain largely overlooked experimental parameters in the context of CHO cell culture. To explore this, we examined the cell culture performance under various low amino acid conditions. Unsurprisingly, the low amino acid concentrations quickly result in amino acid limitation under the batch mode of cultivation. We utilized a continuous feeding strategy to overcome this limitation while maintaining cells under low amino acid concentrations for longer durations. This was achieved using the NutriGels described previously and by continuous feeding in a bioreactor. We observe that though protein expression was not inhibited at the lowest amino acid concentrations evaluated, there is no improvement in culture productivity. Further, we used transcriptomics to understand the molecular changes at low amino acid concentrations. The phenotypic and transcriptional changes were similar to the AAR (Amino acid response) in mammalian cells under amino acid limitation-ATF4/Transporter upregulation and cell cycle arrest. Further experiments at higher amino acid setpoints may help identify the lowest concentration at which the AAR response pathway is not activated.

7.2 Introduction

The cell culture medium chosen to culture cells is a critical part of bioprocessing. Cells invitro are cultured and maintained in specially formulated media containing an osmotically balanced mixture of metabolites that sustain cellular growth and support

proliferation. The extracellular nutrient milieu has an impact on cell culture performance and product titre in mammalian bioprocesses. CHO cells consume nutrients from the medium and divert them for growth and recombinant protein production. However significant fraction of these nutrients is diverted into catabolic by-products and metabolites. Such by-products and metabolites are known to inhibit cell growth and protein synthesis. The impacts of lactate and ammonia accumulation are widely recognized. But CHO culture growth halts even at reduced accumulations of lactate and ammonia, indicating the second tier of novel growth inhibitors.

Limiting amino acid concentration has been shown to help in reducing inhibitor biosynthesis. It is now known that oversupply of these amino acids has been found to cause inhibition of growth due to the production of inhibitory metabolites from various overflow pathways required for catabolizing amino acids [8,241].

Additionally, chemically defined media formulations used for growing cells *ex vivo* generally are nutritionally rich mediums that cannot precisely replicate the moderate micronutrient conditions *in vivo*. These deviations can cause substantial differences *in vivo* and *in vitro* phenotypes, as recently seen by some studies in cancer cell models [11,12,242]. Such reports indicate that commercially available media does not provide a relevant micronutrient context. This can be challenging, especially in patient-derived cell-based therapies that are being increasingly explored for the treatment of a wide variety of diseases.

Utilizing a lean amino acid-based medium can also result in undersupply of specific or a mixture of amino acids. Figure 7.1 summarizes the known effects of single or multiple amino acids. Hence lean nutrient-based medium needs frequent exchange with fresh medium or a complementary feeding system. Otherwise, a lean medium can cause nutrient limitation and, in adverse cases, lead to nutrient starvation-induced cell death, including apoptosis [243,244] and non-apoptotic cell death [245,246].

However, the death mechanism seems to differ by the nutrient or extent of starvation of the same nutrient or by the difference in genetic properties of the cells. In eukaryotic cells, in addition to a response to nutritional stress (glucose and amino acid limitation), integrated stress response (ISR) is activated to adapt to the stress condition in order to restore cellular homeostasis [247]. If the cellular stress is sustained, the ISR will induce cell death. However, whether or how the ISR pathway causes cell death in CHO cells in response to feeding under lean amino acid

conditions is not understood. Effects of lean amino acid-based culture media remain largely overlooked experimental parameter in bioprocessing. In this chapter, we explore the possibility of using a lean amino acid medium in the batch mode and fed-batch mode.

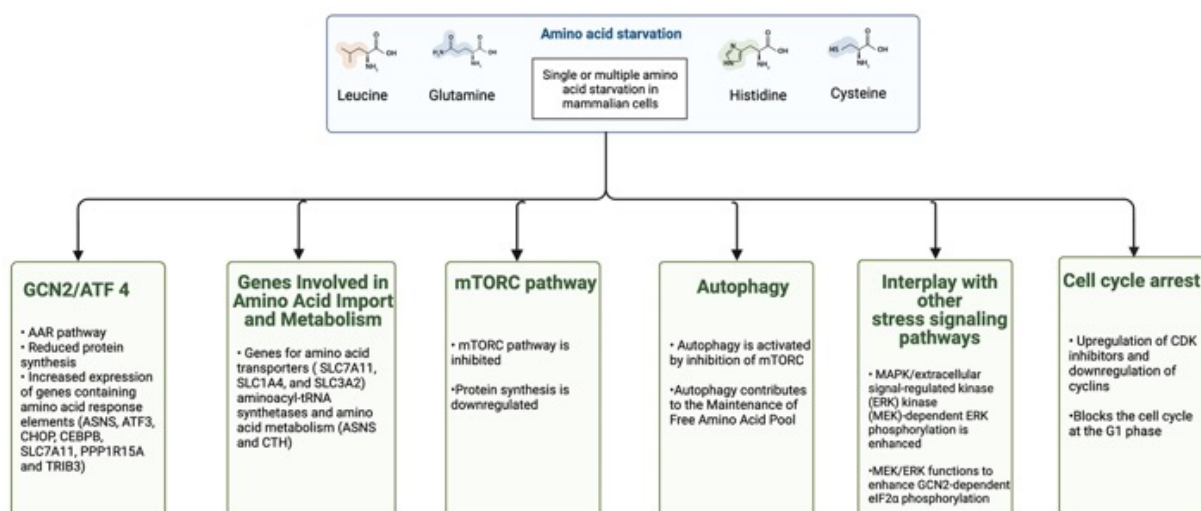


Figure 7.1: Effects of amino acid starvation in mammalian cells

Summary of the reported effects of single or multiple amino acid limitation studies in the literature.

Created with BioRender.com

7.3 Methods

7.3.1 Cell culture

Suspension CHO-DG44 based cells producing recombinant IgG were provided by Inbiopro Solutions (Bengaluru, India). They were regularly passaged in custom made DMEM: F12 based HDFE medium (composition in Appendix 1). All cultures were incubated in a humidified incubator set at 37 °C and 10% CO₂ and shaken at 110 rpm. No antibiotics or serum was used in any of the cultures. A culture volume of 20 mL in a 100 mL glass conical flask with a screw cap was used for all cultures. Cultures were sampled regularly for cell density and extracellular metabolite measurements. Viable cell density was measured on a haemocytometer using the trypan blue dye exclusion method. Glucose concentrations of culture supernatants were measured using a YSI biochemistry analyser (YSI Incorporation, Yellow Springs, OH, USA).

7.3.2 RNA isolation and library preparation

To create the RNA seq library, suspension adapted CHO cells producing IgG regularly passaged in a custom DMEM: F12 based medium without hydrolysate were resuspended in LAA. The different conditions tested were a low amino acid background containing amino acids at 0.1 mM, an equimolar amino acid background containing most amino acids at 1 mM and the passage medium. After 24 hours of an adjustment period, the cells were again resuspended in the respective low or high amino acid media along with the routinely used passaging medium. The cells were seeded at 1×10^6 cells/mL in a 20 mL culture volume. An additional washing step was included with the respective media to minimise carryover from the previous media. Post 24 hours of growth, the cells were counted, and 1×10^6 cells were pelleted by centrifugation at 1000 rpm for 5 mins. The pellet was then washed with PBS once. About 100 μ L of fresh PBS was added to loosen up the pellet and resuspend the cells, followed by the addition of 500 μ L of *RNAlater* (Thermo Scientific, Waltham, Massachusetts, USA), which are then stored at -80° C till RNA extraction.

7.3.3 Transcriptome analysis

RNA was extracted from cells using the TriZol extraction method. The RNA was quality checked, and 1 μ g of RNA from each sample was taken for library preparation. The library was prepared using Illumina TruSeq Stranded Total RNA Library Prep kit as per the manufacturer's instructions. The prepared libraries were quality checked using qubit and Bioanalyzer. The libraries were then sequenced. The Fastq files were quality checked using FastQC [248], and trimming was performed using Trimmomatic [249]. The reads were then analysed using the Tuxedo pipeline FASTQC [250].

Median normalisation was used to normalise the reads obtained. The normalisation factor for a given sample was calculated by dividing the average of all the medians of the samples by the median of all the intensities of the sample. Each sample was then normalised by multiplying each intensity with the normalisation factor of the sample. Fold change was calculated by dividing the mean of all biological replicates of cells cultured in a low amino acid medium by that of control cells cultured in the regularly

used HDFE-3 medium. Base 2 logarithm values of the fold changes are reported. Genes with a p-value lower than 0.05 for p-value and absolute log₂-fold change greater than 0.5 were identified as significantly differentially expressed.

7.3.4 Bioreactor culture

A benchtop bioreactor with a working volume of one litre (Celligen 115, New Brunswick Scientific, Edison, NJ, USA) was used for bioreactor cultures. An initial culture volume of 500 mL was used. Identical basal medium, seeding density, inoculum, feed and feeding strategy were developed from E85 shake flask cultures. Culture temperature was maintained at 37 °C. Dissolved oxygen was maintained above 30% (of saturation) using cascaded control of agitation and gas flow. The culture was agitated using a marine blade impeller between 100 and 130 rpm. Culture pH was maintained at 7±0.02 for cultures. CO₂ gas and 0.1 mM sodium bicarbonate were used as acid and base, respectively, for pH management. An increase in culture volume and increase in cell density were accounted for while feeding the bioreactor. Simethicone was added to control foaming whenever necessary. Clustered heatmaps were plotted using Datawrapper.

7.4 Results

7.4.1 Growth response of CHO cells under diverse amino acid conditions

As already described by numerous reports, the composition of the basal media chosen to culture cells in vitro has a tremendous effect on the outcome [251,252]. Amino Acid Insufficiency or sufficiency may mediate changes in expression levels of various pathways involved in amino acid metabolism and transport. Cell lines producing recombinant proteins have been shown to improve their productivity and product quality and delay apoptosis upon supplementation of customized amino acid feed [4,216,217,233–235]. Depletion of even non-essential amino acids, such as asparagine, can result in the misincorporation of other amino acids in recombinant proteins during translation [236–238]. This indicates the importance of maintaining an

adequate amino acid supply. Such data can be employed to give insights into how these parameters can be controlled to ensure optimal mAb productivity and quality.

Suspension adapted CHO cell line expressing IgG was used to evaluate the effect of three different medium designs: LAA medium (low amino acid medium 0.1 mM), LAA medium supplemented to have amino acid concentrations at High amino acid (1mM AA concentration/HAA), and LAA supplemented to create HDFE-3 (HDFE 3*) the medium in which cells are routinely passaged. Cells were inoculated and were allowed to acclimatize to a nutritionally limited medium by culturing them in a custom made low amino acid LAA medium containing all amino acids at 0.1 mM, glutamine at 0.5 mM, glucose at 2 g/L for 24 hours. Post 24 hours, cells were resuspended in a fresh LAA medium. Improvement in culture performance was observed with LAA medium supplemented to have amino acid concentrations at HAA and HDFE 3* medium. Growth in HDFE 3* is similar to HDFE 3, validating the use of this custom-made media and relative 1.5 and 2.2 fold improvement in productivity in HDFE 3* and High amino acid (1mM AA concentration/HAA) condition. Cell growth under LAA suggests growth inhibition at such low concentrations (Figure 7.2). Though we do not observe any proliferation, there is also no immediate cell death. The culture is able to maintain constant cell density for at least four days. As a positive control, we have also tried to understand the effect on growth with the cells cultured in a relatively rich amino acid composition which is also equimolar with respect to its amino acid composition. The cell culture performance in the HAA is similar to the control HDFE 3* cultures. Though this medium is slightly abundant with amino acids, the effect on viable cell density is minimal. While this preliminary data gives an immediate idea about CHO cell response to a lean amino acid background, it does not give a readout about intracellular genetic responses.

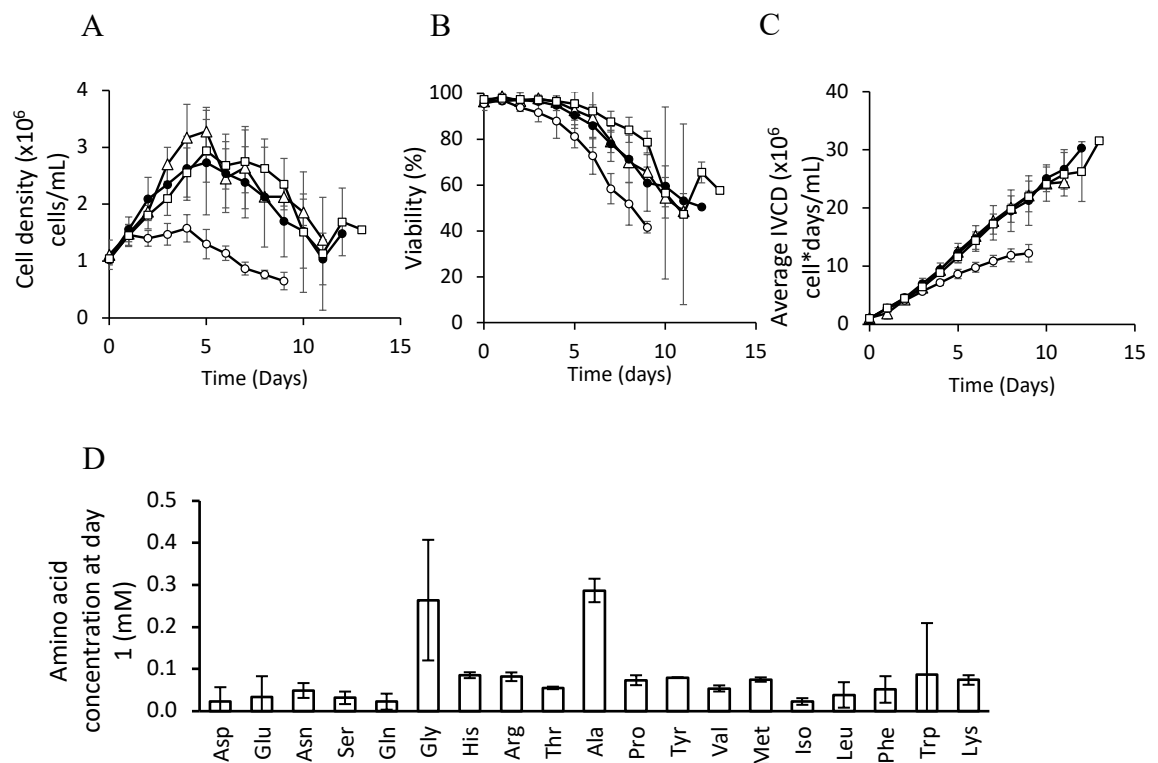


Figure 7.2: Evaluating the effects of diverse media formulation on CHO cell culture performance

CHO-IgG cells were inoculated at a density of 1×10^6 cells/mL in low amino acid condition (LAA), High amino acid condition and the routinely used passaging media. Cells were counted on a hemocytometer every day. Cell density and viability were monitored using trypan blue dye exclusion assay. (A) Cell density \square -HAA condition, Δ -HDFE 3, \circ -LAA Condition, \bullet -HDFE 3* (B) viability \square -HAA condition, Δ -HDFE 3, \circ -LAA Condition, \bullet -HDFE 3* (C) IVCD \square -HAA condition, Δ -HDFE 3, \circ -LAA Condition, \bullet -HDFE 3*. (D) Residual amino acid concentration at day 1 of CHO cell culture in LAA condition. Error bars indicate a 95% confidence interval

We established a lean amino acid-based medium called a low amino acid “LAA” condition that contained all amino acids at a concentration of 0.1 mM, pyruvate at 0.1 mM with 1 g/L glucose and 0.5 mM glutamine. The culture performance provided an initial assessment of the feasibility of maintaining cells under lean amino acid conditions. We observe reduced cell growth and viability when cultured in LAA condition compared to the routinely used medium for culturing these cells under batch mode. We performed RNA-seq to understand the transcriptomics response of cells to culture in low amino acid concentrations in batch conditions. The main objective of

this study was to functionally annotate genes that were differentially regulated in LAA. On average, 16000 transcripts were mapped using the tophat program [250]. In comparison, 143 genes were differentially expressed in LAA, and their GO terms were functionally classified into the biological process (BP), cellular components (CC), and molecular functions (MF). Regarding BP, the genes that were related to the regulation of primary metabolites (59 genes) and regulation of transcription (45) were differentially expressed. Regarding CC and MF, the genes related to the nucleus (54 genes) and cytoplasm (44 genes) were observed to have transcription factor activity (21 genes) or protein binding activity (39 genes). Overall, functional classification using DAVID [253,254] showed the top pathways that were identified as enriched among the differentially expressed genes in LAA were the cell cycle, FoxO signalling pathway, and p53 signalling pathway, PI3K-Akt signalling pathway (Figure 7.3). This is not surprising considering the observed phenotype of slower growth in LAA, which is expected to be accompanied by significant rewiring of the cell cycle and cellular metabolism. These and other transcriptional changes in LAA and HAA are described below in detail.

We observe an adaptational IRS to LAA condition. Among the differentially expressed genes, as expected, are upregulation of various mitochondrial and amino acid transporters like SLC6A9, SLC7A1, SLC38A2, tRNA synthetases and the general control non-derepressable 2/ATF4 pathway in response to nutrient limitation. We also observe growth arrest by upregulation of cyclin kinase inhibitors Cdkn1a and Cdkn2b and upregulation of various signalling pathways. It is important to note that sustained growth arrest and IRS can also lead to apoptosis.

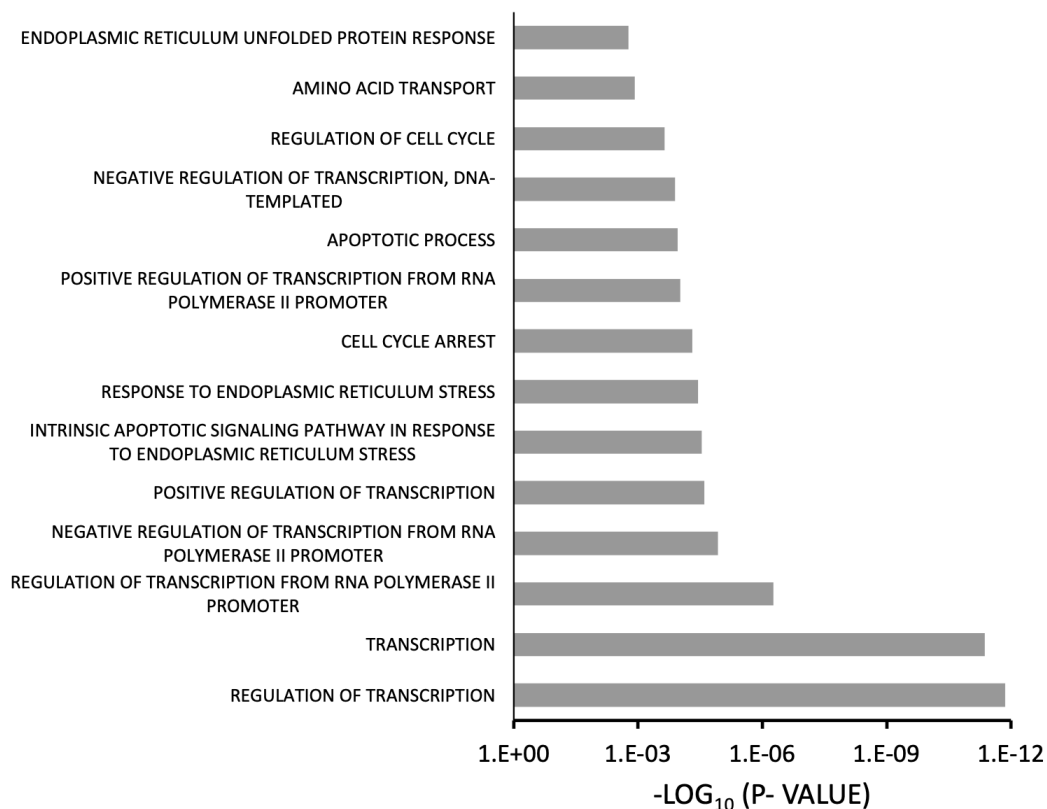


Figure 7.3: Major biological processes enriched during growth in LAA

DAVID Gene Ontology enrichment analysis for the transcriptomics data for the CHO cells cultured in LAA conditions by biological processes

7.4.2 GCNP transcriptional activation as a response to nutrient limitation

When the cells have scarce levels of amino acids, the AAR pathway is activated. The GCN2 kinase binds to uncharged tRNA, which leads to phosphorylation of the translation initiation factor eIF2 α . eIF2 α phosphorylation is a conserved mechanism used from yeasts to mammals to suppress the rate of general protein synthesis under various types of stress [255](Figure 7.4).

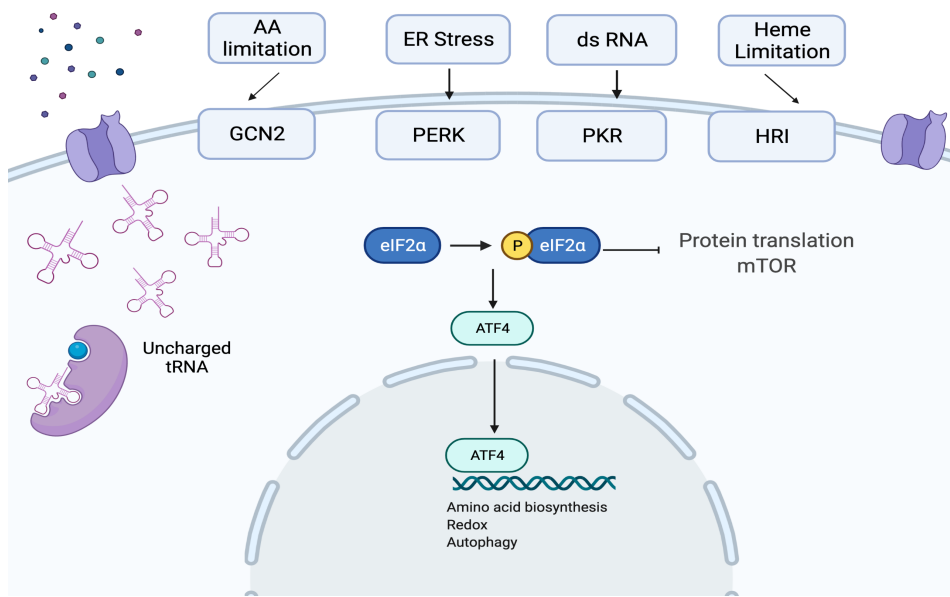


Figure 7.4: GCN2 transcriptional activation in mammalian cells

Created with BioRender.com

Paradoxically there is a simultaneous increase in the expression of certain transcriptional activators whose functions are required for mitigating the stress. Since amino acids are an important class of nutrients, and essential amino acids cannot be synthesized, cells depend upon the nutrient medium for these, and their intracellular concentrations are rigorously controlled by various mechanisms. The AAR pathway in eukaryotes is one such pathway that evolved to recognize and react to amino acid deficiency to mitigate the nutritional deficiency. Limitation of any of the 20 amino acid initiates this response, which initiates a signalling cascade designed to mitigate the amino acid scarcity by increasing amino acid biosynthesis and rescuing global protein synthesis. These regulated events include a spectrum of responses, including chromatin remodelling, RNA splicing and stabilization, translational control, increased expression of transporters, and transcription factors from the basic region/leucine zipper (bZIP) superfamily, growth factors, and metabolic enzymes [256].

Mammalian cells have two recognized pathways for sensing and responding to amino acid availability, the AAR and mammalian target of rapamycin (mTOR) pathway. These two pathways change the rate of protein synthesis in opposing directions; while mTOR detects amino acid sufficiency to support protein synthesis and cell growth,

the GCN2 pathway detects amino acid restriction to maintain intracellular homeostasis.

Limiting the extracellular supply or synthesis of an essential amino acid leads to intracellular disturbance in the cellular pool and leads to increases in uncharged tRNA that is known to bind and activates the GCN2 kinase [256–258]. It is known from studies in *E coli* and yeast that amino acid limitation quickly results in uncharged tRNAs, particularly of the frequently used codes, as various isoacceptor tRNAs exist. The appearance of uncharged tRNAs is a mechanism for detecting amino acid depletion. With uncharged tRNAs as a surrogate, GCN2 protein serves as a primary sensor of amino acid insufficiency. It is important to note deficiency of even one amino acid or suppressed activity for any one of the tRNA synthetases can also trigger the AAR pathway [259]. With uncharged tRNAs and the ratio between uncharged and aminoacylated tRNA molecules as a measure of amino acid availability, GCN2 protein is a primary sensor of amino acid insufficiency [260]. tRNA expression is also regulated in response to stresses such as nutrient availability [261,262]. Leucine sensor LARS1 couples leucine availability to the mTORC1 signalling pathway [263]. WARS1, MARS1, and EPRS are also likely involved in sensing their cognate amino acids along with novel biological roles [264]. In LAA, expression of some tRNA synthetases is upregulated but not sufficiently enough to meet our differential expression criteria (the fold change and *p-value* for all the tRNA synthetases are provided in Annexure 1). TRMO, an enzyme responsible for tRNA methylation, is also upregulated in LAA (*p-value* 0.03, LFC 0.7). Methylation by TRMO is hypothesised to improve the efficiency of the tRNA decoding ability [265].

Once activated, GCN2 kinase phosphorylates eIF2 α , which suppresses global protein synthesis [266]. Under these circumstances, specific mRNAs exhibit increased translation, as first discovered in yeast for transcription factor GCN4 [267], whose mammalian counterpart is ATF4, which is a “master regulator” driving transcriptional dynamics for hundreds of genes under amino acids limitation [268–270]. Phospho-eIF2 α promotes the translation of selected mRNA species; among these are activating transcription factors 4,5 (ATF 4,5), GADD34. GADD34 permits reactivation of translation by dephosphorylating phospho-eIF2 α , permitting translation of the upregulated stress-responsive mRNA species

Three mechanisms are involved in the upregulation of gene expression by amino acid deficiency: (i) mRNA stabilization, e.g. CAT1 (ii) upregulation of the translation rate of one specific transcript, e.g. CAT1; (iii) transcriptional control, e.g. ASNS. We find an increased expression of ATF4 (*p-value* 0.02 FC 0.96). Downstream targets of ATF4/ CHOP (*p-value* 0.05, FC 1.15), which include GADD45A/B (*p-value* 0.05, FC 1.73), TRIB3 (*p-value* 0.07, FC 1.71), ATF3 (*p-value* 0.06, FC 2.02) ATG10, CHAC1 were also found to be upregulated. Mechanisms like the presence of short upstream open reading frames in the GCN4 [267] and ATF4 mRNA [271,272] permit translation of the transcription factor when global protein translation has been suppressed in response to eIF2 α phosphorylation. ATF4 gene targets promote cellular adaptation to the amino acid shortage. ISR inhibits global protein synthesis; increased the expression of genes for amino acid transporters (SLC7A1, SLC7A5, SLC38A2, and SLC3A2), aminoacyl-tRNA synthetases (YARS, SARS, LARS), and, to a limited extent, amino acid metabolism (ASNS) [247].

7.4.3 Differential expression of amino acid sensors

7.4.3.1 Amino acid transporters

Amino acids are not stored intracellularly. Hence the cytosolic pool of each amino acid is tightly regulated. As introduced in chapter 2, intracellular amino acid pools are regulated inside the cells primarily by their import and export through transporters, their biosynthesis and catabolism and protein synthesis and degradation. Seminal work on transporters and recent refinement due to advancements in cloning technologies have led to their classification into systems. The human genome contains ~50 different amino acid transporters, many of which have specialised roles in specific cell types [273,274]. Amino acid transport activities are frequently referred to as “systems” which accept groups of amino acids having similar properties (charge) rather than individual amino acids. Amino acid transporters can further be simply classified into loaders, harmonizers and rescue transporters (Figure 7.5). Loaders import amino acids and help accumulate amino acids in the cytosol. Harmonisers, exchange the accumulated amino acid for another amino acid needed by the cell and hence should have overlapping substrates with amino acid loaders. This exchange mechanism ensures that intracellular exhaustion of a particular amino acid is

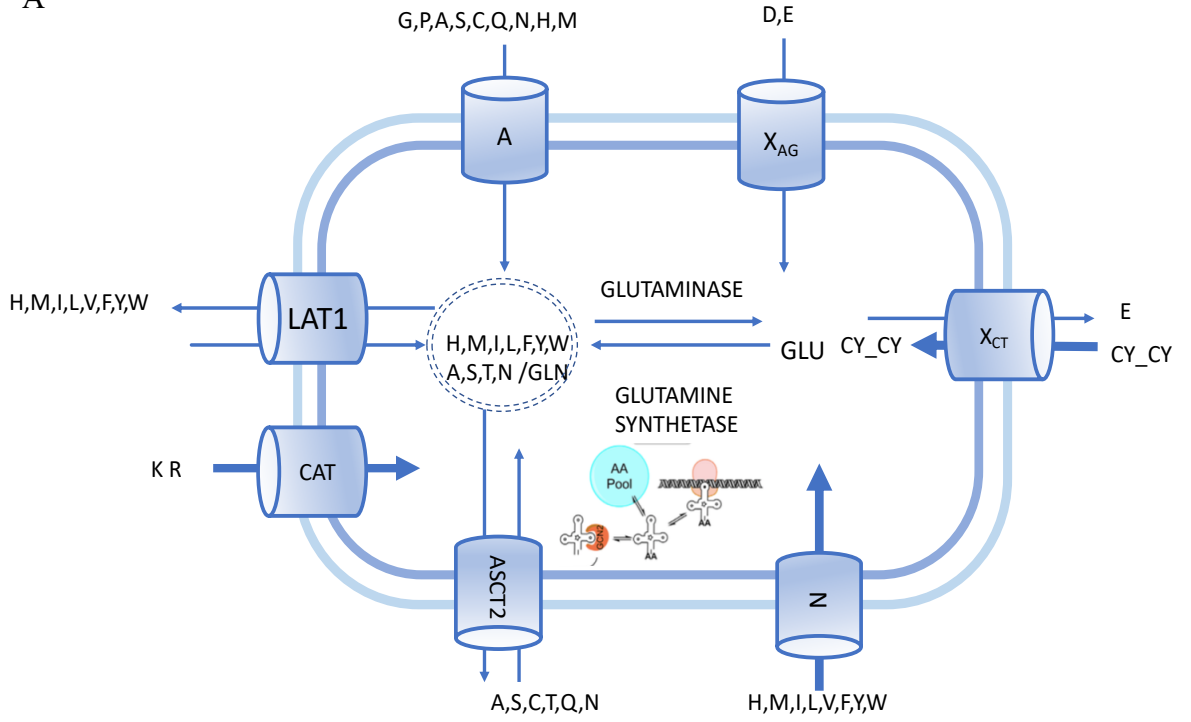
prevented [275]. The homeostasis of the cationic amino acid (lysine, arginine and ornithine) is different owing to the positive charge of these amino acids. Cationic amino acid transporters (CAT1–3) mediate facilitated diffusion [270], which is accumulative due to the negative membrane potential of mammalian cells [277]. It is important to note cationic amino acid transporters are also capable of acting as harmonisers and are reported to be upregulated under amino acid deprivation [278]. As a result, they can serve as a versatile all-in-one loader, harmoniser and rescuer. This explains the upregulation of SLC7A1 (*p-value* 0.07, FC 1.3) which is a cationic amino acid transporter along SLC38A2 (*p-value* 0.02 FC 0.8) SLC6A9 (*p-value* 0.08, FC 1.7) in LAA (Figure 7.5). Interestingly this activation of the amino acid transporter occurs when the limiting amino acid may or may not be a substrate for the upregulated transporter [255]. As mentioned earlier, mechanisms used by transporter gene expression to cope with amino acid deficiency are (i) mRNA stabilization, e.g. CAT1, (ii) upregulation of the translation rate of one specific transcript, e.g. CAT1; (iii) transcriptional control and alternative mechanism make use of uORFs to change the secondary structure of mRNA exposing an internal ribosome entry site (IRES) in the mRNA. This is used to translate CAT-1 more frequently when cap-dependent translation is suppressed due to low levels of eIF2 α ·GTP·Met-tRNAMi [275,279,280].

Such activation of only SNAT and CAT transporters is intriguing and may point towards explanations that support the existence of a minimum set of transporters required to sustain a cell. As seen in Figure 7.6, transporter transcript levels for 917 cancer cell lines were analysed, and only a few transporter genes were observed to have high expression in all cancer cell lines (upward-pointing blue bars across the x-axis). These transporters were hypothesized to be indispensable for maintaining intracellular amino acid homeostasis, whereas other transporters were likely to have specialised roles.

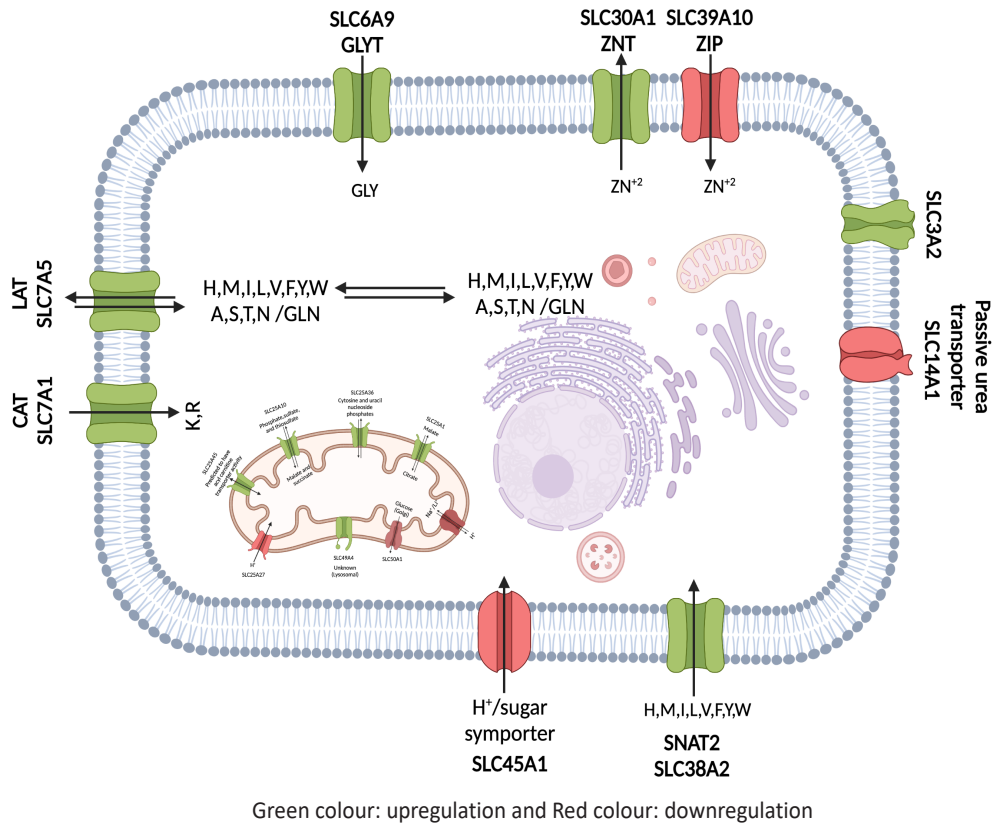
In our data set, 17 SLCs were found to be altered. They can be divided into amino acid transporter encoding genes (5 genes) and genes encoding non-amino acid transporters (9 genes), putative SLCs (2 genes), or atypical SLCs (1 gene). Amino acid transporters like CAT-1, LAT, and SNAT2 are upregulated along with the ancillary protein required by many transporters. Indicating AAR response to maintain

amino acid homeostasis. About 15 genes encoding SLC amino acid transporters were found to upregulated including SLC7A11, SLC6A9, SLC7A1, SLC1A4, SLC7A5, SLC1A5, SLC38A7, SLC38A1, SLC3A2, SLC38A2, SLC25A26, SLC15A4, and SLC16A10 on subjecting N25/2 cells to amino acid starvation [281]. We find similar genes to be upregulated. Among the genes encoding non-amino acid transporters, atypical SLCs (12 genes) 6 genes are upregulated, 6 genes are downregulated. These were transporters for sugars, ions, zinc, nucleosides, and H⁺ mostly occurring in the mitochondria indicating modulation in mitochondrial activity and hence metabolism. Transporter for various vitamins and carbohydrates were also downregulated though not to the same level.

A



B



C

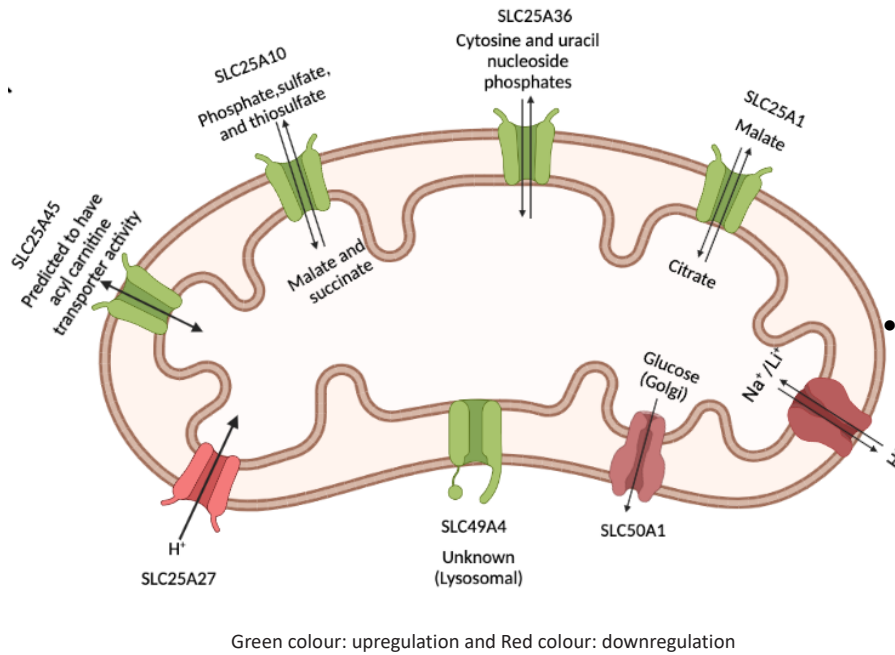


Figure 7.5: Alterations in SLC transporter gene expression following growth in LAA condition

(A) Description of typical transport systems present in a cell. (B) Differentially expressed SLC transporters on the cell membrane (C) Differentially expressed SLC transporters on the intracellular organelles. The green colour represents upregulation; the red colour represents downregulation. Created with BioRender.com

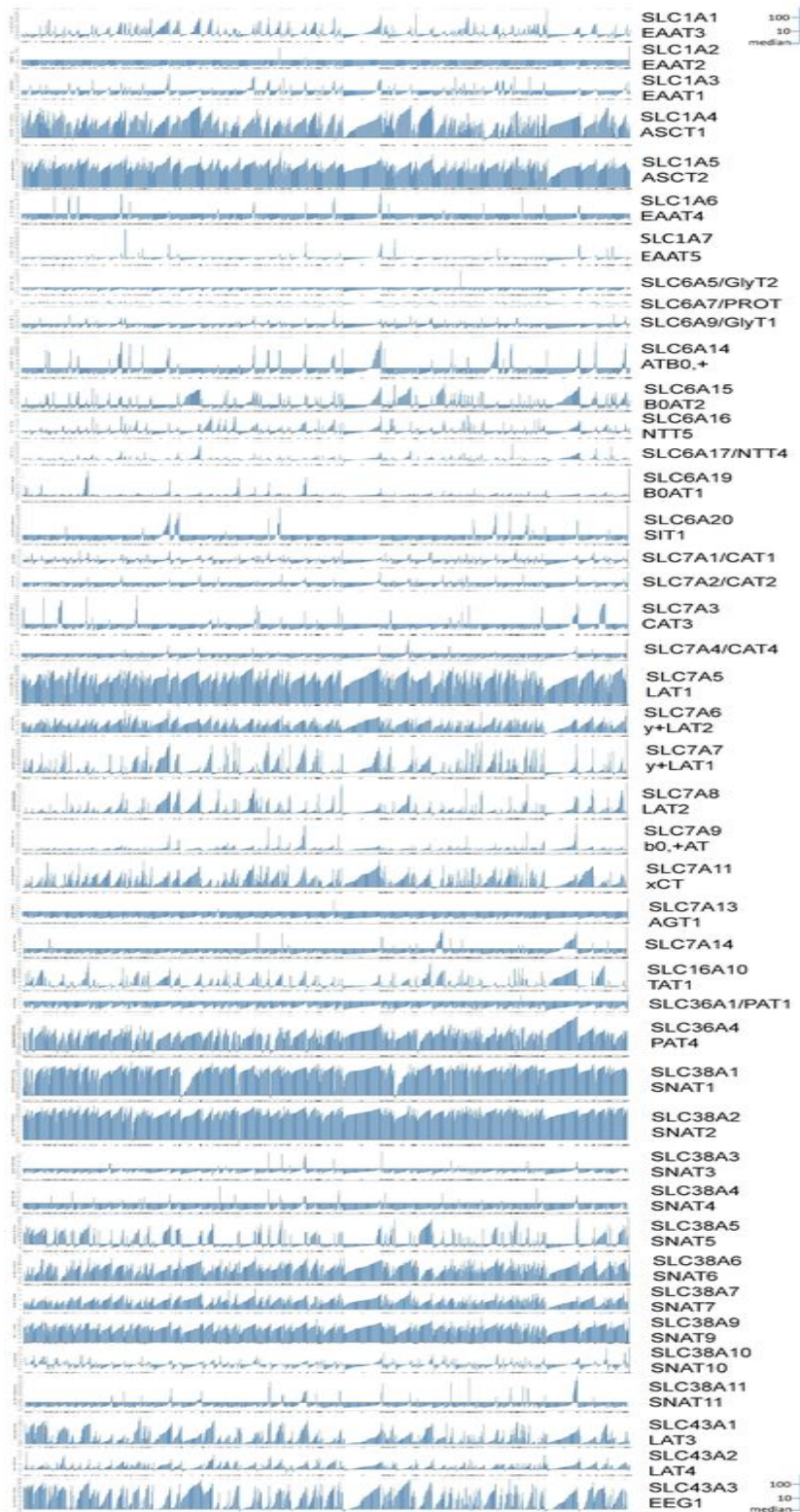


Figure 7.6: The amino acid transporters in cancer cells.

Adapted from Broer et al. [269], Amino acid transporter transcript levels were analysed for 917 cancer cell lines and are depicted as vertical blue bars. Data are depicted as log₂ expression levels relative to the median expression of all genes in the genome. Blue-coloured bars pointing indicate well-expressed genes; bars pointing downwards indicate weakly expressed genes.

Table 5: Differentially expressed SLC genes

	<i>p-Value</i>	Fold change
Slc6a9	0.083	1.62
Slc7a1	0.066	1.26
Slc38a2	0.019	0.77
Slc30a1	0.019	0.99
Slc39a10	0.005	-0.66
Slc25a36	0.001	0.57
Slc3a2	0.107	0.57
Slc45a1	0.060	-0.58
Slc25a10	0.019	0.44
Slc25a45	0.179	0.45
Slc49a4	0.020	0.48
Slc25a1	0.003	-0.49
Slc50a1	0.026	-0.47
Slc14a1	0.014	-0.42
Slc25a27	0.256	-0.42
Slc9b2	0.127	-0.41

7.4.3.2 mTOR

The mTOR pathway, specifically the mTORC1 complex, is the most important cellular amino acid sensor that promotes protein synthesis [282–286] [287,288]. An active mTORC1 complex will stimulate protein biosynthesis and suppress autophagy to increase the anabolic state of the cell, while an inactive mTORC1 complex does the opposite. mTORC1 integrates multiple signals to do that, though not everything is understood about its activation. Growth factors, protein kinase AKT (growth factors), AMPK or ERK (mitogens) activate mTORC through Tuberous sclerosis complex 2 (TSC2). mTORC1 can only be activated by amino acids as long as TSC2 remains inoperative, as TSC2 has GTPase activity towards mTORC1 activator Rheb, inactivating Rheb by hydrolysing its GTP to GDP [289,290]. In a starved state,

mTORC1 is found throughout the cytoplasm. Upon the addition of amino acids, mTORC1 translocates to the lysosomal surface, where it is activated by Rheb [291].

Amino acids activate mTORC1, the major ones being leucine, glutamine and arginine [282]. The mTORC1 complex has sensors for amino acids in the lysosome and the cytosol; however, the precise mechanism is not understood. When cells are deprived of amino acids, other essential elements are the vacuolar H⁺-ATPase, the regulator complex, Rag GTPases (Rag A/B and C/D) and the lysosomal arginine transporter SLC38A9 (lysosomal arginine sensor- it is reported that depletion of lysosomal amino acids through overexpression of the lysosomal transporter (SLC38A1) inactivates mTORC1 signalling pathway) [292–295]. Cytosolic amino acid levels change the nucleotide-bound state of Rag GTPases associated with mTORC1 (Starving induces a GDP-bound state, and sufficiency induces a GTP-bound state). The exchange between GDP and GTP appears to be regulated by proteins associated with amino acid sensing like castor and GATOR. Castor1/2 act as cytosolic arginine-binding proteins to activate mTORC1 [287,290], which is mediated through GATOR1 and/or GATOR2. The GATOR1 complex inhibits mTORC1 activity by hydrolysing Rag-bound GTP to GDP. Sestrin2 is thought to act as a cytosolic leucine-binding protein, also regulating mTORC1 via GATOR1 and/or 2 [266,296]. Some aspects of this model are still disputed, and alternative models have been put forward [263,284]. Alternative models for leucine sensors have also been proposed; for example, leucyl-tRNA synthetase (LARS) has been suggested as the cytosolic leucine sensor for mTORC1 acting as a GTPase-activating protein (GAP) for RagD [263], however, sestrin (SESNs) as a possible leucine sensor is debated [297]. It has also been found that lysosomal transporters PAT1/4 are required for amino acid signalling by mTORC1 [284,298]. About 25% of TOP mRNA were downregulated, reducing ribosomal protein levels. SESNs are conserved stress-inducible proteins. ATF4 induces the expression of Sestrin2 (*p-value* 0.04, FC 2.4), which persists suppression of mTORC1 by blocking its lysosomal localization by inhibiting GATOR2. Elevated DDIT4 and TRIB3 expression inhibit mTORC1. DDIT4 relieves inhibition of the TSC1/TSC2 complex, which is a negative regulator of mTORC1. TXNIP inhibits mTOR activity by binding to and stabilizing Redd1 protein. mTOR controls ribosome biogenesis by promoting the translation of mRNAs for RPs and by affecting ribosomal RNA (rRNA) synthesis. In yeast, the synthesis of rRNA represents ~60% of total transcriptional activity, and

the synthesis of mRNAs encoding RPs accounts for ~60% of all Pol II transcription initiation events. Inhibition of mTOR signalling leads to downregulation of rRNA transcription and pre-rRNA processing [299]. mTORC1 promotes protein synthesis by directly phosphorylating S6K1 and the eukaryotic initiation factor 4E-BP1. In particular, through 4E-BP1 proteins, mTORC1 stimulates the translation of a subset of mRNAs possessing 5' terminal oligopyrimidine (TOP) motifs, such as mRNAs encoding ribosomal proteins. About 25% of TOP mRNA are affected, reducing the ribosomal synthesis in the cell when cultured under LAA condition, indicating suppressed ribosomal protein synthesis.

Ragulator complex

The multiprotein Ragulator complex is an integral part of the mTORC1 signalling pathway. It comprises p18 [encoded by LAMTOR1 (late endosomal/lysosomal adaptor, MAPK and mTOR activator)], p14 (LAMTOR 2), MP1 (MEK-binding partner 1, encoded by LAMTOR 3), C7orf59 (encoded by LAMTOR 4) and HBXIP (hepatitis B virus X-interacting protein, encoded by LAMTOR 5) [300]. Ragulator functions as a guanine nucleotide exchange factor (GEF). Amongst its components, LAMTOR 1 functions as a scaffold for the Rag GTPases and LAMTOR2/LAMTOR3 and LAMTOR4/LAMTOR5 anchoring the complex to the lysosomal surface. Depletion of Ragulator components disrupts Rag GTPases attaching to the lysosome and prevents the lysosomal recruitment of mTORC1. We observed downregulation of LAMTOR1 and 2 (not statistically significant). A deficiency of LAMTOR 2 can lead to the inactivation of mTOR and ERK pathways, as shown in a recent study in mice [301].

7.3.4 Cell cycle arrest observed when cells are cultured in LAA

The cell cycle is a critical and complex control system essential for cell processes such as mitosis and DNA replication that leads to cell proliferation. The cell cycle is divided into two phases: M-phase (Mitosis) and interphase, which is further subdivided into S (Synthesis), G1(Gap-1) and G2 (Gap-2) phase (Figure 7.7). During G1, the cell prepares for replication of the nuclear material (S-phase); in G2, the cell prepares for cell division, followed by M-phase, where mitosis occurs, giving rise to two daughter cells. The cell cycle control system has stringent checkpoints and does

not let the cell advance into the next phase of the cell cycle until the preceding one has been completed. The cell cycle is controlled by cyclins, cyclin-dependent kinase (CDK), and cyclin-dependent kinase inhibitors (CDKI), regulating the transition to the subsequent cell cycle phase [302]. Typically, cyclin protein levels alternately rise and fall during the cell cycle and periodically activate CDK [303] (Figure 7.7), and different cyclins are necessary at different phases of the cell cycle to proceed on to the next phase of the cell cycle (Figure 7.7). We note that Cyclins D1 and F were downregulated in our transcriptomics data. The D type cyclins (cyclin D1, cyclin D2, cyclin D3) bind to CDK4 and CDK6, and the CDK-cyclin D complexes are obligatory for entering the G1 [304]. A decrease in cyclin D can affect the G1 to S progression in two ways. Firstly, it would reduce the formation of the cyclin D-CDK complexes. Secondly, it would raise the associated CDKI to bind and inhibit the required cyclin E-CDK complex. Cyclin kinase inhibitors CDKN1A and CDKN2B, which form a complex with CDK4/CDK6, and prevents the activation of the CDK kinases, are upregulated, arresting the cell cycle at the G1 phase. The inhibitory activity of CKI results in growth suppression. Hence, alterations of at least one of the cell cycle regulators is found in nearly all human cancers [305–307]. Apart from acting as a growth sensor, Cyclin D also links cell cycle and mitogenic stimuli. Cyclin D1 binds to CDK4 and CDK6 in the early G1 phase.

The FoxO forkhead transcription factors are important physiological targets of phosphatidylinositol-3 kinase (PI3K)/Akt signalling. FOXO3A (*p-value* 0.01, LFC 0.6), upregulated in LAA, has been shown to induce cell cycle arrest at G1 phase and is known to be associated with longevity [308]. Cell-cycle machinery is known to be linked with the control of the cytoskeleton. Genes like SAPCD2 (*p-value* 0.01, LFC -0.6), TUBB4B (*p-value* 0.05, LFC 0.7), CCN1 (*p-value* 0.01, LFC 1.1), RND3 (*p-value* 0.04, LFC 0.9), MTSS2 (*p-value* <0.01, LFC 0.7), FHOD1 (*p-value* 0.04, LFC -0.8), FLRT3 (*p-value* 0.04, LFC 0.6), TMEM107 (*p-value* <0.01, LFC -0.6), WASF1 (*p-value* 0.02, LFC 0.7), MICALL2 (*p-value* 0.03, LFC -0.7), involved in mitotic spindle formation, microtubule structure, cytoskeletal organisation and plasma membrane dynamics are also differentially expressed in LAA. These transcriptional changes are consistent with the reticent growth observed in LAA.

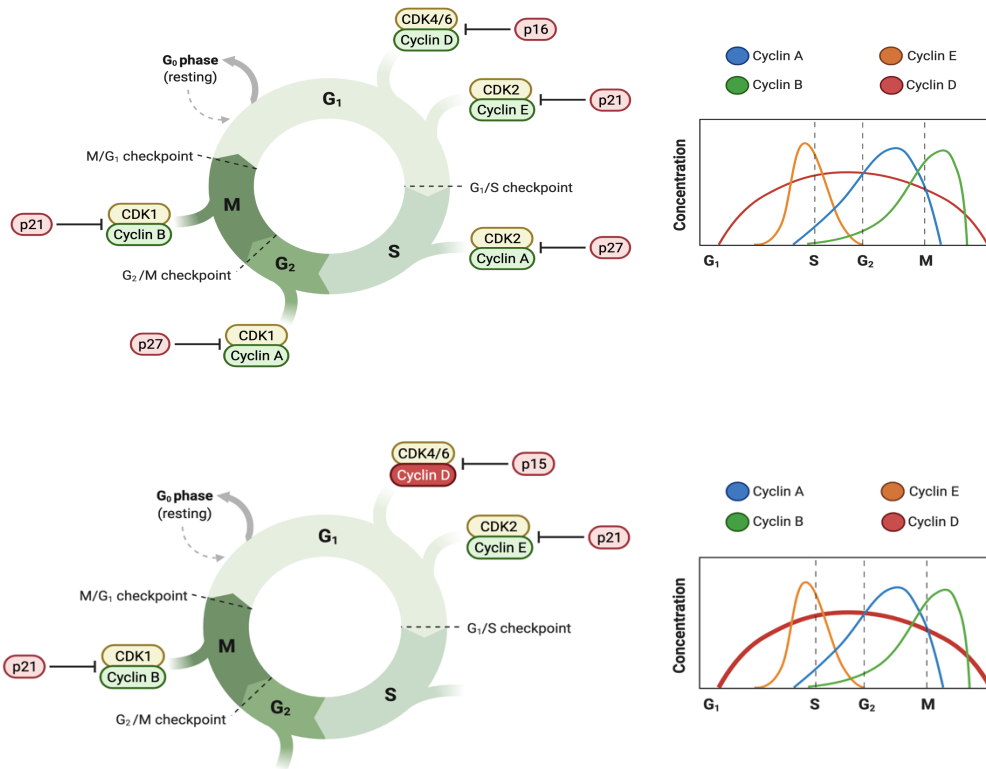


Figure 7.7 Disruption in cell cycle regulation following growth in LAA condition

Differentially expressed genes involved in cell cycle regulation are highlighted in red. Created with BioRender.com

7.4.5 Autophagy

Autophagy is a conserved cellular process to recycle non-essential nutrients and organelles to enable cells to adapt to strenuous conditions. During autophagy initiation, a membrane will be isolated to form a phagophore. The phagophore membrane will then engulf the desired cargo to form a closed double-membrane organelle, called an autophagosome which fuses with a lysosome upon maturation (Figure 7.8). Core proapoptotic like BCL-2, BAX, BAD, BAM and caspases were unaffected in our dataset. DRAM, ULK1, BNIP3L, ATG10, and ATG12 were affected (Figure 7.8), These genes are essential in the autophagic process, as they mediate the formation of the autophagosome. It is also essential for the restoration of mTORC1 signalling. Amino acid sufficiency represses autophagy; amino acid starvation is known to stimulate autophagy. The amino acid limitation is linked to the activation of autophagy by mTOR, which integrates signals from extensive metabolic stimuli [309]. As already mentioned, upregulation of TRIB3 inactivates mTORC1,

activating autophagy. ATF4 also regulates autophagy by controlling the expression of various autophagy genes [310,311]. It has been demonstrated that the eIF2 α /ATF4 directs an autophagy gene transcriptional response to amino acid starvation or ER stress. eIF2 α kinases GCN2 and PERK and the transcription factors ATF4 and CHOP are also required to increase the transcription of genes implicated in the formation, elongation and function of the autophagosome [310]. As the autophagosome continues to expand, ATGs are increasingly recruited into the autophagy system. The autophagic machinery consists of three major systems consisting of ATG1, ATG2, ATG9, ATG18 system, the vacuolar protein sorting 34 (VPS34) complex and ATG8, ATG12, ATG7, ATG10, ATG3, ATG4, ATG16 [312]. The downstream effect of eIF2 α phosphorylation on autophagy is transcriptional, as transcription of ATG12 is upregulated by phosphorylated eIF2 α in eukaryotic cells [313]. Withdrawal of amino acids provokes an increase in cytosolic Ca²⁺. Amino acid starvation could activate autophagy through Ca²⁺ signalling, which can also be measured to further confirm autophagy.

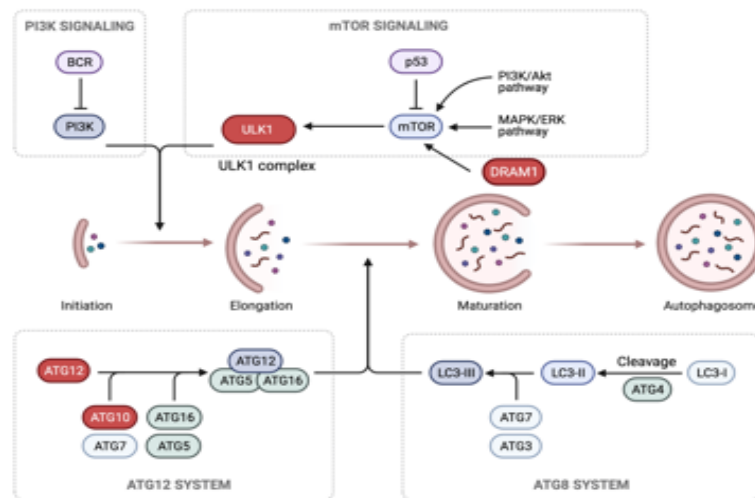


Figure 7.8: Disruption in cell cycle regulation following growth in LAA condition

Genes involved in autophagy are differentially expressed and highlighted in red. Created with BioRender.com

7.4.6 Other differentially expressed genes

Other important differentially expressed genes involved a lot of transcription factors and genes involved in the p53, ERK FOXO pathways. Upregulation of these is routinely observed in several cancer models

Mafk

Mafk is a member of the basic region leucine zipper (bZIP)-type transcription factor family [286]. Mafs lack the transcriptional activation domain; hence, Mafs participate in transcriptional activation or repression depending on their heterodimeric associate molecule and the cellular context. sMAFs have also been implicated in modulating enzymes methionine adenosyltransferase II A (MATIIA), heme oxygenase-1 [314,315].

RNF182

Ubiquitylation is a post-translational modification which involves the conjugation of ubiquitin to the lysine residues of various cellular target proteins. It is catalyzed by a three-enzyme cascade consisting of Ub-activating enzymes (E1s), Ub-conjugating enzymes (E2s), and Ub ligases (E3s). RNF182 is an E3 ubiquitin-protein ligase facilitating the direct transfer of ubiquitin from E2-ubiquitin intermediates to the target protein [316]. Intriguingly, RNF182 is associated with the mTORC signalling pathway since RNF182 silencing and treatment with an mTORC inhibitor negates the effect of RNF182 silencing. Thus, it is likely that RNF182 silencing activates the mTORC signalling pathway. However, the target substrate of RNF182 has not yet been identified [317]. ATP6V0C is a multi-subunit enzyme present in intracellular organelles, endosomes, lysosomes, and the Golgi complex, where it plays a role in their acidification and maintenance of endocytic and exocytic pathways. RNF182 also mediates the ubiquitination of ATP6V0C and targets it to degradation via the ubiquitin-proteasome pathway.

KLHL24

KLHL24 belongs to a family of proteins with a Kelch-like motif part of a ubiquitination-ligase complex [318]. KLHL24 is a significantly upregulated gene

related to the regulation of cell structure, stress responses, and cell proliferation [319][320]. KLHL24 is the receptor of the cullin 3 (CUL3)–RBX1–KLHL24 ubiquitin-ligase complex, with K14 (genes encoding the basal cell keratins) being the ubiquitination substrate. Cullin RING ubiquitin E3 ligases (CRL) is the largest family of ubiquitin E3 ligases, and CRL is a multiprotein complex in which cullin serves as a scaffold linking a ubiquitin donor, E2 ubiquitin-conjugating enzyme, to a ubiquitin acceptor, substrate. KLHL24 is a p73-regulated gene associated with autophagy and metabolism, identifying mTOR as a key signalling pathway upstream of p73 [321].

KLF5

KLF5 and members of the KLF family of transcription factors belong to the Krüppel-like factor family and mediate cell proliferation, cell cycle, apoptosis, migration, differentiation, and stemness by regulating gene expression [322]. The expression and activity of KLF5 are regulated by multiple signalling pathways like Ras/MAPK, PKC, TNF α and TGF β , and various posttranslational modifications, including phosphorylation, acetylation, ubiquitination, and sumoylation. Consistently, KLF5 regulates a number of important target genes, such as cyclin D1, cyclin B, PDGF α , and FGF-BP. KLF5 has essential roles in cell cycle regulation, apoptosis, migration, and differentiation. KLF5 interacts with components of the transcriptional machinery, including initiation factors, TFIIB, TFIIEb, and TFIIIFb, as well as the TATA box-binding protein (TBP). KLF5 can also mediate the modification of histone to regulate chromatin in gene regulation. Munemasa et al. recently found that KLF5 recruits histone chaperone, acidic nuclear phosphoprotein 32B onto gene promoter, repressing the transcription of a gene downstream KLF5 [323]. The KLF5 protein has been shown to associate with various transcription factors, such as retinoic acid receptor, NF κ B, p53, C/EBP β /d, FOXA1 and SREBP-1, to regulate gene transcription. Fujiu et al. reported that KLF5 forms transcriptional complexes with RAR/RXR heterodimer on PDGF promoter [324]. KLF5 has been shown to be ubiquitinated. Chen et al. found that KLF5 is degraded through the ubiquitin-proteasome pathway [325]. KLF5 also has an anti-apoptosis function. KLF5 promotes cell proliferation by accelerating the G1/S and G2/M cell cycle progression.

TNFAIP3

The TNFAIP3 (tumour necrosis factor- α -induced protein 3) gene encodes a ubiquitin editing enzyme, A20, a cytoplasmic protein that restricts NF- κ B-dependent signalling. Trp53-dependent cell-cycle control is determined largely by the Trp53-responsive Cdkn1a, which induces G1 and G2 growth arrest [327].

Trp53inp1

TRP53INP1 is induced by ROS [328] and was previously isolated as a TRP53-inducible protein that participates in Trp53-dependent apoptosis by regulating TRP53 function [329]. Studies showed that it also regulates ROS and autophagy [328,330,331]. TRP53INP1 binds to HIPK2, PRKCD, and TRP53 to mediate the phosphorylation of TRP53. This increases TRP53 stability and transcriptional activity, leading to activation of TRP53 target genes such as TP53AIP1, cell growth arrest, and apoptosis upon DNA damage [332,333].

CHAC1

Amino acid starvation is known to induce CHAC1 expression. Cystine starvation induces CHAC1 expression, and a GSH degradation study showed that ATF4 activated the transcription of CHAC1 to augment ferroptosis [15]. CHAC1 induces GSH degradation [35]. This implies that ATF4 upregulation also leads to GSH degradation [334]. ATF4, ATF3, and CEBP β regulate CHAC1 transcription. CHAC1 protein overexpression thus depletes glutathione. CHAC1 degrades glutathione into 5-oxoproline and Cys-Gly dipeptide, thus depleting intracellular GSH levels [335]. CHAC1 was one of the largest changes in the gene expression induced by cystine starvation in the three TNBC cells [334] [336].

TRIB

TRIB3 physically interacts with Akt [337,338], NF- κ B [339], caspase-3 [340], mTOR [341] and MAPKKs [342], linking TRIB3 and the regulation of cellular stress responses. TRIB3 has been found to enact both pro-survival [343,344] as well as pro-death [302,304] roles in cells subjected to stress. TRIB3 limits excessive CHAC1

activity downstream of ATF4 and also enacts a critical role in cytotoxic conditions [345].

SGK

The SGK1 gene encodes a 50 kDa protein that is a member of the “AGC” family of serine/threonine protein kinases. AGC kinases, including PKA, PKB, PKC (protein kinase C), p70S6K and SGK, all contain a conserved A loop targeted for activating phosphorylation by PDK1. SGK1 upregulates ion channels, carriers, and the Na⁺/K⁺-ATPase. SGK1 regulates enzymes and transcription factors participating in the regulation of transport, hormone release, inflammation, coagulation, cell proliferation and apoptosis. Insulin and growth factors stimulate the activation of SGK1 as well as other AGC kinases, such as Akt, S6K, RSK and PKC isoforms, by enhancing the phosphorylation of these enzymes. SGK1 gene is upregulated by cell shrinkage. SGK1 is under dual control: protein levels are under transcriptional control, while its activity is PI3K dependent. The kinase is activated by insulin and growth factors via PI3K, phosphoinositide-dependent kinase (PDK1) and mTORC2. SGK1 is also a mTORC1 substrate and links mTORC1 and cell-cycle regulation by SGK1-dependent phosphorylation of p27. PI3K and mTOR-raptor-independent pathways may also activate SGK1. SGK1 overexpression promotes cancer cell proliferation through multiple pathways, including effects on FOXO3 α , c-fms, and NF- κ B [346–348] and inhibition of MEKK3 [349]. As for Akt, SGK phosphorylates bRaf, GSK3- β , and FKHRL1 [350,351]. SGK1 alternates between cytoplasm in G1 and nucleus in S and G2/M [352]. Phosphorylation of p27 by SGK1 delays nuclear import of newly synthesized p27 in the G1 phase of the cell cycle to facilitate cyclin D-Cdk assembly. In oncogenic cells, activation of PI3K and mTOR pathway recruits SGK1 to drive cytoplasmic mislocalization of p27, thereby impeding its inhibition of cyclin-Cdk2.

Elovl6

Elovl6 is a microsomal enzyme involved in the elongation of C16 saturated and monounsaturated FAs to form C18 FAs. Elovl6 belongs to a family of ER enzymes involved in synthesising long-chain fatty acids. This enzyme catalyses the elongation of saturated and monounsaturated fatty acids with 12, 14, and 16 carbons and is an essential enzyme responsible for endogenous fatty acid synthesis [353].

CHD5

Nonhistone chromosomal proteins play important roles in regulating gene expression and in the replication and repair of DNA. Chromodomain helicase DNA binding protein 5 (CHD5) belongs to a superfamily of SWI2/SNF2-related ATPases, a significant group of nonhistone chromosomal proteins. CHD5 is identified as a novel tumour suppressor gene (TSG) [354]. By regulating chromatin structure, CHD5 can function to stabilize p53 [355]. It has also been reported that CHD5 expression is suppressed epigenetically by promoter hypermethylation [356]. CHD5 possess a unique combination of chromo, helicase, and DNA binding motifs, suggesting that CHD5 may epigenetically modify chromatin to regulate gene expression affecting cellular development.

EGR1

The early growth response gene 1 (EGR1) transcription factor regulates the HIF-1 α gene during hypoxia. EGR1 targets include the tumour suppressors PTEN, p53 and c-Jun. The absence of EGR1 keeps cell proliferation and growth signals in check by allowing the growth suppressors to act unopposed. A variety of growth factors can initiate EGR1 expression by interacting with serum response elements sequence in the EGR1 promoter region. The EGR1 promoter contains an EGR1-binding sequence (EBS), forming a negative feedback loop to control EGR1 expression. EGR1 can be activated through the MAPK signalling pathway, RAS–RAF–MEK1/2–ERK1/2 signal transduction pathway, and activated EGR1 can either initiate or inhibit the expression of its target genes, thus transcriptionally regulating them [357]. EGR1 plays an important role in cell proliferation and cell survival. EGR1 suppresses transformation and apoptosis via coordinated activation of TGF- β 1, FN, p21Waf1/Cip1, and FAK via enhanced cell adhesion and reduced caspase activity [358,359]. As a downstream protein of the MAPK signalling pathway [303] [360], EGR1 can affect cell cycle proteins; for example, it promotes the transcription of cyclin D1 in many oncogenic cells and maintains the mitosis of tumour cells [361]. It can lead to cell proliferation by advancing cells from the G1 phase to the S phase. EGR1 can also induce cell proliferation by upregulating cell cycle associate proteins such as cyclin D2 and CDK4.

Pim 3

Pim 3 is a Ser/Thr protein kinase associated with MYC coexpression. It plays a role in regulating signalling cascades, contributing to cell proliferation and survival. Pim-3 caused increases in phosphorylation of several downstream proteins such as BAD (Ser112), MDM2 (S166), and STAT3 (Y705), which results in increased expression of c-Myc and Bcl-xL. Overexpression of MYC leads to G2 cell cycle arrest through p53, regulating cellular transcription and cell cycle processes in conjunction with the Myc pathway. Pim-3 is known to prevent apoptosis and promote cell survival and protein translation, thereby enhancing cell proliferation of normal and malignant cells [362].

GPER1

G protein-coupled oestrogen receptor 1 (GPER1) is a G protein-coupled receptor (GPCR) that was recently found to bind 17 β -estradiol (E2) and mediate oestrogenic signals. GPER1 couples to G proteins and modulates secondary signalling pathways via cyclic-AMP and Ca²⁺[363]. Recent studies indicate that GPER1 activation leads to mTOR phosphorylation downstream of PI3-kinase [364].

NNMT

NNMT catalyzes the methylation of nicotinamide (NAM) using the universal methyl donor SAM to generate S-adenosyl-L-homocysteine (SAH) and N1-methyl nicotinamide (MNAM). NAM is a precursor for NAD⁺, a cofactor that donates electrons to the mitochondrial complex I in the electron transport chain and for multiple oxidoreductases. Enzymes like sirtuins and poly-ADP-ribosyltransferases (PARPs) use NAD⁺ as a co-substrate for deacetylation and ADP-ribosylation reactions and regulate multiple metabolic processes. Both sirtuins and PARP are NAD⁺-consuming enzymes, utilizing NAD⁺ as a substrate and releasing NAM, inhibiting their enzymatic activity. Thus, changes in NNMT activity might potentially influence intracellular NAM and NAD⁺ levels and the activity of multiple pathways. The affinity of NNMT for NAM is relatively low at around 430 mM, while the affinity of NAM phosphoribosyltransferase (NAMPT), the rate-limiting step in NAD⁺ biosynthesis, is less than 1 mM. NAMPT is considered saturated with NAM, and thus it is unlikely that increased NNMT expression would decrease intracellular NAM to

limiting levels for NAD⁺ synthesis by NAMPT. It has been reported that NNMT does not directly modulate intracellular NAM and NAD⁺ levels. NNMT is required for glucose independence and enables glucose-deprived cells to utilize alternative carbohydrate sources as energy sources [365]. NNMT modulates energy expenditure in adipose tissue and controls glucose, cholesterol, and triglyceride metabolism in hepatocytes through interaction with sirtuins [366]. PERK-ATF4 pathway activation is the main contributor to ER stress-mediated NNMT upregulation in the liver. Activation of the lipogenic pathway by NNMT was independent of its NAD⁺ enhancing action; however, increased cellular NAD⁺, resulting from NNMT inhibition, was associated with marked AMPK activation [361]. Elevated NNMT activity can decrease cellular NAM levels and effectively inhibit apoptosis. Recent studies show that the activity of NNMT can also regulate post-translational modifications like acetylation and methylation.

MED12

The mediator complex is a set of proteins essential for transcription by RNA polymerase II. MED12 is a component of the transcriptional MEDIATOR adaptor complex that serves as a link between the transcription and its upstream activators [368]. MED12 is a subunit of the “kinase” module of the MEDIATOR complex (kinase module also contains MED13, CYCLIN C, and CDK8). As part of the kinase module, MED12 can interact with methyltransferase to induce histone methylation, thereby repressing gene transcription [369]. By this, MED12 negatively regulates the activity of the Mediator Complex. MED12 can also interact with different factors to regulate diverse biological activities. MED12 is in part cytoplasmic, where it negatively regulates TGF-βR2 by physical interaction. MED12 suppression results in activation of TGF-βR signalling by increasing TGF-βR2 protein levels. TGF-β signalling causes RAS-MEK/ERK activation [370]. MED12 suppresses TGF-βR2 in a posttranscriptional manner [368]. The activation of CDK8 kinase is unique from other CDKs in that its activation is not dependent on cyclin phosphorylation. Instead, the activation happens via physical binding between MED12 and CCNC [371]. It is interesting to note that in contrast to other CDKs, the activity of CDK8 does not fluctuate with phases of the cell cycle. However, CDK8 causes cell cycle arrest by activating the transcription of p21, a CDK inhibitor, in response to genotoxic stress

[372]. It is also known to phosphorylate cyclin H inhibiting CDK1 activation and suppressing mitosis [373]. Mutations of MED12 increases AKT signalling leading to inhibition of gsk3 β and activation of mTORC concurrently.

GFOD1

GFOD1 (Glucose-Fructose Oxidoreductase Domain Containing 1) gene that has oxidoreductase activity.

INSIG1

INSIG1 is an important endoplasmic reticulum membrane protein that regulates cholesterol metabolism, lipogenesis, and glucose homeostasis. It binds the sterol-sensing domains of sterol regulatory element-binding protein (SREBP), cleavage-activating protein (SCAP) and 3-hydroxy-3-methylglutaryl-coenzyme A reductase (HMG-CoA reductase). It is essential for the sterol-mediated trafficking of these two proteins. It promotes the endoplasmic reticulum retention of SCAP and the ubiquitin-mediated degradation of HMG-CoA reductase.

IRS1

This gene encodes a protein which is phosphorylated by insulin receptor tyrosine kinase and mediate the control of various cellular processes by insulin. When phosphorylated by the insulin receptor binds specifically to various cellular proteins containing SH2 domains such as phosphatidylinositol 3-kinase p85 subunit or GRB2. Activates phosphatidylinositol 3-kinase when bound to the regulatory subunit

ALDOA

ALDOA is a glycolytic enzyme that catalyzes the reversible conversion of fructose-1,6-bisphosphate to glyceraldehyde 3-phosphate and dihydroxyacetone phosphate.

DNA2

DNA2 is a helicase family nuclease involved in maintaining mitochondrial and nuclear DNA stability.

DUSP14 and DUSP7

Dual-specificity phosphatases (DUSPs) constitute a large heterogeneous subgroup of the type I cysteine-based protein-tyrosine phosphatase superfamily. DUSPs are characterized by their ability to dephosphorylate both tyrosine and serine/threonine residues. They have been implicated as major modulators of critical signalling pathways. DUSP14 contains the consensus DUSP C-terminal catalytic domain but lacks the N-terminal CH2 domain found in the MKP (mitogen-activated protein kinase phosphatase) class of DUSPs. Involved in the inactivation of MAP kinases. Dephosphorylates ERK, JNK and p38 MAP-kinases. DUSPs constitute a large heterogeneous subgroup of the type I cysteine-based protein-tyrosine phosphatase superfamily. DUSPs are characterized by their ability to dephosphorylate both tyrosine and serine/threonine residues. DUSP7 dephosphorylate MAPK (proteins ERK), JNK, and p38 with specificity distinct from that of individual MKP proteins. MKPs contain a highly conserved C-terminal catalytic domain and an N-terminal Cdc25 -like (CH2) domain. MAPK activation cascades mediate various physiologic processes, including cellular proliferation, apoptosis, differentiation, and stress responses

CREBRF

CREBRF (CREB3 Regulatory Factor) Acts as a negative regulator of the endoplasmic reticulum stress response or unfolded protein response (UPR). Represses the transcriptional activity of CREB3 during the UPR.

Table 6: List of differential expressed genes in CHO cells cultured in LAA

Gene	<i>p-Value</i>	Fold change
SLC6A9	0.083	1.624
SLC7A1	0.066	1.257
SLC38A2	0.019	0.767
SLC30A1	0.019	0.988
SESN2	0.039	2.398
TRIB3	0.067	1.714
7SK	0.066	-1.617
TRP53INP1	0.005	1.482
CHAC1	0.016	1.366
ENSCGRG00001010711	0.041	-1.258
GPR176	0.048	1.206
CCN1	0.007	1.135
TXNIP	0.013	1.117
CDKN2B	0.027	1.049
HERPUD1	0.015	1.001
ENSCGRG00001008121	0.011	-1.000
ENSCGRG00001015394	0.084	0.975
JUN	0.055	0.967
NR1D2	0.020	0.964
0610009B22RIK	0.006	-0.941
ENSCGRG00001008456	0.076	-0.931
CREBL2	0.078	0.929
ENSCGRG00001003984	0.041	0.929
ENSCGRG00001001109	0.061	-0.917
RND3	0.043	0.913
ENSCGRG00001011231	0.030	-0.900
ARID5B	0.019	0.892
SMIM20	0.075	0.882
B630019K06RIK	0.092	0.882
KCTD9	0.001	0.867
MXD4	0.008	0.853
INSR	0.004	0.845
PDK4	0.038	0.841
TWIST2	0.072	-0.834
ZC3H6	0.072	0.831
GM24455	0.095	-0.828
ING3	0.016	0.821
BC031181	0.076	0.819

CIART	0.016	0.815
EGR1	0.077	0.786
BCL7B	0.043	0.781
ENSCGRG00001011179	0.042	-0.775
YARS	0.074	0.771
ENSCGRG00001007219	0.035	-0.771
ENSCGRG00001005504	0.067	0.766
GCC1	0.067	0.765
PLGRKT	0.015	-0.754
RNF212	0.063	-0.751
CCDC112	0.001	0.751
TRMO	0.030	0.742
SPRY2	0.020	0.733
MTSS2	0.001	0.733
CCNF	0.015	-0.718
WASF1	0.020	0.716
CHD2	0.020	0.716
MAFK	0.003	0.712
LENG1	0.015	-0.709
NFE2L1	0.063	0.706
DRAM1	0.032	0.703
KLF5	0.002	0.703
CCNE2	0.008	-0.700
ELOVL6	0.058	-0.701
PTGER4	0.048	0.704
MICALL2	0.028	-0.705
LURAP1L	0.048	-0.710
ZBTB43	0.003	0.713
PIM3	0.083	0.717
GPER1	0.022	-0.723
KMT5B	0.067	0.737
ARL4A	0.037	0.744
RAB40C	0.042	0.745
FHOD1	0.035	-0.748
VGLL3	0.005	0.760
LRIG3	0.059	0.768
ID1	0.002	-0.769
TNFAIP3	0.027	0.776
IL6ST	0.066	0.782
ZKSCAN16	0.027	-0.788
ENSCGRG00001012782	0.029	-0.790
SGK1	0.002	0.800

ENSCGRG00001014273	0.001	-0.814
CDC6	0.071	-0.819
NATD1	0.037	0.821
CHD5	0.041	0.826
RELB	0.067	0.833
TAF1A	0.042	0.834
MED12	0.013	-0.840
ENSCGRG00001010756	0.031	0.848
KLHL24	0.017	0.852
ENSCGRG00001010828	0.006	-0.876
RNF182	0.005	0.880
SNORA33	0.021	-0.925
CAML	0.082	0.945
ENSCGRG00001016292	0.012	0.954
GM22748	0.054	-0.962
ATF4	0.015	0.963
2610008E11RIK	0.038	0.973
GM23751	0.083	0.989
GM24313	0.097	-0.995
GFOD1	0.002	1.024
KLF6	0.011	1.046
ENSCGRG00001024555	0.092	1.051
BBC3	0.029	1.065
CEBPG	0.064	1.083
CHST12	0.035	-1.107
ANKRD1	0.017	1.145
DDIT3	0.046	1.145
ENSCGRG00001017398	0.048	1.149
CDKN2AIP	0.038	1.155
ATF5	0.086	1.160
CITED2	0.032	1.162
RASSF1	0.059	1.176
NNMT	0.057	1.192
ENSCGRG00001018983	0.048	-1.216
ENSCGRG00001004990	0.042	-1.226
SLPI	0.086	-1.248
NFIL3	0.018	1.296
ENSCGRG00001016427	0.056	1.306
MYC	0.019	1.440
IER5L	0.006	-1.471
ENSCGRG00001003263,ENSCGRG00001007615	0.055	1.531
PPP1R15A	0.012	1.667

GADD45A	0.054	1.734
NUPR1	0.038	1.864
PLK2	0.038	1.959
ATF3	0.062	2.017

7.4.7 Supplementation of single amino acid in a lean amino acid background does not improve growth or productivity in CHO cell culture

Phenotype and transcriptomics suggest a possible amino acid limitation is causing cell cycle arrest. To confirm whether deficiency of a specific amino acid is responsible for these transcriptional changes, we examined the effect of replenishing single amino acids under the basal LAA condition. We wanted to mitigate these phenotypic effects on cell proliferation by supplementation of a single amino acid in a lean amino acid background.

Suspension adapted CHO cell line expressing IgG was used to evaluate the effect of individual amino acid supplementation on cell growth and productivity. Cells were allowed to acclimatize to a nutritionally limited medium by culturing them in a custom made LAA condition containing all amino acids at 0.1 mM, glutamine at 0.5 mM, and glucose at 2 g/L for 24 hours. Post 24 hours, cells were resuspended in fresh LAA medium, along with 2 mM of individual amino acids and unsupplemented control culture. To minimize carryover from the previous medium, an additional wash with LAA medium was included at each resuspension. Cells were sampled on alternate days for 6 days and viable cell density and viability, and glucose consumption. Surprisingly, no significant improvement or adverse impact in peak cell density, IVCD or growth rate was observed as seen in Figure 7.9. IgG titer for the control cells was 192 µg/mL on the 6th day, and there was no significant improvement with amino acid supplementation (Figure 7.9). Serine and glutamine have positive effects on IVCD, explained by their importance in maintaining homeostasis (Figure 7.9). It is not surprising that serine and glutamine are among the highest consumed amino acids essential, participating in many cellular processes. The primary donor in the one-carbon metabolism in cells, serine is the second highest consumed amino acid determined [374,375]. More than 70% of the serine consumed by CHO cells contributes to nucleotide synthesis by transforming into glycine [375]. Despite the critical role of serine, reduced serine concentration in media (1 mM) is reported to

have a minor impact on cell growth. However, serine depletion in the medium is reported to have a negative impact, including increased asparagine consumption along with increased alanine, lactate and ammonium generation, which at high concentrations can potentially be growth inhibitory [376]. Considering the excessive consumption and the detrimental effects of depletion, serine is supplied at a high concentration in the medium as additional serine in the medium can improve titers and improve peak cell density [57].

Glutamine is also utilized as a major energy source in CHO cell culture which can explain the improved IVCD. As already mentioned, glutamine is metabolized via glutaminolysis and enters the TCA cycle via α -ketoglutarate. Glutamine is an essential nutrient in CHO cell culture, and its absence is reported to impede the exponential growth phase [67]. Supplementation of glutamine has been reported to improve cell viability, reduce lactate production and improve productivity, even in the case of CHO-GS cells which produce can produce de novo glutamine via the transfected glutamine synthetase [68,69]. However, glutamine is converted to glutamate during glutaminolysis, resulting in the production of free ammonium in the medium [70]. High ammonium concentration in the medium can have detrimental effects on the cell culture by potentially reducing cell growth rate, increasing the glycoform heterogeneity, and affecting the consumption of other amino acids [71,72]. Cystine supplementation resulted in higher specific glucose consumption and hence higher lactate accumulation. The effect of cystine on glucose has also been reported in cells by Zhang, Shihai, et al. [377]. It is possible that because of the batch mode of cultivation, multiple amino acids being limited that cannot be rescued by supplementation of single amino acid. Combinations of amino acids studied belonging to the same transporter families can be further explored. Such effects can be explained by the complex interplay of cell signalling, gene expression and amino acid transporters to maintain homeostasis. Some changes in intracellular metabolites might need further evaluation. Impact on glucose consumption by supplementation of cystine was observed, which agrees with previously reported studies [377].

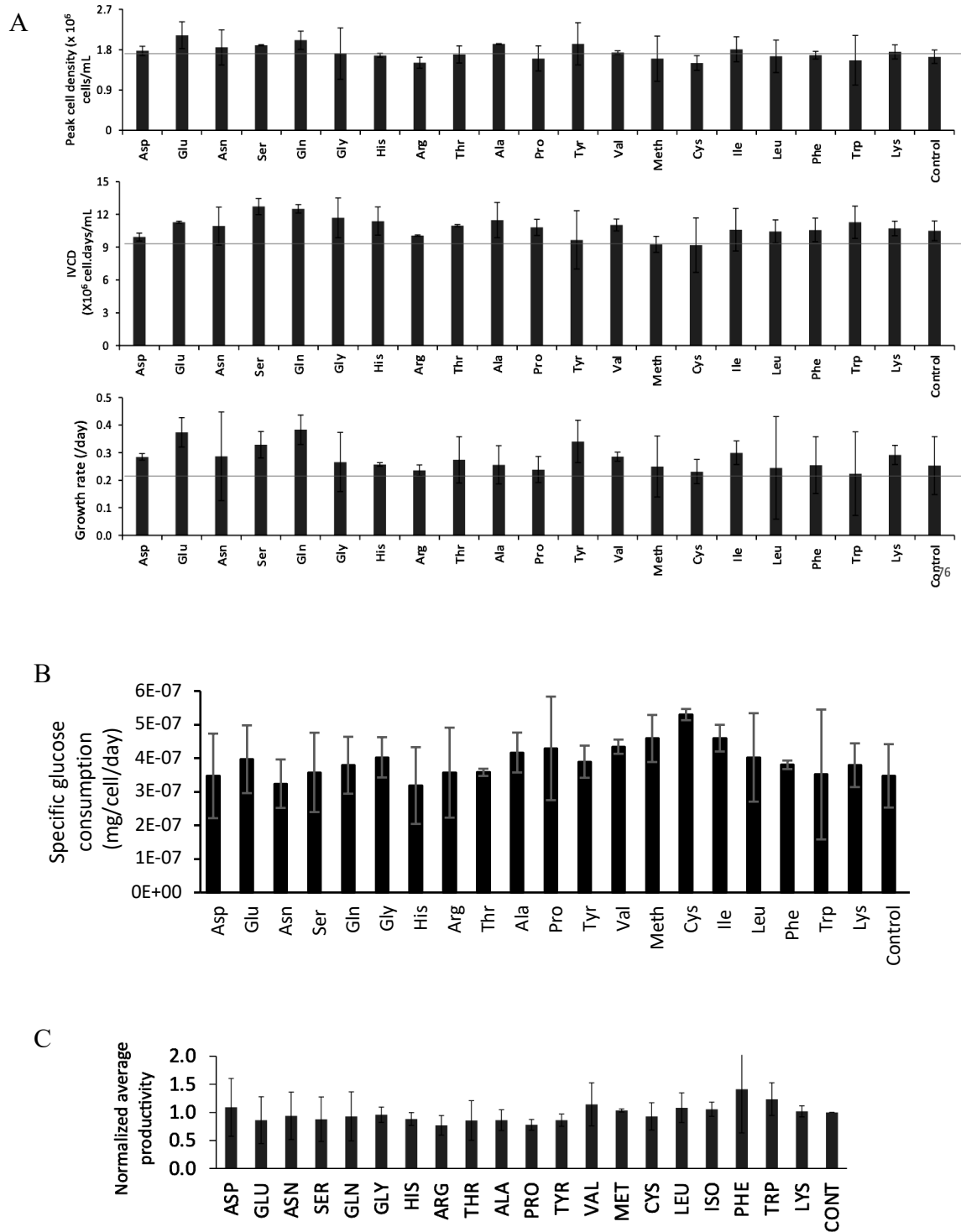


Figure 7.9: No significant difference in cell culture performance with single amino acid supplementation under LAA background

Suspension adapted CHO cell line expressing IgG were cultured in LAA condition 2 mM of each amino acid was supplemented. (A) Effect on peak cell density, IVCD and growth rate (B) Effect on specific glucose consumption (C) Normalized productivity

7.4.8 Developing a feeding strategy to complement LAA condition while maintaining low amino acid concentrations

Transcriptomic alteration and phenotypic characteristic hints toward a genetic and metabolic readjustment for adaptation in a nutrient-limited medium. A feeding system, either through a NutriGel or through motorized feeding in a bioreactor, could prevent the ISR to amino acid limitation. To ensure no amino acid exhaustion and ISR, a continuous feed source is also required to support the culture. As demonstrated in chapters 5 and 6, a NutriGel based feeding system can be tailored to feed amino acids for specific applications. Because of restricted amino acid availability and hence cell cycle arrest, it was expected that there may be no substantial cell growth. The amino acid feed was tailored according to the composition of the recombinant IgG expressed by the cell and was tailored to achieve 2 g/L of protein titer. We utilized a NutriGel to maintain low amino acid concentration by culturing an IgG-producing CHO cell line in LAA. The amino acid feed composition was tailored according to the composition of the recombinant IgG. To determine the amino acid composition, sequence of a human IgG was run on ProtParam [378]. Cells were seeded at a high density of 15×10^6 cells/mL to maintain amino acids at low concentrations. LAA medium supplemented with this NutriGel could maintain CHO cell viability (Figure 7.10)

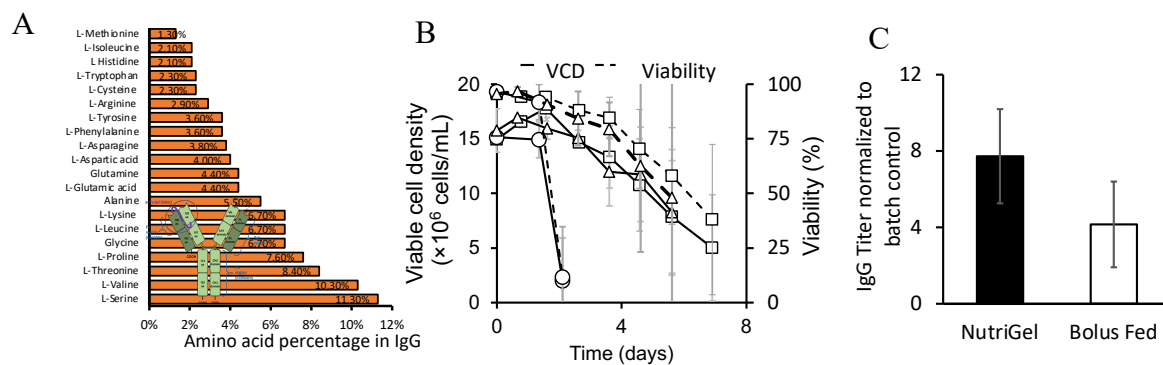


Figure 7.10: In situ, continuous feeding of amino acids through NutriGel in low amino acid (LAA) conditions can sustain CHO cell culture

Suspension adapted CHO cell line expressing IgG were seeded at 15×10^6 cells/mL in LAA condition (A) IgG composition used for synthesizing the NutriGel (B) Viable cell density (solid lines) and viability (dashed lines) Δ -Bolus fed culture \circ -Batch culture \square - Culture supplemented with NutriGel (C) Normalized productivity

The use of a hydrogel-based system supported the maintenance of the CHO cells at a high density for four days and improved the culture longevity compared to batch control. As a positive control, we also supplemented CHO cells with a traditional bolus feed equivalent to the nutrient payload in the NutriGel, and the culture performance is comparable between the NutriGel and the bolus fed cultures (Figure 7.11). However, on performing amino acid quantification, it was observed that all amino acids like aspartate, glutamate, leucine, isoleucine, and glutamine were depleted from the medium (Figure 7.11). Glucose is also nondetectable after day 2, suggesting a possible carbohydrate limitation. The release of amino acids through NutriGels decreases over time, and there is little amino acid delivery beyond 7 days. But on a scale-down model, it was possible to sustain cells in LAA condition with continuous feeding without having an adverse effect on protein translation.

Hence to maintain amino acid feeding over a longer duration, we next utilized a bioreactor to feed amino acids and found comparable culture profiles. We designed a feeding strategy based on release rates from NutriGel. Continuous and sustained feeding led to similar culture performance on a bench-scale bioreactor system comparable to the culture performance in a shake flask. With the ability to continuously feed cultures while maintaining low residual concentration, we attempted to improve the continuous feeding strategy.

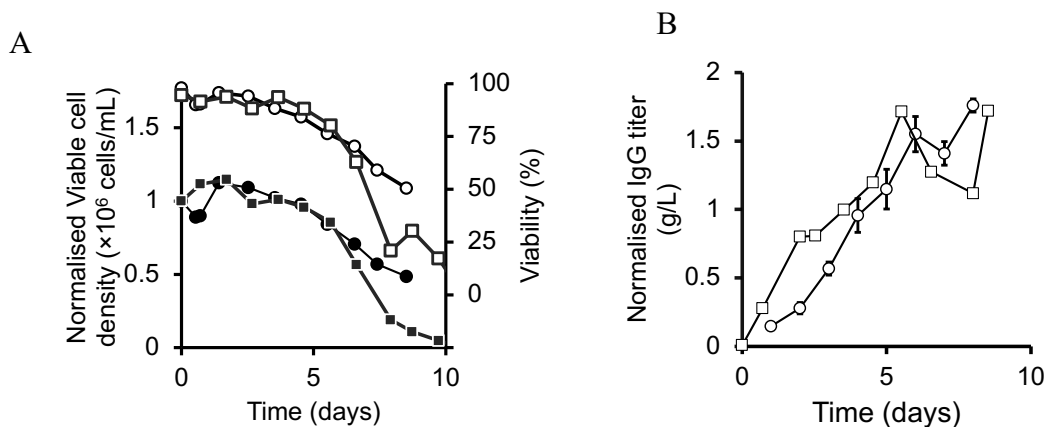


Figure 7.11: Feeding strategy designed on release rates from NutriGel led to culture performance on a bench scale comparable bioreactor system

Suspension adapted CHO cell lines expressing IgG were cultured in a bioreactor and compared to the shake flask cultures from Figure 7.10 supplemented with a NutriGel (A) Viable cell density ■-Shake flask cultures ●-bioreactor culture, and viability □-Shake flask cultures ○-bioreactor culture (B) Normalized productivity □-Shake flask cultures ○-bioreactor culture

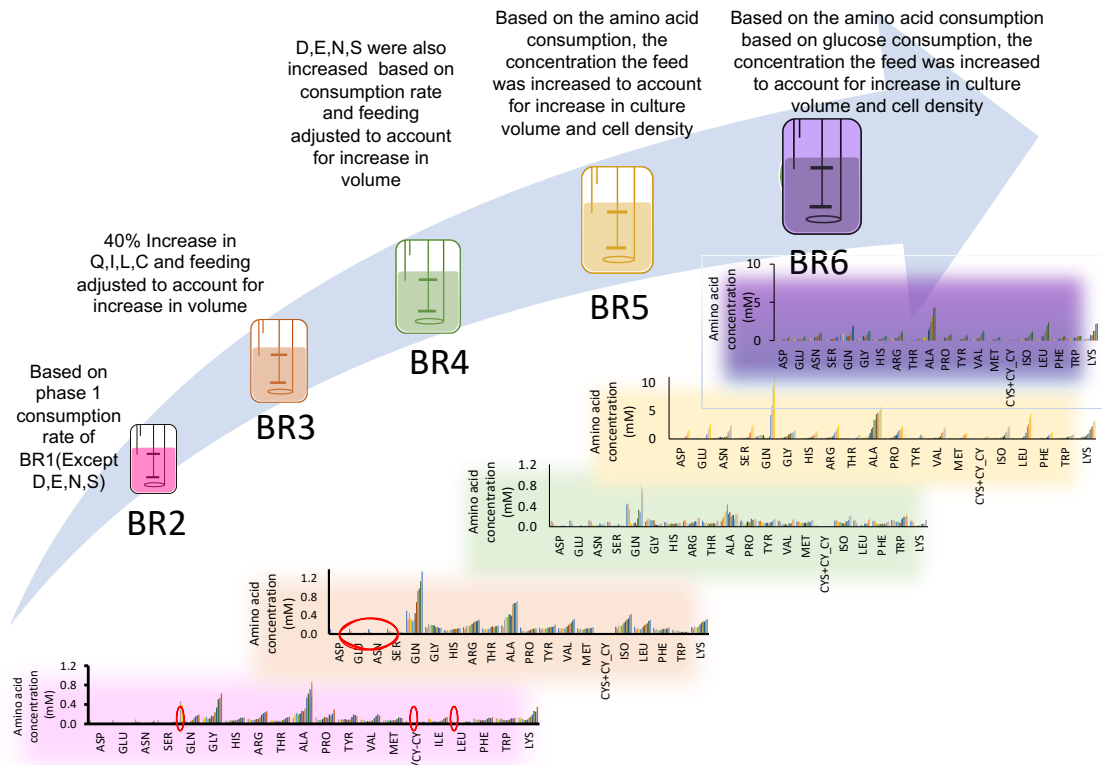


Figure 7.12: Representation of the defined continuous feeding approach developed in this study

In order to further improve the culture performance while maintaining low amino acid concentration, we utilized an iterative approach and empirically tested various feeding strategies (Figure 7.12). The basal medium utilized for all the bioreactor runs was LAA. The feeding strategy utilized amino acid consumption, accounting for the increase in culture volume due to continuous feeding, the increase in cell density and glucose consumption. The concentration for various feeds developed is given in table 7. BR2 utilized the specific amino acid consumption rates from BR1, except for aspartate, glutamate, asparagine and serine. In BR3, amino acids getting exhausted during the course of the reactor were increased by 40%, along with accounting for the increase in culture volume due to continuous feeding. In BR4, the feeding was based on the amino acid consumption profile for all amino acids and accounted for an increase in culture volume. In BR5, the feeding was based on amino acid consumption rates for BR4, accounting for the increased viable cell density over the course of the culture. In BR6, the feeding approach was further refined by utilizing amino acid consumption rates for BR4 and accounting for the increased viable cell density over the course of the culture and glucose consumption rates to manage the

accumulation of amino acids. The DO was maintained at at least 30% in all the reactor runs. And the pH was maintained at 7 with a bandwidth of 0.02. The feeding strategy based on utilizing the amino acid consumption and glucose consumption rates lead to improved cell densities among the various iterations of the bioreactor cultures. Various feeding strategies used to maintain low amino acid concentration had a diverse impact on VCD and productivity.

Table 7: Feed composition for the various reactor runs

	Feed 1 composition (mg/mL)	Feed 2 composition (mg/mL)	Feed 3 composition (mg/mL)	Feed 4 composition (mg/mL)	Feed 5 Based on consumption (mg/mL)	Feed 6 Based on consumption (mg/mL)
Asp	0.009	0.009	0.01	0.009	0.19	0.19
Glu	0.010	0.01	0.01	0.010	0.27	0.27
Asn	0.008	0.008	0.01	0.060	0.24	0.24
Ser	0.029	0.029	0.03	0.082	0.21	0.21
Gln	0.007	0.87	1.22	1.216	1.55	1.55
His	0.022	0.06	0.07	0.065	0.11	0.11
Arg	0.011	0.17	0.17	0.173	0.26	0.26
Thr	0.029	0.09	0.09	0.086	0.08	0.08
Pro	0.004	0.09	0.00	0.004	0.08	0.08
Tyr	0.005	0.12	0.09	0.092	0.14	0.14
Val	0.021	0.06	0.12	0.121	0.18	0.18
Met	0.004	0.06	0.06	0.056	0.08	0.08
Cys	0.002	0.11	0.11	0.154	0.30	0.30
Iso	0.002	0.1	0.16	0.159	0.19	0.19
Leu	0.004	0.06	0.14	0.140	0.39	0.39
Phe	0.006	0.05	0.06	0.062	0.12	0.12
Trp	0.008	0.16	0.05	0.050	0.06	0.06
Lys	0.009	0.004	0.16	0.161	0.42	0.42
Glucose	0.2	2.1	2.6	2.7	5.32	5.32

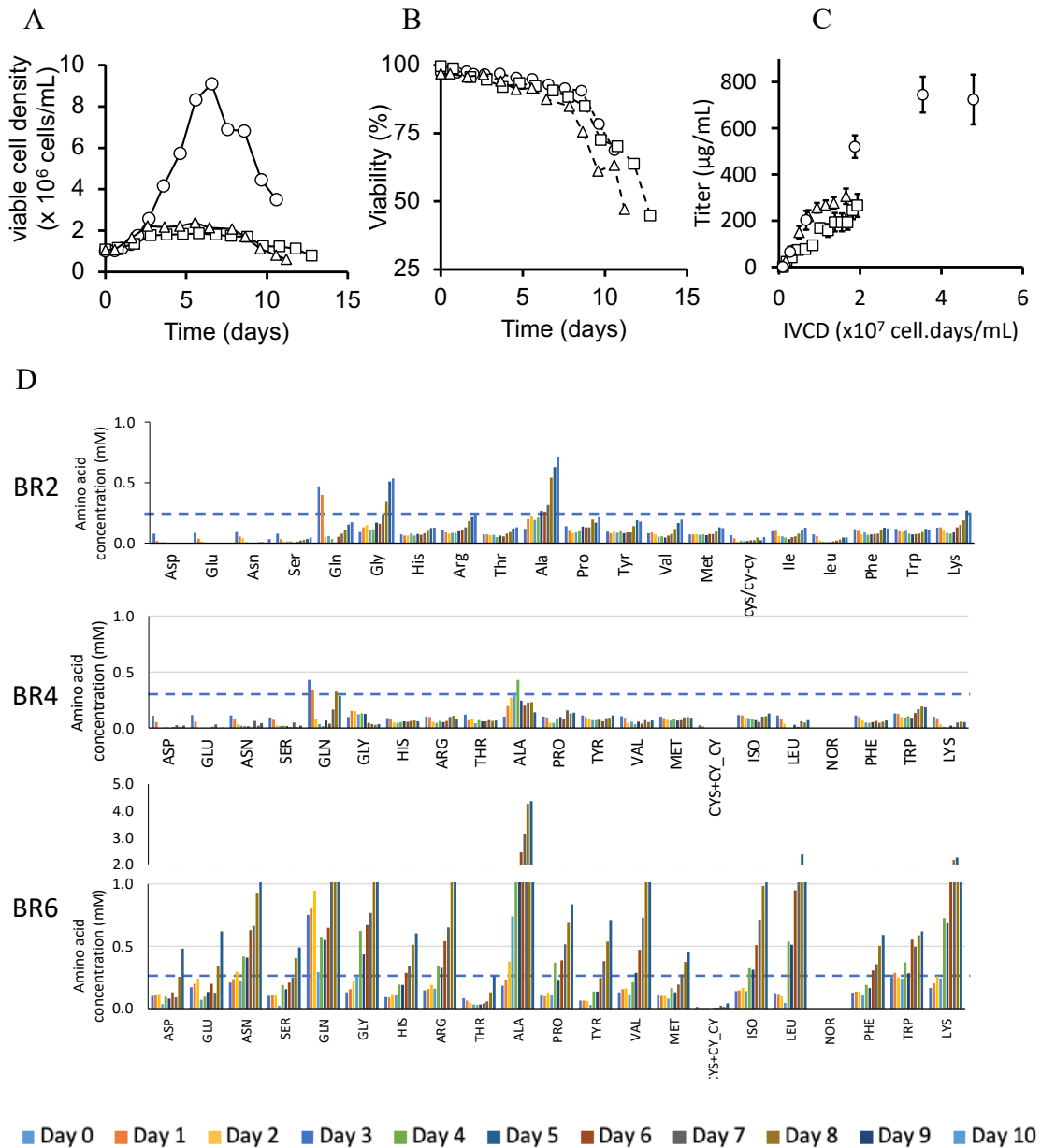


Figure 7.13: Optimizing cell culture performance in low amino acid media by utilizing specific amino acid consumption rates

Bioreactor culture of CHO cell line expressing IgG was cultured in LAA with diverse feeding strategies (A) Effect on viable cell density \square -BR2, \square -BR6, Δ -BR4 (B) Viability \square -BR2, \square -BR6, Δ -BR4 (C) IVCD \square -BR2, \square -BR6, Δ -BR4 (D) Residual amino acid concentration for BR2, BR4 and BR6 from day 0 onwards

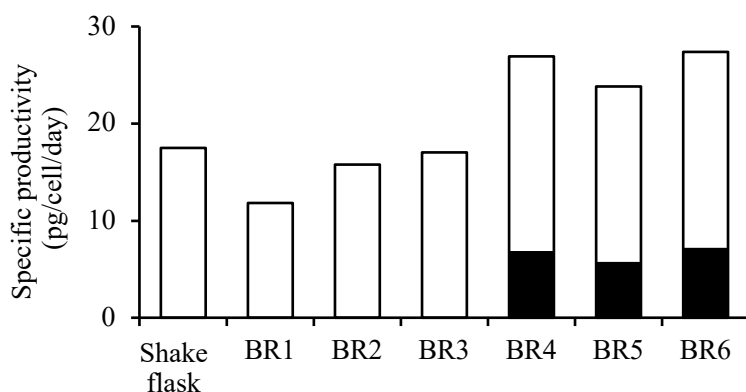


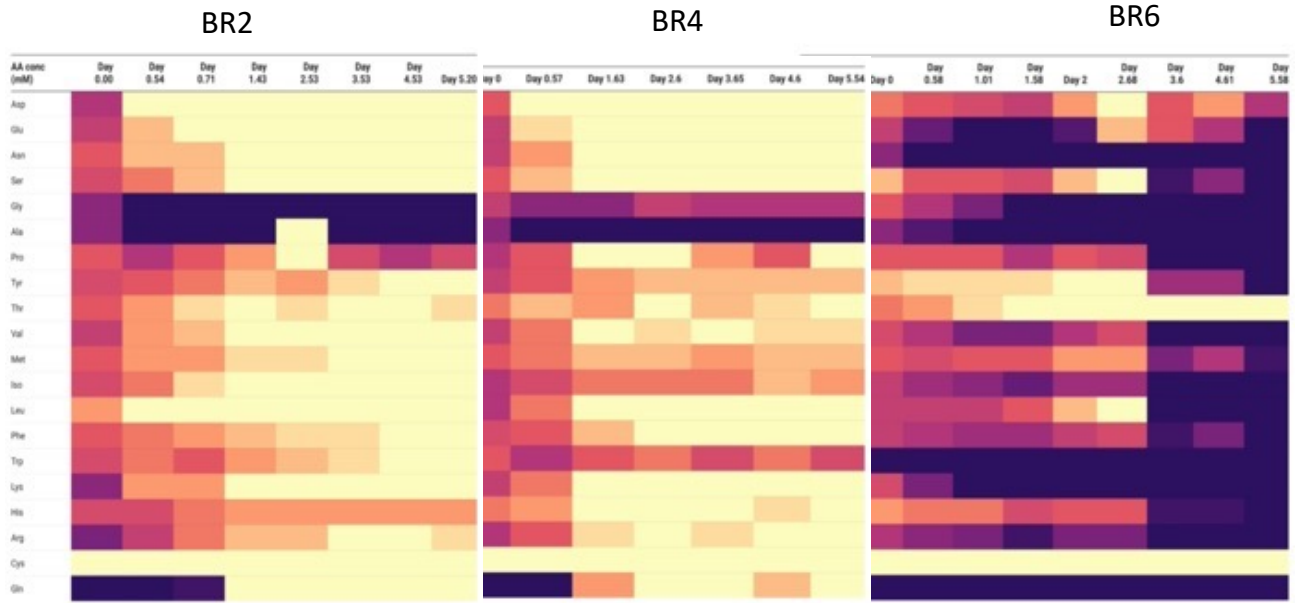
Figure 7.14: Improved specific productivity is observed as amino acid concentration is maintained above 0.1 mM with an improved feeding strategy

A comparison of the specific productivity across all the bioreactor cultures, white bars-phase one specific productivity, black bars- phase two specific productivity

All feeding strategies led to viability (>50%) for 10 days. Feeding based on cell growth and consumption rates resulted in the highest growth and productivity. With diverse feeding strategies, most amino acids could be maintained low for at least 7 days. As the feeding strategies had amino acids at more growth permissive concentrations, amino acid accumulation was observed in the stationary phase. Amino acids like glycine and alanine are observed to accumulate over time (BR5 and BR6) (Figure 7.13). Investigating other feeding strategies is required. Accumulation of amino acids, especially during the stationary phase, is reduced but is not completely avoided in BR6. With LAA and continuous feeding, we could overcome the growth restrictive effects of ISR without adversely impacting protein translation. As we utilized relatively abundant feeds in amino acids (BR4, BR5, BR6), we also observed an improvement in specific productivity (Figure 7.14). Better feeding strategies that can enhance productivity can be further developed.

On performing a meta-analysis of the residual amino acid concentration, we can observe growth is correlated when amino acid concentration can be maintained above 0.1 mM. The heatmap of residual amino acid concentration in the bioreactor cultures suggests a cell growth inhibition in BR1, BR2, and BR3 when amino acid concentrations are below 0.1 mM (Figure 7.15, data for BR1 and BR3 shown in appendix). In BR4, we do observe some growth as the amino acids feeding is

relatively higher. However the feeding rate in BR4 calculated from the specific consumption rates did not take into account the increase in cell density until the next sampling point. This is again corroborated in the range plot that displays the relationship between the initial and final amino acid concentration on day 5 (Figure 7.15). In BR5 and BR6, we can observe amino acids maintained at 0.1 mM. BR5 and 6 have the same feeding profile but having significant differences in peak cell density. One possible explanation for this difference can be the difference in the glucose feeding strategy. On plotting heatmaps for residual glucose to residual amino acid concentration in BR5 and BR6, it is observed that residual glucose concentration is slightly higher in BR6 (Figure 7.16). Glucose feeding was linked to amino acid feeding in BR6. The ratio of residual glucose to residual amino acid is between 2-3 for BR6. This hints during continuous feeding, amino acids have to be maintained low, and glucose also should be maintained low.



A

B

C

D

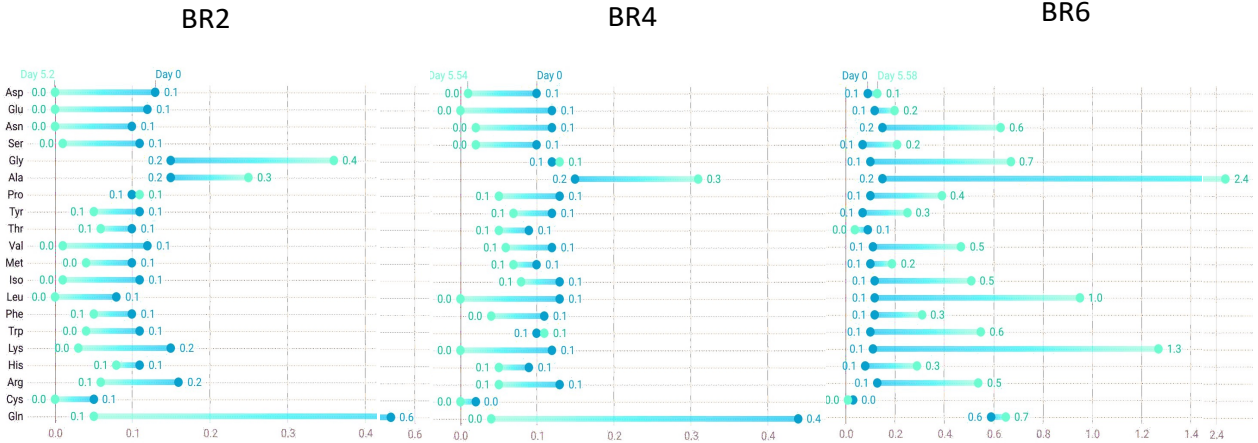
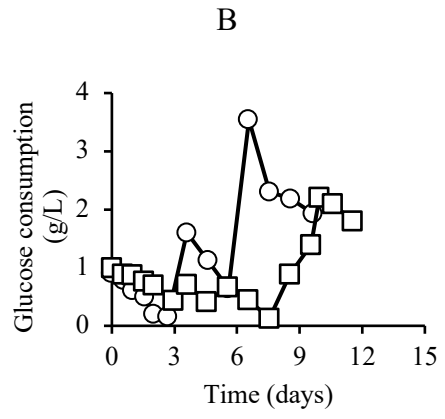
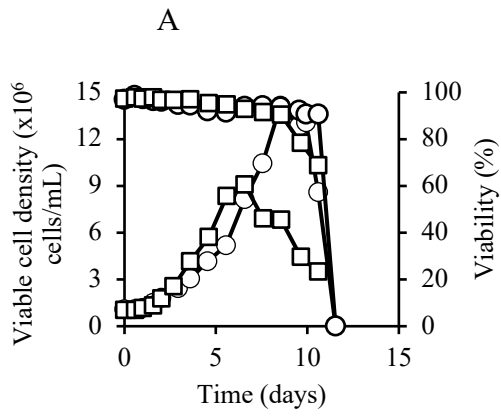


Figure 7.15: Optimizing cell culture performance in low amino acid media by utilizing specific amino acid consumption rates

Clustered heatmaps were plotted for residual amino acid concentration. The colour scheme denotes concentration across culture profiles. (A) BR2 (B) BR4 (C) BR6 (D) Range plot for BR2, BR4 and 6 indicate residual concentration from day 0 to day 5. Created with Datawrapper

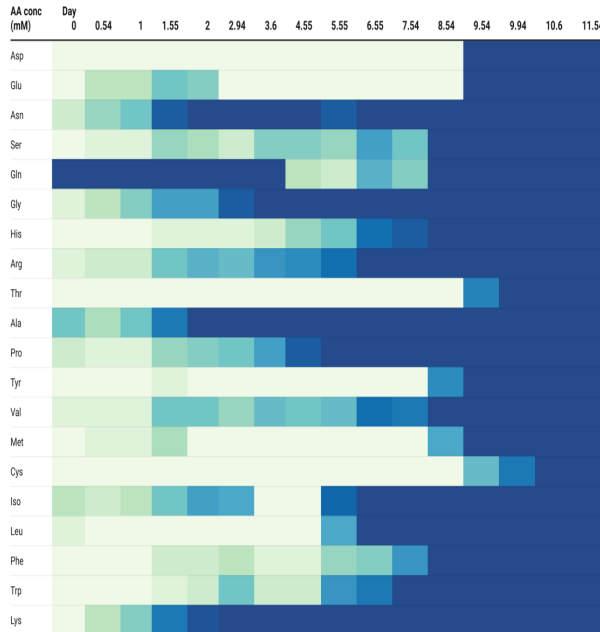


C

BR5

Amino acid concentration (mM)

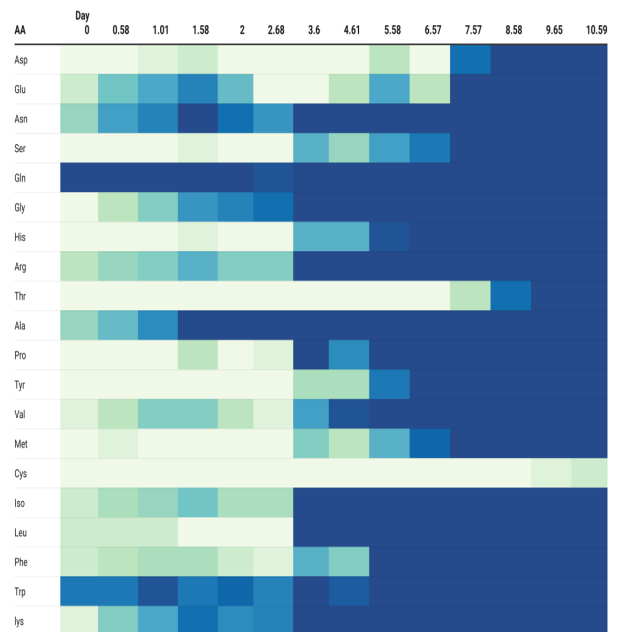
0.1 0.3



BR6

Amino acid concentration (mM)

0.1 0.3



D

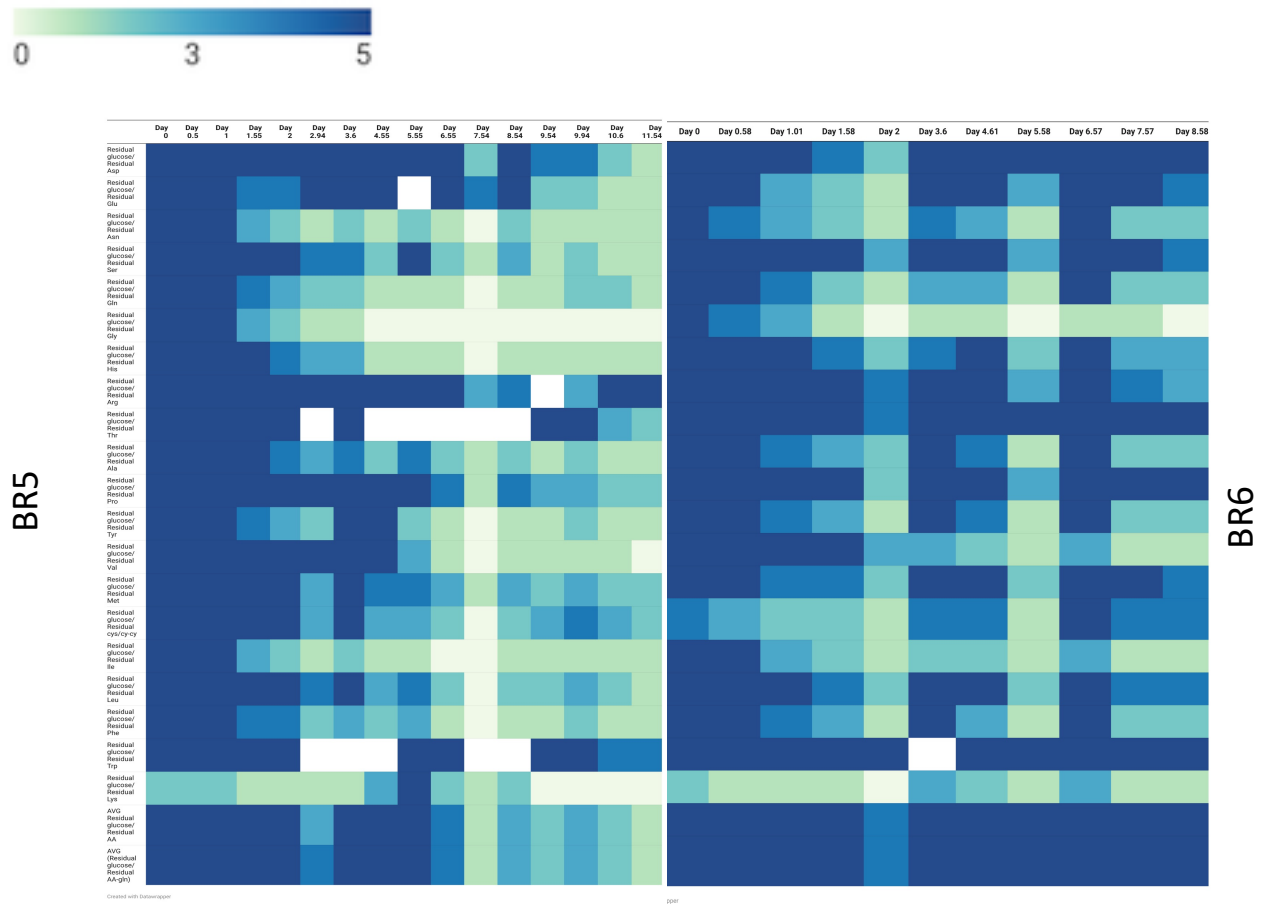


Figure 7.16: Controlling glucose while maintaining low amino acid concentration contributes to higher cell densities

Bioreactor culture, BR5 and BR6 of CHO cell line expressing IgG were cultured in LAA with diverse feeding strategies (A) Effect on viable cell density and Viability \square -BR6, \circ -BR5 (B) Glucose concentration profile \square -BR6, \circ -BR5, (C) Residual amino acid concentration BR5 and BR6 from day 0 onwards (D) Clustered heatmaps comparing the ratio of residual glucose to an amino acid concentration between BR5 and BR6. Created with Datawrapper

7.5 Conclusions

Continuous feeding through a NutriGel in a shake flask (for small-scale culture platforms) allowed preliminary evaluation of low amino acid availability on cell viability. Cell growth is arrested at lower feeding rates, but with better-optimized feeds in bioreactors, cell growth could be achieved while maintaining amino acids at a low concentration indicating the concentrations employed are growth permissive.

Protein translation is not inhibited at these low amino acid concentrations, as seen from IgG accumulation in the culture. However, specific productivity is affected as compared to rich conditions. The feeding strategy can be further improved to maintain amino acids at low concentrations while improving culture performance by incorporating other parameters like growth rate. To maintain LAA conditions, techniques like temperature and pH shifts can limit the high amino acid consumption and avoid nutrient exhaustion in the logarithmic growth phase. Exploring a slightly higher basal amino acid concentration in the basal media can also be attempted. Further experiments at higher amino acid setpoints may help identify the lowest concentration at which the AAR response pathway is not activated.

Chapter VIII.

Conclusions

The development of bioprocesses for the production of recombinant proteins begins with the generation of a robust clone whose selection is usually performed in small scale culture platforms. Small scale culture platforms like shake flasks lack control over parameters like pH, DO or feeding and have lower throughput unless accessorized with sophisticated robotic and monitoring systems. This may cause the selection of low producers since the product titer and quality can be affected by the actual process conditions [185]. Hence an economical alternative that makes shake flask an appropriate scale down model is desired. TGE is routinely used to generate a desired recombinant protein-producing cell line. When performed on a large scale, it can shorten process development timelines as it bypasses the selection and amplification steps. But TGE bioprocesses have been difficult to scale up in large stirred tank bioreactors with volumes of more than 1.5 L. Inadequate production levels are frequently achieved, but the causes have not yet been elucidated [379,380]. Shear stress is an important parameter that needs to be reviewed with reference to transient transfection. In a stirred tank reactor, the distribution of the hydrodynamic stress varies depending on the region of the reactor and covers several orders of magnitudes. A small-scale device capable of mimicking the varying hydrodynamic stress regions while giving the possibility to establish a cell line-specific threshold is required.

In chapter 4, we have demonstrated the effect of shear stress on the efficiency of transient transfection and toxicity on cell culture under various magnitudes of shear stress observed typically in a large scale bioreactor. Increased toxicity and reduced transfection efficiency observed are due to the synergistic effect of shear on the cells and lipoplex. This makes the large-scale transient transfection process heedful of the effects of shear stress, which can be reduced by decreasing agitation during the first

few hours when lipid-mediated transfection is at its maximum rate [381,382]. Another implication of shear stress can be a large number of lipofection agents being developed for gene therapy clinical trials. Consistent with this, lipoplexes with low toxicity in vitro, when injected into the bloodstream where they are subjected to shear, have resulted in significant toxicity to blood cells in the form of transient leukopenia and neutropenia in animal models and human clinical trials [179,181,182,383–386]. However, we did not observe a similar effect of higher toxicity in the presence of shear in K562 cells. K562 cells were not efficiently transfected by the lipoplex used in this study, whereas CHO-S are efficiently transfected. It remains to be seen whether transfectability has any role in the relationship between shear and toxicity of the lipoplex.

Manual bolus feeding leads to frequent operator handling and makes the culture more prone to contamination in fed-batch cultures. In chapters 5 and 6, we explore an alternate application of hydrogels for in situ continuous delivery of a complex nutrient feed comprising 18 amino acids, vitamins, antioxidants, and trace elements. The hydrogel includes the complex nutrient feed in the form of a solid in the central reservoir. This prevents dilution of the culture seen in traditional fed-batch cultures where the feed is added as a concentrated solution whose strength is limited by the solubility of the nutrients included. Release rates of individual amino acids can be modulated through NutriGel by changing their initial loading in the central reservoir. This can ease modulating amino acid feed to tailor to specific cell culture applications. This study provides proof of the concept that hydrogels can enable completely closed in situ feeding for mammalian cell culture, requiring no external intervention. Such systems can help small-scale single-use animal cell culture platforms to achieve nutrient feeding in a completely closed use-and-throw platform without any additional infrastructure while maintaining the sophistication of continuous feeding. In situ nutrient feeding reported in this study, in addition to in situ pH management described previously, can enable completely closed systems in single-use platforms requiring no operator intervention, which may be of use as a screening tool for animal cell-based bioprocesses and in the production of patient-specific cell-based therapies [387,388].

Medium formulations have critical roles in bioprocess development as they directly impact productivity. It is known that underfeeding is a problem that can be resolved by optimization of medium and feed formulation, but overfeeding is also an evolving concern as novel inhibitors are being discovered [8,241]. Currently, there is a limited understanding of a lean cell culture medium formulation and its implication on culture performance. Chapter 8 pursues the feasibility of utilizing the LAA medium. We have compared growth performance and transcriptomics to understand the cellular response to a low amino acid-based medium. We find Phenotypic and transcriptional changes were similar to those reported in mammalian cells under amino acid limitation-ATF4/transporter upregulation. Further, to utilize a medium with lean amino acid background, we show that amino acids should be maintained at a low but growth permissive concentration of 0.1mM for this CHO cell. We demonstrate that optimized continuous feeding can assist in utilizing a lean amino acid-based medium, maintaining low amino acid concentration without inhibiting protein translation.

8.1 Future directions

Applications of NutriGels to assist in screening and process development can be explored. NutriGels can be further improved by trying to incorporate pH control through the same gel. Such sophisticated feeding systems can be tested with WAVE bioreactors. The feeding strategy can be further improved to maintain amino acids at low concentration, while improving culture performance by attempting to incorporate other parameters like growth rate

To maintain LAA conditions, techniques like temperature and pH shifts can be utilized to limit the high amino acid consumption and avoid nutrient exhaustion in the logarithmic growth phase

Exploring a slightly higher concentration of basal amino acid concentration in the basal media can also be attempted with continuous feeding

Appendix

Custom medium formulation

HDFF3 (Routinely used medium for CHO cell culture)

Amino acids	Concentration (mg/L)
Glycine	37.6
L-Alanine	8.9
L-Arginine hydrochloride	294.5
L-Asparagine monohydrate	15
L-Aspartic acid	13.3
L-Cysteine hydrochloride monohydrate	48.9
L-Cystine dihydrochloride	60.59
L-Glutamic acid	14.7
L-Histidine hydrochloride monohydrate	52.5
L-Isoleucine	107
L-Leucine	111
L-Lysine hydrochloride	164
L-Methionine	32.2
L-Phenylalanine	68.5
L-Proline	34.6
L-Serine	52.6
L-Threonine	101
L-Tryptophan	17
L-Tyrosine disodium salt	100
L-Valine	99.7
L-Glutamine	730

Inorganic salts	
Ammonium metavanadate	5.80E-04
Ammonium molybdate tetrahydrate	6.18E-03
Calcium nitrate tetrahydrate	90
Copper sulphate pentahydrate	1.30E-03
Disodium hydrogen phosphate	355
Ferric nitrate nonahydrate	5.00E-02
Ferrous sulphate heptahydrate	0.4
Magnesium chloride anhydrous	29
Magnesium sulphate heptahydrate	100
Manganese chloride	1.25E-04
Nickel chloride	1.20E-04
Potassium chloride	312
Sodium chloride	6996
Sodium dihydrogen phosphate	271.5
Sodium metasilicate nonahydrate	1.42E-02
Sodium selenite	6.24E-03
Stannous chloride dihydrate	1.10E-04
Zinc sulphate heptahydrate	0.432

Vitamins	
Ca-D-Pantothenic acid	2.240
Choline chloride	8.98
D-Biotin	3.50E-03
Folic acid	2.66
Niacinamide	2.020
Pyridoxal hydrochloride	2
Pyridoxine hydrochloride	3.10E-02
Riboflavin	0.219
Thiamine hydrochloride	2.17
Vitamin B12	0.68
Myo-Inositol	12.6
Ascorbic acid	20
Others	
DL-Thioctic acid	0.105
Ethanolamine	21.59
Glutathione	1.8
HEPES buffer	3574.5
Hypoxanthine	2.4
Linoleic acid	4.20E-02
Lipid mixture I, chemically defined (Sigma L0288)	1x
β -mercaptoethanol	1.4
Phenol red sodium salt	8.63
Putrescine hydrochloride	8.10E-02
Protein hydrolysate	1000
Sodium bicarbonate	2200
Sodium pyruvate	55
Thymidine	0.365
Glucose	3000

LAA medium formulation

Amino acids	Concentration (mg/L)
Glycine	7.51
Alanine	8.91
L-Arginine hydrochloride	21.07
L-Asparagine monohydrate	15.01
L-Aspartic acid	13.31
L-Cysteine dihydrochloride	8.78
L-Cystine hydrochloride monohydrate	15.66
L-Glutamic acid	14.62
L Histidine	21.27
L-Isoleucine	13.12
L-Leucine	13.12
L-Lysine hydrochloride	18.27
L-Methionine	14.92
L-Phenylalanine	16.52
L-Proline	11.51
L-Serine	10.51
L-Threonine	11.91
L-Tryptophan	20.42
L-Tyrosine disodium salt	22.52
L-Valine	11.72
Glutamine	73.07

Inorganic salt	
Ammonium metavanadate	0.00087
Ammonium molybdate tetrahydrate	0.00927
Calcium nitrate tetrahydrate	90
Copper sulphate pentahydrate	0.00195
Disodium hydrogen phosphate	355
Ferric nitrate nonahydrate	0.075
Ferrous sulphate heptahydrate	0.6255
Magnesium chloride anhydrous	29

Magnesium sulphate heptahydrate	100
Manganese chloride	1.25E-04
Nickel chloride	0.00018
Potassium chloride	312
Sodium chloride	6996
Sodium dihydrogen phosphate	271.5
Sodium metasilicate nonahydrate	0.0213
Sodium selenite	0.00936
Stannous chloride dihydrate	0.000165
Zinc sulphate heptahydrate	0.648

Vitamins	
Ca-D-Pantothenic acid	3.36
Choline chloride	13.47
D-Biotin	0.00525
Folic acid	3.99
Niacinamide	3.03
Pyridoxal hydrochloride	3
Pyridoxine hydrochloride	0.0465
Riboflavin	0.3285
Thiamine hydrochloride	3.255
Vitamin B12	1.02
Myo-Inositol	18.9
Ascorbic acid	30
Others	
DL-Thioctic acid	0.105
Ethanolamine	21.59
Glutathione	1.8
HEPES buffer	3574.5
Hypoxanthine	2.4
Linoleic acid	4.20E-02
Lipid mixture I, chemically defined (Sigma L0288)	1X

β -mercaptoethanol	1.4
Phenol red sodium salt	8.63
Putrescine hydrochloride	8.10E-02
Protein hydrolysate	1000
Sodium bicarbonate	2200
Sodium pyruvate	55
Thymidine	0.365
Glucose	1000

Medium formulation for Equimolar amino acid concentration

Amino acids	Concentration (mg/L)
Glycine	75.05
L-Alanine	89.09
L-Arginine hydrochloride	210.66
L-Asparagine monohydrate	150.14
L-Aspartic acid	133.10
L-Cysteine hydrochloride monohydrate	8.78
L-Cystine dihydrochloride	93.97
L-Glutamic acid	146.15
L-Histidine hydrochloride monohydrate	212.65
L-Isoleucine	131.17
L-Leucine	131.17
L-Lysine hydrochloride	182.65
L-Methionine	149.21
L-Phenylalanine	165.19
L-Proline	115.13
L-Serine	105.09
L-Threonine	119.12
L-Tryptophan	204.23
L-Tyrosine	225.15
L-Valine	117.15
L-Glutamine	146.14
Inorganic salts	
Ammonium metavanadate	0.00087
Ammonium molybdate tetrahydrate	0.00927
Calcium nitrate tetrahydrate	90
Copper sulphate pentahydrate	0.00195
Disodium hydrogen phosphate	355
Ferric nitrate nonahydrate	0.075
Ferrous sulphate heptahydrate	0.6255
Magnesium chloride anhydrous	29

Magnesium sulphate heptahydrate	100
Manganese chloride	1.25E-04
Nickel chloride	0.00018
Potassium chloride	312
Sodium chloride	6996
Sodium dihydrogen phosphate	271.5
Sodium metasilicate nonahydrate	0.0213
Sodium selenite	0.00936
Stannous chloride dihydrate	0.000165
Zinc sulphate heptahydrate	0.648

Vitamins	
Ca-D-Pantothenic acid	3.36
Choline chloride	13.47
D-Biotin	0.00525
Folic acid	3.99
Niacinamide	3.03
Pyridoxal hydrochloride	3
Pyridoxine hydrochloride	0.0465
Riboflavin	0.3285
Thiamine hydrochloride	3.255
Vitamin B12	1.02
Myo-Inositol	18.9
Ascorbic acid	30

Others	
DL-Thioctic acid	0.105
Ethanolamine	21.59
Glutathione	1.8
HEPES buffer	3574.5
Hypoxanthine	2.4
Linoleic acid	4.20E-02

Lipid mixture I, chemically defined (Sigma L0288)	1X
β -mercaptoethanol	1.4
Phenol red sodium salt	8.63
Putrescine hydrochloride	8.10E-02
Protein hydrolysate	1000
Sodium bicarbonate	2200
Sodium pyruvate	55
Thymidine	0.365
Glucose	1000

Residual amino acid concentration in BR1

The colour scheme denotes concentration across culture profiles. The red colour denotes concentration below 0.1 mM and green colour denotes concentration over 0.1 mM

Time (Days)	0.00	0.54	0.71	1.43	2.53	3.53	4.53	5.20
Asp conc (mM)	0.13	0.05	0.02	0.01	0.01	0.01	0.00	0.00
Glu conc (mM)	0.12	0.07	0.03	0.01	0.01	0.01	0.00	0.00
Asn conc (mM)	0.10	0.07	0.07	0.04	0.03	0.02	0.00	0.00
Ser conc (mM)	0.11	0.09	0.07	0.02	0.01	0.01	0.01	0.01
Gly conc (mM)	0.15	0.21	0.22	0.27	0.33	0.33	0.30	0.36
Ala conc (mM)	0.15	0.32	0.31	0.34	0.00	0.27	0.32	0.25
Pro conc (mM)	0.10	0.13	0.10	0.08	0.00	0.11	0.13	0.11
Tyr conc (mM)	0.11	0.10	0.09	0.07	0.08	0.06	0.04	0.05
Thr conc (mM)	0.10	0.08	0.06	0.05	0.06	0.04	0.04	0.06
Val conc (mM)	0.12	0.08	0.07	0.03	0.04	0.01	0.00	0.01
Met conc (mM)	0.10	0.08	0.08	0.06	0.06	0.05	0.04	0.04
Iso conc (mM)	0.11	0.09	0.06	0.03	0.02	0.01	0.01	0.01
Leu conc (mM)	0.08	0.04	0.03	0.01	0.01	0.00	0.00	0.00
Phe conc (mM)	0.10	0.09	0.08	0.07	0.06	0.06	0.05	0.05
Trp conc (mM)	0.11	0.09	0.10	0.08	0.07	0.06	0.04	0.04
Lys conc (mM)	0.15	0.08	0.08	0.04	0.04	0.03	0.02	0.03
His conc (mM)	0.11	0.11	0.09	0.08	0.08	0.08	0.08	0.08
Arg conc (mM)	0.16	0.12	0.09	0.07	0.07	0.05	0.05	0.06
Cys conc (mM)	0.05	0.01	0.01	0.00	0.00	0.00	0.00	0.00
Gln conc (mM)	0.57	0.26	0.19	0.01	0.01	0.04	0.04	0.05
IVCD (x10 ⁶ cell.days/mL)	0.99	1.5	1.65	2.36	3.6	4.6	5.61	6.5

Residual amino acid concentration in BR3

The colour scheme denotes concentration across culture profiles. The red colour denotes concentration below 0.1 mM and green colour denotes concentration over 0.1 mM

Time (Days)	0	0.8	2.1	3.0	3.9	4.9	5.8	6.8	7.8	8.8	9.7	10.7	11.7
Asp conc (mM)	0.11	0.03	0.01	0.00	0.00	0.00	0.00	0.00	0.01	0.01	0.00	0.00	0.00
Glu conc (mM)	0.11	0.06	0.02	0.01	0.00	0.00	0.00	0.00	0.02	0.01	0.02	0.00	0.04
Asn conc (mM)	0.11	0.05	0.03	0.02	0.01	0.00	0.00	0.01	0.01	0.01	0.01	0.01	0.01
Ser conc (mM)	0.12	0.06	0.06	0.05	0.04	0.02	0.02	0.02	0.04	0.03	0.03	0.03	0.04
Gly conc (mM)	0.15	0.14	0.22	0.19	0.20	0.20	0.19	0.15	0.15	0.16	0.14	0.13	0.13
Ala conc (mM)	0.19	0.15	0.31	0.37	0.37	0.41	0.42	0.39	0.60	0.64	0.67	0.67	0.71
Pro conc (mM)	0.13	0.06	0.07	0.05	0.05	0.06	0.08	0.09	0.11	0.11	0.11	0.12	0.12
Tyr conc (mM)	0.13	0.09	0.12	0.11	0.10	0.12	0.14	0.14	0.15	0.15	0.15	0.17	0.21
Thr conc (mM)	0.12	0.08	0.11	0.09	0.10	0.12	0.15	0.17	0.13	0.14	0.16	0.17	0.18
Val conc (mM)	0.13	0.08	0.13	0.12	0.11	0.14	0.17	0.20	0.21	0.22	0.24	0.29	0.32
Met conc (mM)	0.13	0.08	0.12	0.10	0.09	0.11	0.12	0.12	0.13	0.13	0.12	0.14	0.15
Iso conc (mM)	0.15	0.11	0.17	0.18	0.17	0.21	0.24	0.28	0.29	0.31	0.33	0.41	0.43
Leu conc (mM)	0.15	0.09	0.12	0.11	0.10	0.12	0.16	0.19	0.20	0.21	0.23	0.28	0.31
Phe conc (mM)	0.14	0.08	0.10	0.09	0.08	0.09	0.10	0.11	0.11	0.11	0.11	0.13	0.14
Trp conc (mM)	0.09	0.05	0.06	0.08	0.06	0.05	0.04	0.05	0.04	0.05	0.05	0.04	0.04
Lys conc (mM)	0.15	0.11	0.17	0.15	0.14	0.17	0.21	0.25	0.27	0.27	0.27	0.30	0.33
His conc (mM)	0.08	0.06	0.08	0.08	0.08	0.09	0.10	0.11	0.12	0.12	0.12	0.12	0.13
Arg conc (mM)	0.15	0.11	0.17	0.17	0.16	0.19	0.22	0.24	0.26	0.27	0.27	0.29	0.31
Cys conc (mM)	0.02	0.01	0.00	0.00	0.00	0.00	0.00	0.00	0.00	0.00	0.00	0.00	0.01
Gln conc (mM)	0.50	0.32	0.45	0.33	0.26	0.31	0.45	0.69	0.82	0.93	0.98	1.15	1.35
IVCD (x10 ⁶ cell.days/mL)	0.93	1.7	2.8	3.7	4.7	5.8	7.1	8.4	9.8	10.9	12	12.9	13.7

References

- [1] A. Mullard, 2020 FDA drug approvals, *Nat. Rev. Drug Discov.* 20 (2021) 85–90. doi:10.1038/D41573-021-00002-0.
- [2] BIOPHARMACEUTICALS MARKET - GROWTH, TRENDS, COVID-19 IMPACT, AND FORECASTS (2021 - 2026), 2020. <https://www.mordorintelligence.com/industry-reports/global-biopharmaceuticals-market-industry>.
- [3] G. Walsh, Biopharmaceutical benchmarks 2018, *Nat. Biotechnol.* 36 (2018) 1136. <https://doi.org/10.1038/nbt.4305>.
- [4] F. Torkashvand, B. Vaziri, S. Maleknia, A. Heydari, M. Vossoughi, F. Davami, F. Mahboudi, Designed Amino Acid Feed in Improvement of Production and Quality Targets of a Therapeutic Monoclonal Antibody, *PLoS One.* 10 (2015) e0140597. doi:10.1371/journal.pone.0140597.

- [5] Priyanka, J. Kumar, J. Gomes, A.S. Rathore, Implementing Process Analytical Technology for the Production of Recombinant Proteins in *Escherichia coli* Using an Advanced Controller Scheme, *Biotechnol. J.* 14 (2019). doi:10.1002/BIOT.201800556.
- [6] A.J. Porter, A.J. Dickson, A.J. Racher, Strategies for selecting recombinant CHO cell lines for cGMP manufacturing: realizing the potential in bioreactors., *Biotechnol. Prog.* 26 (2010) 1446–1454. doi:10.1002/btpr.442.
- [7] A.J. Porter, A.J. Racher, R. Preziosi, A.J. Dickson, Strategies for selecting recombinant CHO cell lines for cGMP manufacturing: improving the efficiency of cell line generation, *Biotechnol. Prog.* 26 (2010) 1455–1464.
- [8] B.C. Mulukutla, J. Kale, T. Kalomeris, M. Jacobs, G.W. Hiller, Identification and control of novel growth inhibitors in fed-batch cultures of Chinese hamster ovary cells, *Biotechnol. Bioeng.* 114 (2017) 1779–1790. doi:10.1002/bit.26313.
- [9] A. Bedoya-López, K. Estrada, A. Sanchez-Flores, O.T. Ramírez, C. Altamirano, L. Segovia, J. Miranda-Rios, M.A. Trujillo-Roldan, N.A. Valdez-Cruz, Effect of temperature downshift on the transcriptomic responses of Chinese hamster ovary cells using recombinant human tissue plasminogen activator production culture, *PLoS One.* 11 (2016) e0151529.
- [10] J. Pfizenmaier, L. Junghans, A. Teleki, R. Takors, Hyperosmotic stimulus study discloses benefits in ATP supply and reveals miRNA/mRNA targets to improve recombinant protein production of CHO cells, *Biotechnol. J.* 11 (2016) 1037–1047.
- [11] J.R. Cantor, M. Abu-Remaileh, N. Kanarek, E. Freinkman, X. Gao, A. Louissaint, C.A. Lewis, D.M. Sabatini, Physiologic Medium Rewires Cellular Metabolism and Reveals Uric Acid as an Endogenous Inhibitor of UMP Synthase, *Cell.* (2017). doi:10.1016/j.cell.2017.03.023.
- [12] J. Vande Voorde, T. Ackermann, N. Pfetzer, D. Sumpton, G. Mackay, G. Kalna, C. Nixon, K. Blyth, E. Gottlieb, S. Tardito, Improving the metabolic fidelity of cancer models with a physiological cell culture medium, *Sci. Adv.* (2019). doi:10.1126/sciadv.aau7314.
- [13] E. Baek, C.L. Kim, M.G. Kim, J.S. Lee, G.M. Lee, Chemical inhibition of autophagy: Examining its potential to increase the specific productivity of recombinant CHO cell lines, *Biotechnol. Bioeng.* 113 (2016) 1953–1961. doi:10.1002/bit.25962.
- [14] Y.J. Kim, E. Baek, J.S. Lee, G.M. Lee, Autophagy and its implication in Chinese hamster ovary cell culture, *Biotechnol. Lett.* 35 (2013) 1753–1763. doi:10.1007/s10529-013-1276-5.
- [15] A. Tintó, C. Gabernet, J. Vives, E. Prats, J.J. Cairó, L. Cornudella, F. Gòdia, The protection of hybridoma cells from apoptosis by caspase inhibition allows culture recovery when exposed to non-inducing conditions, *J. Biotechnol.* 95 (2002) 205–214.

- [16] M. Butler, Animal cell cultures: recent achievements and perspectives in the production of biopharmaceuticals, *Appl. Microbiol. Biotechnol.* 68 (2005) 283–291.
- [17] J.A. Zanghi, W.A. Renner, J.E. Bailey, M. Fussenegger, The growth factor inhibitor suramin reduces apoptosis and cell aggregation in protein-free CHO cell batch cultures, *Biotechnol. Prog.* 16 (2000) 319—325. doi:10.1021/bp0000353.
- [18] J. von Hagen, C. Hecklau, R. Seibel, S. Pering, A. Schnellbaecher, M. Wehsling, T. Eichhorn, A. Zimmer, Simplification of Fed-Batch Processes with a Single-Feed Strategy, *Bioprocess Int.* (2017).
- [19] B.P. Weegman, P. Nash, A.L. Carlson, K.J. Voltzke, Z. Geng, M. Jahani, B.B. Becker, K.K. Papas, M.T. Firpo, Nutrient Regulation by Continuous Feeding Removes Limitations on Cell Yield in the Large-Scale Expansion of Mammalian Cell Spheroids, *PLoS One.* 8 (2013). doi:10.1371/journal.pone.0076611.
- [20] N.K. Tripathi, A. Shrivastava, Recent Developments in Bioprocessing of Recombinant Proteins: Expression Hosts and Process Development, *Front. Bioeng. Biotechnol.* 7 (2019) 420. doi:10.3389/FBIOE.2019.00420.
- [21] F.K. Agbogbo, D.M. Ecker, A. Farrand, K. Han, A. Khoury, A. Martin, J. McCool, U. Rasche, T.D. Rau, D. Schmidt, M. Sha, N. Treuheit, Current perspectives on biosimilars, *J. Ind. Microbiol. Biotechnol.* 46 (2019) 1297–1311. doi:10.1007/S10295-019-02216-Z.
- [22] J.M. Bielser, M. Wolf, J. Souquet, H. Broly, M. Morbidelli, Perfusion mammalian cell culture for recombinant protein manufacturing – A critical review, *Biotechnol. Adv.* 36 (2018) 1328–1340. doi:10.1016/J.BIOTECHADV.2018.04.011.
- [23] S. Chung, J. Tian, Z. Tan, J. Chen, J. Lee, M. Borys, Z.J. Li, Industrial bioprocessing perspectives on managing therapeutic protein charge variant profiles, *Biotechnol. Bioeng.* 115 (2018) 1646–1665. doi:10.1002/BIT.26587.
- [24] T.A. Grein, D. Loewe, H. Dieken, T. Weidner, D. Salzig, P. Czermak, Aeration and Shear Stress Are Critical Process Parameters for the Production of Oncolytic Measles Virus, *Front. Bioeng. Biotechnol.* 7 (2019) 78. doi:10.3389/FBIOE.2019.00078.
- [25] S. Ringer, A further Contribution regarding the influence of the different Constituents of the Blood on the Contraction of the Heart, *J. Physiol.* 4 (1883) 29-42.3.
- [26] S. Ringer, Concerning the Influence exerted by each of the Constituents of the Blood on the Contraction of the Ventricle, *J. Physiol.* 3 (1882) 380–393.
- [27] A. Carrel, On the permanent life of tissues outside of the organism, *J. Exp. Med.* 15 (1912) 516–528.

- [28] A. Carrel, Artificial activation of the growth in vitro of connective tissue, *J. Exp. Med.* 17 (1913) 14–19.
- [29] R.G. Harrison, M.J. Greenman, F.P. Mall, C.M. Jackson, Observations of the living developing nerve fiber, *Anat. Rec.* 1 (1907) 116–128.
- [30] P. Flodin, J. Killander, Fractionation of human-serum proteins by gel filtration., *Biochim. Biophys. Acta.* 63 (1962) 402–410.
- [31] A. Melkonian, J.D.S. Gaylor, R.B. Cousins, M.H. Grant, Growth and viability of Hep G2 cells in medium containing high serum concentrations, *Biochem. Soc. Trans.* 21 (1993) 69S LP-69S.
- [32] A.J. Kniazeff, L.J. Wopschall, H.E. Hopps, C.S. Morris, Detection of bovine viruses in fetal bovine serum used in cell culture, *Vitr. Cell. Dev. Biol.* 11 (1975) 400–403.
- [33] C.W. Boone, N. Mantel, T.D. Caruso, E. Kazam, R.E. Stevenson, Quality control studies on fetal bovine serum used in tissue culture, *Vitr. Cell. Dev. Biol.* 7 (1971) 174–189.
- [34] K. V Honn, J.A. Singley, W. Chavin, Fetal bovine serum: a multivariate standard, *Proc. Soc. Exp. Biol. Med.* 149 (1975) 344–347.
- [35] M.S. Even, C.B. Sandusky, N.D. Barnard, Serum-free hybridoma culture: ethical, scientific and safety considerations, *Trends Biotechnol.* 24 (2006) 105–108. doi:<http://dx.doi.org/10.1016/j.tibtech.2006.01.001>.
- [36] B. Griffiths, Can cell culture medium costs be reduced? Strategies and possibilities, *Trends Biotechnol.* 4 (1986) 268–272.
- [37] B. Halliwell, Albumin—An important extracellular antioxidant?, *Biochem. Pharmacol.* 37 (1988) 569–571. doi:[http://dx.doi.org/10.1016/0006-2952\(88\)90126-8](http://dx.doi.org/10.1016/0006-2952(88)90126-8).
- [38] G.L. Francis, Albumin and mammalian cell culture: implications for biotechnology applications, *Cytotechnology.* 62 (2010) 1–16. doi:[10.1007/s10616-010-9263-3](https://doi.org/10.1007/s10616-010-9263-3).
- [39] C. Sheahan, M. Ross, T. Mitina, T. Linke, T. Robinson, S. Grosvenor, L. Chirkova, Recombinant Albumin as an Animal-Free Supplement to Enhance Cell Culture Performance BT - Proceedings of the 21st Annual Meeting of the European Society for Animal Cell Technology (ESACT), Dublin, Ireland, June 7-10, 2009, in: N. Jenkins, N. Barron, P. Alves (Eds.), Springer Netherlands, Dordrecht, 2012: pp. 481–485. doi:[10.1007/978-94-007-0884-6_81](https://doi.org/10.1007/978-94-007-0884-6_81).
- [40] K. Abe, M. Ikeda, Y. Ariumi, H. Dansako, N. Kato, Serum-free cell culture system supplemented with lipid-rich albumin for hepatitis C virus (strain O of genotype 1b) replication, *Virus Res.* 125 (2007) 162–168. doi:<http://dx.doi.org/10.1016/j.virusres.2006.12.015>.
- [41] J. Keenan, M. Dooley, D. Pearson, M. Clynes, Recombinant human albumin in

cell culture: evaluation of growth-promoting potential for NRK and SCC-9 cells in vitro, *Cytotechnology*. 24 (1997) 243–252.

- [42] P.M. Hayter, E.M.A. Curling, A.J. Baines, N. Jenkins, I. Salmon, P.G. Strange, J.M. Tong, A.T. Bull, Glucose-limited chemostat culture of chinese hamster ovary cells producing recombinant human interferon- γ , *Biotechnol. Bioeng.* (1992). doi:10.1002/bit.260390311.
- [43] R.I. Freshney, R.I. Freshney, *Culture of Specific Cell Types*, in: *Cult. Anim. Cells*, John Wiley & Sons, Inc., 2005. doi:10.1002/0471747599.cac023.
- [44] S. Gorfien, R. Fike, G. Godwin, J. Dzimian, D.A. Epstein, D. Gruber, P. Price, Serum-free mammalian cell culture medium, and uses thereof, (2013).
- [45] H. Eagle, S. Barban, M. Levy, H.O. Schulze, The utilization of carbohydrates by human cell cultures., *J. Biol. Chem.* 233 (1958) 551–558.
- [46] M. Lao, D. Toth, Effects of ammonium and lactate on growth and metabolism of a recombinant Chinese hamster ovary cell culture, *Biotechnol. Prog.* 13 (1997) 688–691.
- [47] H. Ronald Zielke, P.T. Ozand, J. Tyson Tildon, D.A. Sevdalian, M. Cornblath, Reciprocal regulation of glucose and glutamine utilization by cultured human diploid fibroblasts, *J. Cell. Physiol.* 95 (1978) 41–48.
- [48] C.A. Wilkens, C. Altamirano, Z.P. Gerdtzen, Comparative metabolic analysis of lactate for CHO cells in glucose and galactose, *Biotechnol. Bioprocess Eng.* 16 (2011) 714–724. doi:10.1007/s12257-010-0409-0.
- [49] C. Altamirano, C. Paredes, J.J.J. Cairo, F. Godia, Improvement of CHO Cell Culture Medium Formulation: Simultaneous Substitution of Glucose and Glutamine, *Biotechnol. Prog.* 16 (2000) 69–75. doi:10.1021/bp990124j.
- [50] F.-Q. Zhao, A.F. Keating, Functional properties and genomics of glucose transporters, *Curr. Genomics.* 8 (2007) 113–128.
- [51] C. Altamirano, C. Paredes, A. Illanes, J.J. Cairo, F. Godia, Strategies for fed-batch cultivation of t-PA producing CHO cells: substitution of glucose and glutamine and rational design of culture medium, *J. Biotechnol.* 110 (2004) 171–179.
- [52] H. Eagle, V.I. Oyama, M. Levy, Amino acid requirements of normal and malignant human cells in tissue culture, *Arch. Biochem. Biophys.* 67 (1957) 432–446.
- [53] H. Eagle, The specific amino acid requirements of a human carcinoma cell (strain HeLa) in tissue culture, *J. Exp. Med.* 102 (1955) 37–48.
- [54] H. Eagle, The specific amino acid requirements of a mammalian cell (strain L) in tissue culture., *J. Biol. Chem.* 214 (1955) 839–852.
- [55] R.G. Ham, An improved nutrient solution for diploid Chinese hamster and

- human cell lines, *Exp. Cell Res.* 29 (1963) 515–526.
- [56] R.Z. Lockart, H. Eagle, Requirements for Growth of Single Human Cells, *Science* (80-.). 129 (1959) 252–254.
- [57] C. Altamirano, A. Illanes, R. Canessa, S. Becerra, Specific nutrient supplementation of defined serum-free medium for the improvement of CHO cells growth and t-PA production, *Electron. J. Biotechnol.* 9 (2006) 61–67. doi:10.2225/vol9-issue1-fulltext-8.
- [58] D. Duval, C. Demangel, K. Munier-Jolain, S. Miossec, I. Geahel, Factors controlling cell proliferation and antibody production in mouse hybridoma cells: I. Influence of the amino acid supply, *Biotechnol. Bioeng.* 38 (1991) 561–570.
- [59] M. Palacín, R. Estévez, J. Bertran, Z. Antonio, Molecular Biology of Mammalian Plasma Membrane Amino Acid Transporters, *Physiol. Rev.* 78 (1998) 969 LP – 1054.
- [60] W.W. Souba, A.J. Pacitti, Review: How Amino Acids Get Into Cells: Mechanisms, Models, Menus, and Mediators, *J. Parenter. Enter. Nutr.* 16 (1992) 569–578. doi:10.1177/0148607192016006569.
- [61] S. Kyriakopoulos, Amino acid metabolism in Chinese hamster ovary cell culture, (2014).
- [62] L. Levintow, H. Eagle, K.A. Piez, The role of glutamine in protein biosynthesis in tissue culture, *J. Biol. Chem.* 227 (1957) 929–941.
- [63] H. Eagle, V.I. Oyama, M. Levy, C.L. Horton, R. Fleischman, The growth response of mammalian cells in tissue culture to L-glutamine and L-glutamic acid., *J. Biol. Chem.* 218 (1956) 607–616.
- [64] M.W. Glacken, Catabolic control of mammalian cell culture, *Nat. Biotechnol.* 6 (1988) 1041–1050.
- [65] H.R. Zielke, C.M. Sumbilla, D.A. Sevdalian, R.L. Hawkins, P.T. Ozand, Lactate: a major product of glutamine metabolism by human diploid fibroblasts, *J. Cell. Physiol.* 104 (1980) 433–441.
- [66] M. Donnelly, I.E. Scheffler, Energy metabolism in respiration-deficient and wild type chinese hamster fibroblasts in culture, *J. Cell. Physiol.* 89 (1976) 39–51.
- [67] J.A.H. Bort, B. Stern, N. Borth, CHO-K1 host cells adapted to growth in glutamine-free medium by FACS-assisted evolution, *Biotechnol. J.* 5 (2010) 1090–1097.
- [68] P. Xu, X. Dai, E. Graf, R. Martel, R. Russell, Effects of glutamine and asparagine on recombinant antibody production using CHO-GS cell lines, *Biotechnol. Prog.* 30 (2014) 1457–1468.

- [69] F. Zhang, X. Sun, X. Yi, Y. Zhang, Metabolic characteristics of recombinant Chinese hamster ovary cells expressing glutamine synthetase in presence and absence of glutamine, *Cytotechnology*. (2006). doi:10.1007/s10616-006-9010-y.
- [70] L.-E. Quek, S. Dietmair, J.O. Krömer, L.K. Nielsen, Metabolic flux analysis in mammalian cell culture, *Metab. Eng.* 12 (2010) 161–171.
- [71] P. Chen, S.W. Harcum, Effects of amino acid additions on ammonium stressed CHO cells, *J. Biotechnol.* 117 (2005) 277–286.
- [72] M. Yang, M. Butler, Effect of ammonia on the glycosylation of human recombinant erythropoietin in culture, *Biotechnol. Prog.* 16 (2000) 751–759.
- [73] B.P. Bode, Recent molecular advances in mammalian glutamine transport, *J. Nutr.* 131 (2001) 2475S-2485S.
- [74] Y.D. Bhutia, V. Ganapathy, Glutamine transporters in mammalian cells and their functions in physiology and cancer, *Biochim. Biophys. Acta (BBA)-Molecular Cell Res.* 1863 (2016) 2531–2539.
- [75] V.K. Pasupuleti, A.L. Demain, *Protein hydrolysates in biotechnology*, Springer Science & Business Media, 2010.
- [76] C.C. Burteau, F.R. Verhoeve, J.F. Mols, J.-S. Ballez, S.N. Agathos, Y.-J. Schneider, Fortification of a Protein-Free Cell Culture Medium with Plant Peptones Improves Cultivation and Productivity of an Interferon- γ -Producing CHO Cell Line, *Vitr. Cell. Dev. Biol.* 39 (2003) 291–296.
- [77] B. Farges-Haddani, B. Tessier, S. Chenu, I. Chevalot, C. Harscoat, I. Marc, J.L. Goergen, A. Marc, Peptide fractions of rapeseed hydrolysates as an alternative to animal proteins in CHO cell culture media, *Process Biochem.* 41 (2006) 2297–2304.
- [78] J.S. Ballez, J. Mols, C. Burteau, S.N. Agathos, Y.J. Schneider, Plant protein hydrolysates support CHO-320 cells proliferation and recombinant IFN- γ production in suspension and inside microcarriers in protein-free media, *Cytotechnology*. 44 (2004) 103–114. doi:10.1007/s10616-004-1099-2.
- [79] J. Mols, C. Peeters-Joris, S.N. Agathos, Y.-J. Schneider, Origin of rice protein hydrolysates added to protein-free media alters secretion and extracellular proteolysis of recombinant interferon- γ as well as CHO-320 cell growth, *Biotechnol. Lett.* 26 (2004) 1043–1046. doi:10.1023/B:BILE.0000032960.06112.31.
- [80] X. Gu, L. Xie, B.J. Harmon, D. I C. Wang, Influence of Primatone RL supplementation on sialylation of recombinant human interferon-g produced by Chinese hamster ovary cell culture using serum-free media, *Biotechnol. Bioeng.* 56 (1997) 353–360.
- [81] R. Heidemann, C. Zhang, H. Qi, J. Larrick Rule, C. Rozales, S. Park, S. Chuppa, M. Ray, J. Michaels, K. Konstantinov, D. Naveh, The use of peptones

- as medium additives for the production of a recombinant therapeutic protein in high density perfusion cultures of mammalian cells, *Cytotechnology*. 32 (2000) 157–167. doi:10.1023/A:1008196521213.
- [82] F. Franěk, H. Katinger, Specific Effects of Synthetic Oligopeptides on Cultured Animal Cells, *Biotechnol. Prog.* 18 (2002) 155–158. doi:10.1021/bp0101278.
- [83] F. Franěk, M. Fussenegger, Survival Factor-Like Activity of Small Peptides in Hybridoma and CHO Cells Cultures, *Biotechnol. Prog.* 21 (2005) 96–98. doi:10.1021/bp0400184.
- [84] I. Rubio-Aliaga, H. Daniel, Mammalian peptide transporters as targets for drug delivery, *Trends Pharmacol. Sci.* 23 (2002) 434–440.
- [85] D.E. Smith, B. Cléménçon, M.A. Hediger, Proton-coupled oligopeptide transporter family SLC15: physiological, pharmacological and pathological implications, *Mol. Aspects Med.* 34 (2013) 323–336.
- [86] H. Eagle, The minimum vitamin requirements of the L and HeLa cells in tissue culture, the production of specific vitamin deficiencies, and their cure, *J. Exp. Med.* 102 (1955) 595–600.
- [87] K.K. Sanford, L.T. Dupree, A.B. Covalsky, Biotin, B12, and other vitamin requirements of a strain of mammalian cells grown in chemically defined medium, *Exp. Cell Res.* 31 (1963) 345–375.
- [88] V.J. Evans, J.C. Bryant, W.T. McQuilkin, M.C. Fioramonti, K.K. Sanford, B.B. Westfall, W.R. Earle, Studies of nutrient media for tissue cells in vitro II. An improved protein-free chemically defined medium for long-term cultivation of strain L-929 cells, *Cancer Res.* 16 (1956) 87.
- [89] H. Eagle, V.I. Oyama, A.E. Freeman, Myo-Inositol as an essential growth factor for normal and malignant human cells in tissue culture., *J. Biol. Chem.* 226 (1957) 191–205.
- [90] I. Lieberman, P. Ove, Control of growth of mammalian cells in culture with folic acid, thymidine, and purines, *J. Biol. Chem.* 235 (1960) 1119–1123.
- [91] T. Yao, Y. Asayama, Animal-cell culture media: History, characteristics, and current issues, *Reprod. Med. Biol.* 16 (2017) 99–117.
- [92] H. Eagle, Nutrition needs of mammalian cells in tissue culture, *Science* (80-.). 122 (1955) 501–504.
- [93] L. He, K. Vasiliou, D.W. Nebert, Analysis and update of the human solute carrier (SLC) gene superfamily, *Hum. Genomics.* 3 (2009) 195.
- [94] G.R. Buettner, The pecking order of free radicals and antioxidants: lipid peroxidation, α -tocopherol, and ascorbate, *Arch. Biochem. Biophys.* 300 (1993) 535–543.
- [95] A.J. Michels, B. Frei, Myths, artifacts, and fatal flaws: identifying limitations

and opportunities in vitamin C research, *Nutrients*. 5 (2013) 5161–5192.

- [96] L. Packer, E.H. Witt, H.J. Tritschler, Alpha-lipoic acid as a biological antioxidant, *Free Radic. Biol. Med.* 19 (1995) 227–250.
- [97] H. Moini, L. Packer, N.-E.L. Saris, Antioxidant and prooxidant activities of α -lipoic acid and dihydrolipoic acid, *Toxicol. Appl. Pharmacol.* 182 (2002) 84–90.
- [98] J. Bustamante, J.K. Lodge, L. Marcocci, H.J. Tritschler, L. Packer, B.H. Rihn, α -Lipoic acid in liver metabolism and disease, *Free Radic. Biol. Med.* 24 (1998) 1023–1039.
- [99] K.P. Shay, R.F. Moreau, E.J. Smith, A.R. Smith, T.M. Hagen, Alpha-lipoic acid as a dietary supplement: Molecular mechanisms and therapeutic potential, *Biochim. Biophys. Acta.* 1790 (2009) 1149–1160. doi:10.1016/j.bbagen.2009.07.026.
- [100] N. Takaishi, K. Yoshida, H. Satsu, M. Shimizu, Transepithelial transport of α -lipoic acid across human intestinal Caco-2 cell monolayers, *J. Agric. Food Chem.* 55 (2007) 5253–5259.
- [101] B. Zehnpfennig, P. Wiriyasermkul, D.A. Carlson, M. Quick, Interaction of α -lipoic acid with the human Na⁺/multivitamin transporter (hSMVT), *J. Biol. Chem.* 290 (2015) 16372–16382.
- [102] J.P. Mather, G.H. Sato, The use of hormone-supplemented serum-free media in primary cultures, *Exp. Cell Res.* 124 (1979) 215–221.
- [103] S.E. Hutchings, G.H. Sato, Growth and maintenance of HeLa cells in serum-free medium supplemented with hormones., *Proc. Natl. Acad. Sci. U. S. A.* 75 (1978) 901–904.
- [104] R. Perez-Rodriguez, A. Franchi, J. Pouyssegur, Growth factor requirements of Chinese hamster lung fibroblasts in serum free media: high mitogenic action of thrombin, *Cell Biol. Int. Rep.* 5 (1981) 347–357.
- [105] M.D. Rosenthal, Accumulation of neutral lipids by human skin fibroblasts: differential effects of saturated and unsaturated fatty acids, *Lipids.* 16 (1981) 173–182.
- [106] S.I. Grammatikos, P. V Subbaiah, T.A. Victor, W.M. Miller, Diverse effects of essential (n-6 and n-3) fatty acids on cultured cells, in: *Cell Cult. Eng. IV*, Springer, 1994: pp. 31–50.
- [107] A.A. Spector, S.N. Mathur, T.L. Kaduce, Lipid nutrition and metabolism of cultured mammalian cells, *Prog. Lipid Res.* 19 (1980) 155–186.
- [108] W. Whitford, J. Manwaring, Lipids in cell culture media, *Art To Sci. Lab. Inc. P.* (2004) 1–5.
- [109] M. Butler, N. Huzel, The effect of fatty acids on hybridoma cell growth and

- antibody productivity in serum-free cultures, *J. Biotechnol.* 39 (1995) 165–173.
- [110] R.P. Henry, Multiple roles of carbonic anhydrase in cellular transport and metabolism, *Annu. Rev. Physiol.* 58 (1996) 523–538.
- [111] R.G. Ham, W.L. McKeehan, [5] Media and growth requirements, *Methods Enzymol.* 58 (1979) 44–93.
- [112] W.L. McKeehan, W.G. Hamilton, R.G. Ham, Selenium is an essential trace nutrient for growth of WI-38 diploid human fibroblasts, *Proc. Natl. Acad. Sci.* 73 (1976) 2023–2027.
- [113] D.H. Holben, A.M. Smith, The diverse role of selenium within selenoproteins: a review, *J. Am. Diet. Assoc.* 99 (1999) 836–843.
- [114] D. Mustacich, G. Powis, Thioredoxin reductase, *Biochem. J.* 346 (2000) 1 LP – 8.
- [115] A. Holmgren, M. Bjornstedt, [21] Thioredoxin and thioredoxin reductase, *Methods Enzymol.* 252 (1995) 199–208. doi:[http://dx.doi.org/10.1016/0076-6879\(95\)52023-6](http://dx.doi.org/10.1016/0076-6879(95)52023-6).
- [116] J. Bottenstein, I. Hayashi, S. Hutchings, H. Masui, J. Mather, D.B. McClure, S. Ohasa, A. Rizzino, G. Sato, G. Serrero, [6] The growth of cells in serum-free hormone-supplemented media, *Methods Enzymol.* 58 (1979) 94–109.
- [117] P.T. Lieu, M. Heiskala, P.A. Peterson, Y. Yang, The roles of iron in health and disease, *Mol. Aspects Med.* 22 (2001) 1–87. doi:[http://dx.doi.org/10.1016/S0098-2997\(00\)00006-6](http://dx.doi.org/10.1016/S0098-2997(00)00006-6).
- [118] J. Osredkar, N. Sustar, Copper and zinc, biological role and significance of copper/zinc imbalance, *J. Clin. Toxicol. S.* 3 (2011) 1.
- [119] A.L.V. Arigony, I.M. de Oliveira, M. Machado, D.L. Bordin, L. Bergter, D. Prá, J.A. Pêgas Henriques, The influence of micronutrients in cell culture: a reflection on viability and genomic stability, *Biomed Res. Int.* 2013 (2013).
- [120] H. Murakami, H. Masui, G.H. Sato, N. Sueoka, T.P. Chow, T. Kano-Sueoka, Growth of hybridoma cells in serum-free medium: ethanolamine is an essential component, *Proc. Natl. Acad. Sci.* 79 (1982) 1158–1162.
- [121] S. Bannai, N. Tateishi, Role of membrane transport in metabolism and function of glutathione in mammals, *J. Membr. Biol.* 89 (1986) 1–8.
- [122] M. Pastor-Anglada, F.J. Casado, Nucleoside transport into cells, in: *Deoxynucleoside Analog. Cancer Ther.*, Springer, 2006: pp. 1–28.
- [123] R. Gheshlaghi, J.M. Scharer, M. Moo-Young, P.L. Douglas, Medium optimization for hen egg white lysozyme production by recombinant *Aspergillus niger* using statistical methods, *Biotechnol. Bioeng.* 90 (2005) 754–760.

- [124] P.L. Wejse, K. Ingvorsen, K.K. Mortensen, Xylanase production by a novel halophilic bacterium increased 20-fold by response surface methodology, *Enzyme Microb. Technol.* 32 (2003) 721–727.
- [125] Q. Zhao, W. Zhang, M. Jin, X. Yu, M. Deng, Formulation of a basal medium for primary cell culture of the marine sponge *Hymeniacidon perleve*, *Biotechnol. Prog.* 21 (2005) 1008–1012.
- [126] C. Chun, K. Heineken, D. Szeto, T. Ryll, S. Chamow, J.D. Chung, Application of factorial design to accelerate identification of CHO growth factor requirements, *Biotechnol. Prog.* 19 (2003) 52–57.
- [127] E.J. Kim, N.S. Kim, G.M. Lee, Development of a serum-free medium for the production of humanized antibody from Chinese hamster ovary cells using a statistical design, *Vitr. Cell. Dev. Biol.* 34 (1998) 757–761.
- [128] G.M. Lee, E.J. Kim, N.S. Kim, S.K. Yoon, Y.H. Ahn, J.Y. Song, Development of a serum-free medium for the production of erythropoietin by suspension culture of recombinant Chinese hamster ovary cells using a statistical design, *J. Biotechnol.* 69 (1999) 85–93.
- [129] E.J. Kim, N.S. Kim, G.M. Lee, Development of a serum-free medium for dihydrofolate reductase-deficient Chinese hamster ovary cells (DG44) using a statistical design: beneficial effect of weaning of cells, *Vitr. Cell. Dev. Biol.* 35 (1999) 178–182.
- [130] C.-H. Liu, I.-M. Chu, S.-M. Hwang, Factorial designs combined with the steepest ascent method to optimize serum-free media for CHO cells, *Enzyme Microb. Technol.* 28 (2001) 314–321.
- [131] N.K. Tripathi, A. Shrivastava, Recent Developments in Bioprocessing of Recombinant Proteins: Expression Hosts and Process Development, *Front. Bioeng. Biotechnol.* 7 (2019). doi:10.3389/FBIOE.2019.00420/XML/NLM.
- [132] E. Petiot, F. Fournier, C. Gény, H. Pinton, A. Marc, Rapid screening of serum-free media for the growth of adherent vero cells by using a small-scale and non-invasive tool, *Appl. Biochem. Biotechnol.* 160 (2010) 1600–1615.
- [133] R.R. Deshpande, C. Wittmann, E. Heinzle, Microplates with integrated oxygen sensing for medium optimization in animal cell culture, *Cytotechnology.* 46 (2004) 1–8.
- [134] I.J. González-Leal, L.M. Carrillo-Cocom, A. Ramírez-Medrano, F. López-Pacheco, D. Bulnes-Abundis, Y. Webb-Vargas, M.M. Alvarez, Use of a plackett-burman statistical design to determine the effect of selected amino acids on monoclonal antibody production in CHO cells, *Biotechnol. Prog.* 27 (2011) 1709–1717. doi:10.1002/btpr.674.
- [135] J. Dean, P. Reddy, Metabolic analysis of antibody producing CHO cells in fed-batch production, *Biotechnol. Bioeng.* (2013). doi:10.1002/bit.24826.
- [136] L. xiang Zhang, W. yan Zhang, C. Wang, J. tao Liu, X. cun Deng, X. ping Liu,

- L. Fan, W. song Tan, Responses of CHO-DHFR cells to ratio of asparagine to glutamine in feed media: cell growth, antibody production, metabolic waste, glutamate, and energy metabolism, *Bioresour. Bioprocess.* (2016). doi:10.1186/s40643-015-0072-6.
- [137] F. Rispoli, V. Shah, A new efficient mixture screening design for optimization of media, *Biotechnol. Prog.* 25 (2009) 980–985.
- [138] T.S. Stoll, K. Mühlethaler, U. Von Stockar, I.W. Marison, Systematic improvement of a chemically-defined protein-free medium for hybridoma growth and monoclonal antibody production, *J. Biotechnol.* 45 (1996) 111–123.
- [139] M. Jordan, D. Voisard, A. Berthoud, L. Tercier, B. Kleuser, G. Baer, H. Broly, Cell culture medium improvement by rigorous shuffling of components using media blending, *Cytotechnology.* 65 (2013) 31–40.
- [140] C. Didier, M. Etcheverrigaray, R. Kratje, H.C. Goicoechea, Crossed mixture design and multiple response analysis for developing complex culture media used in recombinant protein production, *Chemom. Intell. Lab. Syst.* 86 (2007) 1–9.
- [141] Z. Li, J. Dullmann, B. Schiedlmeier, M. Schmidt, C. von Kalle, J. Meyer, M. Forster, C. Stocking, A. Wahlers, O. Frank, Murine leukemia induced by retroviral gene marking, *Science* (80-.). 296 (2002) 497.
- [142] J. Varley, J. Birch, Reactor design for large scale suspension animal cell culture, *Cytotechnology.* 29 (1999) 177–205.
- [143] J. Costes, J.P. Couderc, Study by laser Doppler anemometry of the turbulent flow induced by a Rushton turbine in a stirred tank: influence of the size of the units—I. Mean flow and turbulence, *Chem. Eng. Sci.* 43 (1988) 2751–2764.
- [144] G. Zhou, S.M. Kresta, Distribution of energy between convective and turbulent-flow for 3 frequently used impellers, *Chem. Eng. Res. Des.* 74 (1996) 379–389.
- [145] G. Zhou, S.M. Kresta, Impact of tank geometry on the maximum turbulence energy dissipation rate for impellers, *AIChE J.* 42 (1996) 2476–2490.
- [146] M. Mollet, N. Ma, Y. Zhao, R. Brodkey, R. Taticek, J.J. Chalmers, Bioprocess equipment: characterization of energy dissipation rate and its potential to damage cells, *Biotechnol. Prog.* 20 (2004) 1437–1448.
- [147] W. Hu, C. Berdugo, J.J. Chalmers, The potential of hydrodynamic damage to animal cells of industrial relevance: current understanding, *Cytotechnology.* 63 (2011) 445.
- [148] N. Ma, K.W. Koelling, J.J. Chalmers, Fabrication and use of a transient contractional flow device to quantify the sensitivity of mammalian and insect cells to hydrodynamic forces, *Biotechnol. Bioeng.* 80 (2002) 428–437.

- [149] R. Godoy-Silva, J.J. Chalmers, S.A. Casnocha, L.A. Bass, N. Ma, Physiological responses of CHO cells to repetitive hydrodynamic stress, *Biotechnol. Bioeng.* 103 (2009) 1103–1117.
- [150] J.M. Barnes, J.T. Nauseef, M.D. Henry, Resistance to fluid shear stress is a conserved biophysical property of malignant cells, *PLoS One.* 7 (2012) e50973.
- [151] M.J. Mitchell, M.R. King, Computational and experimental models of cancer cell response to fluid shear stress, *Front. Oncol.* 3 (2013) 44.
- [152] Y.S. Chatzizisis, A.U. Coskun, M. Jonas, E.R. Edelman, C.L. Feldman, P.H. Stone, Role of endothelial shear stress in the natural history of coronary atherosclerosis and vascular remodeling: molecular, cellular, and vascular behavior, *J. Am. Coll. Cardiol.* 49 (2007) 2379–2393.
- [153] J.H. Haga, Y.-S.J. Li, S. Chien, Molecular basis of the effects of mechanical stretch on vascular smooth muscle cells, *J. Biomech.* 40 (2007) 947–960.
- [154] J. Heo, F. Sachs, J. Wang, S.Z. Hua, Shear-induced volume decrease in MDCK cells, *Cell. Physiol. Biochem.* 30 (2012) 395–406.
- [155] N. Resnick, H. Yahav, A. Shay-Salit, M. Shushy, S. Schubert, L.C.M. Zilberman, E. Wofovitz, Fluid shear stress and the vascular endothelium: for better and for worse, *Prog. Biophys. Mol. Biol.* 81 (2003) 177–199.
- [156] P.F. Davies, C.F. Dewey, S.R. Bussolari, E.J. Gordon, M.A. Gimbrone, Influence of hemodynamic forces on vascular endothelial function. In vitro studies of shear stress and pinocytosis in bovine aortic cells., *J. Clin. Invest.* 73 (1984) 1121–1129.
- [157] V. Rizzo, C. Morton, N. DePaola, J.E. Schnitzer, P.F. Davies, Recruitment of endothelial caveolae into mechanotransduction pathways by flow conditioning in vitro, *Am. J. Physiol. Circ. Physiol.* 285 (2003) H1720–H1729.
- [158] C.R. White, J.A. Frangos, The shear stress of it all: the cell membrane and mechanochemical transduction, *Philos. Trans. R. Soc. B Biol. Sci.* 362 (2007) 1459–1467.
- [159] Y. Xu, F.C. Szoka, Mechanism of DNA release from cationic liposome/DNA complexes used in cell transfection, *Biochemistry.* 35 (1996) 5616–5623.
- [160] V.R.S. Patil, C.J. Campbell, Y.H. Yun, S.M. Slack, D.J. Goetz, Particle diameter influences adhesion under flow, *Biophys. J.* 80 (2001) 1733–1743.
- [161] P. Charoenphol, R.B. Huang, O. Eniola-Adefeso, Potential role of size and hemodynamics in the efficacy of vascular-targeted spherical drug carriers, *Biomaterials.* 31 (2010) 1392–1402.
- [162] A. Lin, A. Sabnis, S. Kona, S. Nattama, H. Patel, J. Dong, K.T. Nguyen, Shear-regulated uptake of nanoparticles by endothelial cells and development of endothelial-targeting nanoparticles, *J. Biomed. Mater. Res. Part A An Off. J.*

- Soc. Biomater. Japanese Soc. Biomater. Aust. Soc. Biomater. Korean Soc. Biomater. 93 (2010) 833–842.
- [163] N. Doshi, B. Prabhakarandian, A. Rea-Ramsey, K. Pant, S. Sundaram, S. Mitragotri, Flow and adhesion of drug carriers in blood vessels depend on their shape: a study using model synthetic microvascular networks, *J. Control. Release.* 146 (2010) 196–200.
- [164] J. Han, B.J. Zern, V. V Shuvaev, P.F. Davies, S. Muro, V. Muzykantov, Acute and chronic shear stress differently regulate endothelial internalization of nanocarriers targeted to platelet-endothelial cell adhesion molecule-1, *ACS Nano.* 6 (2012) 8824–8836.
- [165] H. Klingberg, S. Loft, L.B. Oddershede, P. Møller, The influence of flow, shear stress and adhesion molecule targeting on gold nanoparticle uptake in human endothelial cells, *Nanoscale.* 7 (2015) 11409–11419.
- [166] P.J. Butler, G. Norwich, S. Weinbaum, S. Chien, Shear stress induces a time- and position-dependent increase in endothelial cell membrane fluidity, *Am. J. Physiol. Physiol.* 280 (2001) C962–C969.
- [167] M.A. Haidekker, N. L’Heureux, J.A. Frangos, Fluid shear stress increases membrane fluidity in endothelial cells: a study with DCVJ fluorescence, *Am. J. Physiol. Circ. Physiol.* 278 (2000) H1401–H1406.
- [168] M. Kogan, B. Feng, B. Nordén, S. Rocha, T. Beke-Somfai, Shear-induced membrane fusion in viscous solutions, *Langmuir.* 30 (2014) 4875–4878.
- [169] S.S. Harris, T.D. Giorgio, Convective flow increases lipoplex delivery rate to in vitro cellular monolayers, *Gene Ther.* 12 (2005) 512–520.
- [170] T. Fujiwara, H. Akita, K. Furukawa, T. Ushida, H. Mizuguchi, H. Harashima, Impact of convective flow on the cellular uptake and transfection activity of lipoplex and adenovirus, *Biol. Pharm. Bull.* 29 (2006) 1511–1515.
- [171] E. Mennesson, P. Erbacher, M. Kuzak, C. Kieda, P. Midoux, C. Pichon, DNA/cationic polymer complex attachment on a human vascular endothelial cell monolayer exposed to a steady laminar flow, *J. Control. Release.* 114 (2006) 389–397.
- [172] H.S. Shin, H.J. Kim, S.J. Sim, N.L. Jeon, Shear stress effect on transfection of neurons cultured in microfluidic devices, *J. Nanosci. Nanotechnol.* 9 (2009) 7330–7335.
- [173] A. Sharei, J. Zoldan, A. Adamo, W.Y. Sim, N. Cho, E. Jackson, S. Mao, S. Schneider, M.-J. Han, A. Lytton-Jean, A vector-free microfluidic platform for intracellular delivery, *Proc. Natl. Acad. Sci.* 110 (2013) 2082–2087.
- [174] D.M. Hallow, R.A. Seeger, P.P. Kamaev, G.R. Prado, M.C. LaPlaca, M.R. Prausnitz, Shear-induced intracellular loading of cells with molecules by controlled microfluidics, *Biotechnol. Bioeng.* 99 (2008) 846–854.

- [175] A. McQueen, E. Meilhoc, J.E. Bailey, Flow effects on the viability and lysis of suspended mammalian cells, *Biotechnol. Lett.* 9 (1987) 831–836.
- [176] B. Vickroy, K. Lorenz, W. Kelly, Modeling shear damage to suspended CHO cells during cross-flow filtration, *Biotechnol. Prog.* 23 (2007) 194–199.
- [177] S. Kudo, K. Ikezawa, M. Ikeda, K. Oka, K. Tanishita, Albumin concentration profile inside cultured endothelial cells exposed to shear stress, in: *Am. Soc. Mech. Eng. Bioeng. Div. BED*, 1997: pp. 547–548.
- [178] S.H. Mardikar, K. Niranjana, Observations on the shear damage to different animal cells in a concentric cylinder viscometer, *Biotechnol. Bioeng.* 68 (2000) 697–704.
- [179] K.K. Son, D.H. Patel, D. Tkach, A. Park, Cationic liposome and plasmid DNA complexes formed in serum-free medium under optimum transfection condition are negatively charged, *Biochim. Biophys. Acta (BBA)-Biomembranes.* 1466 (2000) 11–15.
- [180] B. Dalby, S. Cates, A. Harris, E.C. Ohki, M.L. Tilkins, P.J. Price, V.C. Ciccarone, Advanced transfection with Lipofectamine 2000 reagent: primary neurons, siRNA, and high-throughput applications, *Methods.* 33 (2004) 95–103.
- [181] B.D. Freimark, H.P. Blezinger, V.J. Florack, J.L. Nordstrom, S.D. Long, D.S. Deshpande, S. Nochumson, K.L. Petrak, Cationic lipids enhance cytokine and cell influx levels in the lung following administration of plasmid: cationic lipid complexes, *J. Immunol.* 160 (1998) 4580–4586.
- [182] S. Li, S.-P. Wu, M. Whitmore, E.J. Loeffert, L. Wang, S.C. Watkins, B.R. Pitt, L. Huang, Effect of immune response on gene transfer to the lung via systemic administration of cationic lipidic vectors, *Am. J. Physiol. Cell. Mol. Physiol.* 276 (1999) L796–L804.
- [183] F.E. Ruiz, J.P. Clancy, M.A. Perricone, Z. Bebok, J.S. Hong, S.H. Cheng, D.P. Meeker, K.R. Young, R.A. Schoumacher, M.R. Weatherly, A clinical inflammatory syndrome attributable to aerosolized lipid–DNA administration in cystic fibrosis, *Hum. Gene Ther.* 12 (2001) 751–761.
- [184] L.M. Barnes, C.M. Bentley, A.J. Dickson, Characterization of the stability of recombinant protein production in the GS-NS0 expression system, *Biotechnol. Bioeng.* 73 (2001) 261–270.
- [185] J.A. Serrato, L.A. Palomares, A. Meneses-Acosta, O.T. Ramírez, Heterogeneous conditions in dissolved oxygen affect N-glycosylation but not productivity of a monoclonal antibody in hybridoma cultures, *Biotechnol. Bioeng.* 88 (2004) 176–188.
- [186] A. Khetan, Y.M. Huang, J. Dolnikova, N.E. Pederson, D. Wen, H. Yusuf-Makagiansar, P. Chen, T. Ryll, Control of misincorporation of serine for asparagine during antibody production using CHO cells, *Biotechnol. Bioeng.* (2010). doi:10.1002/bit.22771.

- [187] J. Glazyrina, M. Krause, S. Junne, F. Glauche, D. Strom, P. Neubauer, Glucose-limited high cell density cultivations from small to pilot plant scale using an enzyme-controlled glucose delivery system, *N. Biotechnol.* 29 (2012) 235–242.
- [188] P. Philip, K. Meier, D. Kern, J. Goldmanns, F. Stockmeier, C. Bähr, J. Büchs, Systematic evaluation of characteristics of the membrane-based fed-batch shake flask, *Microb. Cell Fact.* 16 (2017) 1–17.
- [189] W. Wellenbeck, J. Mampel, C. Naumer, A. Knepper, P. Neubauer, Fast-track development of a lactase production process with *Kluyveromyces lactis* by a progressive parameter-control workflow, *Eng. Life Sci.* 17 (2017) 1185–1194.
- [190] Q. Long, X. Liu, Y. Yang, L. Li, L. Harvey, B. McNeil, Z. Bai, The development and application of high throughput cultivation technology in bioprocess development, *J. Biotechnol.* 192 (2014) 323–338.
- [191] O. Wichterle, D. Lim, Hydrophilic Gels for Biological Use, *Nature.* 185 (1960) 117. <http://dx.doi.org/10.1038/185117a0>.
- [192] P. Agarwal, I.D. Rupenthal, Injectable implants for the sustained release of protein and peptide drugs, *Drug Discov. Today.* 18 (2013) 337–349.
- [193] E.M. Ahmed, Hydrogel: Preparation, characterization, and applications: A review, *J. Adv. Res.* 6 (2015) 105–121. doi:10.1016/J.JARE.2013.07.006.
- [194] J. Panula-Perälä, J. Šiurkus, A. Vasala, R. Wilmanowski, M.G. Casteleijn, P. Neubauer, Enzyme controlled glucose auto-delivery for high cell density cultivations in microplates and shake flasks, *Microb. Cell Fact.* 7 (2008) 31.
- [195] M. Jeude, B. Dittrich, H. Niederschulte, T. Anderlei, C. Knocke, D. Klee, J. Büchs, Fed-batch mode in shake flasks by slow-release technique, *Biotechnol. Bioeng.* 95 (2006) 433–445.
- [196] R. Sanil, V. Maralingannavar, M. Gadgil, In situ pH management for microbial culture in shake flasks and its application to increase plasmid yield, *J. Ind. Microbiol. Biotechnol.* 41 (2014) 647.
- [197] M. Scheidle, M. Jeude, B. Dittrich, S. Denter, F. Kensy, M. Suckow, D. Klee, J. Büchs, High-throughput screening of *Hansenula polymorpha* clones in the batch compared with the controlled-release fed-batch mode on a small scale, *FEMS Yeast Res.* 10 83–92. doi:10.1111/J.1567-1364.2009.00586.X.
- [198] M. Scheidle, B. Dittrich, J. Klinger, H. Ikeda, D. Klee, J. Büchs, Controlling pH in shake flasks using polymer-based controlled-release discs with pre-determined release kinetics, *BMC Biotechnol.* 2011 111. 11 (2011) 1–11. doi:10.1186/1472-6750-11-25.
- [199] A. Wilming, C. Bähr, C. Kamerke, J. Büchs, Fed-batch operation in special microtiter plates: a new method for screening under production conditions, *J. Ind. Microbiol. Biotechnol.* 41 (2014) 513–525. doi:10.1007/s10295-013-1396-x.

- [200] C. Blesken, T. Olfers, A. Grimm, N. Frische, The microfluidic bioreactor for a new era of bioprocess development, *Eng. Life Sci.* 16 (2016) 190–193.
- [201] A. Buchenauer, M.C. Hofmann, M. Funke, J. Büchs, W. Mokwa, U. Schnakenberg, Micro-bioreactors for fed-batch fermentations with integrated online monitoring and microfluidic devices, *Biosens. Bioelectron.* 24 (2009) 1411–1416. doi:<https://doi.org/10.1016/j.bios.2008.08.043>.
- [202] K. Pradhan, T. Pant, M. Gadgil, In situ pH maintenance for mammalian cell cultures in shake flasks and tissue culture flasks, *Biotechnol. Prog.* 28 (2012) 1605–1610.
- [203] W.A. Duetz, Microtiter plates as mini-bioreactors: miniaturization of fermentation methods, *Trends Microbiol.* 15 (2007) 469–475. doi:[10.1016/J.TIM.2007.09.004](https://doi.org/10.1016/J.TIM.2007.09.004).
- [204] K. Chaturvedi, S.Y. Sun, T. O'Brien, Y.J. Liu, J.W. Brooks, Comparison of the behavior of CHO cells during cultivation in 24-square deep well microplates and conventional shake flask systems, *Biotechnol. Reports.* 1–2 (2014) 22–26. doi:[10.1016/j.btre.2014.04.001](https://doi.org/10.1016/j.btre.2014.04.001).
- [205] W.A. Duetz, M. Chase, G. Bills, Miniaturization of fermentations, *Man. Ind. Microbiol. Biotechnol.* (2010) 99–116.
- [206] F. Kensy, G.T. John, B. Hofmann, J. Büchs, Characterisation of operation conditions and online monitoring of physiological culture parameters in shaken 24-well microtiter plates, *Bioprocess Biosyst. Eng.* 28 (2005) 75–81. doi:[10.1007/s00449-005-0010-7](https://doi.org/10.1007/s00449-005-0010-7).
- [207] A.S. Kocincova, S.M. Borisov, C. Krause, O.S. Wolfbeis, Fiber-Optic Microsensors for Simultaneous Sensing of Oxygen and pH, and of Oxygen and Temperature, *Anal. Chem.* 79 (2007) 8486–8493. doi:[10.1021/ac070514h](https://doi.org/10.1021/ac070514h).
- [208] M. Funke, A. Buchenauer, U. Schnakenberg, W. Mokwa, S. Diederichs, A. Mertens, C. Müller, F. Kensy, J. Büchs, Microfluidic biolector—microfluidic bioprocess control in microtiter plates, *Biotechnol. Bioeng.* 107 (2010) 497–505. doi:<https://doi.org/10.1002/bit.22825>.
- [209] A. Chen, R. Chitta, D. Chang, A. Amanullah, Twenty-four well plate miniature bioreactor system as a scale-down model for cell culture process development, *Biotechnol. Bioeng.* 102 (2009) 148–160. doi:<https://doi.org/10.1002/bit.22031>.
- [210] R. Bareither, D. Pollard, A review of advanced small-scale parallel bioreactor technology for accelerated process development: Current state and future need, *Biotechnol. Prog.* (2011). doi:[10.1002/btpr.522](https://doi.org/10.1002/btpr.522).
- [211] W.-T. Hsu, R.P.S. Aulakh, D.L. Traul, I.H. Yuk, Advanced microscale bioreactor system: a representative scale-down model for bench-top bioreactors, *Cytotechnology.* 64 (2012) 667–678. doi:[10.1007/s10616-012-9446-1](https://doi.org/10.1007/s10616-012-9446-1).

- [212] K.E. Royle, I. Jimenez del Val, C. Kontoravdi, Integration of models and experimentation to optimise the production of potential biotherapeutics, *Drug Discov. Today*. 18 (2013) 1250–1255. doi:<https://doi.org/10.1016/j.drudis.2013.07.002>.
- [213] J. Siepmann, F. Siepmann, Mathematical modeling of drug delivery, *Int. J. Pharm.* (2008). doi:[10.1016/j.ijpharm.2008.09.004](https://doi.org/10.1016/j.ijpharm.2008.09.004).
- [214] N.A. Bowden, Modelling the solubility of the 20 proteinogenic amino acids with experimentally derived saturation data, Wageningen University, 2018. <http://edepot.wur.nl/446739>.
- [215] Y. Nishiuch, M. Sasaki, M. Nakayasu, A. Oikawa, Cytotoxicity of cysteine in culture media, *In Vitro*. 12 (1976) 635–638. doi:[10.1007/BF02797462](https://doi.org/10.1007/BF02797462).
- [216] P. Ducommun, P.A. Ruffieux, U. Von Stockar, I. Marison, The role of vitamins and amino acids on hybridoma growth and monoclonal antibody production, *Cytotechnology*. 37 (2001) 65–73. doi:[10.1023/A:1019956013627](https://doi.org/10.1023/A:1019956013627).
- [217] D.Y. Kim, J.C. Lee, H.N. Chang, D.J. Oh, Effects of supplementation of various medium components on Chinese hamster ovary cell cultures producing recombinant antibody, in: *Cytotechnology*, 2005: pp. 37–49. doi:[10.1007/s10616-005-3775-2](https://doi.org/10.1007/s10616-005-3775-2).
- [218] A. Zimmer, R. Mueller, M. Wehsling, A. Schnellbaecher, J. von Hagen, Improvement and simplification of fed-batch bioprocesses with a highly soluble phosphotyrosine sodium salt, *J. Biotechnol.* (2014). doi:[10.1016/j.jbiotec.2014.06.026](https://doi.org/10.1016/j.jbiotec.2014.06.026).
- [219] C. Hecklau, S. Pering, R. Seibel, A. Schnellbaecher, M. Wehsling, T. Eichhorn, J. von Hagen, A. Zimmer, S-Sulfocysteine simplifies fed-batch processes and increases the CHO specific productivity via anti-oxidant activity, *J. Biotechnol.* (2016). doi:[10.1016/j.jbiotec.2015.11.022](https://doi.org/10.1016/j.jbiotec.2015.11.022).
- [220] K.F. Wlaschin, W.-S. Hu, Fedbatch Culture and Dynamic Nutrient Feeding, in: W.-S. Hu (Ed.), *Adv. Biochem. Eng. Biotechnol.*, Springer Berlin Heidelberg, Berlin, Heidelberg, 2006: pp. 43–74. doi:[10.1007/10_015](https://doi.org/10.1007/10_015).
- [221] W. Zhou, J. Rehm, A. Europa, W.S. Hu, Alteration of mammalian cell metabolism by dynamic nutrient feeding, *Cytotechnology*. 24 (1997) 99–108. doi:[10.1023/A:1007945826228](https://doi.org/10.1023/A:1007945826228).
- [222] H.J. Cruz, C.M. Freitas, P.M. Alves, J.L. Moreira, M.J.T. Carrondo, Effects of ammonia and lactate on growth, metabolism, and productivity of BHK cells, *Enzyme Microb. Technol.* 27 (2000) 43–52.
- [223] C. Altamirano, C. Paredes, A. Illanes, J. Cairó, F. Gòdia, Strategies for fed-batch cultivation of t-PA producing CHO cells: substitution of glucose and glutamine and rational design of culture medium, *J. Biotechnol.* 110 (2004) 171–179. doi:[10.1016/j.jbiotec.2004.02.004](https://doi.org/10.1016/j.jbiotec.2004.02.004).
- [224] D. Chee Fung Wong, K. Tin Kam Wong, L. Tang Goh, C. Kiat Heng, M. Gek

- Sim Yap, Impact of dynamic online fed-batch strategies on metabolism, productivity and N-glycosylation quality in CHO cell cultures, *Biotechnol. Bioeng.* 89 (2005) 164–177. doi:10.1002/bit.20317.
- [225] S.L. Barrett, R. Boniface, P. Dhulipala, P. Slade, Y. Tennico, M. Stramaglia, P. Lio, S.F. Gorfien, Attaining next-level titers in CHO fed-batch cultures, *Bioprocess Int.* (2012).
- [226] D.C. Kirouac, P.W. Zandstra, The Systematic Production of Cells for Cell Therapies, *Cell Stem Cell.* 3 (2008) 369–381. doi:10.1016/j.stem.2008.09.001.
- [227] C.-A. Tran, L. Burton, D. Russom, J.R. Wagner, M.C. Jensen, S.J. Forman, D.L. DiGiusto, Manufacturing of Large Numbers of Patient-specific T Cells for Adoptive Immunotherapy, *J. Immunother.* 30 (2007) 644–654. doi:10.1097/CJI.0b013e318052e1f4.
- [228] E. Csaszar, D.C. Kirouac, M. Yu, W. Wang, W. Qiao, M.P. Cooke, A.E. Boitano, C. Ito, P.W. Zandstra, Rapid expansion of human hematopoietic stem cells by automated control of inhibitory feedback signaling, *Cell Stem Cell.* (2012). doi:10.1016/j.stem.2012.01.003.
- [229] W. Zhou, J. Rehm, W. -S Hu, High viable cell concentration fed-batch cultures of hybridoma cells through on-line nutrient feeding, *Biotechnol. Bioeng.* 46 (1995) 579–587. doi:10.1002/bit.260460611.
- [230] A. Amanullah, J.M. Otero, M. Mikola, A. Hsu, J. Zhang, J. Aunins, H.B. Schreyer, J.A. Hope, A.P. Russo, Novel micro-bioreactor high throughput technology for cell culture process development: Reproducibility and scalability assessment of fed-batch CHO cultures, *Biotechnol. Bioeng.* 106 (2010) 57–67. doi:10.1002/bit.2266.
- [231] S. Hegde, T. Pant, K. Pradhan, M. Badiger, M. Gadgil, Controlled release of nutrients to mammalian cells cultured in shake flasks, *Biotechnol. Prog.* 28 (2012) 188–195. doi:10.1002/btpr.729.
- [232] A.M. Hosios, V.C. Hecht, L. V. Danai, M.O. Johnson, J.C. Rathmell, M.L. Steinhauser, S.R. Manalis, M.G. Vander Heiden, Amino Acids Rather than Glucose Account for the Majority of Cell Mass in Proliferating Mammalian Cells, *Dev. Cell.* (2016). doi:10.1016/j.devcel.2016.02.012.
- [233] S. Kishishita, S. Katayama, K. Kodaira, Y. Takagi, H. Matsuda, H. Okamoto, S. Takuma, C. Hirashima, H. Aoyagi, Optimization of chemically defined feed media for monoclonal antibody production in Chinese hamster ovary cells, *J. Biosci. Bioeng.* 120 (2015) 78–84. doi:10.1016/j.jbiosc.2014.11.022.
- [234] L.M. Carrillo-Cocom, T. Genel-Rey, D. Araújo-Hernández, F. López-Pacheco, J. López-Meza, M.R. Rocha-Pizaña, A. Ramírez-Medrano, M.M. Alvarez, Amino acid consumption in naïve and recombinant CHO cell cultures: producers of a monoclonal antibody, *Cytotechnology.* 67 (2015) 809–820. doi:10.1007/s10616-014-9720-5.
- [235] Z. Xing, B. Kenty, I. Koyrakh, M. Borys, S.H. Pan, Z.J. Li, Optimizing amino

- acid composition of CHO cell culture media for a fusion protein production, *Process Biochem.* 46 (2011) 1423–1429. doi:10.1016/j.procbio.2011.03.014.
- [236] D. Wen, M.M. Vecchi, S. Gu, L. Su, J. Dolnikova, Y.M. Huang, S.F. Foley, E. Garber, N. Pederson, W. Meier, Discovery and investigation of misincorporation of serine at asparagine positions in recombinant proteins expressed in Chinese hamster ovary cells, *J. Biol. Chem.* 284 (2009) 32686–32694. doi:10.1074/jbc.M109.059360.
- [237] Z. Zhang, B. Shah, P. V Bondarenko, G/U and Certain Wobble Position Mismatches as Possible Main Causes of Amino Acid Misincorporations, *Biochemistry.* 52 (2013) 8165–8176. doi:10.1021/bi401002c.
- [238] A. Khetan, Y. Huang, J. Dolnikova, N.E. Pederson, D. Wen, H. Yusuf-Makagiansar, P. Chen, T. Ryll, Control of misincorporation of serine for asparagine during antibody production using CHO cells, *Biotechnol. Bioeng.* 107 (2010) 116–123.
- [239] L.B. Sullivan, D.Y. Gui, A.M. Hosios, L.N. Bush, E. Freinkman, M.G. Vander Heiden, Supporting Aspartate Biosynthesis Is an Essential Function of Respiration in Proliferating Cells, *Cell.* 162 (2015) 552–563. doi:10.1016/j.cell.2015.07.017.
- [240] N. Psychogios, D.D. Hau, J. Peng, A.C. Guo, R. Mandal, S. Bouatra, I. Sinelnikov, R. Krishnamurthy, R. Eisner, B. Gautam, N. Young, J. Xia, C. Knox, E. Dong, P. Huang, Z. Hollander, T.L. Pedersen, S.R. Smith, F. Bamforth, R. Greiner, B. McManus, J.W. Newman, T. Goodfriend, D.S. Wishart, The human serum metabolome, *PLoS One.* (2011). doi:10.1371/journal.pone.0016957.
- [241] B. Kuang, V.G. Dhara, D. Hoang, J. Jenkins, P. Ladiwala, Y. Tan, S.A. Shaffer, S.C. Galbraith, M.J. Betenbaugh, S. Yoon, Identification of novel inhibitory metabolites and impact verification on growth and protein synthesis in mammalian cells, *Metab. Eng. Commun.* 13 (2021) e00182. doi:https://doi.org/10.1016/j.mec.2021.e00182.
- [242] A. Muir, M.G. Vander Heiden, The nutrient environment affects therapy, *Science* (80-.). 360 (2018) 962 LP – 963. doi:10.1126/science.aar5986.
- [243] S. Shin, G.R. Buel, L. Wolgamott, D.R. Plas, J.M. Asara, J. Blenis, S.-O. Yoon, ERK2 mediates metabolic stress response to regulate cell fate, *Mol. Cell.* 59 (2015) 382–398.
- [244] X. Tang, J. Wu, C.-K. Ding, M. Lu, M.M. Keenan, C.-C. Lin, C.-A. Lin, C.C. Wang, D. George, D.S. Hsu, Cystine deprivation triggers programmed necrosis in VHL-deficient renal cell carcinomas, *Cancer Res.* 76 (2016) 1892–1903.
- [245] C.A. Changou, Y.-R. Chen, L. Xing, Y. Yen, F.Y.S. Chuang, R.H. Cheng, R.J. Bold, D.K. Ann, H.-J. Kung, Arginine starvation-associated atypical cellular death involves mitochondrial dysfunction, nuclear DNA leakage, and chromatin autophagy, *Proc. Natl. Acad. Sci.* 111 (2014) 14147–14152.

- [246] S.J. Dixon, K.M. Lemberg, M.R. Lamprecht, R. Skouta, E.M. Zaitsev, C.E. Gleason, D.N. Patel, A.J. Bauer, A.M. Cantley, W.S. Yang, Ferroptosis: an iron-dependent form of nonapoptotic cell death, *Cell*. 149 (2012) 1060–1072.
- [247] K. Pakos-Zebrucka, I. Koryga, K. Mnich, M. Ljujic, A. Samali, A.M. Gorman, The integrated stress response, *EMBO Rep.* 17 (2016) 1374–1395.
- [248] S. Andrews, FastQC: a quality control tool for high throughput sequence data. Available online, Retrieved May. 17 (2010) 2018.
- [249] A.M. Bolger, M. Lohse, B. Usadel, Trimmomatic: a flexible trimmer for Illumina sequence data, *Bioinformatics*. 30 (2014) 2114–2120. doi:10.1093/bioinformatics/btu170.
- [250] C. Trapnell, A. Roberts, L. Goff, G. Pertea, D. Kim, D.R. Kelley, H. Pimentel, S.L. Salzberg, J.L. Rinn, L. Pachter, Differential gene and transcript expression analysis of RNA-seq experiments with TopHat and Cufflinks, *Nat. Protoc.* 7 (2012) 562–578.
- [251] S.H. Zainal Ariffin, N.A. Mohamed Rozali, R. Megat Abdul Wahab, S. Senafi, I.Z. Zainol Abidin, Z. Zainal Ariffin, Analyses of basal media and serum for in vitro expansion of suspension peripheral blood mononucleated stem cell, *Cytotechnology*. 68 (2016) 675–686. doi:10.1007/s10616-014-9819-8.
- [252] L. Arodin Selenius, M. Wallenberg Lundgren, R. Jawad, O. Danielsson, M. Björnstedt, The Cell Culture Medium Affects Growth, Phenotype Expression and the Response to Selenium Cytotoxicity in A549 and HepG2 Cells, *Antioxidants* . 8 (2019). doi:10.3390/antiox8050130.
- [253] D.W. Huang, B.T. Sherman, R.A. Lempicki, Systematic and integrative analysis of large gene lists using DAVID bioinformatics resources, *Nat. Protoc.* 4 (2009) 44–57. doi:10.1038/nprot.2008.211.
- [254] D.W. Huang, B.T. Sherman, R.A. Lempicki, Bioinformatics enrichment tools: paths toward the comprehensive functional analysis of large gene lists, *Nucleic Acids Res.* 37 (2009) 1–13. doi:10.1093/nar/gkn923.
- [255] M.S. Kilberg, Y.-X. Pan, H. Chen, V. Leung-Pineda, Nutritional control of gene expression: how mammalian cells respond to amino acid limitation, *Annu. Rev. Nutr.* 25 (2005) 59–85.
- [256] P. Zhang, B.C. McGrath, J. Reinert, D.S. Olsen, L. Lei, S. Gill, S.A. Wek, K.M. Vattam, R.C. Wek, S.R. Kimball, The GCN2 eIF2 α kinase is required for adaptation to amino acid deprivation in mice, *Mol. Cell. Biol.* 22 (2002) 6681–6688.
- [257] J.J. Berlanga, J. Santoyo, C. de Haro, Characterization of a mammalian homolog of the GCN2 eukaryotic initiation factor 2 α kinase, *Eur. J. Biochem.* 265 (1999) 754–762.
- [258] R. Sood, A.C. Porter, D. Olsen, D.R. Cavener, R.C. Wek, A mammalian homologue of GCN2 protein kinase important for translational control by

- phosphorylation of eukaryotic initiation factor-2 α , *Genetics*. 154 (2000) 787–801.
- [259] I.L. Andrulis, G.W. Hatfield, S.M. Arfin, Asparaginyl-tRNA aminoacylation levels and asparagine synthetase expression in cultured Chinese hamster ovary cells., *J. Biol. Chem.* 254 (1979) 10629–10633.
- [260] J.M. Zaborske, J. Narasimhan, L. Jiang, S.A. Wek, K.A. Dittmar, F. Freimoser, T. Pan, R.C. Wek, Genome-wide Analysis of tRNA Charging and Activation of the eIF2 Kinase Gcn2p* \diamond , *J. Biol. Chem.* 284 (2009) 25254–25267.
- [261] M. Raina, M. Ibba, tRNAs as regulators of biological processes , *Front. Genet.* . 5 (2014).
<https://www.frontiersin.org/article/10.3389/fgene.2014.00171>.
- [262] Z. Zhang, Y. Ye, J. Gong, H. Ruan, C.-J. Liu, Y. Xiang, C. Cai, A.-Y. Guo, J. Ling, L. Diao, J.N. Weinstein, L. Han, Global analysis of tRNA and translation factor expression reveals a dynamic landscape of translational regulation in human cancers, *Commun. Biol.* 1 (2018) 234. doi:10.1038/s42003-018-0239-8.
- [263] J.M. Han, S.J. Jeong, M.C. Park, G. Kim, N.H. Kwon, H.K. Kim, S.H. Ha, S.H. Ryu, S. Kim, Leucyl-tRNA synthetase is an intracellular leucine sensor for the mTORC1-signaling pathway, *Cell*. 149 (2012) 410–424.
- [264] Y.C. Yu, J.M. Han, S. Kim, Aminoacyl-tRNA synthetases and amino acid signaling, *Biochim. Biophys. Acta - Mol. Cell Res.* 1868 (2021) 118889. doi:<https://doi.org/10.1016/j.bbamcr.2020.118889>.
- [265] S. Kimura, K. Miyauchi, Y. Ikeuchi, P.C. Thiaville, V. de Crécy-Lagard, T. Suzuki, Discovery of the β -barrel-type RNA methyltransferase responsible for N6-methylation of N6-threonylcarbamoyladenine in tRNAs, *Nucleic Acids Res.* 42 (2014) 9350–9365. doi:10.1093/nar/gku618.
- [266] S.R. Kimball, Regulation of global and specific mRNA translation by amino acids, *J. Nutr.* 132 (2002) 883–886.
- [267] A.G. Hinnebusch, Translational regulation of yeast GCN4: a window on factors that control initiator-tRNA binding to the ribosome, *J. Biol. Chem.* 272 (1997) 21661–21664.
- [268] H.P. Harding, I. Novoa, Y. Zhang, H. Zeng, R. Wek, M. Schapira, D. Ron, Regulated translation initiation controls stress-induced gene expression in mammalian cells, *Mol. Cell.* 6 (2000) 1099–1108.
- [269] K. Natarajan, M.R. Meyer, B.M. Jackson, D. Slade, C. Roberts, A.G. Hinnebusch, M.J. Marton, Transcriptional profiling shows that Gcn4p is a master regulator of gene expression during amino acid starvation in yeast, *Mol. Cell. Biol.* 21 (2001) 4347–4368.
- [270] D. Scheuner, B. Song, E. McEwen, C. Liu, R. Laybutt, P. Gillespie, T. Saunders, S. Bonner-Weir, R.J. Kaufman, Translational control is required for the unfolded protein response and in vivo glucose homeostasis, *Mol. Cell.* 7

- (2001) 1165–1176.
- [271] P.D. Lu, H.P. Harding, D. Ron, Translation reinitiation at alternative open reading frames regulates gene expression in an integrated stress response, *J. Cell Biol.* 167 (2004) 27–33.
- [272] K.M. Vattem, R.C. Wek, Reinitiation involving upstream ORFs regulates ATF4 mRNA translation in mammalian cells, *Proc. Natl. Acad. Sci.* 101 (2004) 11269–11274.
- [273] S. Bröer, M. Palacín, The role of amino acid transporters in inherited and acquired diseases, *Biochem. J.* 436 (2011) 193–211. doi:10.1042/BJ20101912.
- [274] E. Perland, R. Fredriksson, Classification systems of secondary active transporters, *Trends Pharmacol. Sci.* 38 (2017) 305–315.
- [275] S. Bröer, A. Bröer, Amino acid homeostasis and signalling in mammalian cells and organisms, *Biochem. J.* 474 (2017) 1935–1963. doi:10.1042/BCJ20160822.
- [276] E.I. Closs, A. Simon, N. Vékony, A. Rotmann, Plasma Membrane Transporters for Arginine, *J. Nutr.* 134 (2004) 2752S–2759S. doi:10.1093/jn/134.10.2752S.
- [277] M.P. Kavanaugh, Voltage dependence of facilitated arginine flux mediated by the system y⁺ basic amino acid transporter, *Biochemistry.* 32 (1993) 5781–5785.
- [278] J. Fernandez, I. Yaman, R. Mishra, W.C. Merrick, M.D. Snider, W.H. Lamers, M. Hatzoglou, Internal ribosome entry site-mediated translation of a mammalian mRNA is regulated by amino acid availability, *J. Biol. Chem.* 276 (2001) 12285–12291.
- [279] F. Verrey, E.I. Closs, C.A. Wagner, M. Palacin, H. Endou, Y. Kanai, CATs and HATs: the SLC7 family of amino acid transporters, *Pflügers Arch.* 447 (2004) 532–542.
- [280] M. Jeude, B. Dittrich, H. Niederschulte, T. Anderlei, C. Knocke, D. Klee, J. Büchs, Fed-batch mode in shake flasks by slow-release technique, *Biotechnol. Bioeng.* 95 (2006) 433–445. doi:10.1002/BIT.21012.
- [281] S. V Hellsten, E. Lekholm, T. Ahmad, R. Fredriksson, The gene expression of numerous SLC transporters is altered in the immortalized hypothalamic cell line N25/2 following amino acid starvation, *FEBS Open Bio.* 7 (2017) 249–264.
- [282] L. Bar-Peled, D.M. Sabatini, Regulation of mTORC1 by amino acids, *Trends Cell Biol.* 24 (2014) 400–406.
- [283] J. Avruch, X. Long, S. Ortiz-Vega, J. Rapley, A. Papageorgiou, Dai N, Amin. Acid Regul. TOR Complex. 1 (n.d.).
- [284] D.C.I. Goberdhan, C. Wilson, A.L. Harris, Amino acid sensing by mTORC1:

- intracellular transporters mark the spot, *Cell Metab.* 23 (2016) 580–589.
- [285] L. Zheng, W. Zhang, Y. Zhou, F. Li, H. Wei, J. Peng, Recent advances in understanding amino acid sensing mechanisms that regulate mTORC1, *Int. J. Mol. Sci.* 17 (2016) 1636.
- [286] J.L. Jewell, R.C. Russell, K.-L. Guan, Amino acid signalling upstream of mTOR, *Nat. Rev. Mol. Cell Biol.* 14 (2013) 133–139.
- [287] E.A. Dunlop, A.R. Tee, mTOR and autophagy: A dynamic relationship governed by nutrients and energy, *Semin. Cell Dev. Biol.* 36 (2014) 121–129. doi:<https://doi.org/10.1016/j.semcdb.2014.08.006>.
- [288] N. Hosokawa, T. Hara, T. Kaizuka, C. Kishi, A. Takamura, Y. Miura, S. Iemura, T. Natsume, K. Takehana, N. Yamada, J.-L. Guan, N. Oshiro, N. Mizushima, Nutrient-dependent mTORC1 Association with the ULK1–Atg13–FIP200 Complex Required for Autophagy, *Mol. Biol. Cell.* 20 (2009) 1981–1991. doi:[10.1091/mbc.e08-12-1248](https://doi.org/10.1091/mbc.e08-12-1248).
- [289] S. Sengupta, T.R. Peterson, D.M. Sabatini, Regulation of the mTOR complex 1 pathway by nutrients, growth factors, and stress, *Mol. Cell.* 40 (2010) 310–322.
- [290] N. Kimura, C. Tokunaga, S. Dalal, C. Richardson, K. Yoshino, K. Hara, B.E. Kemp, L.A. Witters, O. Mimura, K. Yonezawa, A possible linkage between AMP-activated protein kinase (AMPK) and mammalian target of rapamycin (mTOR) signalling pathway, *Genes to Cells.* 8 (2003) 65–79. doi:<https://doi.org/10.1046/j.1365-2443.2003.00615.x>.
- [291] Y. Sancak, L. Bar-Peled, R. Zoncu, A.L. Markhard, S. Nada, D.M. Sabatini, Ragulator-Rag complex targets mTORC1 to the lysosomal surface and is necessary for its activation by amino acids, *Cell.* 141 (2010) 290–303.
- [292] M. Rebsamen, L. Pochini, T. Stasyk, M.E.G. de Araújo, M. Galluccio, R.K. Kandasamy, B. Snijder, A. Fauster, E.L. Rudashevskaya, M. Bruckner, SLC38A9 is a component of the lysosomal amino acid sensing machinery that controls mTORC1, *Nature.* 519 (2015) 477–481.
- [293] W. Shuyu, T. Zhi-Yang, W.R. L., S. Kuang, W.G. A., P.M. E., Y.E. D., J.T. D., C. Lynne, C. William, W. Tim, B.-P. Liron, Z. Roberto, S. Christoph, K. Choah, P. Jiwon, S.B. L., S.D. M., Lysosomal amino acid transporter SLC38A9 signals arginine sufficiency to mTORC1, *Science (80-.).* 347 (2015) 188–194. doi:[10.1126/science.1257132](https://doi.org/10.1126/science.1257132).
- [294] J. Jennifer, G.H. Marika, B. Christian, Amino Acid-Dependent mTORC1 Regulation by the Lysosomal Membrane Protein SLC38A9, *Mol. Cell. Biol.* 35 (2015) 2479–2494. doi:[10.1128/MCB.00125-15](https://doi.org/10.1128/MCB.00125-15).
- [295] Z. Roberto, B.-P. Liron, E. Alejo, W. Shuyu, S. Yasemin, S.D. M., mTORC1 Senses Lysosomal Amino Acids Through an Inside-Out Mechanism That Requires the Vacuolar H⁺-ATPase, *Science (80-.).* 334 (2011) 678–683. doi:[10.1126/science.1207056](https://doi.org/10.1126/science.1207056).

- [296] W.R. L., C. Lynne, S.R. A., S. Kuang, S.S. M., C.J. R., S.D. M., Sestrin2 is a leucine sensor for the mTORC1 pathway, *Science* (80-.). 351 (2016) 43–48. doi:10.1126/science.aab2674.
- [297] L.J. Hee, C. Uhn-Soo, K. Michael, Sestrin regulation of TORC1: Is Sestrin a leucine sensor?, *Sci. Signal.* 9 (2016) re5–re5. doi:10.1126/scisignal.aaf2885.
- [298] S. Heublein, S. Kazi, M.H. Ögmundsdóttir, E. V Attwood, S. Kala, C.A.R. Boyd, C. Wilson, D.C.I. Goberdhan, Proton-assisted amino-acid transporters are conserved regulators of proliferation and amino-acid-dependent mTORC1 activation, *Oncogene.* 29 (2010) 4068–4079. doi:10.1038/onc.2010.177.
- [299] J.R. Warner, The economics of ribosome biosynthesis in yeast, *Trends Biochem. Sci.* 24 (1999) 437–440.
- [300] A. Colaço, M. Jäättelä, Ragulator—a multifaceted regulator of lysosomal signaling and trafficking, *J. Cell Biol.* 216 (2017) 3895–3898.
- [301] F. Sparber, J.M. Scheffler, N. Amberg, C.H. Tripp, V. Heib, M. Hermann, S.P. Zahner, B.E. Clausen, B. Reizis, L.A. Huber, P. Stoitzner, N. Romani, The late endosomal adaptor molecule p14 (LAMTOR2) represents a novel regulator of Langerhans cell homeostasis, *Blood.* 123 (2014) 217–227. doi:10.1182/blood-2013-08-518555.
- [302] A.J. Obaya, J.M. Sedivy, Regulation of cyclin-Cdk activity in mammalian cells, *Cell. Mol. Life Sci. C.* 59 (2002) 126–142.
- [303] M. Arellano, S. Moreno, Regulation of CDK/cyclin complexes during the cell cycle, *Int. J. Biochem. Cell Biol.* 29 (1997) 559–573.
- [304] J. Kato, M. Matsuoka, K. Polyak, J. Massague, C.J. Sherr, Cyclic AMP-induced G1 phase arrest mediated by an inhibitor (p27Kip1) of cyclin-dependent kinase 4 activation, *Cell.* 79 (1994) 487–496.
- [305] W. Jiang, Y.-J. Zhang, S.M. Kahn, M.C. Hollstein, R.M. Santella, S.-H. Lu, C.C. Harris, R. Montesano, I.B. Weinstein, Altered expression of the cyclin D1 and retinoblastoma genes in human esophageal cancer, *Proc. Natl. Acad. Sci.* 90 (1993) 9026–9030.
- [306] T. Hunter, J. Pines, Cyclins and cancer II: cyclin D and CDK inhibitors come of age, *Cell.* 79 (1994) 573–582.
- [307] K. Okamoto, D. Beach, Cyclin G is a transcriptional target of the p53 tumor suppressor protein., *EMBO J.* 13 (1994) 4816–4822.
- [308] M. Schmidt, S. Fernandez de Mattos, A. van der Horst, R. Klompaker, G.J.P.L. Kops, E.W.-F. Lam, B.M.T. Burgering, R.H. Medema, Cell cycle inhibition by FoxO forkhead transcription factors involves downregulation of cyclin D, *Mol. Cell. Biol.* 22 (2002) 7842–7852.
- [309] X.M. Ma, J. Blenis, Molecular mechanisms of mTOR-mediated translational control, *Nat. Rev. Mol. Cell Biol.* 10 (2009) 307–318.

- [310] W. B'chir, A.-C. Maurin, V. Carraro, J. Averous, C. Jousse, Y. Muranishi, L. Parry, G. Stepien, P. Fafournoux, A. Bruhat, The eIF2 α /ATF4 pathway is essential for stress-induced autophagy gene expression, *Nucleic Acids Res.* 41 (2013) 7683–7699. doi:10.1093/nar/gkt563.
- [311] T. Rzymiski, M. Milani, L. Pike, F. Buffa, H.R. Mellor, L. Winchester, I. Pires, E. Hammond, I. Ragoussis, A.L. Harris, Regulation of autophagy by ATF4 in response to severe hypoxia, *Oncogene.* 29 (2010) 4424–4435.
- [312] W. Dröge, Autophagy and aging—importance of amino acid levels, *Mech. Ageing Dev.* 125 (2004) 161–168. doi:https://doi.org/10.1016/j.mad.2003.12.003.
- [313] Y. Kouroku, E. Fujita, I. Tanida, T. Ueno, A. Isoai, H. Kumagai, S. Ogawa, R.J. Kaufman, E. Kominami, T. Momoi, ER stress (PERK/eIF2 α phosphorylation) mediates the polyglutamine-induced LC3 conversion, an essential step for autophagy formation, *Cell Death Differ.* 14 (2007) 230–239.
- [314] T. Nguyen, H.C. Huang, C.B. Pickett, Transcriptional regulation of the antioxidant response element: activation by Nrf2 and repression by MafK, *J. Biol. Chem.* 275 (2000) 15466–15473.
- [315] M.B. Kannan, V. Solovieva, V. Blank, The small MAF transcription factors MAFF, MAFK and MAFK: current knowledge and perspectives, *Biochim. Biophys. Acta (BBA)-Molecular Cell Res.* 1823 (2012) 1841–1846.
- [316] H. Walden, K. Rittinger, RBR ligase-mediated ubiquitin transfer: a tale with many twists and turns, *Nat. Struct. Mol. Biol.* 25 (2018) 440–445.
- [317] J. Wang, Z. Wei, Y. Gao, C. Liu, J. Sun, Activation of the mammalian target of rapamycin signaling pathway underlies a novel inhibitory role of ring finger protein 182 in ventricular remodeling after myocardial ischemia-reperfusion injury, *J. Cell. Biochem.* 120 (2019) 7635–7648.
- [318] Z. Lin, S. Li, C. Feng, S. Yang, H. Wang, D. Ma, J. Zhang, M. Gou, D. Bu, T. Zhang, Stabilizing mutations of KLHL24 ubiquitin ligase cause loss of keratin 14 and human skin fragility, *Nat. Genet.* 48 (2016) 1508–1516.
- [319] H. Schweikl, K.-A. Hiller, A. Eckhardt, C. Bolay, G. Spagnuolo, T. Stempf, G. Schmalz, Differential gene expression involved in oxidative stress response caused by triethylene glycol dimethacrylate, *Biomaterials.* 29 (2008) 1377–1387.
- [320] F. Laezza, T.J. Wilding, S. Sequeira, A.M. Craig, J.E. Huettner, The BTB/kelch protein, KRIP6, modulates the interaction of PICK1 with GluR6 kainate receptors, *Neuropharmacology.* 55 (2008) 1131–1139.
- [321] R.J. M., M.D. J., P.M. F., T.L. Jia, P.J. A., A Gene Signature-Based Approach Identifies mTOR as a Regulator of p73, *Mol. Cell. Biol.* 28 (2008) 5951–5964. doi:10.1128/MCB.00305-08.
- [322] R. NAGAI, T. SUZUKI, K. AIZAWA, T. SHINDO, I. MANABE,

- Significance of the transcription factor KLF5 in cardiovascular remodeling, *J. Thromb. Haemost.* 3 (2005) 1569–1576. doi:<https://doi.org/10.1111/j.1538-7836.2005.01366.x>.
- [323] Y. Munemasa, T. Suzuki, K. Aizawa, S. Miyamoto, Y. Imai, T. Matsumura, M. Horikoshi, R. Nagai, Promoter region-specific histone incorporation by the novel histone chaperone ANP32B and DNA-binding factor KLF5, *Mol. Cell Biol.* 28 (2008) 1171–1181. doi:10.1128/MCB.01396-07.
- [324] K. Fujiu, I. Manabe, A. Ishihara, Y. Oishi, H. Iwata, G. Nishimura, T. Shindo, K. Maemura, H. Kagechika, K. Shudo, Synthetic retinoid Am80 suppresses smooth muscle phenotypic modulation and in-stent neointima formation by inhibiting KLF5, *Circ. Res.* 97 (2005) 1132–1141.
- [325] C. Chen, X. Sun, Q. Ran, K.D. Wilkinson, T.J. Murphy, J.W. Simons, J.-T. Dong, Ubiquitin–proteasome degradation of KLF5 transcription factor in cancer and untransformed epithelial cells, *Oncogene.* 24 (2005) 3319–3327.
- [326] Y. Oishi, I. Manabe, K. Tobe, K. Tsushima, T. Shindo, K. Fujiu, G. Nishimura, K. Maemura, T. Yamauchi, N. Kubota, Krüppel-like transcription factor KLF5 is a key regulator of adipocyte differentiation, *Cell Metab.* 1 (2005) 27–39.
- [327] E.A. Komarova, K. Christov, A.I. Faerman, A. V Gudkov, Different impact of p53 and p21 on the radiation response of mouse tissues, *Oncogene.* 19 (2000) 3791–3798.
- [328] C.E. Cano, J. Gommeaux, S. Pietri, M. Culcasi, S. Garcia, M. Seux, S. Barelier, S. Vasseur, R.P. Spoto, M.-J. Pébusque, Tumor protein 53–induced nuclear protein 1 is a major mediator of p53 antioxidant function, *Cancer Res.* 69 (2009) 219–226.
- [329] S. Okamura, H. Arakawa, T. Tanaka, H. Nakanishi, C.C. Ng, Y. Taya, M. Monden, Y. Nakamura, p53DINP1, a p53-inducible gene, regulates p53-dependent apoptosis, *Mol. Cell.* 8 (2001) 85–94.
- [330] A. Sancho, J. Duran, A. García-España, C. Mauvezin, E.A. Alemu, T. Lamark, M.J. Macias, R. DeSalle, M. Royo, D. Sala, DOR/Tp53inp2 and Tp53inp1 constitute a metazoan gene family encoding dual regulators of autophagy and transcription, *PLoS One.* 7 (2012) e34034.
- [331] M. Seillier, S. Peugeot, O. Gayet, C. Gauthier, P. N’guessan, M. Monte, A. Carrier, J.L. Iovanna, N.J. Dusetti, TP53INP1, a tumor suppressor, interacts with LC3 and ATG8-family proteins through the LC3-interacting region (LIR) and promotes autophagy-dependent cell death, *Cell Death Differ.* 19 (2012) 1525–1535.
- [332] R. Tomasini, A.A. Samir, A. Carrier, D. Isnardon, B. Cecchinelli, S. Soddu, B. Malissen, J.-C. Dagorn, J.L. Iovanna, N.J. Dusetti, TP53INP1s and homeodomain-interacting protein kinase-2 (HIPK2) are partners in regulating p53 activity, *J. Biol. Chem.* 278 (2003) 37722–37729.
- [333] K. Yoshida, H. Liu, Y. Miki, Protein kinase C δ regulates Ser46

- phosphorylation of p53 tumor suppressor in the apoptotic response to DNA damage, *J. Biol. Chem.* 281 (2006) 5734–5740.
- [334] M.-S. Chen, S.-F. Wang, C.-Y. Hsu, P.-H. Yin, T.-S. Yeh, H.-C. Lee, L.-M. Tseng, CHAC1 degradation of glutathione enhances cystine-starvation-induced necroptosis and ferroptosis in human triple negative breast cancer cells via the GCN2-eIF2 α -ATF4 pathway, *Oncotarget.* 8 (2017) 114588–114602. doi:10.18632/oncotarget.23055.
- [335] A. Kumar, S. Tikoo, S. Maity, S. Sengupta, S. Sengupta, A. Kaur, A. Kumar Bachhawat, Mammalian proapoptotic factor Chac1 and its homologues function as γ -glutamyl cyclotransferases acting specifically on glutathione, *EMBO Rep.* 13 (2012) 1095–1101.
- [336] M. Hamano, S. Tomonaga, Y. Osaki, H. Oda, H. Kato, S. Furuya, Transcriptional Activation of Chac1 and Other Atf4-Target Genes Induced by Extracellular l-Serine Depletion is negated with Glycine Consumption in Hepa1-6 Hepatocarcinoma Cells, *Nutrients.* 12 (2020) 3018.
- [337] R.K. Humphrey, C.J. Newcomb, A.Y. Shu-Mei, E. Hao, D. Yu, S. Krajewski, K. Du, U.S. Jhala, Mixed lineage kinase-3 stabilizes and functionally cooperates with TRIBBLES-3 to compromise mitochondrial integrity in cytokine-induced death of pancreatic beta cells, *J. Biol. Chem.* 285 (2010) 22426–22436.
- [338] K. Du, S. Herzig, R.N. Kulkarni, M. Montminy, TRB3: a tribbles homolog that inhibits Akt/PKB activation by insulin in liver, *Science* (80-.). 300 (2003) 1574–1577.
- [339] M. Wu, L.-G. Xu, Z. Zhai, H.-B. Shu, SINK is a p65-interacting negative regulator of NF- κ B-dependent transcription, *J. Biol. Chem.* 278 (2003) 27072–27079.
- [340] K. Shimizu, S. Takahama, Y. Endo, T. Sawasaki, Stress-inducible caspase substrate TRB3 promotes nuclear translocation of procaspase-3, (2012).
- [341] E. Borsting, S. V Patel, A.-E. Declèves, S.J. Lee, Q.M. Rahman, S. Akira, J. Satriano, K. Sharma, V. Vallon, R. Cunard, Tribbles homolog 3 attenuates mammalian target of rapamycin complex-2 signaling and inflammation in the diabetic kidney, *J. Am. Soc. Nephrol.* 25 (2014) 2067–2078.
- [342] E. Kiss-Toth, S.M. Bagstaff, H.Y. Sung, V. Jozsa, C. Dempsey, J.C. Caunt, K.M. Oxley, D.H. Wyllie, T. Polgar, M. Harte, Human tribbles, a protein family controlling mitogen-activated protein kinase cascades, *J. Biol. Chem.* 279 (2004) 42703–42708.
- [343] R. Schwarzer, S. Dames, D. Tondera, A. Klippel, J. Kaufmann, TRB3 is a PI 3-kinase dependent indicator for nutrient starvation, *Cell. Signal.* 18 (2006) 899–909.
- [344] D. Örd, K. Meerits, T. Örd, TRB3 protects cells against the growth inhibitory and cytotoxic effect of ATF4, *Exp. Cell Res.* 313 (2007) 3556–3567.

- [345] D. Örd, T. Örd, T. Biene, T. Örd, TRIB3 increases cell resistance to arsenite toxicity by limiting the expression of the glutathione-degrading enzyme CHAC1, *Biochim. Biophys. Acta - Mol. Cell Res.* 1863 (2016) 2668–2680. doi:<https://doi.org/10.1016/j.bbamcr.2016.08.003>.
- [346] W. Wu, M. Zou, D.R. Brickley, T. Pew, S.D. Conzen, Glucocorticoid receptor activation signals through forkhead transcription factor 3a in breast cancer cells, *Mol. Endocrinol.* 20 (2006) 2304–2314.
- [347] J. Tangir, N. Bonafé, M. Gilmore-Hebert, O. Henegariu, S.K. Chambers, SGK1, a potential regulator of c-fms related breast cancer aggressiveness, *Clin. Exp. Metastasis.* 21 (2004) 477–483.
- [348] L. Zhang, R. Cui, X. Cheng, J. Du, Antiapoptotic effect of serum and glucocorticoid-inducible protein kinase is mediated by novel mechanism activating I κ B kinase, *Cancer Res.* 65 (2005) 457–464.
- [349] J. Chun, T. Kwon, D.J. Kim, I. Park, G. Chung, E.J. Lee, S.K. Hong, S.-I. Chang, H.Y. Kim, S.S. Kang, Inhibition of mitogen-activated kinase kinase kinase 3 activity through phosphorylation by the serum-and glucocorticoid-induced kinase 1, *J. Biochem.* 133 (2003) 103–108.
- [350] T. Kobayashi, M. Deak, N. Morrice, P. Cohen, Characterization of the structure and regulation of two novel isoforms of serum-and glucocorticoid-induced protein kinase, *Biochem. J.* 344 (1999) 189–197.
- [351] H. Sakoda, Y. Gotoh, H. Katagiri, M. Kurokawa, H. Ono, Y. Onishi, M. Anai, T. Ogihara, M. Fujishiro, Y. Fukushima, Differing roles of Akt and serum-and glucocorticoid-regulated kinase in glucose metabolism, DNA synthesis, and oncogenic activity, *J. Biol. Chem.* 278 (2003) 25802–25807.
- [352] A.C. Maiyar, M.L.L. Leong, G.L. Firestone, Importin- α mediates the regulated nuclear targeting of serum-and glucocorticoid-inducible protein kinase (Sgk) by recognition of a nuclear localization signal in the kinase central domain, *Mol. Biol. Cell.* 14 (2003) 1221–1239.
- [353] T. Matsuzaka, H. Shimano, Elovl6: a new player in fatty acid metabolism and insulin sensitivity, *J. Mol. Med.* 87 (2009) 379–384.
- [354] P.M. Thompson, T. Gotoh, M. Kok, P.S. White, G.M. Brodeur, CHD5, a new member of the chromodomain gene family, is preferentially expressed in the nervous system, *Oncogene.* 22 (2003) 1002–1011.
- [355] A. Bagchi, C. Papazoglu, Y. Wu, D. Capurso, M. Brodt, D. Francis, M. Bredel, H. Vogel, A.A. Mills, CHD5 is a tumor suppressor at human 1p36, *Cell.* 128 (2007) 459–475.
- [356] T. Fujita, J. Igarashi, E.R. Okawa, T. Gotoh, J. Manne, V. Kolla, J. Kim, H. Zhao, B.R. Pawel, W.B. London, CHD5, a tumor suppressor gene deleted from 1p36. 31 in neuroblastomas, *JNCI J. Natl. Cancer Inst.* 100 (2008) 940–949.
- [357] J.-H. Kim, I.-Y. Jeong, Y.-H. Lim, Y.-H. Lee, S.-Y. Shin, Estrogen receptor β

- stimulates Egr-1 transcription via MEK1/Erk/Elk-1 cascade in C6 glioma cells, *BMB Rep.* 44 (2011) 452–457.
- [358] I. de Belle, R.-P. Huang, Y. Fan, C. Liu, D. Mercola, E.D. Adamson, p53 and Egr-1 additively suppress transformed growth in HT1080 cells but Egr-1 counteracts p53-dependent apoptosis, *Oncogene.* 18 (1999) 3633–3642.
- [359] J. Ryu, S.S. Choe, S.-H. Ryu, E.-Y. Park, B.W. Lee, T.K. Kim, C.H. Ha, S. Lee, Paradoxical induction of growth arrest and apoptosis by EGF via the up-regulation of PTEN by activating Redox factor-1/Egr-1 in human lung cancer cells, *Oncotarget.* 8 (2017) 4181.
- [360] J.-L. Schwachtgen, P. Houston, C. Campbell, V. Sukhatme, M. Braddock, Fluid shear stress activation of egr-1 transcription in cultured human endothelial and epithelial cells is mediated via the extracellular signal-related kinase 1/2 mitogen-activated protein kinase pathway., *J. Clin. Invest.* 101 (1998) 2540–2549.
- [361] D. Xiao, D. Chinnappan, R. Pestell, C. Albanese, H.C. Weber, Bombesin regulates cyclin D1 expression through the early growth response protein Egr-1 in prostate cancer cells, *Cancer Res.* 65 (2005) 9934–9942.
- [362] N. Mukaida, Y.-Y. Wang, Y.-Y. Li, Roles of Pim-3, a novel survival kinase, in tumorigenesis, *Cancer Sci.* 102 (2011) 1437–1442.
doi:<https://doi.org/10.1111/j.1349-7006.2011.01966.x>.
- [363] B.-O. Nilsson, B. Olde, L.M.F. Leeb-Lundberg, G protein-coupled oestrogen receptor 1 (GPER1)/GPR30: a new player in cardiovascular and metabolic oestrogenic signalling, *Br. J. Pharmacol.* 163 (2011) 1131–1139.
doi:<https://doi.org/10.1111/j.1476-5381.2011.01235.x>.
- [364] V. Briz, M. Baudry, Estrogen regulates protein synthesis and actin polymerization in hippocampal neurons through different molecular mechanisms, *Front. Endocrinol. (Lausanne).* 5 (2014) 22.
- [365] J. Kanska, P.-J.P. Aspuria, B. Taylor-Harding, L. Spurka, V. Funari, S. Orsulic, B.Y. Karlan, W.R. Wiedemeyer, Glucose deprivation elicits phenotypic plasticity via ZEB1-mediated expression of NNMT, *Oncotarget.* 8 (2017) 26200–26220. doi:[10.18632/oncotarget.15429](https://doi.org/10.18632/oncotarget.15429).
- [366] Y. Gao, N.I. Martin, M.J. van Haren, Nicotinamide N-methyl transferase (NNMT): An emerging therapeutic target, *Drug Discov. Today.* 26 (2021) 2699–2706. doi:<https://doi.org/10.1016/j.drudis.2021.05.011>.
- [367] Q. Song, Y. Chen, J. Wang, L. Hao, C. Huang, A. Griffiths, Z. Sun, Z. Zhou, Z. Song, ER stress-induced upregulation of NNMT contributes to alcohol-related fatty liver development, *J. Hepatol.* 73 (2020) 783–793.
doi:<https://doi.org/10.1016/j.jhep.2020.04.038>.
- [368] S. Huang, M. Hölzel, T. Knijnenburg, A. Schlicker, P. Roepman, U. McDermott, M. Garnett, W. Grenrum, C. Sun, A. Prahallad, F.H. Groenendijk, L. Mittempergher, W. Nijkamp, J. Neefjes, R. Salazar, P. ten Dijke, H.

- Uramoto, F. Tanaka, R.L. Beijersbergen, L.F.A. Wessels, R. Bernards, MED12 Controls the Response to Multiple Cancer Drugs through Regulation of TGF- β Receptor Signaling, *Cell*. 151 (2012) 937–950. doi:<https://doi.org/10.1016/j.cell.2012.10.035>.
- [369] N. Ding, H. Zhou, P.-O. Esteve, H.G. Chin, S. Kim, X. Xu, S.M. Joseph, M.J. Friez, C.E. Schwartz, S. Pradhan, T.G. Boyer, Mediator links epigenetic silencing of neuronal gene expression with x-linked mental retardation, *Mol. Cell*. 31 (2008) 347–359. doi:10.1016/j.molcel.2008.05.023.
- [370] Y.E. Zhang, Non-Smad pathways in TGF- β signaling, *Cell Res*. 19 (2009) 128–139. doi:10.1038/cr.2008.328.
- [371] E. V Schneider, J. Böttcher, M. Blaesse, L. Neumann, R. Huber, K. Maskos, The structure of CDK8/CycC implicates specificity in the CDK/cyclin family and reveals interaction with a deep pocket binder, *J. Mol. Biol.* 412 (2011) 251–266.
- [372] A.J. Donner, S. Szostek, J.M. Hoover, J.M. Espinosa, CDK8 Is a Stimulus-Specific Positive Coregulator of p53 Target Genes, *Mol. Cell*. 27 (2007) 121–133. doi:<https://doi.org/10.1016/j.molcel.2007.05.026>.
- [373] S. Srivastava, R. Kulshreshtha, Insights into the regulatory role and clinical relevance of mediator subunit, MED12, in human diseases, *J. Cell. Physiol.* 236 (2021) 3163–3177.
- [374] N. Carinhas, T.M. Duarte, L.C. Barreiro, M.J.T. Carrondo, P.M. Alves, A.P. Teixeira, Metabolic signatures of GS-CHO cell clones associated with butyrate treatment and culture phase transition, *Biotechnol. Bioeng.* 110 (2013) 3244–3257.
- [375] M.R. NARKEWICZ, S.D. SAULS, S.S. TJOA, C. TENG, P. V FENNESSEY, Evidence for intracellular partitioning of serine and glycine metabolism in Chinese hamster ovary cells, *Biochem. J.* 313 (1996) 991–996.
- [376] T.M. Duarte, N. Carinhas, L.C. Barreiro, M.J.T. Carrondo, P.M. Alves, A.P. Teixeira, Metabolic responses of CHO cells to limitation of key amino acids, *Biotechnol. Bioeng.* 111 (2014) 2095–2106. doi:10.1002/bit.25266.
- [377] S. Zhang, Q. Yang, M. Ren, S. Qiao, P. He, D. Li, X. Zeng, Effects of isoleucine on glucose uptake through the enhancement of muscular membrane concentrations of GLUT1 and GLUT4 and intestinal membrane concentrations of Na⁺/glucose co-transporter 1 (SGLT-1) and GLUT2, *Br. J. Nutr.* 116 (2016) 593–602.
- [378] J.S. Lewis, A.P., Lemon, S.M., Barber, K.A., Murphy, P., Parry, N.R., Peakman, T.C., Sims, M.J., Worden, J. and Crowe, IgG [Homo sapiens], Rescue, Expression, Anal. a Neutralizing Hum. Anti-Hepatitis A Virus Monoclon. Antib. Anti-Hepatitis A Virus Monoclon. Antib. (n.d.). <https://www.ncbi.nlm.nih.gov/protein/AAA02914.1> (accessed October 1, 2019).

- [379] S. Gutiérrez-Granados, L. Cervera, A.A. Kamen, F. Gòdia, Advancements in mammalian cell transient gene expression (TGE) technology for accelerated production of biologics, *Crit. Rev. Biotechnol.* 38 (2018) 918–940.
- [380] P. Chen, J. Demirji, V.B. Ivleva, J. Horwitz, R. Schwartz, F. Arnold, The transient expression of CHIKV VLP in large stirred tank bioreactors, *Cytotechnology.* 71 (2019) 1079–1093. doi:10.1007/s10616-019-00346-x.
- [381] P.L. Felgner, T.R. Gadek, M. Holm, R. Roman, H.W. Chan, M. Wenz, J.P. Northrop, G.M. Ringold, M. Danielsen, Lipofection: a highly efficient, lipid-mediated DNA-transfection procedure, *Proc. Natl. Acad. Sci.* 84 (1987) 7413–7417.
- [382] N. Düzgüneş, S. Nir, Mechanisms and kinetics of liposome–cell interactions, *Adv. Drug Deliv. Rev.* 40 (1999) 3–18.
- [383] L.T. Nguyen, K. Atobe, J.M. Barichello, T. Ishida, H. Kiwada, Complex formation with plasmid DNA increases the cytotoxicity of cationic liposomes, *Biol. Pharm. Bull.* 30 (2007) 751–757.
- [384] M.C. Filion, N.C. Phillips, Toxicity and immunomodulatory activity of liposomal vectors formulated with cationic lipids toward immune effector cells, *Biochim. Biophys. Acta (BBA)-Biomembranes.* 1329 (1997) 345–356.
- [385] M.M. Chang, L. Gaidukov, G. Jung, W.A. Tseng, J.J. Scarcelli, R. Cornell, J.K. Marshall, J.L. Lyles, P. Sakorafas, A.H.A. Chu, K. Cote, B. Tzvetkova, S. Dolatshahi, M. Sumit, B.C. Mulukutla, D.A. Lauffenburger, B. Figueroa, N.M. Summers, T.K. Lu, R. Weiss, Small-molecule control of antibody N-glycosylation in engineered mammalian cells, *Nat. Chem. Biol.* 15 (2019) 730–736. doi:10.1038/S41589-019-0288-4.
- [386] J.D. Tousignant, A.L. Gates, L.A. Ingram, C.L. Johnson, J.B. Nietupski, S.H. Cheng, S.J. Eastman, R.K. Scheule, Comprehensive analysis of the acute toxicities induced by systemic administration of cationic lipid: plasmid DNA complexes in mice, *Hum. Gene Ther.* 11 (2000) 2493–2513.
- [387] N.N. Shah, T. Maatman, P. Hari, B. Johnson, Multi targeted CAR-T cell therapies for B-cell malignancies, *Front. Oncol.* 9 (2019) 146.
- [388] L.J.N. Cooper, L. Ausubel, M. Gutierrez, S. Stephan, R. Shakeley, S. Olivares, L.M. Serrano, L. Burton, M.C.V. Jensen, S.J. Forman, D.L. DiGiusto, Manufacturing of gene-modified cytotoxic T lymphocytes for autologous cellular therapy for lymphoma, *Cytotherapy.* (2006). doi:10.1080/14653240600620176.

ABSTRACT

Name of the Student: Jyoti Rawat

Registration No. : 10BB17J26054

Faculty of Study: Biological Sciences

Year of Submission: 2021

CSIR Lab: National Chemical Laboratory

Name of the Supervisor: Mugdha Gadgil

Title of the thesis: Towards improving cell culture processes for biotherapeutic production: novel tools and strategies

Mammalian cell culture based processes are important for the producing effective recombinant therapeutics such as monoclonal antibodies. A typical production process involves introduction of the gene of interest in the host cell, selecting a clone with desired productivity characteristics, process and medium development for the selected clone followed by production runs in larger scale bioreactors, which are currently predominantly run in fed batch mode. For pre-clinical analysis material can be produced by transient expression of the protein without selecting a clone. Each of these steps has scope for improvement. In this thesis, I have explored three problems associated with these steps (1) Understanding whether shear stress has an effect on the productivity of transient protein expression, which is of importance when scaling up such processes (2) Developing a hydrogel based tool for simultaneous in situ delivery of >20 nutrients in small scale culture which can enable fed batch culture at small scale without any additional infrastructure, and help in better identification of high productivity clones at the screening stage (3) Evaluated whether a medium formulation strategy of maintaining amino acids at low concentrations via continuous feeding may be beneficial for increasing culture longevity and productivity.

Large scale TGE is an important method for rapidly producing large amount of recombinant protein for initial characterizations. Mammalian cells are subjected to varying degrees of shear during various stages of bioprocessing. Effect of shear has been mainly studied in adherent cells but have been studied to a lower degree in suspension cells especially in the bioprocessing context. Shear stress affects transfection efficiency and increases liposomal toxicity. And this effect increases as the magnitude of shear stress increases and is because of the synergistic effect of shear on liposomal toxicity and the cells.

During cell line development, selecting a robust high producer is the primary requirement for any successful cell line development program. Screening clones under conditions similar to the final production process reduces the chances of sub-par clone performance at higher scale. I have investigated whether it is possible to culture cells in fed batch mode in small scale platforms without requiring any additional infrastructure. I have developed a nutrient delivery system for in situ feeding of CHO cells in small scale culture platforms, capable of delivering a large number of nutrients such as amino acids vitamins and trace elements. I have shown that it is possible modulate the delivery of 18 amino acids, improving cell culture

performance. Such system will also aid in creating completely closed system for small scale platforms for cultivating CHO cell.

Medium development is another critical parameter that can affect the process. Recent report caution against the use of nutritionally rich medium, as a result of the catabolic by products of amino acids. I have investigated whether maintaining amino acids at low concentrations through continuous feeding can improve culture performance.. Results from these experiments do not suggest an improvement in culture performance. However with developments in online metabolite measurements, precise at-line control of amino acids may enable further refined experimentation.

List of publications and patent

(1) List of publications and patent

Rawat, Jyoti, and Mugdha Gadgil (2016). “Shear stress increases cytotoxicity and reduces transfection efficiency of liposomal gene delivery to CHO-S cells.” *Cytotechnology* 68.6: 2529-2538.

Rawat, Jyoti, and Mugdha Gadgil (2020). “Towards in situ continuous feeding via controlled release of complete nutrients for fed-batch culture of animal cells.” *Biochemical Engineering Journal* 154: 107436.

Rawat, Jyoti, and Mugdha Gadgil (2020). “A Diffusion Based Closed Hydrogel System For Continuous In Situ Feeding Of Nutrients” *Indian Patent application No.* 201911023888.

Poster presentation

Rawat, Jyoti, and Mugdha Gadgil (2016). “Shear affects growth and reduces transfection efficiency of liposomal gene delivery in CHO-S cells” *Indo-US workshop on cell factories*, IIT Bombay.

Rawat, Jyoti, and Mugdha Gadgil (2020). “Towards in situ continuous feeding via controlled release of complete nutrients for fed-batch culture of animal cells” EMBO Symposium, *Engineering meets evolution: Designing biological systems* IIT Madras.

Oral Presentation

Rawat, Jyoti, and Mugdha Gadgil (2019). “Towards in situ continuous feeding via controlled release of complete nutrients for fed-batch culture of animal cells” *Student Research Foundation conference*, NCL Pune.

(2) Poster presentation

Rawat, Jyoti, and Mugdha Gadgil (2016). “Shear affects growth and reduces transfection efficiency of liposomal gene delivery in CHO-S cells” *Indo-US workshop on cell factories*, IIT Bombay.

Abstract: Shear stress is an inevitable part of bioreactor systems. Shear is known to affect binding of polyplexes and drug delivery vehicles in adherent cells^[1,2]. Moreover, shear has been speculated to be the principle for enhanced uptake in devices fabricated by Hallow et al and Sharei et al^[3,4]. Thus, shear can potentially affect intracellular delivery of cargo such as DNA for transgene expression. We chose lipofectamine 2000, a widely used DNA delivery vehicle, as a model liposome to study the effect of shear on lipofection of suspension CHO-S cells. We find that exposure to shear in the presence of liposome:DNA complex (lipoplex) leads to reduced growth and decreases transfection efficiency. This effect is not due to the effect of shear on the lipoplex itself, and is also not explained by the exposure of cells to shear with liposome alone.

Rawat, Jyoti, and Mugdha Gadgil (2020). “Towards in situ continuous feeding via controlled release of complete nutrients for fed-batch culture of animal cells” EMBO Symposium, *Engineering meets evolution: Designing biological systems* IIT Madras.

Abstract: In fed-batch culture nutrients are replenished by addition of concentrated feed. This is done by manual bolus feeding or by robotic handling systems. We report development of a hydrogel system called NutriGel for in situ continuous delivery of a complex nutrient feed. This feed comprises of 52 nutrients including 18 amino acids, vitamins, antioxidants, and trace element. Amino acid release from NutriGel is sustained for at least seven days. Release rates of individual amino acids can be

independently modulated by changing their initial loading. This study provides a proof of concept that NutriGels can enable a completely closed continuous in situ feeding system for mammalian cell culture



Shear stress increases cytotoxicity and reduces transfection efficiency of liposomal gene delivery to CHO-S cells

Jyoti Rawat · Mugdha Gadgil

Received: 4 February 2016 / Accepted: 19 April 2016 / Published online: 29 April 2016
© Springer Science+Business Media Dordrecht 2016

Abstract Animal cells in suspension experience shear stress in different situations such as in vivo due to hemodynamics, or in vitro due to agitation in large-scale bioreactors. Shear stress is known to affect cell physiology, including binding and uptake of extracellular cargo. In adherent cells the effects of exposure to shear stress on particle binding kinetics and uptake have been studied. There are however no reports on the effect of shear stress on extracellular cargo delivery to suspension cells. In this study, we have evaluated the effect of shear stress on transfection of CHO-S cells using Lipofectamine 2000 in a simple flow apparatus. Our results show decreased cell growth and transfection efficiency upon lipoplex assisted transfection of CHO-S while being subjected to shear stress. This effect is not seen to the same extent when cells are exposed to shear stress in absence of the lipoplex complex and subsequently transfected, or if the lipoplex is subjected to shear stress and subsequently used to transfect the cells. It is also not seen to the same extent when cells are exposed to shear stress in presence of liposome alone, suggesting that the observed effect is dependent on interaction of the lipoplex with cells in the presence of shear stress. These results suggest that studies

involving liposomal DNA delivery in presence of shear stress such as large scale transient protein expression should account for the effect of shear during lipoplex assisted DNA delivery.

Keywords Shear stress · Transfection · Lipoplex · Liposome

Background

Animal cells in suspension are subjected to shear stress under diverse conditions such as due to hemodynamics in vivo or due to agitation during large scale culture of cells in bioreactors. The effect of shear stress has been largely studied in adherent cells primarily due to interest in the effect of shear stress on endothelial cells in blood vessels, and is known to affect various aspects of cell physiology including cell morphology, size and metabolism (Chatzizisis et al. 2007; Haga et al. 2007; Heo et al. 2012; Resnick et al. 2003). In addition, shear stress is also known to affect cellular uptake of extracellular cargo. Indeed, exposure to shear stress is being evaluated as a strategy for delivering macromolecules into cells. Different methods of employing shear stress have led to devices such as those made by Hallow et al. and Sharei et al. that use shear stress as the fundamental principle for intracellular delivery (Hallow et al. 2008; Sharei et al. 2013), though the exact mechanism is yet unclear.

J. Rawat · M. Gadgil (✉)
Chemical Engineering and Process Development
Division, CSIR-National Chemical Laboratory,
Pune 411008, India
e-mail: mc.gadgil@ncl.res.in

Exposure to shear stress has been reported to transiently increase fluid phase endocytosis and caveolae density (Davies et al. 1984; Rizzo et al. 2003; White and Frangos 2007). Endocytosis of extracellular cargo requires association of the cargo with the cell membrane as the first step. Shear stress has been widely reported to affect particle adhesion in endothelial cells, which in turn can affect uptake. These effects vary depending on the particle size and shear stress level. For example, Patil et al. report that at higher shear rates of 400–600 s⁻¹, the rate of attachment of 5–20 µm diameter microspheres coated with a recombinant PSGL-1 construct decreased with increasing size (Patil et al. 2001). Charoenphol et al. showed that binding efficiency for spherical particles of size 100 nm to 10 µm increased with increasing particle size at a shear rate of 200 s⁻¹ and for a given size the binding efficiency increased when the wall shear rate was increased from 200 to 1500 s⁻¹ (Charoenphol et al. 2010). In addition to size, particle shape affects the binding of particles under shear stress: adhesion of elongated and flattened particles was found to be significantly higher than spheres (Doshi et al. 2010). This may be of relevance to the effectiveness in the presence of shear stress of carriers such as liposomes, which can deform in the presence of shear. The duration of cellular exposure to shear stress also affects uptake: chronic exposure of human umbilical vein endothelial cells (HUVECs) to shear stress at 5 dyne/cm² led to a reduced internalization of ~180 nm diameter FITC-labeled polystyrene spheres coated with anti-PECAM, whereas acute exposure led to an increased internalization (Han et al. 2012). This was reproduced in another study where chronic shear stress led to reduced internalization of unmodified 80 nm spherical gold nanoparticles (AuNPs) in HUVEC cells (Klingberg et al. 2015). The magnitude of the shear stress obviously matters for binding/uptake: for example, nanoscale particles showed an inverse relationship between shear stress and particle uptake (Lin et al. 2010). Cell membrane properties can also be affected by shear stress, with membrane fluidity reported to increase with shear stress in endothelial cells, the mechanism of which is unclear (Butler et al. 2001; Haidekker et al. 2000). Shear stress can also induce membrane fusion, suggesting that under some conditions the interaction of liposomal carriers with cells, and hence their ability to deliver cargo, might possibly be affected by shear stress (Kogan et al. 2014).

The effect of shear stress on the uptake of liposomal formulations has been evaluated on adherent cells. Flow can have a positive effect of improving access of the lipoplex to the adhered cell (Harris and Giorgio 2005) which can increase its uptake, but at the same time can reduce the binding affinity of the lipoplex to the cells (Fujiwara et al. 2006). Shear stress has been shown to increase transfection efficiency up to an optimal shear stress level beyond which efficiency decreases (Mennesson et al. 2006; Shin et al. 2009). To our knowledge, there are no reports on the effect of shear stress on carrier-assisted delivery of cargo to suspension cells. Such scenarios are relevant to large-scale transfections carried out in bioreactors for transient expression of recombinant protein, and to liposomal gene and drug delivery to blood cells where the liposomal complex is injected into blood vessels. The primary focus of this study is on suspension adapted CHO-S cells which have been used for large scale transfection in bioreactors to transiently express recombinant protein (Baldi et al. 2007). Mardikar and Niranjana subjected various animal cells in suspension to shear stress and depending on the shear stress level report formation of pores, population and cell shrinkage (Mardikar and Niranjana 2000). It is conceivable that such formation of pores could affect uptake of extracellular cargo.

In this study we use a simple flow apparatus to evaluate the effect of shear stress on the ability of liposomal carriers to deliver DNA to suspension cells for transgene expression. We find that exposure to shear stress during transfection with lipoplex results in a decrease in transfection efficiency and reduced cell density compared to transfection carried out in the absence of shear stress, in well-plates in CHO-S cells, which are efficiently transfected by Lipofectamine 2000. This effect is not seen to the same extent when cells are exposed to shear stress in the absence of the lipoplex and subsequently transfected, or if the lipoplex is exposed to shear stress and subsequently used to transfect cells not exposed to shear.

Materials and methods

Lipofectamine 2000 (11668027) was purchased from Invitrogen Corporation (Carlsbad, CA, USA). CHO-S-SFM II and DMEM were purchased from Invitrogen Corporation (12052-114 and 12320-032, respectively).

Fetal Bovine Serum (RM1112, FBS) was purchased from Hi Media Laboratories (Mumbai, India). Cell culture compatible silicone tubing ID 2 mm × OD 4 mm was purchased from Ami Polymers (Mumbai, India). 24 well plates were purchased from Nest Scientific USA (Rahway, NJ, USA) and used for seeding K562 cells. Ultra low binding 24 well plates were purchased from Sigma-Aldrich (St. Louis, MO, USA) and used for CHO-S cells.

CHO-S cell line was purchased from Invitrogen Corporation. Cells were seeded at a density of 0.2×10^6 cells/ml in CHO-SFM II and passaged every second day. Cells were maintained at 37 °C, 10 % CO₂ and 110 rpm, and used from passage 9–40. K562, human chronic myelogenous leukemic cell line was obtained from National Centre for Cell Sciences (NCCS, Pune, India). K562 cells were maintained in DMEM supplemented with 10 % FBS and cultured at 37 °C, 10 % CO₂ and 110 rpm. K562 cells were used from passage 39–50. Plasmid containing mCherry gene was used for transfection with fluorescent mCherry protein used as a reporter.

Flow apparatus

A flow apparatus with a reservoir for cell suspension and a peristaltic pump (Longer pumps BT100-2J Low Flow Rate Peristaltic Pump with the 6-roller pump head DG-2) was used to flow cells at a flow rate of 19 ml/min through a cell culture compatible silicone tubing (ID 2 mm × OD 4 mm, Ami polymers). For low shear stress, cells were flowed only through the silicone tube of 2 mm inner diameter. A glass capillary of 0.5 mm diameter and length of 8 cm was attached to generate moderate shear stress and a silicone tube of 0.25 mm diameter of length 1.2 cm was inserted to generate high shear stress. Under an assumption of incompressible walls and no slip at the wall, these correspond to a wall shear stress of ~2, 220 and 2000 dynes/cm² under the three conditions respectively. The experiment was repeated at least three times, and cells were seeded into two wells for each repetition. To control for any effect of shear stress due the squeezing action of the peristaltic pump head, the flow rate was kept constant under all three conditions. The pump head design allowed varying occlusion using a ratchet wheel. The extent of cell death observed when cells alone were flowed through the pump head varied for different values of this

parameter with cell death increasing at higher levels of occlusion. The highest occlusion was identified for each cell type such that there was minimal cell death immediately subsequent to exposure to low shear stress, and was then kept constant for all experiments with that cell type. The selected level of this parameter was higher for CHO-S compared to K562.

Transfection

Transfection for CHO-S was performed using Lipofectamine 2000 (Invitrogen Corporation) as per the manufacturer's instructions. Transfections were carried out using cells on the second day of passage. 1 µg DNA and 5 µl Lipofectamine 2000 was used per milliliter of the cell suspension. Depending on the experiment, the lipoplex complex or lipid alone were added to 4 ml of the cell suspension and flowed through the flow apparatus for 2 h. After 2 h, 500 µl of the culture was incubated in 24 well plate at 37 °C, 10 % CO₂ and 110 rpm. Samples were taken for measuring cell density immediately before and after flowing the cells, and after allowing cells to recover for one day after exposure to shear stress. Cell density was measured using a hemocytometer after appropriate dilution and viability was measured using trypan blue dye exclusion method. After 24 h of incubation, some clumping was observed for all transfected CHO-S cultures with clumps of approximately 5–20 cells. Clumps were counted as a single cell for calculation of cell density. Each experiment was repeated at least 3 times.

Transfection for K562 was performed using Lipofectamine 2000 as per a modified protocol suggested by the manufacturer. 2.4 µg DNA and 5 µl Lipofectamine 2000 was used per milliliter of the cell suspension for transfection. The complex was mixed in serum free DMEM medium and incubated for 20 min at room temperature before addition to the culture.

Calculation of transfection efficiency

Twenty-four hours post transfection, cells were harvested from the 24 well plate. After washing with PBS, the CHO-S cells were then imaged on EVOS Fluid Cell Imaging Station (Life Technologies, Carlsbad, CA, USA). Transfection efficiency for CHO-S cells was calculated by counting the percentage of cells that showed red fluorescence due to expression of

fluorescent mCherry protein. A minimum of fifteen fields per well were recorded with the Fluid Cell Imaging Station and the number of fluorescent cells and total cells was counted.

Due to the very low transfection efficiencies for K562 cells, transfection efficiency was measured using flow cytometry (BD Accuri C6 Flow Cytometer, BD Biosciences) and data were analyzed using the BD Accuriflow software (BD Biosciences, San Jose, CA, USA).

Statistical analysis

Two tailed Student's *t* test was used to determine significance of difference between all data sets. All *p*-values lower than significance level of 0.05 are denoted by asterisks in figures. Error bars indicate 95 % confidence interval.

Results

CHO-S cells were subjected to shear stress by pumping them in a closed loop at a constant flow rate using a peristaltic pump. Cells were subjected to shear stress by pumping them for 2 h either through a silicone tube of 2 mm inner diameter (henceforth referred to as 'low shear') or a silicone tube of 2 mm diameter with an attached glass capillary of 0.5 mm inner diameter and length 8 cm (referred to as 'moderate shear') or a silicone tube of 2 mm diameter with a silicone tube of 0.25 mm diameter and length 1.2 cm (referred to as 'high shear'). The use of peristaltic pump allowed aseptic continuous unidirectional flow allowing cells to be exposed to shear stress for extended periods of time.

We first evaluated the effect of shear stress on CHO-S cells to validate the use of the flow apparatus. Both, the immediate effect of shear stress on cell death measured as any decrease in viable cell density (VCD) immediately after exposure to shear stress, and a longer-term effect measured as any effect on cell growth at the end of 24 h after exposure to shear stress, were measured. The immediate decrease in VCD due to shear stress is small at low shear stress (8 % decrease) but increases at high shear stress (50 % decrease, Fig. 1a). Exposure to shear stress also affects subsequent cell growth with cells exposed to low shear stress showing an average 0.9 population doublings over 24 h, compared to growth of cells

maintained throughout in a 24 well plate showing an average 1.2 population doublings. However, cells exposed to high shear stress show a considerable decrease in VCD (average 73 % decrease in 24 h). This is similar to previous reports such as those of flow causing lysis in mouse myeloma cells at a wall shear stress of 1800 dyne/cm², validating the use of our flow apparatus (McQueen et al. 1987; Vickroy et al. 2007). Cell viability is however not substantially reduced after exposure to shear at all levels of shear stress (Fig. 1b), indicating the decrease in viable cell density at high shear stress is likely due to cell lysis. Due to high cell death at high shear stress, the effect of shear stress on transfection of CHO-S cells using lipoplex was further evaluated at low and moderate shear stress.

Exposure to shear stress in presence of lipoplex reduces transfection efficiency and increases cell death

We then further evaluated the effect of exposure of cells to shear stress in the presence of lipoplex (lipofectamine 2000: DNA complex). The immediate effect of shear stress on cell death was similar as in the case when cells were exposed to shear stress without the lipoplex. However surprisingly, in the presence of lipoplex, VCD at 24 h after exposure to shear stress was substantially reduced even at low shear stress (Fig. 2a). An average 25 % decrease in VCD was observed at low shear and 40 % decrease at moderate shear, compared to cell growth at an average 0.4 population doublings observed in cells transfected in the well plate. This decrease in VCD is partly caused due to greater clumping of cells in the presence of shear stress during transfection, though that alone is not sufficient to explain the difference, as verified by including the cells in clumps during cell counting. Viability was again, however, not substantially affected suggesting the decrease in VCD is due to increased cell lysis in the presence of lipoplex during exposure to shear stress (Fig. 2b). Transfection efficiency decreased significantly when cells were subjected to shear stress in the presence of lipoplex (Fig. 2c).

Higher cell death and lower transfection efficiency of the lipoplex in the presence of shear stress could possibly be due to the effect of shear on cells: for example, reduced cell growth upon exposure to shear

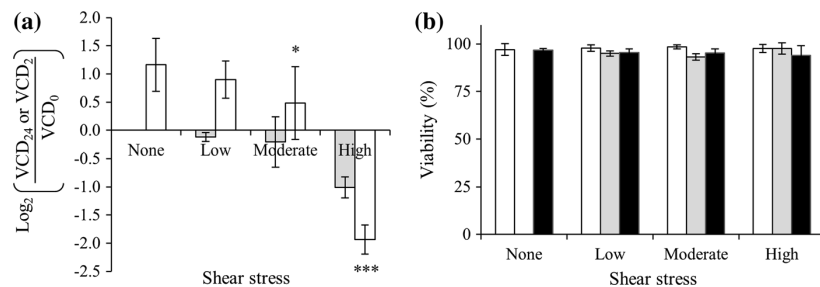


Fig. 1 The effect of shear stress on cell density and viability of CHO-S cells. CHO-S cells were subjected to shear stress (low, moderate and high, see Methods section for details on shear stress levels) for 120 min and monitored for changes in viable cell density and viability immediately after flow and after 24 h of incubation. CHO-S cells not subjected to shear stress were used as control. **a** Viable cell density (VCD) normalized to initial viable cell density. Immediately after subjecting cells to shear stress (filled bars), after 24 h (open bars). Initial viable

cell density (VCD_0), viable cell density immediately after flow (VCD_2), 24 h after flow (VCD_{24}). Log_2 transformation is used to represent cell growth in terms of population doublings, and make the data symmetric for changes in both directions (growth and death). **b** Viability. Initial (white bars), immediately after subjecting the cells to shear stress (grey bars) and after 24 h (black bars). $n \geq 3$, error bars indicate 95 % confidence interval. *** $p < 0.0005$; ** $p < 0.005$; * $p < 0.05$ for comparison to no shear condition

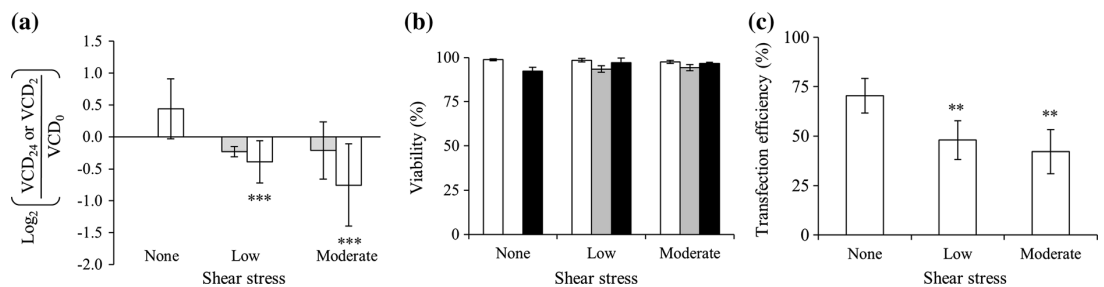


Fig. 2 Cell density, viability and transfection efficiency of CHO-S cells when exposed to shear stress in the presence of lipoplex. CHO-S cells were subjected to shear stress (low and moderate, see Methods section for details on shear stress levels) for 120 min in the presence of lipoplex and monitored for changes in cell density and viability immediately after flow and after 24 h of incubation. Control culture was not subjected to shear stress. **a** Viable cell density (VCD) normalized to initial viable cell density. Immediately after subjecting cells to shear

stress (filled bars), after 24 h (open bars). Initial viable cell density (VCD_0), viable cell density immediately after flow (VCD_2), 24 h after flow (VCD_{24}). **b** Viability. Initial (white bars), immediately after subjecting the cells to shear stress (grey bars) and after 24 h (black bars). **c** Transfection efficiency. $n \geq 3$, error bars indicate 95 % confidence interval. *** $p < 0.0005$; ** $p < 0.005$; * $p < 0.05$ for comparison to no shear condition

stress could lead to reduced transfection efficiency. On the other hand, shear stress could have an effect on the lipoplex characteristics, which in turn affect their ability to cause DNA uptake. Both these mechanisms could by themselves or in a concerted fashion produce the effect of increased toxicity and reduced transfection efficiency in the presence of shear stress. To test whether the observed effect on cell toxicity could be explained solely by the effect of shear stress on cells or on the lipoplex, we next subjected either only the lipoplex or the cells to shear stress prior to

transfection. Further experiments were only carried out at low shear stress.

Shear stress does not affect the transfectability of the lipoplex complex

The lipoplex was exposed to low shear stress for 2 h and subsequently immediately used to transfect CHO-S cells. A control culture was also transfected with lipoplex incubated for the same period of time in the absence of shear stress to control for the effect of

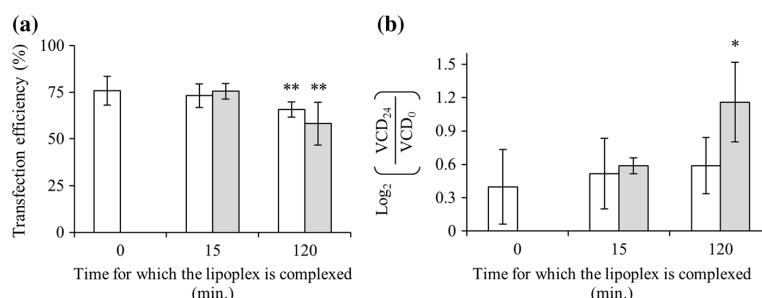


Fig. 3 Shear stress does not affect the transfectability of the lipoplex. Lipoplex subjected to low shear stress for 120 min and its unsheared control were used for transfecting CHO-S cells at different time points. **a** Transfection efficiency. Lipoplex not subjected to shear stress (*white bars*) and sheared lipoplex (*grey bar*) **b** Viable cell density (VCD) normalized to initial viable cell density. Cells transfected with unsheared lipoplex at

indicated time points after complexation (*white bars*), cells transfected with sheared lipoplex at indicated time points (sheared for 15 and 120 min) (*grey bars*). Initial viable cell density (VCD_0), 24 h after flow (VCD_{24}). The *error bars* indicate 95 % confidence interval, $n = 3$. $**p < 0.005$; $*p < 0.05$

increased incubation time on the efficacy of the complex. There is no remarkable difference in the transfection efficiency of lipoplexes sheared for 15 min (Fig. 3a). The slight decrease in transfection efficiency of lipoplex sheared for 2 h maybe attributed to the higher incubation time compared to the manufacturer's suggested optimal duration as it is also seen in the case of the lipoplex incubated for 2 h in the absence of any shear stress. Surprisingly, there is higher cell growth when cells are transfected with lipoplex sheared for 2 h, seen from the 1.2 population doublings for cells transfected with sheared lipoplex compared to the 0.6 population doublings for cells transfected with lipoplex incubated for 2 h without shear (Fig. 3b). Our data do not suggest any explanation for this observation of comparable transfectability and reduced growth inhibition by lipoplex subjected to shear stress.

Shear stress affects the transfectability of CHO-S cells

Next we subjected CHO-S to low shear stress for varying durations of time and subsequently immediately transfected them. Figure 4a shows the transfection efficiency of cells transfected without exposure to shear stress or transfected after 15 and 120 min of exposure to shear stress. A short duration 15 min exposure of cells to shear stress did not decrease their transfectability significantly. The transfection efficiency however decreased significantly when the cells

were subjected to shear stress for 2 h prior to transfection. As expected from the previous results, VCD did not change significantly immediately after exposure of cells to shear stress (see gray bars in Fig. 4b). The average number of 0.9 population doublings in 24 h after exposure to shear stress was significantly higher for cells exposed to shear stress for short duration prior to transfection compared to the cells transfected without exposure to shear (average 0.5 population doublings, see white bars in Fig. 4b).

For both cases where either the lipoplex or cells are subjected to shear stress followed by transfection, VCD increases in the 24 h period post transfection. This is unlike the case when cells are exposed to shear stress in presence of lipoplex where the VCD decreases in the 24 h period after exposure to shear. A comparison of Figs. 2a, 3b and 4b thus suggests that cell growth is adversely affected by the presence of lipoplex during exposure of cells to shear stress.

Toxicity of lipoplex is not solely attributable to liposome

To understand whether the effect of shear stress during lipofection is exclusively due to the liposome, we subjected CHO-S cells to shear stress in the presence of liposome at a concentration equivalent to its concentration in the lipoplex. In the absence of shear stress, an average 1.9 and 1.2 population doublings were observed in 24 h in the absence and presence of

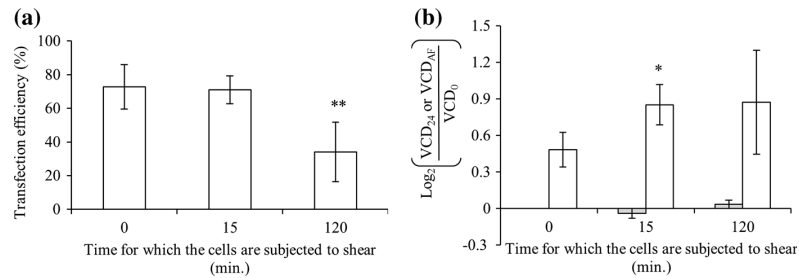


Fig. 4 Shear stress reduces transfectability of CHO-S cells. CHO-S cells were subjected to low shear stress for 120 min and subsequently transfected at different time points. **a** Transfection efficiency **b** Viable cell density (VCD) normalized to initial viable cell density. Immediately after subjecting cells to shear

stress (grey bars), 24 h after subjecting cells to shear stress for indicated time (white bars). Initial viable cell density (VCD_0), viable cell density immediately after flow for the indicated time (VCD_{AF}), 24 h after flow (VCD_{24}). The error bars indicate 95 % confidence interval, $n = 3$. ** $p < 0.005$; * $p < 0.05$

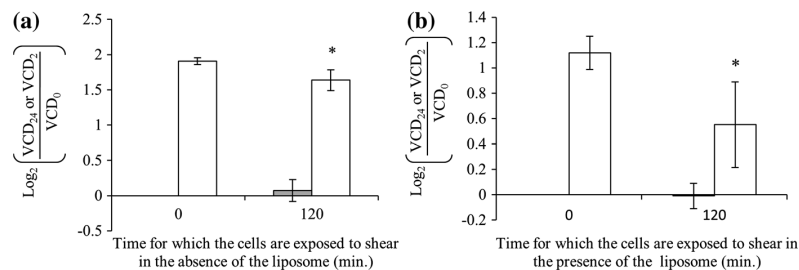


Fig. 5 Exposure of CHO-S cells to shear stress in presence of liposome causes reduction in cell growth. CHO-S cells were subjected to shear stress in the presence or absence of lipofectamine 2000 for 120 min and monitored for changes in cell density immediately after 120 min of flow and after 24 h of incubation. **a** Viable cell density (VCD) normalized to initial viable cell density for CHO-S cells subjected to a low shear stress without the liposome. **b** Viable cell density normalized to

initial viable cell density for CHO-S cells subjected to a low shear stress with the liposome. Viable cell density immediately after subjecting cells to shear stress for 120 min (grey bars), after 24 h of incubation (white bars). Initial viable cell density (VCD_0), viable cell density immediately after flow (VCD_2), 24 h after flow (VCD_{24}). The error bars indicate 95 % confidence interval, $n = 3$. * $p < 0.05$

liposome respectively (Fig. 5). Thus the presence of liposome by itself adversely affects cell growth. When cells are exposed to shear stress in the absence and presence of liposome, cells show growth at a lower average of 1.6 and 0.6 population doublings. Thus the adverse effect of liposomes on cell growth is substantially enhanced in the presence of shear. This is however in contrast to the case when cells are subjected to shear stress in presence of the lipoplex, where a 25 % decrease in VCD was observed (Fig. 2a). This suggests that the adverse effect on cell growth seen when cells are exposed to shear stress in presence of lipoplex is not attributable solely to the liposome.

Shear stress does not affect toxicity of lipoplex in inefficiently transfected K562 cell line

The results above indicate that toxicity of lipoplex is increased in presence of shear stress. We next evaluated whether the same effect is seen in K562 cells, which are not as efficiently transfected by Lipofectamine 2000 as CHO-S cells. There was no substantial cell death immediately after exposure of cells to shear stress, both in absence or presence of lipoplex (grey bars in Fig. 6a, b). The cell density of K562 cells doubled 24 h post transfection irrespective of whether cells were incubated with lipoplex in the absence or presence of shear stress (white bars Fig. 6a, b). The transfection

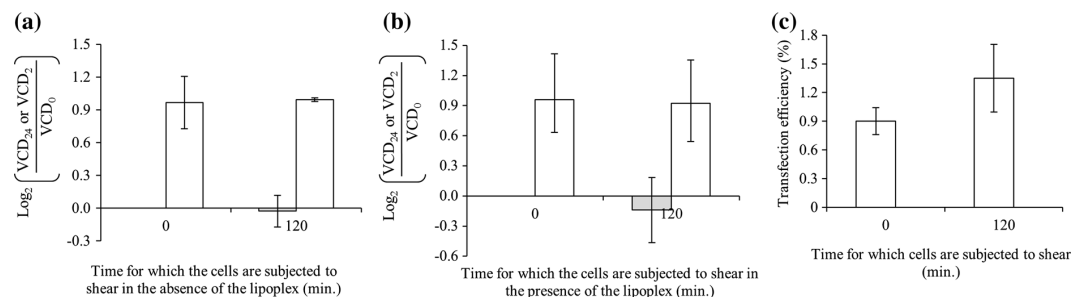


Fig. 6 Effect of shear stress on cell density and transfection efficiency of K562 cells in the presence or absence of the lipoplex. K562 cells were subjected to low shear stress for 120 min in the presence or absence of the lipoplex and monitored for changes in cell density and viability immediately after flow and after 24 h of incubation. **a** Viable cell density (VCD) normalized to initial viable cell density for K562 cells subjected to a low shear stress for 120 min. **b** Viable cell density

normalized to initial viable cell density for K562 cells subjected to a low shear stress in the presence of lipoplex for 120 min. Immediately after subjecting cells to shear stress (grey bars), after 24 h (white bars). Initial viable cell density (VCD_0), viable cell density immediately after flow (VCD_2), 24 h after flow (VCD_{24}). **c** Transfection efficiency. The error bars indicate 95 % confidence interval, $n = 2$

efficiency of K562 cells is low, and is slightly, but not significantly, increased in the presence of shear (Fig. 6c). Thus the adverse effect of lipoplex on cell growth in the presence of shear is not seen in the inefficiently transfected K562 cell line.

Discussion

Shear stress is known to affect various aspects of cell physiology like endocytosis and pinocytosis (Davies et al. 1984; Kudo et al. 1997; Rizzo et al. 2003), membrane fluidity (Butler et al. 2001; Haidekker et al. 2000), inducing membrane fusion (Kogan et al. 2014), and more recently it was shown to facilitate uptake of extracellular macromolecules (Hallow et al. 2008; Sharei et al. 2013), possibly through formation of transient pores in the cell membrane (Mardikar and Niranjana 2000). It is known that high levels of shear stress are deleterious to suspension cells. For example, McQueen et al. subjected mouse myeloma cells to high shear stress in capillary tubes and showed that flow caused lysis which was observed at a wall shear stress of 1800 dyne/cm² (McQueen et al. 1987). Our simple flow apparatus comprising of pumping suspension cells using a peristaltic pump also showed similar results for CHO-S cells with high levels of cell death at high wall shear stress, but not at the low and moderate shear stress levels. The use of a peristaltic pump allows long duration aseptic unidirectional flow

of cells. However, in this set-up, unlike systems using syringe pumps, cells are also subjected to shear stress in the peristaltic pump head, but this effect has been controlled by keeping the fluid flow rate constant and varying the diameter of the fluid path to vary wall shear stress. Though shear stress has been known to affect cell survival, and for reasons described above can be expected to affect liposomal delivery of cargo to suspension cells, to our knowledge there have been no studies explicitly analyzing the effect of shear stress on liposomal DNA delivery to suspension cells.

We report that exposure of CHO-S cells to shear stress in the presence of lipoplex reduced transfection efficiency and cell growth in the subsequent 24 h period while causing greater cell clumping. We further evaluated whether this effect could be attributed simply to the interaction of the cells with lipid in the presence of shear. The size and zeta potential of lipofectamine 2000 has been reported to change upon complexation with DNA (Son et al. 2000). In an uncomplexed state, the reported zeta potential was -4 mV and upon complexation with plasmid DNA, it was -24 mV. The hydrodynamic diameter in a complexed state was reported to increase to 488 nm from 319 nm in an uncomplexed state (Son et al. 2000). Shearing of cells in presence of liposome alone also reduces cell growth in the subsequent 24-h period, though not to an extent similar to that due to the lipoplex. This suggests that the increased toxicity is not entirely explained by interaction of the liposome

alone with the cell in the presence of shear stress. This could be due to the differences in zeta potential and/or size of the liposome and lipoplex reported in the literature. To further check if the increased toxicity due to lipoplex in the presence of shear stress might be due to long-lasting modification of the lipoplex with shear, we subjected the lipoplex to shear, subsequently using the sheared lipoplex for transfection. It was observed that there is only a slight reduction in efficiency following the 2 h incubation of lipoplex both in presence and absence of shear stress. Such slight loss of transfection efficiency was previously reported where the DNA–Lipofectamine 2000 complexes were relatively stable and continued to provide high transfection efficiency even up to 2 h after complexation (Dalby et al. 2004). This however does not preclude a change in shape and therefore increased toxicity when lipoplex is sheared along with cells. Interestingly, there is a slight increase in cell growth when cells are transfected with sheared lipoplex compared to the cell growth upon transfection with lipoplex incubated under static conditions.

The reduced transfection efficiency and increased lipoplex toxicity observed at low shear stress could also possibly be due to the effect of shear stress on cells, making the cells more susceptible to lipoplex toxicity. In that case, these effects should be seen when transfection is carried out immediately after subjecting cells to shear stress. Indeed, subjecting CHO cells to sustained low shear stress prior to transfection (for 2 h), resulted in reducing the transfectability of CHO cells, but did not increase cell death. This indicates that the observed effect of reduced transfection efficiency could be due to shear stress affecting the ability of cells to uptake and/or deliver the foreign DNA to the nucleus. This also suggests that the increased toxicity of lipoplex in presence of shear stress is a result of cellular interaction with lipoplex in the presence of shear stress and likely not due to other long-term cellular changes upon exposure to shear stress. Lipoplexes with low toxicity in vitro, when injected into the blood stream where they are subjected to shear stress, have resulted in significant toxicity to blood cells in the form of transient leukopenia and neutropenia both in animal models and human clinical trials (Freimark et al. 1998; Li et al. 1999; Ruiz et al. 2001; Tousignant et al. 2000; Zhang et al. 2005), though the cause of this is not clear. We did not observe a similar effect of higher toxicity in presence of shear stress in K562 cells. K562 cells were not efficiently transfected by the lipoplex used

in this study whereas CHO-S are efficiently transfected. It remains to be seen whether transfectability has any role in the relationship between shear stress and toxicity of the lipoplex.

In conclusion, enhanced toxicity and reduced transfection efficiency of lipoplex is observed in CHO-S cells exposed to shear stress. Further studies will be necessary to fully understand the mode of toxicity. We propose that this factor should be taken into account in the design and planning for large-scale transfections in bioreactors for transient protein expression. Our results may also be relevant to gene therapy where shear stress may contribute to performance of in vitro static cell cultures not being predictive of performance in animal models where the lipoplex is intravenously injected and evaluation of liposomal delivery agents in the presence of shear stress could be considered as an intermediate testing step before animal studies for gene therapy.

Acknowledgments MG acknowledges funding from CSIR (CSC0302).

References

- Baldi L, Hacker DL, Adam M, Wurm FM (2007) Recombinant protein production by large-scale transient gene expression in mammalian cells: state of the art and future perspectives. *Biotechnol Lett* 29:677–684. doi:10.1007/s10529-006-9297-y
- Butler PJ, Norwich G, Weinbaum S, Chien S (2001) Shear stress induces a time- and position-dependent increase in endothelial cell membrane fluidity. *Am J Physiol Cell Physiol* 280:C962–C969
- Charoenphol P, Huang RB, Eniola-Adefeso O (2010) Potential role of size and hemodynamics in the efficacy of vascular-targeted spherical drug carriers. *Biomaterials* 31:1392–1402. doi:10.1016/j.biomaterials.2009.11.007
- Chatzizisis YS, Coskun AU, Jonas M, Edelman ER, Feldman CL, Stone PH (2007) Role of endothelial shear stress in the natural history of coronary atherosclerosis and vascular remodeling: molecular, cellular, and vascular behavior. *J Am Coll Cardiol* 49:2379–2393. doi:10.1016/j.jacc.2007.02.059
- Dalby B, Cates S, Harris A, Ohki EC, Tilkins ML, Price PJ, Ciccione VC (2004) Advanced transfection with Lipofectamine 2000 reagent: primary neurons, siRNA, and high-throughput applications. *Methods* 33:95–103. doi:10.1016/j.ymeth.2003.11.023
- Davies PF, Dewey CF, Bussolari SR, Gordon EJ, Gimbrone MA (1984) Influence of hemodynamic forces on vascular endothelial function. In vitro studies of shear stress and pinocytosis in bovine aortic cells. *J Clin Invest* 73: 1121–1129

- Doshi N, Prabhakarparandian B, Rea-Ramsey A, Pant K, Sundaram S, Mitragotri S (2010) Flow and adhesion of drug carriers in blood vessels depend on their shape: a study using model synthetic microvascular networks. *J Control Release* 146:196–200. doi:10.1016/j.jconrel.2010.04.007
- Freimark BD et al (1998) Cationic lipids enhance cytokine and cell influx levels in the lung following administration of plasmid: cationic lipid complexes. *J Immunol* 160:4580–4586
- Fujiwara T, Akita H, Furukawa K, Ushida T, Mizuguchi H, Harashima H (2006) Impact of convective flow on the cellular uptake and transfection activity of lipoplex and adenovirus. *Biol Pharm Bull* 29:1511–1515
- Haga JH, Li Y-SJ, Chien S (2007) Molecular basis of the effects of mechanical stretch on vascular smooth muscle cells. *J Biomech* 40:947–960. doi:10.1016/j.jbiomech.2006.04.011
- Haidekker MA, L'Heureux N, Frangos JA (2000) Fluid shear stress increases membrane fluidity in endothelial cells: a study with DCJV fluorescence. *Am J Physiol Heart Circ Physiol* 278:H1401–H1406
- Hallow DM, Seeger RA, Kamaev PP, Prado GR, LaPlaca MC, Prausnitz MR (2008) Shear-induced intracellular loading of cells with molecules by controlled microfluidics. *Biotechnol Bioeng* 99:846–854. doi:10.1002/bit.21651
- Han J, Zern BJ, Shuvaev VV, Davies PF, Muro S, Muzykantsov V (2012) Acute and chronic shear stress differently regulate endothelial internalization of nanocarriers targeted to platelet-endothelial cell adhesion molecule-1. *ACS Nano* 6:8824–8836. doi:10.1021/nl302687n
- Harris SS, Giorgio TD (2005) Convective flow increases lipoplex delivery rate to in vitro cellular monolayers. *Gene Ther* 12:512–520. doi:10.1038/sj.gt.3302397
- Heo J, Sachs F, Wang J, Hua SZ (2012) Shear-induced volume decrease in MDCK cells. *Cell Physiol Biochem* 30:395–406. doi:10.1159/000339033
- Klingberg H, Loft S, Oddershede LB, Moller P (2015) The influence of flow, shear stress and adhesion molecule targeting on gold nanoparticle uptake in human endothelial cells. *Nanoscale* 7:11409–11419. doi:10.1039/c5nr01467k
- Kogan M, Feng B, Nordén B, Rocha S, Beke-Somfai T (2014) Shear-induced membrane fusion in viscous solutions. *Langmuir* 30:4875–4878. doi:10.1021/la404857r
- Kudo S, Ikezawa K, Ikeda M, Oka K, Tanishita K (1997) Albumin concentration profile inside cultured endothelial cells exposed to shear stress. In: *ASME/BED Proceedings of bioengineering conference*, vol. 35, pp. 547–548
- Li S et al (1999) Effect of immune response on gene transfer to the lung via systemic administration of cationic lipidic vectors. *Am J Physiol* 276:L796–L804
- Lin A, Sabnis A, Kona S, Nattama S, Patel H, Dong JF, Nguyen KT (2010) Shear-regulated uptake of nanoparticles by endothelial cells and development of endothelial-targeting nanoparticles. *J Biomed Mater Res A* 93:833–842. doi:10.1002/jbm.a.32592
- Mardikar SH, Niranjan K (2000) Observations on the shear damage to different animal cells in a concentric cylinder viscometer. *Biotechnol Bioeng* 68:697–704. doi:10.1002/(SICI)1097-0290(20000620)68:6<697:AID-BIT14>3.0.CO;2-6
- McQueen A, Meilhoc E, Bailey J (1987) Flow effects on the viability and lysis of suspended mammalian cells. *Biotechnol Lett* 9:831–836. doi:10.1007/bf01026191
- Mennesson E, Erbacher P, Kuzak M, Kieda C, Midoux P, Pichon C (2006) DNA/cationic polymer complex attachment on a human vascular endothelial cell monolayer exposed to a steady laminar flow. *J Control Release* 114:389–397. doi:10.1016/j.jconrel.2006.06.006
- Patil VRS, Campbell CJ, Yun YH, Slack SM, Goetz DJ (2001) Particle diameter influences adhesion under flow. *Biophys J* 80:1733–1743
- Resnick N, Yahav H, Shay-Salit A, Shushy M, Schubert S, Zilberman LCM, Wofovitz E (2003) Fluid shear stress and the vascular endothelium: for better and for worse. *Prog Biophys Mol Biol* 81:177–199. doi:10.1016/S0079-6107(02)00052-4
- Rizzo V, Morton C, DePaola N, Schnitzer JE, Davies PF (2003) Recruitment of endothelial caveolae into mechanotransduction pathways by flow conditioning in vitro. *Am J Physiol Heart Circ Physiol* 285:H1720–H1729. doi:10.1152/ajpheart.00344.2002
- Ruiz FE, Clancy JP, Perricone MA, Bebok Z, Hong JS, Cheng SH, Meecker DP, Young KR, Schoumacker RA, Weatherly MR, Wing L, Morris JE, Sindel L, Rosenberg M, van Ginkel FW, McGhee JR, Kelly D, Lyrene RK, Sorscher EJ (2001) A clinical inflammatory syndrome attributable to aerosolized lipid-DNA administration in cystic fibrosis. *Hum Gene Ther* 12:751–761. doi:10.1089/104303401750148667
- Sharei A, Zoldan J, Adamo A, Sim WY, Cho N, Jackson E, Mao S, Schneider S, Han MJ, Lytton-Jean A, Basto PA, Jhunjhunwala S, Lee J, Heller DA, Kang JW, Hartoularos GC, Kim KS, Anderson DG, Langer R, Jensen KF (2013) A vector-free microfluidic platform for intracellular delivery. *Proc Natl Acad Sci USA* 110:2082–2087. doi:10.1073/pnas.1218705110
- Shin HS, Kim HJ, Sim SJ, Jeon NL (2009) Shear stress effect on transfection of neurons cultured in microfluidic devices. *J Nanosci Nanotechnol* 9:7330–7335
- Son KK, Patel DH, Tkach D, Park A (2000) Cationic liposome and plasmid DNA complexes formed in serum-free medium under optimum transfection condition are negatively charged. *Biochim et Biophys Acta Biomembr* 1466:11–15. doi:10.1016/S0005-2736(00)00176-0
- Tousignant JD, Gates AL, Ingram LA, Johnson CL, Nietupski JB, Cheng SH, Eastman SJ, Scheule RK (2000) Comprehensive analysis of the acute toxicities induced by systemic administration of cationic lipid: plasmid DNA complexes in mice. *Hum Gene Ther* 11:2493–2513. doi:10.1089/10430340050207984
- Vickroy B, Lorenz K, Kelly W (2007) Modeling shear damage to suspended CHO cells during cross-flow filtration. *Biotechnol Prog* 23:194–199. doi:10.1021/bp060183e
- White CR, Frangos JA (2007) The shear stress of it all: the cell membrane and mechanochemical transduction. *Philos Trans R Soc B Biol Sci* 362:1459–1467. doi:10.1098/rstb.2007.2128
- Zhang JS, Liu F, Huang L (2005) Implications of pharmacokinetic behavior of lipoplex for its inflammatory toxicity. *Adv Drug Deliv Rev* 57:689–698. doi:10.1016/j.addr.2004.12.004



Contents lists available at ScienceDirect

Biochemical Engineering Journal

journal homepage: www.elsevier.com/locate/bej

Regular article

Towards in situ continuous feeding via controlled release of complete nutrients for fed-batch culture of animal cells

Jyoti Rawat^{a,b}, Mugdha Gadgil^{a,b,*}^a Chemical Engineering and Process Development, CSIR-National Chemical Laboratory, Pune, 411008, India^b Academy of Scientific and Innovative Research (AcSIR), CSIR-National Chemical Laboratory Campus, Ghaziabad, 201002, India

HIGHLIGHTS

- In situ delivery of a multi-component nutrient feed by hydrogel (NutriGel).
- NutriGel sustains release of amino acids for at least 7 days.
- Independent modulation of release rates of 16 amino acids demonstrated.
- NutriGel enables a completely closed system for fed batch culture of animal cells.
- NutriGel improved IVCD and productivity by 1.8 and 3-fold compared to batch culture.

ARTICLE INFO

Keywords:

In situ nutrient release
CHO cells
Amino acids
Fed-batch
Closed system
Hydrogel for continuous feeding

ABSTRACT

Small-scale culture of animal cells in suspension is of importance for many applications. At a small-scale, fed-batch is achieved either by manual bolus feeding or the use of liquid handling robots. In this study, we report an alternate application of a hydrogel for in situ continuous delivery of a nutrient feed comprising 18 amino acids, vitamins, antioxidants, and trace elements. We show that amino acid release is sustained for at least seven days. Importantly, release rates of individual amino acids can be independently modulated by changing their loading. We demonstrate the application of this hydrogel for complete in situ feeding of nutrients to a suspension adapted CHO cell line expressing IgG leading to 2.7-fold and 4-fold improvement in integral viable cell density (IVCD) and volumetric productivity respectively. This is similar to improvements obtained by bolus liquid feeding. Further, supplying glucose from the same hydrogel to eliminate manual feeding led to a 1.8-fold increase in IVCD accompanied by a 3-fold increase in volumetric productivity as compared to batch culture. In summary, this study provides a proof-of-concept that hydrogels can enable completely closed in situ feeding for mammalian cell culture requiring no external intervention. Such continuous in situ delivery can potentially enable closed culture systems maintaining nutrients at low levels mimicking physiological concentrations.

1. Introduction

Small-scale culture of animal cells in suspension is of importance for many applications such as process development for production of recombinant proteins and viral vaccines, stem cell culture, and cell therapy applications such as the recently FDA approved CAR-T therapy [1]. Increasing culture longevity and/or cell growth is of importance for such applications. In vitro culture of animal cells requires a large number of nutrients including sugars such as glucose, most amino acids, vitamins, antioxidants, bulk ions, and trace elements. Some of these

nutrients, such as glucose and amino acids, are substantially consumed during culture, while others such as bulk salts may not show an appreciable change in concentration [2]. Recent reports indicate that high initial nutrient concentrations above physiological levels may result in metabolic differences in cells in culture, which can result in reduced biological relevance of in vitro cell culture models [3]. Feeding nutrients during the course of the culture enables replenishment of the exhausted nutrients to prevent their limitation while at the same time avoiding initial oversupply and associated waste metabolite production, which could be inhibitory to cell growth [4–6]. The value of such

Abbreviations: HEMA, 2-hydroxyethyl methacrylate; CAR-T, Chimeric antigen receptor T cell; EGDMA, Ethylene glycol dimethacrylate; PITS, Phenylisothiocyanate; IVCD, Integral viable cell density

* Corresponding author at: Chemical Engineering and Process Development, CSIR-National Chemical Laboratory, Pune, 411008, India.

E-mail address: mc.gadgil@ncl.res.in (M. Gadgil).

<https://doi.org/10.1016/j.bej.2019.107436>

Received 31 July 2019; Received in revised form 8 November 2019; Accepted 14 November 2019

Available online 15 November 2019

1369-703X/ © 2019 Elsevier B.V. All rights reserved.

Table 1
Compositions of payloads used in this study.

	L-Amino acids ^{a,b}	HEPES	Glucose	Vitamins	Trace elements	Thioctic acid	Antioxidant	Nucleoside precursors	Linoleic acid
NutriGel ₁	+ ^a	+		+	+	+	+	+	+
NutriGel ₂ ^H	+ ^b	+							
NutriGel ₂ ^G	+ ^b		+						
NutriGel ₁ ^T	+ ^a	+		+	+	+	+	+	+
NutriGel ₁ ^{AA,T,G}	+ ^a		++						
NutriGel ₁ ^{T-V}	+ ^a	+	+		+	+	+	+	
NutriGel ₁ ^{T-TE}	+ ^a	+	+	+		+	+	+	
NutriGel ₁ ^{T-AO}	+ ^a	+	+	+	+	+		+	
NutriGel ₁ ^{T-N}	+ ^a	+	+	+	+	+	+	+	
NutriGel ₁ ^{T-TA}	+ ^a	+	+	+	+	+	+	+	
NutriGel ₂ ^{HVT,T}	+ ^b	+		++++	++++	+	+	+	
NutriGel ₁ ^{T,G}	+ ^a	+	++	+	+	+	+	+	+
L-Amino acids ^a (mg)	Arginine hydrochloride 29, Asparagine monohydrate 2, Aspartic acid 1, Cysteine dihydrochloride 5, Cystine hydrochloride monohydrate 6, Glutamic acid 1.5, Histidine hydrochloride monohydrate 5, Isoleucine 11, Leucine 11, Lysine hydrochloride 16, Methionine 3, Phenylalanine 7, Proline 4, Serine 5, Threonine 10, Tryptophan 1.7, Tyrosine 10, Valine 10, Glutamine 25								
L-Amino acids ^b (mg)	Arginine hydrochloride 8, Asparagine monohydrate 8, Aspartic acid 8, Cysteine dihydrochloride 8, Cystine hydrochloride monohydrate 8, Glutamic acid 8, Histidine hydrochloride monohydrate 8, Isoleucine 8, Leucine 8, Lysine hydrochloride 8, Methionine 8, Phenylalanine 8, Proline 8, Serine 8, Threonine 8, Tryptophan 8, Tyrosine 8, Valine 8, Glutamine 8								
Trace elements (mg)	Ammonium metavanadate 0.00006, Ammonium molybdate tetrahydrate 0.0006, Copper sulphate pentahydrate 0.0001, Ferric nitrate nonahydrate 0.005, Ferrous sulphate heptahydrate 0.04, Nickel chloride 0.00001, Sodium metasilicate nonahydrate 0.001, Sodium selenite 0.001, Stannous chloride dehydrate 0.00001, Zinc sulphate heptahydrate 0.04								
Vitamins (mg)	Ca-D-Pantothenic acid 0.2, Choline chloride 0.9, D-Biotin 0.0004, Folic acid 0.3, Niacinamide 0.2, Pyridoxal hydrochloride 0.2, Pyridoxine hydrochloride 0.003, Riboflavin 0.02, Thiamine hydrochloride 0.2, Vitamin B12 0.07, Myo-Inositol 1.3								
Antioxidants (mg)	L-Ascorbic acid 2, Ethanolamine hydrochloride 1.4, Glutathione reduced 0.2, Putrescine dihydrochloride 0.01								
Nucleoside precursors (mg)	Hypoxanthine 0.2, Thymidine 0.04								
Miscellaneous (mg)	Linoleic acid 0.004								
Glucose (mg)	Glucose 100								
Thioctic acid (mg)	Thioctic acid 0.011								
HEPES (mg)	HEPES 100								

(x-number of + indicates x-times of concentration indicated above, ^{a,b} indicate the amino acid composition type, ^T Indicates the presence of 4 mg tyrosine in the bottom layer of the hydrogel).

feeding strategies to achieve higher cell growth and culture longevity has been amply demonstrated in the development of fed-batch processes for recombinant protein production [2,5,7,8]. In small-scale cultures, nutrient feeding is predominantly made possible by bolus addition of highly concentrated feed solutions. This is usually carried out using liquid handling robots in the case of microreactors or manually for the ubiquitous shake flasks or spinner flasks.

Bolus feed addition has several limitations. The solubility of some components, such as tyrosine, is low at neutral pH, and pH adjustments are necessary to achieve the desired solubility [9,10]. These can contribute to increasing the osmolarity of the culture. Feeding such concentrated solutions can also lead to large step increases in concentration and pH at the time of feeding, which may be undesirable [11,12]. Bolus feeding during process development may lock-in production processes to have intermittent feeding strategies. Manual feeding also requires frequent handling of the cultures, which increases the chances of operator-induced errors. Lesser manual intervention and fewer steps with limited exposure to the environment reduce the probability of contamination. This is especially important for the imminent cell-based therapies where limited quantity of patient-derived cells are available, and cells are the final product of interest that cannot be subjected to sterilization [13].

The disadvantages of manual bolus feeding can be overcome through the use of a continuous feeding process, not requiring manual intervention. Automated closed systems have been demonstrated for ex vivo production of cells such as human placental, human CD4, and CD8 T lymphocytes, [14], and stem cell [15] for cell-derived therapies. Automated continuous feeding for small-scale platforms cannot however, be achieved without upgrading to additional infrastructure and robotic platforms [16–18]. These systems require appreciable capital investment. An alternative approach for continuous feeding is the continuous in situ delivery of nutrients via diffusion through hydrogels. Hydrogels are three-dimensional polymer networks that swell in water

[19]. Hydrogels have been extensively used for biomedical applications like the slow release of drugs, hormones, and growth factors [20]. Our group has previously described the use of hydrogels for continuous in situ feeding of individual nutrients such as glucose in shake flasks [21]. However, mammalian cells in culture require feeding of a complex mixture comprising many nutrients. This study aimed to investigate the feasibility of developing hydrogels for simultaneous in situ release of all nutrients provided in feed formulations for a fed-batch culture of mammalian cells such as glucose, amino acids, and vitamins. Such in situ diffusion-based continuous delivery of nutrients can enable fed-batch culture in a completely closed system requiring only gas exchange.

In this study, we have used suspension adapted CHO cells expressing recombinant IgG as a model system to establish the proof-of-concept for using hydrogels for in situ feeding of all nutrients required for the culture of animal cells. We characterize the individual rate constants for a simultaneous release of amino acids through the hydrogel. Alanine and glycine are formed as waste metabolites during culture and hence are not included in the feed. In the range of loading evaluated, we show that the amino acid release rates are proportional to the initial loading of the amino acid. This feature enables independent control of the release rates for all amino acids as per the requirement of the particular cell line. Tyrosine and cystine are expected to be an exception to this due to their poor solubility, and indeed tyrosine, whose release rate is measured, shows a constant zero-order release. We show that in situ delivery of all nutrients led to a 1.8-fold (p value 0.004) increase in integral viable cell density (IVCD) accompanied by a 3-fold (p value 0.011) increase in volumetric productivity as compared to batch culture. To our knowledge, this study demonstrates, for the first time, the feasibility of achieving a completely closed in situ feeding platform for continuous feeding of complex nutrient feeds to animal cells, which does not require manual intervention or liquid handling technology.

2. Materials and methods

2.1. Hydrogel synthesis

Poly-HEMA hydrogels were synthesized using 2-hydroxyethyl methacrylate (HEMA, 97% pure, Sigma-Aldrich Corp, USA) monomer and ethylene glycol dimethacrylate (EGDMA, Sigma-Aldrich Corp, USA) crosslinker at 86:14 mol/mol HEMA:EGDMA in the presence of an initiator Azobisisobutyronitrile (0.5%, Sigma Aldrich Corp, USA). A bottom layer of the hydrogel was created by polymerizing 200 μ L of the HEMA:EGDMA mixture in a 1.3 cm diameter glass disc at 75 °C for 1.5 h. A cavity was then formed over the bottom layer using an appropriate mould and 400 μ L of the HEMA:EGDMA mixture by incubation at 75 °C for 1.25 h. The diameter of the cavity was 9 mm. Subsequently, the solid powder of the payload was added into this cavity. The exact composition of the payload varies in different experiments and is described in Table 1. Four hundred and fifty microliters of the HEMA:EGDMA mixture was used to create the monolithic central reservoir and final layer of the hydrogel, sealing the cavity. The hydrogels were then washed in sterile ultrapure water for two days. After washing, the hydrogels were sterilized using UV for 25 min on each side of the hydrogel. Hydrogels were incubated overnight in culture medium before addition to the cultures. The HEMA:EGDMA hydrogel was previously assessed for cytotoxicity to CHO cells and found to be non-toxic as processed [21].

2.2. Release kinetics for amino acids

The release kinetics of amino acids were analyzed at 37 °C. The hydrogel was added into phosphate-buffered saline (PBS) with 0.05% sodium azide under shaking conditions to simulate conditions during release in shake flasks. Samples were taken on alternate days for amino acid concentration measurement for 16 days. Amino acid quantification was carried out using HPLC. The samples were subjected to precolumn derivatization with phenylisothiocyanate (PITC) and the derivatized amino acids were quantified on HPLC (Agilent 1200 infinity series) with reverse phase C18 column (Purospher star RP18 (5 μ m) end-capped, Merck, Darmstadt, Germany). Briefly, 100 μ L of the sample was spiked with 15 μ g of norleucine as internal standard and lyophilized. Subsequently, 20 μ L of methanol:water:trimethylamine 2:1:1 (v/v) was added, vortexed and lyophilized. Further, 20 μ L of methanol:water:trimethylamine:PITC 7:1:1:1 (v/v) was added, vortexed, incubated for 20 min at room temperature and lyophilized. Derivatized samples were resuspended in 1 mL of eluent A (85 mM sodium acetate and 0.3 mM sodium azide in 98% water and 2% acetonitrile, pH 5.2, (w/v)). Chromatography was carried out after injecting 5 μ L of derivatized sample using elution gradient of $T_{0 \text{ min}} = 3\%$ eluent B (100% acetonitrile), $T_{25 \text{ min}} = 13\%$ eluent B, $T_{45 \text{ min}} = 50\%$ eluent B, $T_{46 \text{ min}} = 3\%$ eluent B. Flow rate was maintained at 0.8 mL min⁻¹. Eluted derivatives were detected with a diode array detector at 254 nm with a bandwidth of 4 nm. The peak area for each amino acid was normalized to the internal standard. Amino acid concentration was calculated using response factor calculated from the peak area of the respective amino acid (normalized to norleucine) in a standard containing 15 μ g/mL of aspartate, glutamate, glutamine, glycine, asparagine, serine, histidine, threonine, arginine, alanine, proline, tyrosine, valine, methionine, cystine, isoleucine, leucine, phenylalanine, tryptophan and lysine. It is important to note that in this method for amino acid measurement, cysteine and cystine were not resolved as separate peaks but coeluted as a single peak and hence could not be accurately quantified.

2.3. Cell culture

A suspension CHO cell line expressing IgG, provided by Inbiopro Solutions (Bangalore, India), was used to evaluate the effect of the

addition of the hydrogels to increase culture longevity and productivity. Cells were inoculated at a density of 0.3×10^6 cells/mL in 25 mL culture volume in 100 mL Erlenmeyer flasks (Borosil). Cells were regularly passaged in our in-house medium formulation based on DMEM:F12 containing 3 g/L glucose and 5 mM glutamine. The complete medium formulation is provided in Supplementary Table 1. For fed batch experiments, shake flasks cultures were incubated at 37 °C, 10% CO₂, 110 rpm. Glucose was fed to bring its concentration back to 2 g/L: at viability above 85%, glucose was fed when its concentration decreased below 2 g/L, while at viability below 85%, glucose was fed when the concentration decreased below 1.5 g/L. For cultures supplemented with NutriGel₂^{HVT,T}, cells were inoculated at 5×10^6 cells/mL in 50 mL culture volume. These cultures were incubated at 37 °C, 10% CO₂, 130 rpm. Glucose was fed to bring its concentration back to 4 g/L: at viability above 85%, glucose was fed when its concentration decreased below 4 g/L, while at viability below 85% glucose was fed when the concentration decreased below 2.5 g/L. The hydrogel was added on day 3 for all the cultures and at day 0 for the NutriGel₂^{HVT,T} cultures. For bolus fed cultures, cultures were fed with 0.5X of the corresponding feed (20X) on day 3,6,8,10 or day 3,4,6,8. A total of 2X of the feed was added, where 1X corresponds to medium concentration without the bulk salts. A total of 2.5 mL liquid feed was added to 25 mL culture volume of the bolus fed cultures. The hydrogel is added as a pre-swollen solid, so there is no volume change due to hydrogel addition. The composition of the bolus liquid feed was the same as NutriGel^T. The amount of payload in NutriGel^T was 250 mg, while the liquid bolus feed addition resulted in the addition of 125 mg of the feed, both to the same initial culture volume. The hydrogel payload was kept higher due to loss of payload during the initial washing and pre-incubation of the hydrogel for at least 2.5 days to remove unpolymerized monomers. The loss of payload was variable for the different components. Glucose was fed to maintain glucose concentration between 2–2.5 g/L, and a total of 7 mM of glutamine was also fed to the cultures. Samples were taken every alternate day for measuring cell density, viability, glucose concentration. Cell density was quantified by manual counting using a hemocytometer. Viability was assessed using the trypan blue dye exclusion assay. Glucose concentration was measured using a YSI Biochemistry Analyzer. Volumetric IgG titer was determined by a sandwich ELISA. Briefly, ELISA plates were coated with capture antibody-rabbit anti-human IgG and subsequently blocked with 1% bovine serum albumin (BSA) in phosphate-buffered saline (PBS). 0.01% Tween 20 in PBS was used to wash plates. Human IgG was used to generate a standard curve for quantitation. HRP conjugated rabbit anti-human IgG (Merck Millipore, Mumbai, India) was used to detect IgG in culture followed by the addition of substrate TMB/H₂O₂ (Genei Laboratories Pvt Ltd, India). The reaction was stopped using 1 M H₂SO₄. Absorbance was measured at 450 nm on Bio-Rad iMark microplate reader (Bio-Rad Laboratories, Mumbai, India). Samples selected for ELISA had a viability of 60% or more.

2.4. Statistical analysis

Two-tailed Student's *t*-test was used to determine the significance of the difference between each pair of data. All *p* values lower than the significance level of 0.05 are denoted by asterisks in figures. A *p* value < 0.05 is denoted by *, < 0.005 by **, and < 0.0005 by ***.

3. Results and discussion

Glucose and glutamine are the major nutrients consumed by mammalian cells. Amino acids other than glutamine have been shown to account for majority of the cell mass in proliferating mammalian cell lines, also indicating their importance to cell growth [22]. Various cell lines producing recombinant proteins have been shown to improve their productivity, product quality, and delay apoptosis upon supplementation of customized amino acid feed [23–28]. Depletion of even

non-essential amino acids, such as asparagine, has been reported to result in misincorporation of other amino acids during translation. This indicates the importance of maintaining adequate amino acid supply [29–31]. At the same time, recent reports have also shown that high concentrations of amino acids in the culture lead to the accumulation of inhibitory metabolites [32]. Thus, feeding amino acids is essential to maintain an adequate supply of nutrients while avoiding a large initial excess. We have previously reported the use of hydrogels for the in situ delivery of glucose to animal cell cultures. We now explore whether similar hydrogels can enable simultaneous in situ delivery of a mixture including 18 amino acids.

3.1. Hydrogels can maintain a continuous supply of amino acids for an extended duration suitable for supporting animal cell culture

A hydrogel formed by the bulk polymerization of HEMA with EGDMA as a crosslinker was evaluated for in situ release of a nutrient mixture including 18 amino acids. Since alanine and glycine are typically excreted by cells in culture, they were not included in the feed. Briefly, this hydrogel comprises a central monolithic reservoir system surrounded by a hydrogel layer. The nutrient payload is dispersed as a solid powder within the hydrogel matrix in the central reservoir. We first formulated a simple feed mixture having the same composition as the culture medium but without bulk salts. These hydrogels will be henceforth called NutriGel₁ (composition in Table 1). The release of amino acids from washed and pre-swollen NutriGel₁ was monitored in PBS buffer over a duration of 2 weeks. Cysteine/cystine could not be accurately quantified. Fig. 1a, b shows the cumulative release for 17 amino acids in the feed mixture. All amino acids continue to be released from the hydrogel for a period of at least seven days.

Release rate constants were further calculated for all amino acids. Assuming a 0.75 void fraction in the central reservoir and after accounting for the amino acid content lost during the wash, we calculate that at the initial amino acid loadings used, the concentrations of all amino acids in the reservoir except cysteine/cystine and tyrosine will be less than their solubility at 37 °C. Hence, the release rate is assumed to follow first-order release kinetics as described by the equation [33]

$$\frac{dm_i}{dt} = k_i(m_{0i} - m_i), \text{ resulting in } m_i = m_{0i} \left(1 - \frac{1}{e^{k_i t}}\right) \quad (1)$$

for $i = 1-17$, where m_i is the amount of i th amino acid released at time t , m_{0i} is the initial loading of the i th amino acid in the reservoir, and k_i is the rate constant for release for the i th amino acid. The amino acid release data for the first seven days was fit to the above equation (1) for all amino acids except tyrosine to obtain the release rate constants. The r^2 values for all fits were above 0.95 except for proline, phenylalanine ($r^2 > 0.92$) and aspartate ($r^2 > 0.68$). For amino acids with very low solubility i.e., cystine and tyrosine, a zero-order release is expected, described by [33]:

$$\frac{dm_i}{dt} = k_i, \text{ resulting in } m_i = k_i t \quad (2)$$

For tyrosine, the amino acid release data was fit to the above Eq. (2) to obtain the release rate constants ($r^2 > 0.84$). It should be noted that consistent with its low solubility, the release rate for tyrosine is very low, and the release rate of cysteine/cystine is also expected to be very low. Fig. 1e and f shows the release rate constants for all amino acids. As per equation (1), the amino acid release rates are proportional to the initial loading of the amino acid within the central reservoir. Thus, this provides a very simple tool to vary individual amino acid release rates for all amino acids (except cysteine/cystine and tyrosine) by varying

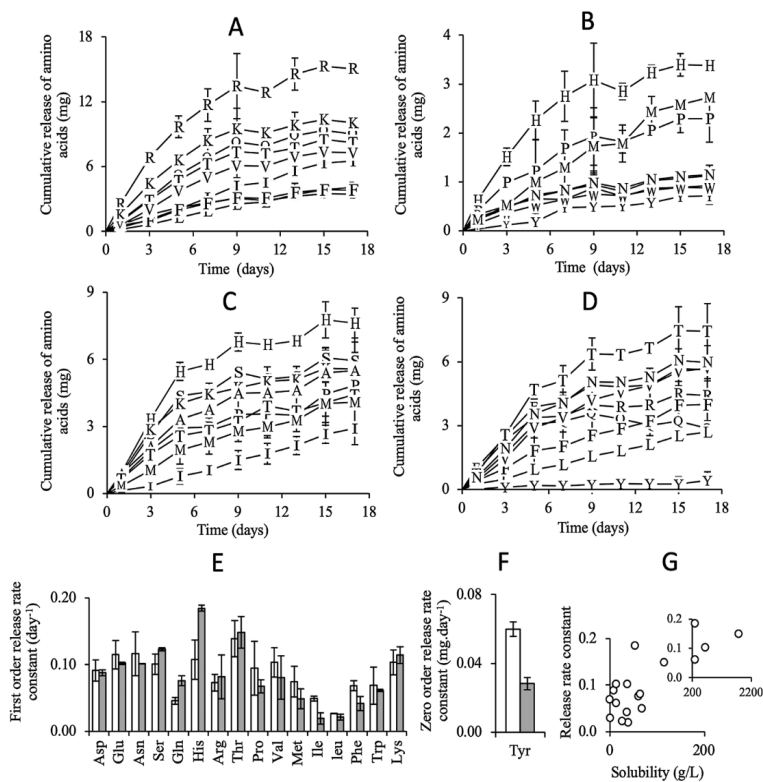


Fig. 1. Cumulative amino acid release profile from two different compositions of amino acid in the NutriGel payload viz NutriGel₁ and NutriGel₂^H. Release kinetics of amino acids for prewashed NutriGel₁ or NutriGel₂^H were characterized in 25 mL PBS with 0.05% sodium azide incubated at 37 °C under shaking conditions. Amino acid concentrations were quantified by reversed phase HPLC. (A,B) Cumulative amino acid release profile from NutriGel₁. Markers depict single amino acid abbreviations. (C,D) Cumulative amino acid release profile from NutriGel₂^H. Markers depict single amino acid abbreviations. (E,F) Release rate constants for NutriGel₁ gel (white bar) and NutriGel₂^H (grey bar). (G) Relationship between release rate constant and solubility. Error bars indicate 95% confidence interval, n = 2.

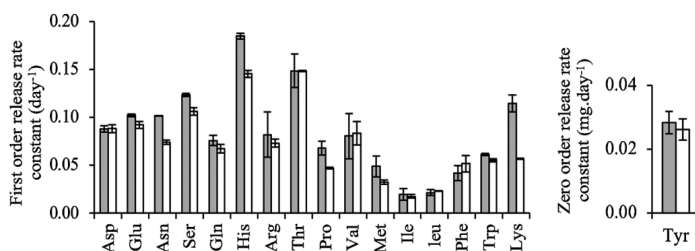


Fig. 2. Effect of inclusion of HEPES in the payload on the release rate constant. Release kinetics of amino acids for prewashed NutriGel₂^H or NutriGel₂^G were characterized in 25 mL PBS with 0.05% sodium azide at 37 °C under shaking conditions. Amino acid concentrations were quantified by reversed phase HPLC. Release rate constants for NutriGel₂^H (grey bars) and for NutriGel₂^G (white bars). Release rate constants for NutriGel₂^H are taken from Fig. 1E,F. Error bars indicate 95% confidence interval, n = 2.

their initial loading.

To independently confirm the effect of initial loading in the central reservoir on the release rate, we next evaluated a feed mixture comprising 8 mg each of all 18 amino acids along with 100 mg HEPES (composition in Table 1). These hydrogels will be referred to as NutriGel₂^H. Figs. 1c, d, and e, f shows the cumulative release profile and release rate constants for release of all amino acids from NutriGel₂^H. The release rate constants are similar to those calculated for NutriGel₁, indicating that the release rate is indeed proportional to the initial loading of the amino acid in the reservoir except for tyrosine and is not substantially affected by changes in the composition of the other amino acids in the reservoir.

A plot of release rate constant in NutriGel₂^H vs. solubility at 37 °C shows a weak positive correlation (Fig. 1g) (amino acid solubility at 37 °C was calculated using the Sober equation, δ and θ for the equation were obtained from Bowden, 2018 [34]). There is no correlation between the release rate constants of the amino acids and their molecular weight (data not shown). This is not surprising since the molecular weights of all amino acids lie within a narrow range. The local pH in the reservoir, which is not known, could affect the charge on the amino acids and hence their release. Due to the buffering action of HEPES and the effect of pH on the solubility of amino acids, we next assessed whether the presence of HEPES in the payload had any effect on release rates. The release rates for the amino acid formulations in NutriGel₂ were then analyzed in the presence of an equal amount of glucose instead of HEPES (NutriGel₂^G). With the exception of lysine, there was no substantial difference between the release rate constants in the presence or absence of HEPES (Fig. 2).

To increase the release rates of tyrosine, the amino acid with the lowest release rate constant, we dispersed 4 mg of tyrosine directly in the bottom layer of the hydrogel. Release kinetics of tyrosine from such a matrix was separately measured and found to be 0.09 mg/day. All hydrogels containing tyrosine thus dispersed are indicated by including ^T in the superscript in the name of the hydrogel. Since an oversupply of cysteine can cause toxicity [35], no further loading of cysteine/cystine was evaluated. However, a similar strategy can be used to increase the supply of cysteine/cystine if desired.

With the demonstrated ability of NutriGels to release amino acids over at least a week, we next explored whether such hydrogels could be

used to achieve a closed in situ feeding system for animal cell culture. Though the release rate of only amino acids has been measured here, other low abundance components of cell culture medium like vitamins, trace elements, antioxidants also play an essential role [26,28] and have been included in the feed mixture payload of the hydrogels used for cell culture. We have used a recombinant CHO cell line expressing IgG as a model culture system to assess whether in situ feeding of amino acids and other micronutrients can enable an increase in longevity of the culture in order to increase productivity. We first use a hydrogel with a nutrient feed payload having the same composition as the culture medium but without the bulk salts (NutriGel₁).

3.2. Continuous feeding of complex nutrient feed using NutriGel₁ improves culture longevity and volumetric productivity of recombinant CHO cell culture

NutriGel₁^T was evaluated with a suspension CHO cell culture producing IgG to assess whether the in situ supply of nutrients through the hydrogel has a beneficial effect on productivity and/or culture longevity. A culture without NutriGel₁^T served as control. Glucose was bolus fed to all the cultures, as described in the methods section. The NutriGel₁^T hydrogel was added on the 3rd day of the culture inoculated at a density of 0.3×10^6 cells/mL. Fig. 3 shows the effect of the addition of NutriGel₁^T on culture performance for a representative culture. The biological replicate cultures had differences in cell density in the later stages of the culture beyond day 13 and are hence not averaged. We also compared NutriGel₁^T to the traditional bolus fed cultures, where the bolus feed had the same composition as the payload of NutriGel₁^T and was supplemented as a liquid feed at fixed intervals. Fig. 3 also provides a comparison between the continuous mode of feeding through a hydrogel and the manual bolus mode of feeding. The viability of the cultures without the hydrogel decreased below 60% beyond day 8, while the addition of NutriGel₁^T or bolus feed resulted in maintenance of viability above 60% for at least 13 days among all replicates, thus substantially increasing the culture longevity. This is reflected in an average 2.7-fold (p value 0.0023) increase in integral viable cell density (IVCD) and an average 4 fold and 4-fold (p value 0.0012) increase in volumetric productivity of IgG (Fig. 3d) with NutriGel₁^T. Bolus feeding led to an average 2-fold (p value 0.0027) increase in IVCD

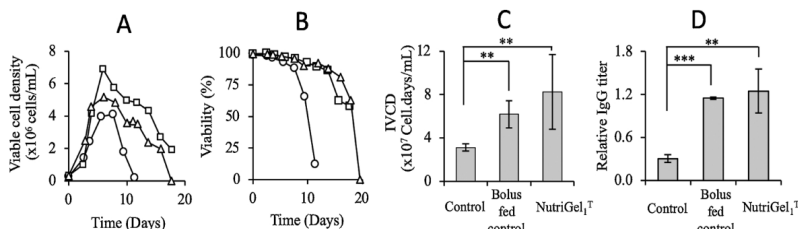


Fig. 3. In situ delivery of nutrients through NutriGel₁^T leads to improved culture performance. Suspension adapted CHO cells expressing IgG were inoculated at 0.3×10^6 cells/mL. Cultures were either bolus fed only glucose (control), bolus-fed complete nutrient feed (bolus fed control) or NutriGel₁^T was added to the culture on the 3rd day and cultures were bolus fed glucose as required (NutriGel₁^T). (A) Viable cell density. A

representative growth curve is shown. (B) Viability (C) IVCD (D) Relative IgG titer. ○ – control, Δ – bolus fed control, □ – NutriGel₁^T. Error bars indicate 95% confidence interval, n = 5 for cultures supplemented with NutriGel₁^T, n = 4 for control cultures, n = 2 for bolus-fed control cultures.

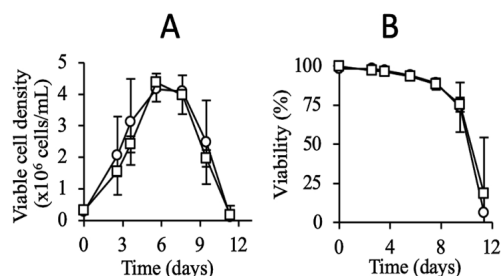


Fig. 4. In situ release of only amino acids does not result in improved cell growth. Suspension adapted CHO cells expressing IgG were inoculated at 0.3×10^6 cells/mL. NutriGel^{AA,T,G} was added on the 3rd day. Cultures were bolus-fed with glucose as required. (A) Viable cell density. (B) Viability. \circ – control, \square – NutriGel^{AA,T,G}. Error bars indicate 95% confidence interval, $n = 2$ for control cultures and $n = 3$ for cultures supplemented with NutriGel^{AA,T,G}.

and an average 3.8 (p value 0.0001) fold increase in volumetric productivity of IgG compared to the control. The differences between the bolus and NutriGel fed cultures are not statistically different. Thus, supplying the feed nutrient mixture through the hydrogel led to significantly increased culture longevity and volumetric productivity compared to the control demonstrating the proof-of-concept that a large number of nutrients can be simultaneously supplied in situ to support cell culture. It should be noted that the composition of the nutrient feed mixture loaded into the hydrogel is identical to the medium formulation, with the exception of the omission of bulk salts and glucose, and has not been optimized for improved culture performance.

Nutrients in cell culture medium other than amino acids such as vitamins, trace elements, and antioxidants also have a significant impact on cells in culture and have been shown to improve growth and productivity [28]. The NutriGel^T hydrogels have a payload of vitamins, antioxidants, trace elements, and other micronutrients, as listed in Table 1, in addition to amino acids. Though the release rates of these other nutrients included in small quantities in the payload have not been quantified, we questioned whether the release of any of these other nutrients contributed to the increased culture longevity. We investigated this by making hydrogels identical to NutriGel^T, but without particular classes of nutrients such as vitamins, trace elements and antioxidants and analyzing their effect on culture longevity.

3.3. NutriGel₁ hydrogels also supply other classes of nutrients that help in improving culture longevity

We first formulated NutriGel^{AA,T,G} with a payload of only amino acids in a composition identical to that in NutriGel₁ along with glucose. The NutriGel^{AA,T,G} were similarly added to the culture on day 3, and the culture was fed with glucose as a bolus when the glucose concentration decreased below 2 g/L. The culture data shown in Fig. 4 indicates that in situ supply of only amino acids through NutriGel^{AA,T,G}

does not result in a culture performance similar to NutriGel₁^T (Fig. 4). Viable cell densities of cultures supplemented with NutriGel^{AA,T,G} are similar to control cultures without the hydrogel and show no increase in IVCD. This supports the conclusion that at least some of the other micro-nutrients are being delivered to the culture through the NutriGel₁^T and their release contributes to the improved culture longevity.

3.4. Vitamins and trace elements are released from the NutriGels and contribute to improving culture longevity

To identify the nutrients essential for enhanced culture longevity in NutriGel₁^T as compared to NutriGel^{AA,T,G}, we supplemented CHO cultures with hydrogels identical to NutriGel₁^T, but with one category of micro-nutrients absent. The payload in these experiments was assembled by mixing all individual components in solid form for the macronutrients, while the micronutrients were added as a stock solution followed by drying, due to their low levels. These hydrogels were NutriGel₁^{T-V}, NutriGel₁^{T-TE}, NutriGel₁^{T-AO}, NutriGel₁^{T-TA}, and NutriGel₁^{T-N} lacking vitamins, trace elements, antioxidants (ethanolamine, putrescine, glutathione, and vitamin C), thioctic acid and nucleoside precursors respectively. Fig. 5 shows the IVCD, and peak viable cell density for NutriGel₁^T, NutriGel₁^{T-V}, NutriGel₁^{T-TE}, NutriGel₁^{T-AO}, NutriGel₁^{T-TA}, and NutriGel₁^{T-N}. The absence of vitamins in the hydrogel led to the lowest IVCD followed by the absence of trace elements indicating their importance in maintaining culture longevity. When NutriGel^{AA,T} was supplemented with vitamins and trace elements in the payload, the IVCD was restored to levels similar to NutriGel₁^T (data not shown).

3.5. Use of NutriGel₂^{HVT,T} to reduce the differences in release rates of all amino acids in fed-batch cultures

The amino acid composition in the payload for NutriGel₁ is similar to the culture medium. As shown above, the release rates of amino acids are proportional to the initial loading in the reservoir. Thus, amino acids, such as arginine, which are already in high abundance in the medium, have a high release rate. It is increasingly becoming evident that excessive supplementation of amino acids can lead to the production of inhibitory metabolites [32]. Amino acids, like arginine have also been shown to have a negative impact on protein production [36]. At the same time, amino acids like aspartate, which are present at low concentrations in the medium, have low release rates, which could limit their availability [37]. Consequently, in order to support cultures at higher viable cell density, we next examined the effect of using NutriGel₂^H hydrogels containing 8 mg each of all amino acids instead of NutriGel₁^T. Additional vitamin and trace element loading was included in the NutriGel₂^H hydrogels since the release of these two groups of micro-nutrients was seen to be essential for the increased culture longevity. This hydrogel is referred to henceforth as NutriGel₂^{HVT,T}.

We evaluated the effect of in situ feeding cultures seeded at a higher cell density of 5×10^6 cells/mL. NutriGel₂^{HVT,T} was added to the culture at the time of inoculation while no hydrogel was added to the

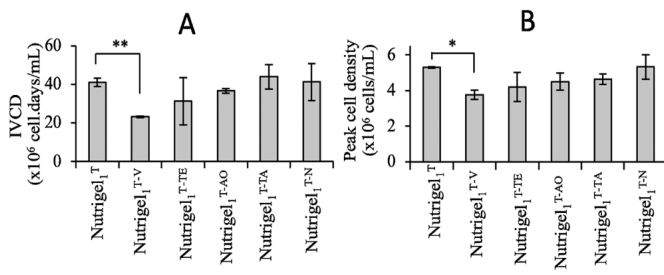


Fig. 5. Effect of exclusion of different classes of nutrients from the payload of the NutriGel on culture longevity. Suspension adapted CHO cells expressing IgG were inoculated at 0.3×10^6 cells/mL. NutriGels deficient in a single class of nutrients were added on the 3rd day and cultures were bolus fed glucose as required. NutriGel₁^T, NutriGel₁^{T-V} (without vitamins), NutriGel₁^{T-TE} (without trace elements), NutriGel₁^{T-N} (without nucleoside precursor), NutriGel₁^{T-AO} (without antioxidants), NutriGel₁^{T-TA} (without thioctic acid). See Table 1 for the detail formulation of the NutriGels. (A) IVCD and (B) Peak viable cell density. Error bars indicate 95% confidence interval, $n = 2$.

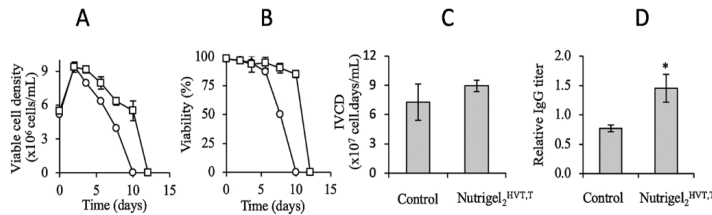


Fig. 6. Use of NutriGel₂^{HVT,T} hydrogel to reduce the differences in release rates of all amino acids in fed-batch cultures. Suspension adapted CHO cells expressing IgG were inoculated at 5×10^6 cells/mL. NutriGel₂^{HVT,T} was added on day zero and cultures were bolus fed glucose as required. Control cultures were bolus fed only glucose. (A) Viable cell density. A representative growth curve is shown. (B) Viability (C) IVCD (D) Relative IgG titer. \circ – Control, \square – NutriGel₂^{HVT,T}. Error bars indicate 95% confidence interval, n = 2.

control culture. Both cultures were bolus fed glucose as described in the methods section. There is no difference in peak viable cell density with the addition of NutriGel₂^{HVT,T} indicating the per cell supply of nutrients achieved in this condition does not support higher cell growth. In the absence of NutriGel₂^{HVT,T}, cell viability was maintained above 80% till day 6. Addition of NutriGel₂^{HVT,T} led to viability above 80% till day 10 with an average 1.2-fold higher IVCD (p value 0.24) and a 1.9-fold (p value 0.014) increase in volumetric productivity of IgG compared to the control. Volumetric productivity of 1.5 g/L was achieved with NutriGel₂^{HVT,T} (Fig. 6). This again demonstrates the ability to improve culture performance by in situ release of nutrients. Though this particular hydrogel loading formulation did not support higher growth, culture volume and/or amino acid loading can be trivially changed to adjust the per cell release rates to further optimize the release rates per unit volume for increased growth if desired.

3.6. A completely closed continuous in situ feeding via hydrogels for animal cell culture requiring no operator handling

With NutriGel₁^T, we successfully demonstrated the utility of a hydrogel to feed amino acids and other nutrients to improve culture performance in terms of growth and productivity, but glucose was supplied via bolus additions. To make a complete in situ feeding system, glucose was also further delivered through the same hydrogel to avoid any bolus feeding. NutriGel₁^{T,G} has an identical payload as NutriGel₁^T with the addition of 200 mg glucose. Release kinetics for hydrogels loaded with 200 mg of glucose is shown in Fig. 7a. Cultures supplemented with NutriGel₁^{T,G} hydrogel on day 3 led to improved culture longevity with an average 1.8-fold (p value 0.004) higher IVCD along with a 3-fold (p value 0.011) higher volumetric productivity of IgG compared to the control cultures in batch mode (Fig. 7e, f).

Importantly, with the addition of NutriGel₁^{T,G}, there is no requirement for operator handling for the feeding of cultures (Fig. 7). The statistical significance of the differences between this completely closed culture and the NutriGel added cultures which were bolus fed glucose as described above is $p = 0.03$ and $p = 0.21$ for IVCD and titer, respectively. This indicates no significant difference in titer when glucose is either fed as a bolus or through the NutriGel. The difference in IVCD may be due to the nature of the glucose release kinetics through the hydrogel. A separate hydrogel could be used for glucose delivery to provide independent control on the rate and duration of glucose release. The use of other slowly metabolizing sugars in addition to glucose may result in further improvements to the culture performance. A separate glucose loaded hydrogel can also be used to obtain independent control over the glucose release rate.

4. Conclusion

In this study, we report for the first time, the development and application of a diffusion-based inexpensive hydrogel system for continuous in situ feeding of a complex mixture of all nutrients required for mammalian cell cultures, including amino acids, vitamins, and trace elements. The hydrogel includes the complex nutrient feed dispersed in the form of a solid in a central reservoir. This prevents dilution of the culture seen in traditional fed-batch cultures where the feed is added as a concentrated solution whose strength is limited by the solubility of the nutrients included. At the end of the culture, the culture can be pipetted/pumped out from the culture vessel leaving the hydrogel behind. No additional separation step is required. We demonstrate that it is possible to modulate the release rates of individual amino acids through this hydrogel by changing their initial loading in the central reservoir, with the exception of low solubility amino acids tyrosine and

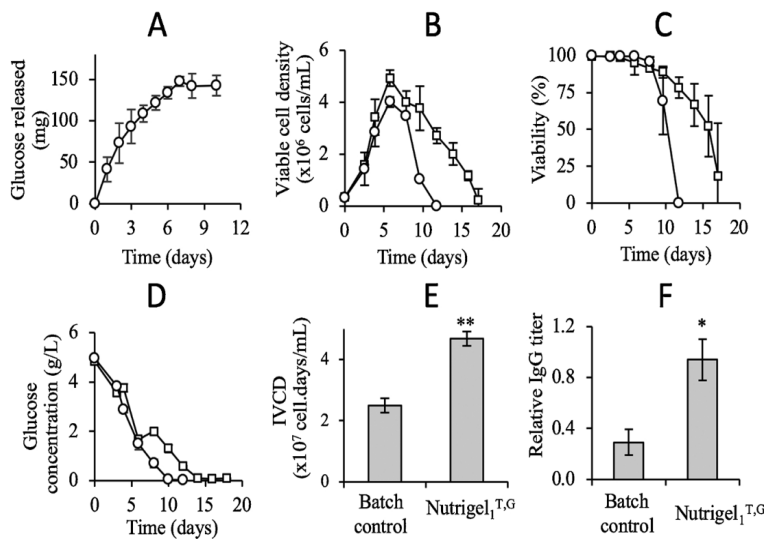


Fig. 7. Complete in situ continuous delivery of all nutrients through NutriGel₁^{T,G} also results in improved culture performance. (A) Cumulative glucose released through NutriGel₁^{T,G}, n = 3. (B) Suspension adapted CHO cells expressing IgG were inoculated at 0.3×10^6 cells/mL and NutriGel₁^{T,G} was added on the 3rd day. Control cultures are operated in batch mode with no feeding. Viable cell density (C) Viability (D) Glucose concentration in the culture supernatant. \circ – batch control, \square – NutriGel₁^{T,G}. (E) IVCD (F) Relative IgG titer. n = 2 for control and n = 3 for cultures supplemented with NutriGel₁^{T,G}. Error bars indicate 95% confidence interval.

possibly cystine/cysteine. This provides the ability to tailor release rates for individual amino acids as required for the specific application. The release rates of these low solubility amino acids can be increased if required by loading them outside the reservoir of the hydrogel. The use of higher solubility/stability modified amino acids, such as phosphotyrosine disodium salt can also allow control over the release rate of the low solubility amino acids through the reservoir if desired [10,38]. Though the release rates of the other micronutrients like vitamins and trace elements were not measured, we show that their incorporation was essential for the improved culture performance. This indirectly confirms that at least some of the other nutrients are indeed delivered through the hydrogel. Further characterization of release rates of micronutrients will help in the optimization of the feed loaded in the reservoir.

Such systems can help small-scale animal cell culture platforms to achieve continuous nutrient feeding in a completely closed use-and-throw format without any additional infrastructure. We have not evaluated the shear sensitivity of the NutriGel, but such studies can guide exploration of application in small scale single-use bioreactors like the WAVE bioreactor. In situ continuous feeding at small-scales can also allow the development and use of leaner culture medium, which is more representative of conditions encountered by cells in vivo [39] since cell growth will no longer be limited by the initial nutrient concentrations in the medium. In situ nutrient feeding reported in this study, in addition to in situ pH management described previously [40], can enable completely closed systems in single-use platforms requiring no operator intervention which may be of use in bioprocessing as a screening tool for animal cell-based bioprocesses and in production of patient-specific cell-based therapies.

Declaration of Competing Interest

MG and JR declare a provisional patent application titled "A method for sustaining a cell culture system using a hydrogel composition" filed by CSIR, which is based on results reported in this study.

Acknowledgements

MG acknowledges funding from Council of Scientific and Industrial Research, India (CSIR)YSA000426 and MLP035526). JR acknowledges senior research fellowship from CSIR. The authors thankfully acknowledge help from Dr RV Gadre with establishing HPLC analysis protocols for amino acid quantitation.

Appendix A. Supplementary data

Supplementary material related to this article can be found, in the online version, at doi:<https://doi.org/10.1016/j.bej.2019.107436>.

References

- [1] G. Walsh, Biopharmaceutical benchmarks 2018, *Nat. Biotechnol.* 36 (2018) 1136, <https://doi.org/10.1038/nbt.4305>.
- [2] K.F. Wlaschin, W.-S. Hu, Fedbatch culture and dynamic nutrient feeding, in: W.-S. Hu (Ed.), *Adv. Biochem. Eng. Biotechnol.* Springer Berlin Heidelberg, Berlin, Heidelberg, 2006, pp. 43–74, https://doi.org/10.1007/10_015.
- [3] J. Vande Voorde, T. Ackermann, N. Pfetzer, D. Sumpton, G. Mackay, G. Kalna, C. Nixon, K. Blyth, E. Gottlieb, S. Tardito, Improving the metabolic fidelity of cancer models with a physiological cell culture medium, *Sci. Adv.* (2019), <https://doi.org/10.1126/sciadv.aau7314>.
- [4] P.M. Hayter, E.M.A. Curling, A.J. Baines, N. Jenkins, I. Salmon, P.G. Strange, J.M. Tong, A.T. Bull, Glucose-limited chemostat culture of chinese hamster ovary cells producing recombinant human interferon- γ , *Biotechnol. Bioeng.* (1992), <https://doi.org/10.1002/bit.260390311>.
- [5] W. Zhou, J. Rehm, A. Europa, W.S. Hu, Alteration of mammalian cell metabolism by dynamic nutrient feeding, *Cytotechnology.* 24 (1997) 99–108, <https://doi.org/10.1023/A:1007945826228>.
- [6] H.J. Cruz, C.M. Freitas, P.M. Alves, J.L. Moreira, M.J.T. Carrondo, Effects of ammonia and lactate on growth, metabolism, and productivity of BHK cells, *Enzyme Microb. Technol.* 27 (2000) 43–52.
- [7] C. Altamirano, C. Paredes, A. Illanes, J. Cairó, F. Gòdia, Strategies for fed-batch cultivation of t-PA producing CHO cells: substitution of glucose and glutamine and rational design of culture medium, *J. Biotechnol.* 110 (2004) 171–179, <https://doi.org/10.1016/j.jbiotec.2004.02.004>.
- [8] D. Chee Fung Wong, K. Tin Kam Wong, L. Tang Goh, C. Kiat Heng, M. Gek Sim Yap, Impact of dynamic online fed-batch strategies on metabolism, productivity and N-glycosylation quality in CHO cell cultures, *Biotechnol. Bioeng.* 89 (2005) 164–177, <https://doi.org/10.1002/bit.20317>.
- [9] S.L. Barrett, R. Boniface, P. Dhulipala, P. Slade, Y. Tennico, M. Stramaglia, P. Lio, S.F. Gorfien, Attaining next-level titers in CHO fed-batch cultures, *Bioprocess Int.* (2012).
- [10] A. Zimmer, R. Mueller, M. Wehsling, A. Schnellbaeher, J. von Hagen, Improvement and simplification of fed-batch bioprocesses with a highly soluble phosphotyrosine sodium salt, *J. Biotechnol.* (2014), <https://doi.org/10.1016/j.jbiotec.2014.06.026>.
- [11] J. von Hagen, C. Hecklau, R. Seibel, S. Pering, A. Schnellbaeher, M. Wehsling, T. Eichhorn, A. Zimmer, Simplification of fed-batch processes with a single-feed strategy, *Bioprocess Int.* (2017).
- [12] B.P. Weegman, P. Nash, A.L. Carlson, K.J. Voltzke, Z. Geng, M. Jahani, B.B. Becker, K.K. Pappas, M.T. Firpo, Nutrient regulation by continuous feeding removes limitations on cell yield in the large-scale expansion of mammalian cell spheroids, *PLoS One* 8 (2013), <https://doi.org/10.1371/journal.pone.0076611>.
- [13] D.C. Kirouac, P.W. Zandstra, The systematic production of cells for cell therapies, *Cell Stem Cell* 3 (2008) 369–381, <https://doi.org/10.1016/j.stem.2008.09.001>.
- [14] C.-A. Tran, L. Burton, D. Russom, J.R. Wagner, M.C. Jensen, S.J. Forman, D.L. DiGiusto, Manufacturing of large numbers of patient-specific T cells for adoptive immunotherapy, *J. Immunother.* 30 (2007) 644–654, <https://doi.org/10.1097/CJI.0b013e318052e1f4>.
- [15] E. Csaszar, D.C. Kirouac, M. Yu, W. Wang, W. Qiao, M.P. Cooke, A.E. Boitano, C. Ito, P.W. Zandstra, Rapid expansion of human hematopoietic stem cells by automated control of inhibitory feedback signaling, *Cell Stem Cell* (2012), <https://doi.org/10.1016/j.stem.2012.01.003>.
- [16] W. Zhou, J. Rehm, W.-S. Hu, High viable cell concentration fed-batch cultures of hybridoma cells through on-line nutrient feeding, *Biotechnol. Bioeng.* 46 (1995) 579–587, <https://doi.org/10.1002/bit.260460611>.
- [17] A. Amanullah, J.M. Otero, M. Mikola, A. Hsu, J. Zhang, J. Aunins, H.B. Schreyer, J.A. Hope, A.P. Russo, Novel micro-bioreactor high throughput technology for cell culture process development: reproducibility and scalability assessment of fed-batch CHO cultures, *Biotechnol. Bioeng.* 106 (2010) 57–67, <https://doi.org/10.1002/bit.2266>.
- [18] R. Bareither, D. Pollard, A review of advanced small-scale parallel bioreactor technology for accelerated process development: current state and future need, *Biotechnol. Prog.* (2011), <https://doi.org/10.1002/btpr.522>.
- [19] O. Wichterle, D. Lím, Hydrophilic gels for biological use, *Nature.* 185 (1960) 117, <https://doi.org/10.1038/185117a0>.
- [20] P. Agarwal, I.D. Rupenthal, Injectable implants for the sustained release of protein and peptide drugs, *Drug Discov. Today* 18 (2013) 337–349.
- [21] S. Hegde, T. Pant, K. Pradhan, M. Badiger, M. Gadgil, Controlled release of nutrients to mammalian cells cultured in shake flasks, *Biotechnol. Prog.* 28 (2012) 188–195, <https://doi.org/10.1002/btpr.729>.
- [22] A.M. Hosios, V.C. Hecht, L.V. Danai, M.O. Johnson, J.C. Rathmel, M.L. Steinhauer, S.R. Manalis, M.G. Vander Heiden, Amino acids rather than glucose account for the majority of cell mass in proliferating mammalian cells, *Dev. Cell* (2016), <https://doi.org/10.1016/j.devcel.2016.02.012>.
- [23] F. Torkashvand, B. Vaziri, S. Maleknia, A. Heydari, M. Vossoughi, F. Davami, F. Mahboudi, Designed amino acid feed in improvement of production and quality targets of a therapeutic monoclonal antibody, *PLoS One* 10 (2015) e0140597, <https://doi.org/10.1371/journal.pone.0140597>.
- [24] S. Kishishita, S. Katayama, K. Kodaira, Y. Takagi, H. Matsuda, H. Okamoto, S. Takuma, C. Hirashima, H. Aoyagi, Optimization of chemically defined feed media for monoclonal antibody production in Chinese hamster ovary cells, *J. Biosci. Bioeng.* 120 (2015) 78–84, <https://doi.org/10.1016/j.jbiosc.2014.11.022>.
- [25] L.M. Carrillo-Coccom, T. Genel-Rey, D. Araúz-Hernández, F. López-Pacheco, J. López-Meza, M.R. Rocha-Pizaña, A. Ramírez-Medrano, M.M. Alvarez, Amino acid consumption in naive and recombinant CHO cell cultures: producers of a monoclonal antibody, *Cytotechnology.* 67 (2015) 809–820, <https://doi.org/10.1007/s10616-014-9720-5>.
- [26] P. Ducommun, P.A. Ruffieux, U. Von Stockar, I. Marison, The role of vitamins and amino acids on hybridoma growth and monoclonal antibody production, *Cytotechnology.* 37 (2001) 65–73, <https://doi.org/10.1023/A:1019956013627>.
- [27] Z. Xing, B. Kenty, I. Koyrak, M. Borys, S.H. Pan, Z.J. Li, Optimizing amino acid composition of CHO cell culture media for a fusion protein production, *Process Biochem.* 46 (2011) 1423–1429, <https://doi.org/10.1016/j.procbio.2011.03.014>.
- [28] D.Y. Kim, J.C. Lee, H.N. Chang, D.J. Oh, Effects of supplementation of various medium components on Chinese hamster ovary cell cultures producing recombinant antibody, *Cytotechnology* (2005) 37–49, <https://doi.org/10.1007/s10616-005-3775-2>.
- [29] D. Wen, M.M. Vecchi, S. Gu, L. Su, J. Dolnikova, Y.M. Huang, S.F. Foley, E. Garber, N. Pederson, W. Meier, Discovery and investigation of misincorporation of serine at asparagine positions in recombinant proteins expressed in Chinese hamster ovary cells, *J. Biol. Chem.* 284 (2009) 32686–32694, <https://doi.org/10.1074/jbc.M109.059360>.
- [30] Z. Zhang, B. Shah, P.V. Bondarenko, G/U and certain wobble position mismatches as possible main causes of amino acid misincorporations, *Biochemistry.* 52 (2013) 8165–8176, <https://doi.org/10.1021/bi401002c>.
- [31] A. Khetan, Y. Huang, J. Dolnikova, N.E. Pederson, D. Wen, H. Yusuf-Makgiansar, P. Chen, T. Ryll, Control of misincorporation of serine for asparagine during

- antibody production using CHO cells, *Biotechnol. Bioeng.* 107 (2010) 116–123.
- [32] B.C. Mulukutla, J. Kale, T. Kalomeris, M. Jacobs, G.W. Hiller, Identification and control of novel growth inhibitors in fed-batch cultures of Chinese hamster ovary cells, *Biotechnol. Bioeng.* 114 (2017) 1779–1790, <https://doi.org/10.1002/bit.26313>.
- [33] J. Siepmann, F. Siepmann, Mathematical modeling of drug delivery, *Int. J. Pharm.* (2008), <https://doi.org/10.1016/j.ijpharm.2008.09.004>.
- [34] N.A. Bowden, Modelling the Solubility of the 20 Proteinogenic Amino Acids With Experimentally Derived Saturation Data, Wageningen University, 2018, <http://edepot.wur.nl/446739>.
- [35] Y. Nishiuchi, M. Sasaki, M. Nakayasu, A. Oikawa, Cytotoxicity of cysteine in culture media, *In Vitro* 12 (1976) 635–638, <https://doi.org/10.1007/BF02797462>.
- [36] I.J. González-Leal, L.M. Carrillo-Cocom, A. Ramírez-Medrano, F. López-Pacheco, D. Bulnes-Abundis, Y. Webb-Vargas, M.M. Alvarez, Use of a plackett-burman statistical design to determine the effect of selected amino acids on monoclonal antibody production in CHO cells, *Biotechnol. Prog.* 27 (2011) 1709–1717, <https://doi.org/10.1002/btpr.674>.
- [37] L.B. Sullivan, D.Y. Gui, A.M. Hosios, L.N. Bush, E. Freinkman, M.G. Vander Heiden, Supporting Aspartate Biosynthesis Is an Essential Function of Respiration in Proliferating Cells, *Cell*. 162 (2015) 552–563, <https://doi.org/10.1016/j.cell.2015.07.017>.
- [38] C. Hecklau, S. Pering, R. Seibel, A. Schnellbaecher, M. Wehsling, T. Eichhorn, J. von Hagen, A. Zimmer, S-Sulfofocysteine simplifies fed-batch processes and increases the CHO specific productivity via anti-oxidant activity, *J. Biotechnol.* (2016), <https://doi.org/10.1016/j.jbiotec.2015.11.022>.
- [39] N. Psychogios, D.D. Hau, J. Peng, A.C. Guo, R. Mandal, S. Bouatra, I. Sinelnikov, R. Krishnamurthy, R. Eisner, B. Gautam, N. Young, J. Xia, C. Knox, E. Dong, P. Huang, Z. Hollander, T.L. Pedersen, S.R. Smith, F. Bamforth, R. Greiner, B. McManus, J.W. Newman, T. Goodfriend, D.S. Wishart, The human serum metabolome, *PLoS One* (2011), <https://doi.org/10.1371/journal.pone.0016957>.
- [40] R. Sanil, V. Maralingannavar, M. Gadgil, In situ pH management for microbial culture in shake flasks and its application to increase plasmid yield, *J. Ind. Microbiol. Biotechnol.* 41 (2014) 647.